

Date Received for Clearance Process (MM/DD/YYYY) 06/23/2021 07/08/2021 ^{JRR}	INFORMATION CLEARANCE FORM																																				
A. Information Category <input type="checkbox"/> Abstract <input type="checkbox"/> Journal Article <input type="checkbox"/> Summary <input type="checkbox"/> Internet <input type="checkbox"/> Visual Aid <input type="checkbox"/> Software <input type="checkbox"/> Full Paper <input type="checkbox"/> Report <input type="checkbox"/> Other _____	B. Document Number DOE/ORP-2021-02 Revision 0 C. Title Department of Energy Responses to the Nuclear Regulatory Commission Request for Additional Information on the Draft Waste Incidental to Reprocessing Evaluation for Vitrification of Low Activity Waste																																				
E. Required Information (MANDATORY) 1. Is document potentially Classified? <input checked="" type="radio"/> No <input type="radio"/> Yes Trenchard, Glyn D Approved via att. IDMS data file. _____ Manager Required (Print and Sign) If Yes _____ ADC Required (Print and Sign) <input type="radio"/> No <input type="radio"/> Yes Classified 2. Official Use Only <input checked="" type="radio"/> No <input type="radio"/> Yes Exemption No. _____ 3. Export Controlled Information <input checked="" type="radio"/> No <input type="radio"/> Yes OOU Exemption No. 3 4. UCNi <input checked="" type="radio"/> No <input type="radio"/> Yes 5. Applied Technology <input checked="" type="radio"/> No <input type="radio"/> Yes OOU Exemption No. 5 6. Other (Specify) _____	7. Does Information Contain the Following: a. New or Novel (Patentable) Subject Matter? <input checked="" type="radio"/> No <input type="radio"/> Yes If "Yes", OOU Exemption No. 3 If "Yes", Disclosure No.: _____ b. Commercial Proprietary Information Received in Confidence, Such as Proprietary and/or Inventions? <input checked="" type="radio"/> No <input type="radio"/> Yes If "Yes", OOU Exemption No. 4 c. Corporate Privileged Information? <input checked="" type="radio"/> No <input type="radio"/> Yes If "Yes", OOU Exemption No. 4 d. Government Privileged Information? <input checked="" type="radio"/> No <input type="radio"/> Yes If "Yes", Exemption No. 5 e. Copyrights? <input checked="" type="radio"/> No <input type="radio"/> Yes If "Yes", Attach Permission. f. Trademarks? <input checked="" type="radio"/> No <input type="radio"/> Yes If "Yes", Identify in Document. 8. Is Information requiring submission to OSTI? <input checked="" type="radio"/> No <input type="radio"/> Yes 9. Release Level? <input checked="" type="radio"/> Public <input type="radio"/> Limited																																				
F. Complete for a Journal Article																																					
1. Title of Journal _____																																					
G. Complete for a Presentation																																					
1. Title for Conference or Meeting _____ 2. Group Sponsoring _____ 3. Date of Conference _____ 4. City/State _____ 5. Will Information be Published in Proceedings? <input checked="" type="radio"/> No <input type="radio"/> Yes 6. Will Material be Handed Out? <input checked="" type="radio"/> No <input type="radio"/> Yes																																					
H. Information Owner/Author/Requestor Pyles, Gary L Approved via att. IDMS data file. _____ (Print and Sign)	Responsible Manager Trenchard, Glyn D Approved via att. IDMS data file. _____ (Print and Sign)																																				
Approval by Direct Report to President (Speech/Articles Only) _____ (Print and Sign)																																					
I. Reviewers	Signature																																				
<table border="0" style="width:100%;"> <tr> <td style="width:15%;"><input checked="" type="checkbox"/> Yes</td> <td style="width:15%;"><input type="checkbox"/> Print</td> <td style="width:55%;"></td> <td style="width:15%;"></td> </tr> <tr> <td><input checked="" type="checkbox"/></td> <td><input type="checkbox"/></td> <td><input type="checkbox"/></td> <td><input type="checkbox"/></td> </tr> </table>	<input checked="" type="checkbox"/> Yes	<input type="checkbox"/> Print			<input checked="" type="checkbox"/>	<input type="checkbox"/>	<input type="checkbox"/>	<input type="checkbox"/>	<table border="0" style="width:100%;"> <tr> <td style="width:15%;"></td> <td style="width:15%;"></td> <td style="width:55%;"></td> <td style="width:15%;"></td> </tr> <tr> <td>General Counsel</td> <td><input checked="" type="checkbox"/></td> <td>Hellstrom, George W</td> <td>Approved via att. IDMS data file. <input checked="" type="radio"/> Y / N</td> </tr> <tr> <td>Office of External Affairs</td> <td><input checked="" type="checkbox"/></td> <td>Tyree, Geoffrey T</td> <td>Approved via att. IDMS data file. <input checked="" type="radio"/> Y / N</td> </tr> <tr> <td>DOE</td> <td><input type="checkbox"/></td> <td>_____</td> <td>Y / N</td> </tr> <tr> <td>Other</td> <td><input type="checkbox"/></td> <td>_____</td> <td>Y / N</td> </tr> <tr> <td>Other</td> <td><input type="checkbox"/></td> <td>_____</td> <td>Y / N</td> </tr> <tr> <td>Other</td> <td><input type="checkbox"/></td> <td>_____</td> <td>Y / N</td> </tr> </table>					General Counsel	<input checked="" type="checkbox"/>	Hellstrom, George W	Approved via att. IDMS data file. <input checked="" type="radio"/> Y / N	Office of External Affairs	<input checked="" type="checkbox"/>	Tyree, Geoffrey T	Approved via att. IDMS data file. <input checked="" type="radio"/> Y / N	DOE	<input type="checkbox"/>	_____	Y / N	Other	<input type="checkbox"/>	_____	Y / N	Other	<input type="checkbox"/>	_____	Y / N	Other	<input type="checkbox"/>	_____	Y / N
<input checked="" type="checkbox"/> Yes	<input type="checkbox"/> Print																																				
<input checked="" type="checkbox"/>	<input type="checkbox"/>	<input type="checkbox"/>	<input type="checkbox"/>																																		
General Counsel	<input checked="" type="checkbox"/>	Hellstrom, George W	Approved via att. IDMS data file. <input checked="" type="radio"/> Y / N																																		
Office of External Affairs	<input checked="" type="checkbox"/>	Tyree, Geoffrey T	Approved via att. IDMS data file. <input checked="" type="radio"/> Y / N																																		
DOE	<input type="checkbox"/>	_____	Y / N																																		
Other	<input type="checkbox"/>	_____	Y / N																																		
Other	<input type="checkbox"/>	_____	Y / N																																		
Other	<input type="checkbox"/>	_____	Y / N																																		
J. Comments Document has been formally submitted to NRC by DOE/HQ and needs to be public released to share with other stakeholders.																																					
Information Clearance Approval <div style="border: 1px solid green; padding: 5px; display: inline-block; color: green; font-weight: bold;">APPROVED</div> <small>By Julia Raymer at 8:32 am, Jul 08, 2021</small> <div style="border: 1px solid blue; padding: 5px; display: inline-block; color: blue; font-weight: bold;">Approved for Public Release; Further Dissemination Unlimited</div>																																					

```

- <workflow name="(JRR) DOE/ORP-2021-02-00" id="307803359">
- <task name="Clearance Process" id="0" date-initiated="20210623T1056"
  performer="JULIA R RAYMER" performer-id="164931488"
  username="h3310581">
  <comments>Please approve DOE/ORP-2021-02, Rev. 0 for public release.
  Thank you, Julia Raymer, Information Clearance</comments>
</task>
<task name="Add XML" id="1" date-done="20210623T1056" />
<task name="Manager Approval" id="41" date-due="20210628T1056" date-
done="20210701T1112" performer="GLYN D TRENCHARD" performer-
id="692578" username="h0078302" disposition="Approve"
authentication="true" />
<task name="Document Reviewer1" id="54" date-due="20210706T1112" date-
done="20210702T0850" performer="GEORGE W HELLSTROM" performer-
id="273013663" username="h8579141" disposition="Public Release"
authentication="true" />
<task name="Document Reviewer2" id="53" date-due="20210706T1112" date-
done="20210707T1352" performer="GEOFFREY T TYREE" performer-
id="6158846" username="h0068565" disposition="Public Release"
authentication="true" />
<task name="Doc Owner Clearance Review" id="13" date-due="20210708T1352"
date-done="20210707T1401" performer="GARY L PYLES" performer-
id="147601648" username="h6400308" disposition="Send On"
authentication="true" />
<task name="Milestone 1" id="24" date-done="20210707T1402" />
<task name="Milestone 2" id="62" date-done="20210707T1402" />
<task name="Verify Doc Consistency" id="4" date-due="20210708T1401" date-
done="20210708T0725" performer="JULIA R RAYMER" performer-
id="164931488" username="h3310581" disposition="Cleared"
authentication="true" />
</workflow>

```

Department of Energy Responses to the Nuclear Regulatory Commission Request for Additional Information on the Draft Waste Incidental to Reprocessing Evaluation for Vitrification of Low Activity Waste

Prepared for the U.S. Department of Energy
Assistant Secretary for Environmental Management



P.O. Box 450
Richland, Washington 99352

Department of Energy Responses to the Nuclear Regulatory Commission Request for Additional Information on the Draft Waste Incidental to Reprocessing Evaluation for Vitrification of Low Activity Waste

D. B. Darling
Washington River Protection Solutions

D. J. Swanberg
Washington River Protection Solutions

K. P. Lee
ORANO

L. H. Cree
Washington River Protection Solutions

Date Published
June 2021

Prepared for the U.S. Department of Energy
Assistant Secretary for Environmental Management

Office of River Protection

**P.O. Box 450
Richland, Washington 99352**

APPROVED

By Julia Raymer at 8:33 am, Jul 08, 2021

Release Approval

Date

TRADEMARK DISCLAIMER

Reference herein to any specific commercial product, process, or service by tradename, trademark, manufacturer, or otherwise, does not necessarily constitute or imply its endorsement, recommendation, or favoring by the United States Government or any agency thereof or its contractors or subcontractors.

This report has been reproduced from the best available copy.

Printed in the United States of America



**Department of Energy Responses to the
Nuclear Regulatory Commission
Request for Additional Information on the
Draft Waste Incidental to Reprocessing
Evaluation for Vitrification of Low Activity
Waste**

June 2021

This page intentionally left blank.

TABLE OF CONTENTS

1.0	INTRODUCTION.....	1
2.0	NRC’S INTRODUCTORY STATEMENT IN THE REQUEST FOR ADDITIONAL INFORMATION RELATED TO SECONDARY WASTE	3
3.0	REMOVAL OF KEY RADIONUCLIDES TO THE MAXIMUM EXTENT PRACTICAL.....	6
	RAI 1-1 (Removal of 90Sr to the Maximum Extent Practicable)	6
	RAI 1-2 (Percentage of Key Radionuclide Removal)	10
	RAI 1-3 (Percentage of 99Tc and 129I Recycled versus Removed).....	18
	RAI 1-4 (Alternative Technology Evaluation Impacting 99Tc and 129I).....	22
	RAI 1-5 (Removal and Disposal of Separated 129I).....	24
4.0	RADIONUCLIDE INVENTORY AND RELEASE RATES	27
	RAI 2-1 (Scope of PA Compared to Scope of Draft WIR Evaluation)	27
	RAI 2-2 (Model Support for the Performance Assessment).....	30
	RAI 2-3 (PA Modeling Discretization).....	32
	RAI 2-4 (Near-field and UZ Modeling Approach).....	40
	RAI 2-5 (Disposition of Nitrate).....	42
	RAI 2-6 (Glass Wasteform and Volatile Species Distribution).....	46
	RAI 2-7 (Glass Wasteform Fractional Release Rate).....	48
	RAI 2-8 (Glass Cracking).....	69
	RAI 2-9 (Glass Stage III).....	72
	RAI 2-10 (Volatile Species and Glass).....	81
	RAI 2-11 (Comparison of STOMP and GWB)	86
	RAI 2-12 (Sensitivity and Uncertainty Analyses)	89

RAI 2-13 (Quality Assurance).....	92
RAI 2-14 (Geologic Uncertainty).....	93
RAI 2-15 (Vadose Zone Parameters).....	116
RAI 2-16 (Saturated Zone Hydraulic Conductivity)	149
RAI 2-17 (Intruder).....	168
RAI 2-18 (90Sr Inventory Uncertainty).....	178
RAI 2-19 (Releases from the ETF-LSW Waste)	184
RAI 2-20 (I Sorption on the SSW-GAC and SSW-AGM Wasteforms).....	195
RAI 2-21 (Releases from Cementitious Wasteforms)	205
5.0 ASSESSMENT OF WASTE CONCENTRATION AND CLASSIFICATION	209
6.0 REFERENCES.....	210

TABLE OF ATTACHMENTS

ATTACHMENT A	213
--------------------	-----

TABLE OF FIGURES

Figure 1-2-1. Data from Table 2-3 in the Draft Waste Incidental to Reprocessing Evaluation.	10
Figure 1-3-1. Iodine-129 Distribution across Waste Forms as Percent of Best-Basis Inventory by Case.	19
Figure 1-3-2. Technetium-99 Distribution across Waste Forms as Percent of Best-Basis Inventory by Case.	19
Figure 2-3-1. Two-Dimensional Vertical Cross-Section Model of Integrated Disposal Facility Showing Numerical Grid and Surface Barrier Materials.	33
Figure 2-3-2. CLD3-Infiltration: 33.0 mm/yr Spatial Distribution of Saturation (Top) and Magnitude of Water Fluxes (Middle), and Vertical Fluxes (Bottom) at 750 years [After Cover/Liner Degradation].....	34
Figure 2-4-1. Grids for Alternative Disposal Configurations Involving One Waste Package or Four Vertically Stacked Waste Packages.	41
Figure 2-5-1. Low-Activity Waste/Supplemental Low-Activity Waste Nitrogen Balance in Kmol by Contributor.....	43
Figure 2-7-1. Sodium Ion Exchange Rate vs. Reciprocal Temperature for LAWABP1 Glass.....	48
Figure 2-7-2. Normalized Glass Dissolution Rate, Based on Boron, as a Function of pH(T) for LAWA44.....	49
Figure 2-7-3. Distribution of Fractional Dissolution Rates from the Applied Uncertainties for LAWA44 Glass.	55
Figure 2-7-4. Distribution of Fractional Dissolution Rates from the Applied Uncertainties for LAWC22 Glass.	56
Figure 2-7-5. Example of Principal Component Analysis of the Dilute Rate Model Parameters for a Borosilicate Glass.	58
Figure 2-7-6. Scatter Plot of Individually Varied Glass Components (in mass fractions) in the Statistically-Designed Glass Formulations Representative of the Enhanced Immobilized Low-Activity Waste Glass Compositional Region.	59
Figure 2-7-7. Scatterplot of 15 Glass Compositions for Which Sodium Ion Exchange Was Measured by Single-Pass Flow-Through (12 red full circles), by Single-Pass Flow-Through and Pulse Flow Test (3 black diamonds), and by Pulse Flow Test Only (3 blue triangles).	63
Figure 2-7-8. Images of the Field Lysimeter Test Facility a) Aerial Photograph of the Facility, b) Artist Three-Dimensional Drawing of the Facility, c) Depiction of the Layout of Buried Waste Forms and Sampling Devices Within a Single Lysimeter Tube, d) Photograph of the Lower Level of Buried Cementitious Waste Forms, and e) Photograph of the Underground Sampling Bay Showing the Two Rows of Lysimeter Tubes.....	65
Figure 2-9-1. PCT-B (static dissolution) Results (90 °C and S/V of 2,000 m ⁻¹) for the Ten Integrated Disposal Facility Glasses (Total available normalized boron release is 100 g/L at S/V of 2,000 m ⁻¹).....	74

Figure 2-9-2. PCT-B Results (40 °C and S/V of 2,000 m-1) for the Ten Integrated Disposal Facility Glasses (Total available normalized boron release is 100 g/L at S/V of 2,000 m⁻¹). 75

Figure 2-9-3. Scatter Plot of Individually Varied Glass Components (in mass fractions) in the Statistically-Designed Glass Formulations Representative of the Enhanced Immobilized Low-Activity Waste Glass Compositional Region. 76

Figure 2-9-4. Graphical Depiction of the Four Types of Responses Measured for Hanford Immobilized Low-Activity Waste Glasses Exposed to an Aqueous Solution and Seeded with Zeolite P2. 77

Figure 2-9-5. Ratio of Predicted Stage III Rates (from seeded tests) to Stage II Rates (using the rate prior to seeding) at 15 °C. 78

Figure 2-9-6. Images of the Field Lysimeter Test Facility a) Aerial Photograph of the Facility, b) Artist Three-Dimensional Drawing of the Facility, c) Depiction of the Layout of Buried Waste Forms and Sampling Devices Within a Single Lysimeter Tube, d) Photograph of the Lower Level of Buried Cementitious Waste Forms, and e) Photograph of the Underground Sampling Bay Showing the Two Rows of Lysimeter Tubes..... 79

Figure 2-14-1. Hanford South Geologic Framework Model Ringold E Well Control..... 93

Figure 2-14-2. Plan View Comparison of Central Plateau and Integrated Disposal Facility Geologic Framework Models at 114.5 Meters. 94

Figure 2-14-3. Ringold Formation Member of Wooded Island – Unit E Structure Elevation (feet) in 200 East Area with Extent Limiting Polygon in Orange. 105

Figure 2-14-4. Boreholes near the Integrated Disposal Facility Used to Develop Structural Contours of Hydrostratigraphic Unit Tops. 106

Figure 2-14-5. Location of Cross-Sections through the Central Plateau Vadose Zone Geologic Framework Model near the Integrated Disposal Facility..... 107

Figure 2-14-6. North-South Cross-Sections through the Central Plateau Vadose Zone Geologic Framework Model near the Integrated Disposal Facility, Section B (top) and Section C (bottom). 108

Figure 2-14-7. West-East Cross Sections of Central Plateau Vadose Zone Geologic Framework Model near the Integrated Disposal Facility, Section D (top) and Section E (bottom). 109

Figure 2-14-8. Saturated Thickness of the Cold Creek Gravel Unit near the Integrated Disposal Facility..... 110

Figure 2-14-9. Location of the High Conductivity Zone (Hanford Channel) Modeled in Central Plateau Groundwater Model Version 8.4.5 and Plateau to River Groundwater Model Version 8.3 and the Tank Closure and Waste Management Environmental Impact Statement..... 112

Figure 2-15-1. Fitted Log-Normal Distribution to the van Genuchten “Alpha” Parameter Data Set Used for the H2 Unit..... 116

Figure 2-15-2. Cumulative Distribution Function of Vertical Pore Velocity Assuming a Vertical Darcy Flux of 1.7 mm/yr. 120

Figure 2-15-3. Distribution of Predicted H2 Sand Volumetric Moisture Content for 200 Realizations of Uncertain Vadose Zone Property Sets..... 122

Figure 2-15-4. Cross-Plots of Predicted H2 Sand Volumetric Moisture Content versus Uncertain Vadose Zone Parameter Values for a Vertical Darcy Flux of 1.7 mm/yr..... 123

Figure 2-15-5. Comparison of Vadose Zone Hydraulic Parameter Sets for the H2 Sand. 126

Figure 2-15-6. Predicted Vertical Moisture Profile Under Integrated Disposal Facility for Different Hydraulic Parameter Sets..... 127

Figure 2-15-7. Calculated Moisture Content in the Middle of H2 Sand at 169-meter Elevation with Different Vadose Zone Hydraulic Parameter Sets and Background Infiltration Rates..... 129

Figure 2-15-8. Predicted H2 Sand Moisture Content for Uncertain Vadose Zone Hydraulic Parameter Values for Vertical Darcy Fluxes of 0.9 mm/yr and 100 mm/yr..... 136

Figure 2-15-9. Technetium-99 Breakthrough at Water Table from Solid Secondary Waste Sources for Different Vadose Zone Conceptual Models and Property Sets – Distributed Infiltration 3.5 mm/yr..... 140

Figure 2-15-10. Iodine-129 Breakthrough Curves for Cases Vzp00 and Vzp14 at Location of Peak Impact Along the 100-meter Buffer Boundary for Release from Immobilized Low-Activity Waste Glass and Solid Secondary Waste. 142

Figure 2-15-11. Iodine-129 Breakthrough Curves for Cases Vzp00 and Vzp04 at Location of Peak Impact Along the 100-meter Buffer Boundary for Release from Immobilized Low-Activity Waste Glass and Solid Secondary Waste. 143

Figure 2-15-12. Technetium-99 Breakthrough Curves for Cases Vzp00 and Vzp14 at Location of Peak Impact along the 100-meter Buffer Boundary for Release from Immobilized Low-Activity Waste Glass and Solid Secondary Waste..... 144

Figure 2-15-13. Technetium-99 Breakthrough Curves for Cases Vzp00 and Vzp04 at Location of Peak Impact along the 100-meter Buffer Boundary for Release from Immobilized Low-Activity Waste Glass and Solid Secondary Waste..... 145

Figure 2-16-1. Hanford Formation Hydraulic Conductivity Based on Slug Tests, Pumping Tests, and Groundwater Flow Models..... 150

Figure 2-16-2. Adjustments to the Hanford Channel Zonation in Layers 1, 2 and 3 of the Central Plateau Groundwater Model Version 8.4.5 in the 200 East Area of the Central Plateau (a) Initial, (b) Modified in Central Plateau Groundwater Model Version 8.4.5. 156

Figure 2-16-3. Location of the Hanford Channel Included Prior to and After Calibration of the Plateau to River (P2R) Groundwater Flow Model Version 8.2..... 157

Figure 2-16-4. Calibrated Hydraulic Conductivity of Hanford Channel – Plateau to River Groundwater Model Version 8.2. 158

Figure 2-16-5. Location of the High Conductivity Zone Analysis Area used in the Plateau to River Version 8.3..... 159

Figure 2-16-6. Calibrated Hydraulic Conductivity for Plateau to River Version 8.3 Model Layer 1.	160
Figure 2-16-7. Calibrated Hydraulic Conductivity for Plateau to River Version 8.3 Model Layer 2.	161
Figure 2-16-8. Calibrated Hydraulic Conductivity for Plateau to River Version 8.3 Model Layer 3.	162
Figure 2-16-9. Calibrated Hydraulic Conductivity for Plateau to River Version 8.3 Model Layer 4.	163
Figure 2-16-10. Calibrated Hydraulic Conductivity for Plateau to River Version 8.3 Model Layer 5.	164
Figure 2-16-11. Calibrated Transmissivity for Plateau to River Version 8.3.	165
Figure 2-17-1. Monthly Radionuclide Sum of Fractions for Vitrified Low-Activity Waste.	172
Figure 2-17-2. Monthly Radionuclide Sum of Fractions for Supplemental Vitrified Low-Activity Waste (after Direct Feed Low Activity Waste Mission).	173
Figure 2-18-1. Strontium-90 Inventory in All Waste Phases in the Best-Basis Inventory with Estimates of Sample Uncertainty.	179
Figure 2-18-2. Estimate of Strontium-90 Inventory Uncertainty in Supernate from Best-Basis Inventory Records.	181
Figure 2-19-1. Comparison of Laboratory Measured Effective Diffusion Coefficients for Iodine and Sodium.	187
Figure 2-19-2. Distribution of Iodine Apparent Diffusion Coefficients in Integrated Disposal Facility Performance Assessment Uncertainty Analysis.	188
Figure 2-19-3. Comparison of Fractional Release Rates to Vadose Zone from Solidified Liquid Secondary Waste for Background Infiltration Rates of 1.7 mm/yr: Iodine-129.	189
Figure 2-19-4. Comparison of Fractional Release Rates to Vadose Zone from Solidified Liquid Secondary Waste for Background Infiltration Rates of 3.5 mm/yr: Iodine-129.	190
Figure 2-19-5. System Model Development of the Diffusive Length in the Backfill near Packages of Liquid Secondary Waste: Iodine-129.	192
Figure 2-19-6. System Model Development of the Diffusive Length in the Backfill near Packages of Liquid Secondary Waste: Technetium-99.	193
Figure 2-20-1. Iodine-129 Release Rate to Vadose Zone from Carbon Adsorption Media: Solid Secondary Waste-Granular Activated Carbon Sensitivity Studies a) System Model, b) Process Model (fractional release rate).	201
Figure 2-20-2. Iodine-129 Cumulative Release to Vadose Zone from Solidified Carbon Adsorption Media: Solid Secondary Waste-Granular Activated Carbon Sensitivity Studies.	202
Figure 2-20-3. Iodine-129 Groundwater Concentration and Annual Dose Solidified Carbon Adsorption Media: Solid Secondary Waste-Granular Activated Carbon Sensitivity Studies.	203
Figure 2-21-1. Mix Design Worksheet for Hanford Grout Mix 5.	207

TABLE OF TABLES

Table 1-1-1. Values from Table 6-7 of RPP-RPT-57991.....	9
Table 1-2-1. Radionuclide Content in Supernate, Saltcake, Sludge and Vitrified Low-Activity Waste.....	12
Table 1-2-2. Radionuclides in Others of Table 1-2.1.	14
Table 1-2-3. Run Case 7 Radionuclides.	15
Table 2-7-1. Summary of Rate Law Parameters for LD6-5412, LAWABP1, LAWA44, LAWB45, and LAWC22 at 15 °C.	50
Table 2-8-1. Summary of Studies Examining Surface Area Increases Due to Thermal Fracturing.	70
Table 2-14-1. Evolution of Geologic Framework Models in the Vicinity of the Integrated Disposal Facility.....	96
Table 2-14-2. Formation Tops and Elevations in Boreholes near the Integrated Disposal Facility.....	103
Table 2-15-1. van Genuchten-Mualem Parameter Values used for Base Case and Sensitivity Analyses.	121
Table 2-15-2. H2 Sand Moisture Content Data in Boreholes Drilled near the Integrated Disposal Facility.....	134
Table 2-15-3. Comparison of Vadose Zone Hydraulic Parameter Realizations with Lowest Predicted Moisture Contents for Best-Estimate Undisturbed and Disturbed Recharge Rates.....	137
Table 2-15-4. Predicted Moisture Content in the H2 Sand for Different Vadose Zone Hydraulic Property Sets and Recharge Rates.....	139
Table 2-15-5. Comparison of Peak Groundwater Concentration for Base Case (Vzp00) and Alternative Vadose Zone Hydraulic Property Set (Vzp04 and Vzp14).....	146

LIST OF TERMS

Acronyms and Abbreviations

2D	two dimensional
3D	three-dimensional
ADT	Advective-Diffusive Transport
asl	above sea level
BBI	Best-Basis Inventory
CA	composite analysis
CAB	carbon adsorber bed
CCU	Cold Creek Unit
CCUg	CCU gravel unit
CDF	Cumulative Distribution Function
CERCLA	<i>Comprehensive Environmental Response, Compensation, and Liability Act of 1980</i>
CFR	<i>Code of Federal Regulations</i>
CHEM	Chemical
CHPRC	CH2M HILL Plateau Remediation Company
COPC	constituent of potential concern
CPGWM	Central Plateau Groundwater Model
CPM	Central Plateau Model/Central Plateau Groundwater flow model
CPVZ	Central Plateau Vadose Zone
Cs	cesium
CST	crystalline silicotitanate
CY	calendar year
DFLAW	Direct-Feed Low-Activity Waste
DIW	de-ionized water
DOE	U.S. Department of Energy
DOE M	DOE Manual
DOE O	DOE Order
ECF	environmental calculation file
EIS	Environmental Impact Statement
EMF	Effluent Management Facility
ERDF	Environmental Restoration Disposal Facility
ETF	Effluent Treatment Facility
EWG	enhanced waste glass
FFTF	Fast Flux Test Facility
FLTF	Field Lysimeter Test Facility
FY	fiscal year
GAC	granular activated carbon
GFM	geologic framework model
GWB	GeoChemists Workbench [®]
HCZ	high conductivity zone
H2	Hanford formation sand unit
H3/Hf3	Hanford formation gravel unit

HEIS	Hanford Environmental Information System
HEPA	high-efficiency particulate air
HLW	high-level radioactive waste
HMS	Hanford Meteorological Station
HSU	hydrostratigraphic unit
HTWOS	Hanford Tank Waste Operations Simulator
I	iodine
IDF	Integrated Disposal Facility
IDF PA	RPP-RPT-59958, <i>Performance Assessment for the Integrated Disposal Facility, Hanford Site, Washington</i>
ILAW	immobilized low-activity waste (synonymous with VLAW)
IX	ion exchange
LAW	low-activity waste or Low-Activity Waste Vitrification Facility
LDR	Land Disposal Restrictions
LERF	Liquid Effluent Retention Facility
LFRG	Low-Level Waste Disposal Facility Federal Review Group
LLW	low-level radioactive waste
LSW	liquid secondary waste
MCL	maximum contaminant level
MDA	moisture-dependent anisotropy
NRC	U.S. Nuclear Regulatory Commission
ORP	DOE Office of River Protection
OU	operable unit
P2R	Plateau to River Groundwater Model
PA	Performance Assessment
PA-TCT	power averaged tensorial-connectivity-tortuosity
PCT	product consistency test
PNNL	Pacific Northwest National Laboratory
PT	Pretreatment
RAI	request for additional information
RCRA	<i>Resource Conservation and Recovery Act of 1976</i>
RL	DOE Richland Operations Office
RLD	Radioactive Liquid Waste Disposal
Rtf	Ringold Taylor Flats unit
Rwie	Ringold Unit E
RWMB	Radioactive Waste Management Basis
SBS	submerged bed scrubber
SCR	selective catalytic reducer
SMRN	secondary mineral reaction network
SPFT	single-pass flow-through
SRCA	Stirred Reactor Coupon Analysis
Sr	strontium
SSW	solid secondary waste
STLP	Supplemental Treated LAW Evaporation Process
TBR	WHC-SD-WM-TI-699, <i>Technical Basis for Classification of Low-Activity Waste Fraction from Hanford Site Tanks</i>

Tc	technetium
TC&WM EIS	Tank Closure and Waste Management Environmental Impact Statement
TED	total effective dose
TLP	Treated LAW Evaporation Process
TSCR	Tank-Side Cesium Removal
TST	transition-state theory
U.S.	United States
VLAW	vitrified low-activity waste (synonymous with ILAW)
VSL	Vitreous State Laboratory
WAC	Waste Acceptance Criteria
WESP	wet electrostatic precipitator
WIR	Waste Incidental to Reprocessing
WMA	Waste Management Area
WTP	Hanford Tank Waste Treatment and Immobilization Plant; Waste Treatment Plant
VZPW	vadose zone pore water

Units

µg	microgram
Ci	curie
cm	centimeter
ft	foot
ft ²	square foot
ft ³	cubic foot
g	gram
gal	gallon
in	inch
kg	kilogram
km	kilometer
L	liter
m	meter
m ³	cubic meter
mrem	millirem
nCi	nanocurie
pCi	picocurie
psi	pounds per square inch
psig	pounds per square inch gauge pressure
yr	year

1.0 INTRODUCTION

In accordance with DOE Order (O) 435.1, *Radioactive Waste Management* and its accompanying manual, DOE Manual (M) 435.1-1, *Radioactive Waste Management Manual*, the United States (U.S.) Department of Energy (DOE) manages radioactive waste in a manner that protects the public, workers and the environment, and that complies with applicable federal, state and local laws. Certain waste resulting from reprocessing of spent nuclear fuel that is incidental to reprocessing is not high-level radioactive waste (HLW) and is managed in accordance with the requirements for low-level radioactive waste (LLW). In April 2020, DOE issued the *Draft Waste Incidental to Reprocessing Evaluation for Vitrified Low-Activity Waste Disposed Onsite at the Hanford Site, Washington* (herein referred to as the Draft WIR Evaluation) (DOE/ORP-2020-01).

By means of an interagency agreement between DOE and the U.S. Nuclear Regulatory Commission (NRC), NRC is conducting a consultative technical review of DOE's Draft WIR Evaluation. Prior to preparation of the Draft WIR Evaluation, DOE prepared the *Performance Assessment for the Integrated Disposal Facility, Hanford Site, Washington* (herein referred to as the IDF PA) (RPP-RPT-59958), which is a technical reference document for the Draft WIR Evaluation. The IDF PA has undergone independent review by DOE's Low Level Waste Disposal Facility Review Group (LFRG). DOE also engaged in extensive discussions and scoping meetings, including discussions with states and Tribal Nations, regarding the fundamental technical bases, approaches, and key parameter values to be used in developing the IDF PA. The IDF PA was issued in 2019, and the Draft WIR Evaluation was subsequently issued for NRC consultation and comments by states, Tribal Nations, and the public in April 2020.

The DOE and the NRC staff have engaged in a series of public meetings to clarify the approaches and rationales documented in the Draft WIR Evaluation and IDF PA. DOE, NRC and Washington River Protection Solutions, LLC, participated in public meetings that were held on September 28 and October 6, 2020 to review and get clarifications on the NRC List of Topics that was provided regarding potential questions on the Draft WIR Evaluation. On November 6, 2020, NRC staff submitted requests for additional information (RAIs) (External letter "Request for Additional Information on the Draft Waste Incidental to Reprocessing Evaluation for Vitrified Low-Activity Waste Disposed Onsite at the Hanford Site, Washington" [NRC 2020]).

This document provides DOE's responses to many of the NRC RAIs, to facilitate NRC's completion of a Technical Evaluation Report (TER) on the Draft WIR Evaluation. For each of the 26 RAIs, the NRC comment, basis information, and proposed path forward is quoted directly as received from NRC (with minor typographical corrections, and the addition of 508 compliant graphics explanations). These are followed by DOE's technical response to many of the RAIs. For others, DOE's response will be provided in Revision 1 of this document. The topics discussed herein are technical in nature. The RAIs and responses are part of the ongoing interaction between DOE and NRC staff regarding the review of the Draft WIR Evaluation and its references, including the IDF PA, and can only be understood in that context; a working knowledge of those documents is assumed.

The RAIs were organized by NRC according to the three criteria contained in DOE Manual (M) 435.1-1, Section II.B(2)(a). Those criteria provide, in relevant part, that the wastes:

- “(1) Have been processed, or will be processed, to remove key radionuclides to the maximum extent that is technically and economically practical; and
- (2) Will be managed to meet safety requirements comparable to the performance objectives set out in 10 CFR 61 Subpart C, *Performance Objectives*; and
- (3) Are to be managed, pursuant to DOE’s authority under the *Atomic Energy Act of 1954*, as amended, and in accordance with the provisions of Chapter IV of this Manual [*DOE M 435.1-1*], provided the waste will be incorporated in a solid physical form at a concentration that does not exceed the applicable concentration limits for Class C low-level waste as set out in 10 CFR 61.55, *Waste Classification*[.]”

The RAI responses are organized according to applicable categories based upon these criteria, as presented in Sections 3.0, 4.0, and 5.0 below.

2.0 NRC'S INTRODUCTORY STATEMENT IN THE REQUEST FOR ADDITIONAL INFORMATION RELATED TO SECONDARY WASTE

NRC's Introductory Statement in the Request for Additional Information Related to Secondary Waste

NRC stated in the last paragraph on page 1 and continuing onto page 2 of the Request for Additional Information (RAI), under "Structure of Comments": "DOE indicated that the scope for the VLAW draft waste incidental to reprocessing (WIR) evaluation was limited to vitrified waste generated as part of the Direct Feed Low Activity Waste (DFLAW) process (DOE-ORP-2020-01, 2020). Secondary solid wastes (SSW) generated by the process were not within the scope of the draft waste evaluation though those secondary wastes were evaluated in the PA as they would be disposed in the same facility as the VLAW. NRC evaluated the scope of the evaluation in the acceptance review and determined that the DOE approach was not consistent with the intent of the incidental waste process. DOE's election of vitrification as the primary waste production process results in some key radionuclides that are volatilized and effectively separated from the waste (e.g., ¹²⁹I), or are removed in other processing steps. If the majority of that activity that is separated or removed will be disposed in near-surface disposal (i.e., as other than high-level waste), then the resulting waste forms and waste streams are within the scope of the draft waste evaluation, especially for DOE M 435.1-1 Criterion 2 as the key radionuclides drive the long-term risk for the disposal. As a result, NRC has included secondary SSW within the scope of the review."

DOE Response to NRC's Introductory Statement Related to Secondary Waste

Because several of the NRC's RAIs involve secondary waste, DOE is providing the following comments and observations here as a matter of convenience, to avoid repeating the same information in the applicable RAI responses. As NRC notes, the scope of the *Draft Waste Incidental to Reprocessing Evaluation for Vitrified Low-Activity Waste Disposed Onsite at the Hanford Site* (Draft WIR Evaluation) focuses on the separated, pretreated and vitrified low activity waste (VLAW). DOE has not included other wastes, including solid secondary waste (SSW), within the scope of the Draft WIR Evaluation.

As background, the Hanford Site currently stores radioactive waste in underground storage tanks. The waste was generated, in part, by the prior reprocessing of spent nuclear fuel. DOE is retrieving waste from the Hanford tanks, and has decided to separate the tank waste into a low-activity waste stream and a high-level radioactive waste stream.¹

The Draft WIR Evaluation concerns the low-activity waste from some of the Hanford tanks. For the low-activity waste at issue in the Draft WIR Evaluation, DOE has decided to use the direct-feed low-activity waste (DFLAW) pretreatment approach.² The DFLAW pretreatment approach is a two-phased approach (Phase 1 and Phase 2, described below) that will separate and pretreat

¹ See "Record of Decision: Final Tank Closure and Waste Management Environmental Impact Statement for the Hanford Site, Richland, Washington", 78 FR 75913 (Dec. 31, 2013).

² See "Amended Record of Decision for the Direct-Feed Low-Activity Waste Approach at the Hanford Site, Washington", 84 FR 424 (Jan. 28, 2019).

supernate (essentially the upper-most layer of tank waste that contains low concentrations of long-lived radionuclides) from the applicable tanks.

The DFLAW pretreatment approach will entail in-tank settling, decanting, filtration, and cesium ion exchange removal, using the Tank Side Cesium Removal (TSCR) System for Phase 1 and either a second TSCR unit or a filtration and cesium removal facility for Phase 2. As explained in the Draft WIR Evaluation, the DFLAW pretreatment process will remove over 99% of the cesium, as well as other key radionuclides. After pretreatment using the DFLAW approach, the resulting, pretreated waste stream – called Low Activity Waste or LAW-- will be vitrified in the Low Activity Waste Vitrification Facility.³ LAW from which key radionuclides have been removed to the maximum extent technically and economically practical during the pretreatment process, will be managed and disposed of as LLW, subject to the analysis and commitments of the Final WIR Evaluation and WIR Determination. The vitrified LAW (also called VLAW) will meet the performance objectives and measures for LLW disposal, as demonstrated in the Draft WIR Evaluation,⁴ and be disposed of in the Integrated Disposal Facility (IDF).

During vitrification of the LAW, some radionuclides, including ⁹⁹Tc and ¹²⁹I, will volatilize. The LAW Vitrification Facility will, by design, maximize the capture of the volatilized ⁹⁹Tc and ¹²⁹I into the VLAW. Since the completion of the *Performance Assessment for the Integrated Disposal Facility, Hanford Site, Washington* (IDF PA), the latest flowsheet modeling shows that approximately 98% of the ⁹⁹Tc and approximately 96% of the ¹²⁹I will be captured into the VLAW, and approximately 99% of all radioactivity in the pretreated LAW will be incorporated into the VLAW.⁵ In sum, the vast majority of all radionuclides in the LAW, including ⁹⁹Tc and ¹²⁹I, will be captured in the VLAW and will not be entrained in secondary waste.

The SSW and other secondary solid waste⁶ – including HEPA filters, carbon bed adsorbers, a submerged bed scrubber, a wet electrostatic precipitator, and certain solidified evaporator waste -

³ The LAW will meet the waste acceptance criteria for the Low Activity Waste Vitrification Facility, which has been designed to meet the applicable requirements in DOE regulations, Orders and standards.

⁴ In addition, the VLAW will be in a solid physical form that does not exceed Class C LLW concentrations, as shown in Section 6 of the Draft WIR Evaluation.

⁵ The latest flowsheet modeling discussed above, RPP-RPT-57991, 2019, *One System River Protection Project Integrated Flowsheet*, Revision 3, Washington River Protection Solutions, LLC, Richland, Washington and MR-50461 - 00, *2019 Flowsheet Integration Joint Scenarios*, were prepared after the IDF PA and will be appropriately considered as part of maintenance of the IDF PA. ³H and ¹⁴C are volatile radionuclides which will not be captured in the VLAW and are considered in the IDF PA to the extent those radionuclides are entrained in secondary waste. It bears emphasizing that after pretreatment using the DFLAW approach, the pretreated LAW stream will contain approximately 1% of the radioactivity from the applicable tank waste, and the VLAW will capture approximately 99% of all radioactivity in the pretreated LAW. See e.g., responses to RAIs 1-2, 2-1, 2-10 and 2-17.

The response to RAI 2-17 compares the revised VLAW inventory (based on the latest flowsheet modeling) to the disposal concentration limits developed to protect an inadvertent intruder (IDF-00002, *Waste Acceptance Criteria for the Integrated Disposal Facility*, Table G-1). The evaluation demonstrates that the updated VLAW inventory will meet DOE's performance measures for inadvertent intrusion into the VLAW.

⁶ SSW, which is discussed in the Draft WIR Evaluation for additional background information, is radioactive solid waste derived from Waste Treatment Plant (WTP) operations and will include a wide variety of wastes from routine maintenance activities, non-routine maintenance activities, and day-to-day operating activities. The SSW includes carbon bed adsorbers and HEPA filters generated by the off gas system at the LAW Vitrification Facility, as well as Effluent Treatment Facility-Generated (ETF- Generated) SSW. For additional information, and as

- will be generated by, or derived from, the off gas system associated with the vitrification of the pretreated LAW. Importantly, after pretreatment using the DFLAW approach, the pretreated LAW stream will contain approximately 1% of the radioactivity from the applicable tank waste, and the VLAW will capture approximately 99% of all radioactivity in the pretreated LAW.⁷ Otherwise put, the relevant secondary wastes, in combination, will contain approximately 1% of 1% (.0001) of the radioactivity initially in the reprocessing waste from the applicable tanks.

If DOE issues a Final WIR Evaluation and WIR Determination in the future, then the pretreated LAW—from which key radionuclides will have been removed to the maximum extent technically and economically practical – may be appropriately managed and disposed of as LLW, subject to the analysis and commitments of the Final WIR Evaluation and WIR Determination. Secondary waste generated from processes associated with further treatment, stabilization, solidification, storage, transport or disposal of this pretreated LAW must necessarily continue to be managed and disposed of as LLW and cannot be considered HLW.⁸ This secondary waste can be disposed of in the IDF, if it is properly characterized and meets the waste acceptance criteria (WAC)⁹ for the IDF, including radionuclide concentration limits to ensure protection of a hypothetical inadvertent intruder.¹⁰

DOE notes that the IDF PA correctly includes SSW because SSW is planned to be disposed of at IDF. This does not mean, however, that the SSW should be included within the scope of the Draft WIR Evaluation.

Several of NRC’s RAIs pertain to secondary waste. DOE has responded to such RAIs to provide additional information and clarification.

described in sections 2.5.1.4 and 2.5.3 and in footnotes 33 and 40 of the Draft WIR Evaluation, the liquid off-gas system condensate generated by the LAW Vitrification Facility will be sent to the Effluent Management Facility, where evaporator liquid concentrate will be recycled to the LAW stream for vitrification and the evaporator overheads will be sent to ETF, which in turn will generate treated and solidified ETF liquid secondary waste (ETF-LSW). For convenience here, the above-mentioned wastes are collectively referred to as secondary waste, except as otherwise noted. The secondary waste will be properly characterized and classified prior to disposal, and must meet the waste acceptance criteria for the disposal facility (currently planned as the IDF).

⁷ See e.g., responses to RAIs 1-2, 2-1, 2-10 and 2-17.

⁸ DOE has previously determined that such secondary waste is not HLW. The citation WIR determinations for Hanford, DOE-ORP-PPD-EM-50168 Waste Incidental to Reprocessing Determinations, Revision 2 (Dec. 9, 2020), encompassed secondary waste, and explained that such waste is not from the reprocessing of spent nuclear fuel. Alternatively, a citation WIR could be based on the factual situation that the relevant secondary wastes, in combination, will contain approximately 1% of 1% (.0001) of the radioactivity initially in the reprocessing waste from the applicable tanks as explained above, and thus such waste is akin to “contaminated job wastes including laboratory items such as clothing, tools, and equipment” described in Chapter II.B.(1) of DOE Manual 435.1-1 concerning citation WIR determinations. Under either approach, the result is the same: the secondary waste is not HLW.

⁹ IDF-00002, 2019, *Waste Acceptance Criteria for the Integrated Disposal Facility*, Rev. 0, CH2M HILL Plateau Remediation Company, Richland, Washington.

¹⁰ As demonstrated in the IDF PA base case, potential doses attributable to secondary waste will be well-below the performance objectives and performance measures for LLW disposal. See also the response to RAI 2-17.

3.0 REMOVAL OF KEY RADIONUCLIDES TO THE MAXIMUM EXTENT PRACTICAL

RAI 1-1 (Removal of ⁹⁰Sr to the Maximum Extent Practicable)

Comment

Additional information is needed on the amount of soluble ⁹⁰Sr expected to be in the waste processed for Direct-Feed Low-Activity Waste (DFLAW) and the technologies that may be used to remove it to the maximum extent practical.

Basis

In the draft WIR evaluation, DOE states that most of the ⁹⁰Sr is insoluble but strontium can be soluble in some tanks with higher organic concentrations. Tanks with soluble ⁹⁰Sr are not currently planned to be part of the DFLAW campaigns and therefore are not discussed in the draft WIR evaluation. DOE indicated there would likely be a separate WIR evaluation for the tanks beyond DFLAW. However, in the draft WIR evaluation, DOE stated that the Integrated Disposal Facility (IDF) PA includes VLAW from tanks with soluble ⁹⁰Sr (see footnote 51). The NRC is reviewing the total risk from the disposal of waste in the IDF, including the potential for soluble ⁹⁰Sr to be part of the inventory for IDF, as within the scope of this evaluation, and therefore is requesting additional information on what amount of soluble ⁹⁰Sr is expected in the tanks and the technologies that may be used to remove soluble ⁹⁰Sr to the maximum extent practical.

Table 3-29 of the PA document¹¹ shows that nearly 100% of the ⁹⁰Sr is assumed to remain in the high-level waste (HLW) (i.e., not listed as waste going to IDF) under Case 7, 8B, 9, 10A, and 10B. It is unclear if any of these cases include the processing of the tanks with the soluble ⁹⁰Sr waste.

Waste Form	Case 7	Case 8B	Case 9	Case 10A	Case 10B
Non-IDF (HLW)	99.46%	99.61%	99.71%	99.54%	99.63%
ILAW Glass	0.54%	0.39%	0.29%	0.45%	0.36%
LAW Melters	0.00%	0.00%	0.00%	0.00%	0.00%
ETF-Generated Secondary Solid Waste	0.00%	0.00%	0.00%	0.00%	0.00%
Secondary Solid Waste	0.00%	0.00%	0.00%	0.00%	0.00%
IDF Total	0.54%	0.39%	0.29%	0.46%	0.37%

Path Forward

Please provide additional information on what percentage of the ⁹⁰Sr is estimated to be soluble versus insoluble in the tanks. Please provide additional basis for what percentage of the soluble ⁹⁰Sr DOE estimates can be extracted using the ion exchange columns, or other technologies planned to be used.

¹¹ The PA document is RPP-RPT-59958 Rev. 1, Performance Assessment for the Integrated Disposal Facility, Hanford Site, Washington, Department of Energy, Richland, WA, August 2018. The PA consists of computer files (models) as well as a supporting document.

DOE Response

In the total inventory of tank waste stored in the Hanford Tank Farms single-shell and double-shell tanks, it is estimated that 4% of the ^{90}Sr is soluble (demonstrated in “Calculation” below). Under the DFLAW approach, nearly all of the ^{90}Sr that is not soluble is expected to be removed from the tank waste via the settle and decant process combined with the filter within the Tank Side Cesium Removal (TSCR) unit for Phase 1, and either a second TSCR unit or a filtration and cesium removal facility for Phase 2. With respect to soluble ^{90}Sr , process modeling in support of the IDF PA and the VLAW WIR, (described in RPP-ENV-58562, *Inventory Data Package for the Integrated Disposal Facility Performance Assessment* and RPP-RPT-57991, *River Protection Project Integrated Flowsheet*, respectively) conservatively assumed that all soluble ^{90}Sr present in staged DFLAW campaigns (19% of the total tank farms soluble ^{90}Sr , or less than 1% of the total tank farms inventory of ^{90}Sr) would remain in the DFLAW feed. However, there is recent laboratory data showing that almost all of the soluble ^{90}Sr will be removed by the crystalline silicotitanate (CST) within the TSCR unit (PNNL-28945, *Characterization of Cs-Loaded CST Used for Treatment of Hanford Tank Waste in Support of Tank-Side Cesium Removal*). Nevertheless, to bound the analysis, DOE assumed no ^{90}Sr is removed by CST ion exchange.

DOE intends to characterize the amount of ^{90}Sr in the low-activity waste (LAW) feed/VLAW after startup by sampling and analyzing every batch received in the LAW Vitrification Facility concentrate receipt vessels (24590-LAW-PL-PENG-17-0001, *ILAW Product Compliance Plan*) and tracking it through the vitrification process. Characterization of strontium in the LAW feed will be used to reduce the conservatism in the assumption that CST does not remove ^{90}Sr .

Furthermore, each waste package destined for the IDF will have a certified waste profile that is prepared by the waste generator. The radionuclide concentrations in the shipment cannot exceed the concentrations in the certified waste profile. The IDF waste acceptance team will review the certified waste profile to ensure each profile meets the requirements in the IDF Waste Acceptance Criteria (WAC) (IDF-00002, *Waste Acceptance Criteria for the Integrated Disposal Facility*). Annually, the IDF will prepare a report that summarizes waste receipts from the past fiscal year together with all past receipts (DOE M 435.1-1). The intent is to compare actual waste receipt volumes and inventories to the volume and activity levels evaluated in the IDF PA to ensure the continued adequacy of the PA and also provide an indication for the remaining capacity (volume and/or activity) of the IDF.

DOE plans to track the radionuclides, including strontium, in the VLAW, as well as other wastes, disposed of at the IDF to provide information for future closure of the IDF, including updated PA analyses. Prior to IDF closure, a revision to the IDF PA, using data provided by the LAW Vitrification Facility and other waste generators, will evaluate whether there is reasonable expectation that the performance objectives and performance measures are met for protection of the member of the public and inadvertent intruder from dose consequences from ^{90}Sr and other radionuclides in the VLAW, as well as all other waste streams, disposed of in the IDF.

Calculation

The amount of soluble strontium, and insoluble strontium present in the Hanford tank waste was estimated using data directly from RPP-RPT-57991. Due to the assumptions used in the flowsheet, explained in the response to RAI 1-1, all soluble strontium present in the Hanford Tank Farms is assumed to be routed as feed to the LAW Vitrification Facility¹² and assumed supplemental LAW¹³ treatment facilities, and all insoluble strontium is routed as feed to the HLW Vitrification Facility during the full-scale mission. Thus, the concentration information for ⁹⁰Sr, combined with the stream volume for the representative streams from Table 6-7 of RPP-RPT-57991, can be used to calculate the percentage of soluble ⁹⁰Sr in the tank waste, as demonstrated below:

$$\begin{aligned}
 \text{Total soluble } ^{90}\text{Sr inventory (Ci)} &= \left[C_{28}^{90\text{Sr}} \left(\frac{\text{Ci}}{\text{L}} \right) * V_{28}(\text{gal}) + C_{41}^{90\text{Sr}} \left(\frac{\text{Ci}}{\text{L}} \right) * V_{41}(\text{gal}) + C_{45}^{90\text{Sr}} \left(\frac{\text{Ci}}{\text{L}} \right) * V_{45}(\text{gal}) \right. \\
 &\quad \left. + C_{46}^{90\text{Sr}} \left(\frac{\text{Ci}}{\text{L}} \right) * V_{46}(\text{gal}) \right] * 3.785 \left(\frac{\text{L}}{\text{gal}} \right) = 8.2E + 05 \text{ Ci} \\
 \text{Total insoluble } ^{90}\text{Sr inventory (Ci)} &= \left[C_{35}^{90\text{Sr}} \left(\frac{\text{Ci}}{\text{L}} \right) * V_{35}(\text{gal}) \right] * 3.785 \left(\frac{\text{L}}{\text{gal}} \right) \\
 &= 1.9E + 07 \text{ Ci} \\
 \% \text{ soluble } ^{90}\text{Sr} &= \frac{\text{Total soluble } ^{90}\text{Sr inventory}}{\left(\text{Total soluble } ^{90}\text{Sr inventory} + \text{Total insoluble } ^{90}\text{Sr inventory} \right)} \\
 &= 4\%
 \end{aligned}$$

where,

$C_X^{90\text{Sr}}$ = concentration of ⁹⁰Sr in stream X, Ci/L

V_X = total volume of stream X, gal

X = Stream number from Table 6-7 of RPP-RPT-57991

¹² Vitrification at the Hanford Tank Waste Treatment and Immobilization Plant (WTP) LAW Vitrification Facility includes DFLAW operations as well as vitrification in the WTP LAW Vitrification Facility following pre-treatment at the WTP Pre-Treatment Facility after the DFLAW mission is completed. Vitrification in the WTP LAW Vitrification Facility following the DFLAW mission is provided for additional information and completeness, and is outside the scope of the Draft WIR Evaluation.

¹³ Information concerning supplemental LAW is provided in this RAI response for additional information and completeness, and is outside the scope of both the Draft WIR Evaluation and DOE decisions concerning supplemental LAW treatment. DOE has not made decisions concerning the potential path forward for supplemental LAW treatment, as explained in footnote 7 of the Draft WIR Evaluation and 78 FR 75913, "Record of Decision: Final Tank Closure and Waste Management Environmental Impact Statement for the Hanford Site, Richland, Washington." As explained in section 1.2 of the Draft WIR Evaluation, the Draft WIR Evaluation does not address or include in its scope supplemental LAW. To bound the IDF PA analysis, the IDF PA assumed that supplemental LAW may potentially be vitrified and disposed of in the IDF, although, as explained above, DOE has made no decisions concerning the potential path forward for supplemental LAW treatment.

Table 1-1-1. Values from Table 6-7 of RPP-RPT-57991.

	Stream Number, X				
	28 ^a	35 ^b	41 ^c	45 ^d	46 ^e
C_x^{90Sr} (Ci/L)	2.00E-03	3.17E-01	1.45E-03	1.50E-03	1.59E-03
V_x (gal)	2.35E+07	1.54E+07	6.33E+07	3.00E+07	2.06E+07

^a Stream 28 represents the treated low-activity waste (LAW) waste stream sent to the LAW Vitrification Facility, used during the Direct-Feed Low-Activity Waste mission. This stream contains only soluble ⁹⁰Sr.

^b Stream 35 represents the treated high-level radioactive waste (HLW) waste stream sent from the Hanford Tank Waste Treatment and Immobilization Plant (WTP) Pretreatment facility to the HLW Vitrification Facility. This stream contains only ⁹⁰Sr that is not soluble.

^c Stream 41 represents the treated LAW waste stream sent from the WTP Pretreatment facility to the LAW Vitrification Facility. This stream contains only soluble ⁹⁰Sr.

^d Stream 45 represents the treated LAW waste stream sent from the WTP Pretreatment facility to the potential supplemental LAW facility (see footnote 12). This stream contains only soluble ⁹⁰Sr.

^e Stream 46 represents the treated LAW waste stream sent to the potential supplemental LAW facility (see footnote 12). This stream contains only soluble ⁹⁰Sr.

Reference: RPP-RPT-57991, *River Protection Project Integrated Flowsheet*.

References

- 78 FR 75913, 2013, “Record of Decision: Final Tank Closure and Waste Management Environmental Impact Statement for the Hanford Site, Richland, Washington,” *Federal Register*, Vol. 78, pp. 75913–75919 (December 13).
- 24590-LAW-PL-PENG-17-0001, 2021, *ILAW Product Compliance Plan*, Rev. 2, Bechtel, River Protection Project Waste Treatment Plant, Richland, Washington.
- DOE M 435.1-1, 2011, *Radioactive Waste Management Manual*, Change 2, U.S. Department of Energy, Washington, D.C.
- IDF-00002, 2019, *Waste Acceptance Criteria for the Integrated Disposal Facility*, Rev. 0, CH2M HILL Plateau Remediation Company, Richland, Washington.
- PNNL-28945, 2019, *Characterization of Cs-Loaded CST Used for Treatment of Hanford Tank Waste in Support of Tank-Side Cesium Removal*, RPT-TCT-005, Rev. 0, Pacific Northwest National Laboratory, Richland, Washington.
- RPP-ENV-58562, 2016, *Inventory Data Package for the Integrated Disposal Facility Performance Assessment*, Rev. 3, Washington River Protection Solutions, LLC, Richland, Washington.
- RPP-RPT-57991, 2019, *River Protection Project Integrated Flowsheet*, 24590-WTP-RPT-MGT-14-023, Rev. 3, Washington River Protection Solutions, LLC, Richland, Washington.
- RPP-RPT-59958, 2018, *Performance Assessment for the Integrated Disposal Facility, Hanford Site*, Rev. 1, Washington, Department of Energy, Richland, Washington.

RAI 1-2 (Percentage of Key Radionuclide Removal)

Comment

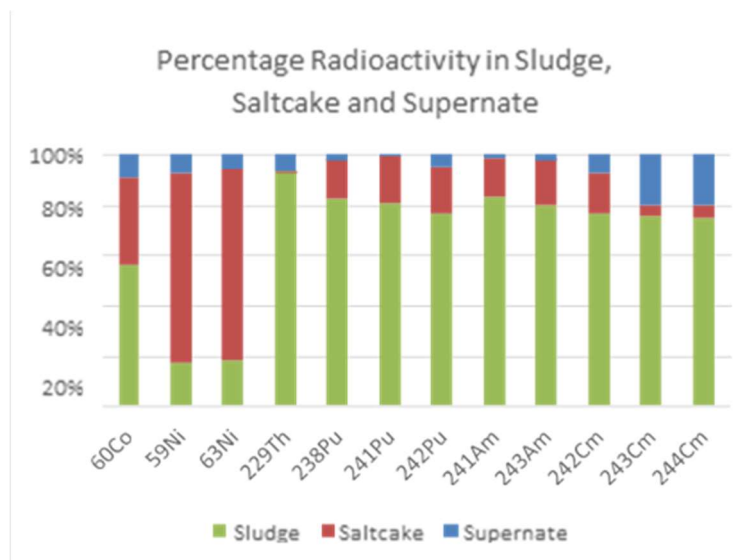
Additional information is needed on the percentage of key radionuclides removed from the waste that will be disposed in the integrated disposal facility.

Basis

Table 3-29 in the PA document lists the wastefrom distributions resulting from the five cases considered to potentially be disposed of in IDF for 11 of the 25 key radionuclides identified by DOE. The 14 key radionuclides that are not listed in Table 3-29 are ^{60}Co , ^{59}Ni , ^{63}Ni , ^{228}Rn , ^{229}Th , ^{232}Th , ^{238}Pu , ^{241}Pu , ^{242}Pu , ^{241}Am , ^{243}Am , ^{242}Cm , ^{243}Cm , ^{244}Cm . (Note that ^{233}U and ^{235}U are listed in Table 3-29 but they are not listed as a key radionuclide in the draft WIR evaluation.)

In Table 2-3 of the draft WIR evaluation DOE lists the estimated total radioactivity in the 177 underground waste tanks, broken down by how much radioactivity is in the supernate, saltcake, and sludge for certain radionuclides (Note that key radionuclides ^{228}Rn , ^{232}Th are not listed in Table 2-3 of the draft WIR evaluation). For 12 of the 14 key radionuclides that are not listed in Table 3-29, Table 2-3 of the draft WIR evaluation shows that there is some percentage of these radionuclides that remains in the supernate or saltcake. For example, more than 80% of the ^{59}Ni and ^{63}Ni is in the saltcake or supernate, and about 45% of the ^{60}Co is in the saltcake or supernate. About 20-25% of the ^{238}Pu , ^{241}Pu , ^{242}Pu , ^{241}Am , ^{243}Am , ^{242}Cm , ^{243}Cm , and ^{244}Cm are not in the sludge. In the draft WIR evaluation, DOE states that ^{59}Ni is present in very low concentrations in the vitrified LAW and is an insignificant contributor to dose after IDF closure. However, it is unclear what percentage of these radionuclides may be present in the various waste forms that will be disposed of at IDF and what was removed by processing.

Figure 1-2-1. Data from Table 2-3 in the Draft Waste Incidental to Reprocessing Evaluation.



Path Forward

Please provide the percentages of key radionuclides removed for those key radionuclides (see Table 4-3 of the draft WIR evaluation) that are not already included in Table 3-29.

DOE Response

Table 4-3 in the Draft WIR Evaluation identifies key radionuclides. The second and third columns of Table 4-3 identify as key radionuclides those radionuclides listed in Title 10, *Code of Federal Regulations* (CFR), Part 61, “Licensing Requirements for Land Disposal of Radioactive Waste,” Subpart D—Technical Requirements for Land Disposal Facilities, §61.55, “Waste Classification” (10 CFR 61.55)¹⁴, and the last column identifies those radionuclides important to the IDF PA (RPP-RPT-59958)¹⁵.

The DFLAW approach is currently planned for waste from tanks without significant soluble ⁹⁰Sr, as explained in the Draft WIR Evaluation in footnote 51. For the applicable tanks, the DFLAW pretreatment approach will use settling, decanting, filtration and ion exchange, which will remove over 99% of the ¹³⁷Cs as well as other key radionuclides, as shown in the Draft WIR Evaluation Section 4 and Table 1-2-1 below.

The curies in the supernate, saltcake, sum of saltcake and supernate, and sludge in the applicable tanks are identified in Columns 1, 2, 3 and 4 of Table 1-2-1, respectively. Column 5 of Table 1-2-1 is the total curies in the applicable tanks. Column 6 of Table 1-2-1 is the curies that will remain in the pretreated LAW during the DFLAW approach. In general, column 6 is that portion of Column 3 treated during DFLAW approach with more than 99.9% reduction in Cs (RPP-CALC-63643, *Sum of Fractions Calculations for DFLAW Immobilized LAW Glass*)¹⁶. The expected removal of each key radionuclide using the DFLAW approach is provided in Column 7 of Table 1-2-1. Under the DFLAW approach, the total curies in the pretreated LAW are anticipated to be approximately 1% of the initial total curies in the applicable tanks, as shown in the last row of Column 7 of Table 1-2-1.

The expected inventory in the VLAW glass from RPP-CALC-63643 is provided in Column 8. For the DFLAW approach, approximately 99% of the radionuclides in the pretreated LAW will be captured in the VLAW, as shown in Column 9 of Table 1-2-1. Approximately 96% of the ¹²⁹I and approximately 98% of the ⁹⁹Tc in the pretreated LAW sent to the LAW Vitrification Facility will be captured in the VLAW.¹⁷ The VLAW will contain approximately 99% of the total curies in the pretreated LAW as provided in the last row of Column 9 of Table 1-2-1.

¹⁴ Some are of lesser importance due to their low concentrations in the waste, their small dose conversion factors, short half-life, or both.

¹⁵ To provide a bounding radiological risk analysis in the IDF PA, no credit is taken in flowsheet modeling for removal of key radionuclides other than ¹³⁷Cs by the ion exchange media. However, other radionuclides are expected to be removed by the ion exchange media. As explained in Section 4.2.2.1 of the Draft WIR Evaluation, the DFLAW approach includes “Passing through crystalline silicotitanate (CST) ion exchange media to remove ¹³⁷Cs, and large fractions of Ca, U, ⁹⁰Sr, Np and Pu if present in soluble form (PNNL-28783, *Dead-End Filtration and Crystalline Silicotitanate Cesium Ion Exchange with Hanford Tank Waste AW-102*).”

¹⁶ In general, sludge is separated through decanting and filtration prior to cesium removal during the DFLAW approach. The percentage of ¹³⁷Cs removed per DFLAW campaign is 99.95% or greater per RPP-CALC-63643. Table 1-2-1 rounds this value to three significant figures.

¹⁷ ³H and ¹⁴C are volatile radionuclides which will not be captured in the VLAW.

Table 1-2-1. Radionuclide Content in Supernate, Saltcake, Sludge and Vitrified Low-Activity Waste.¹ (2 sheets)

Radionuclide	Supernate (Ci)	Saltcake (Ci)	Supernate + Saltcake (Ci)	Sludge (removed via settle / decant) (Ci)	Total in DFLAW Tanks (Ci)	Radionuclide Content in Pretreated LAW Sent to LAW Vit Facility (Ci)	Percent Removed by DFLAW Approach	Radionuclide Content in VLAW Glass (Ci)	Percent of LAW Radionuclides in VLAW Glass
	(1)	(2)	(3)	(4)	(5)	(6)	(7)	(8)	(9)
Column Formula	BBI	BBI	(1)+(2)	BBI	(3)+(4)	RPP-CALC-63643	(6)/(5)*100	RPP-CALC-63643	(8)/(6)*100
³ H	1.27E+02	2.09E+02	3.36E+02	8.81E+01	4.24E+02	1.37E+02	67.7%	0.00E+00	0%
¹⁴ C	6.47E+01	1.64E+02	2.29E+02	8.63E+00	2.38E+02	1.43E+02	39.7%	0.00E+00	0%
⁶⁰ Co	9.30E+01	9.92E+01	1.92E+02	5.41E+02	7.33E+02	2.44E+01	96.7%	2.44E+01	99.9%
⁵⁹ Ni	4.44E+01	1.93E+02	2.37E+02	9.77E+01	3.35E+02	3.17E+01	90.5%	3.17E+01	99.9%
⁶³ Ni	2.52E+03	1.69E+04	1.94E+04	8.83E+03	2.83E+04	2.01E+03	92.9%	2.01E+03	99.9%
⁹⁰ Sr	4.72E+04	1.15E+06	1.20E+06	1.49E+07	1.61E+07	2.12E+05	98.7%	2.12E+05	99.8%
⁹⁴ Nb ²	NA	NA	NA	NA	NA	—	—	—	—
⁹⁹ Tc	9.44E+03	6.70E+03	1.61E+04	5.86E+02	1.67E+04	7.48E+03	55.2%	7.36E+03	98.4%
¹²⁶ Sn	1.34E+02	7.79E+01	2.12E+02	1.73E+01	2.30E+02	5.47E+01	76.2%	5.46E+01	99.9%
¹²⁹ I	1.15E+01	5.33E+00	1.68E+01	7.67E-01	1.76E+01	9.71E+00	45.0%	9.34E+00	96.2%
¹³⁷ Cs	1.58E+07	6.12E+06	2.19E+07	1.06E+06	2.30E+07	1.47E+03	100%	1.46E+03	99.2%
²²⁹ Th	1.81E-01	3.19E-03	1.84E-01	2.63E-03	1.87E-01	1.14E-01	39.1%	1.14E-01	99.9%
²³³ U	6.55E-01	4.16E+01	4.23E+01	7.33E+00	4.96E+01	8.01E-01	98.4%	7.99E-01	99.8%
²³⁴ U	4.96E-01	1.34E+01	1.39E+01	2.91E+01	4.30E+01	5.68E-01	98.7%	5.67E-01	99.8%
²³⁵ U	6.55E-01	4.16E+01	4.23E+01	7.33E+00	4.96E+01	2.12E-02	98.7%	2.12E-02	99.8%
²³⁸ U	3.82E-01	1.16E+01	1.20E+01	2.14E+01	3.33E+01	4.45E-01	98.7%	4.44E-01	99.8%
²³⁷ Np	1.92E+00	2.48E+01	2.67E+01	4.02E+01	6.70E+01	2.82E+00	95.8%	2.82E+00	99.8%
²³⁸ Pu	9.11E+00	1.12E+02	1.21E+02	1.02E+03	1.14E+03	6.79E+00	99.4%	6.78E+00	99.9%
²³⁹ Pu	5.95E+01	1.92E+03	1.98E+03	9.56E+03	1.15E+04	9.20E+01	99.2%	9.19E+01	99.9%
²⁴⁰ Pu	1.36E+01	4.44E+02	4.58E+02	2.45E+03	2.91E+03	2.06E+01	99.3%	2.06E+01	99.9%

Table 1-2-1. Radionuclide Content in Supernate, Saltcake, Sludge and Vitrified Low-Activity Waste.¹ (2 sheets)

Radionuclide	Supernate (Ci)	Saltcake (Ci)	Supernate + Saltcake (Ci)	Sludge (removed via settle / decant) (Ci)	Total in DFLAW Tanks (Ci)	Radionuclide Content in Pretreated LAW Sent to LAW Vit Facility (Ci)	Percent Removed by DFLAW Approach	Radionuclide Content in VLAW Glass (Ci)	Percent of LAW Radionuclides in VLAW Glass
	(1)	(2)	(3)	(4)	(5)	(6)	(7)	(8)	(9)
²⁴¹ Pu	1.30E+02	2.49E+03	2.62E+03	2.40E+04	2.66E+04	9.07E+01	99.7%	9.06E+01	99.9%
²⁴² Pu	9.44E-02	3.49E-02	1.29E-01	3.45E-01	4.74E-01	7.09E-02	85.0%	7.09E-02	99.9%
²⁴¹ Am	7.18E+01	5.94E+03	6.01E+03	8.39E+04	9.00E+04	9.76E+01	99.9%	9.75E+01	99.9%
²⁴³ Am	3.15E-02	3.58E+00	3.61E+00	3.86E+01	4.22E+01	4.78E-02	99.9%	4.77E-02	99.9%
²⁴² Cm	1.87E-01	1.56E+01	1.58E+01	6.98E+01	8.57E+01	2.21E+00	97%	2.20E+00	99.8%
²⁴³ Cm	3.54E-02	2.09E+00	2.13E+00	7.51E+00	9.63E+00	1.46E-01	98.5%	1.45E-01	99.8%
²⁴⁴ Cm	6.63E-01	4.13E+01	4.20E+01	1.49E+02	1.91E+02	2.63E+00	98.6%	2.62E+00	99.8%
Others ³	1.52E+07	7.36E+06	2.26E+07	1.67E+07	3.93E+07	3.51E+05	99.1%	3.50E+05	99.8%
Totals	3.11E+07	1.47E+07	4.58E+07	3.28E+07	7.85E+07	5.75E+05	99.3%	5.73E+05	99.8%

Source: RPP-CALC-63643, *Sum of Fractions Calculations for DFLAW Immobilized LAW Glass*, Rev. 4 and associated Excel[®] (a registered trademark of Microsoft Corporation in the U.S. and other countries) file.

Note: Numbers are rounded to three significant figures.

¹ The Draft WIR Evaluation (DOE/ORP-2020-01, *Draft Waste Incidental to Reprocessing Evaluation for Vitrified Low-Activity Waste Disposed Onsite at the Hanford Site, Washington*) uses the term vitrified low-activity waste (VLAW) which is also called immobilized low-activity waste (ILAW). Reference documents may use ILAW and as such this is synonymous with VLAW.

² As noted in the Draft WIR Evaluation, Table 4-3 Footnote c, ⁹⁴Nb is a key radionuclide identified in 10 CFR 61.55 that is not applicable to Hanford tank waste. The total amount of ⁹⁴Nb created from 1944 to 1989 in all Hanford reactors is about 0.1 Ci. ⁹⁴Nb is primarily produced in reactors from activation of natural niobium in stainless steel and Incone1[®] (a registered trademark of Special Metals Corporation, New Hartford, New York), neither of which were used at Hanford in the fuels that were reprocessed. Therefore, ⁹⁴Nb is not a key radionuclide in vitrified LAW (RPP-13489, *Activity of Fuel Batches Processed Through Hanford Separations Plants, 1944 Through 1989*, Table H-1). It is not a standard analyte for the Best-Basis Inventory (BBI) and thus content information is not available.

³ Others are identified in Table 1-2.2.

DFLAW = Direct-Feed Low-Activity Waste

The information in Table 1-2-1 will be added to the final WIR Evaluation. ^{233}U and ^{235}U are also included in Table 1-2-1, but were omitted from Table 4-3 in the Draft WIR Evaluation. These radionuclides will be added to Table 4-3 of the final WIR evaluation.

The following Table 1-2-2 provides the list of radionuclides included in the row Others of Table 1-2-1.

Table 1-2-2. Radionuclides in Others of Table 1-2.1.

^{106}Ru
$^{113\text{m}}\text{Cd}$
^{125}Sb
^{134}Cs
$^{137\text{m}}\text{Ba}$
^{151}Sm
^{152}Eu
^{154}Eu
^{155}Eu
^{226}Ra
^{227}Ac
^{228}Ra
^{231}Pa
^{232}Th
^{232}U
^{236}U
^{79}Se
^{90}Y
$^{93\text{m}}\text{Nb}$
^{93}Zr

It bears emphasizing that the vast majority of the curies in the tanks will not be disposed of in the IDF. For the entire Hanford cleanup mission¹⁸, the Table 1-2-3 provides Base Case 7 modelling

¹⁸ The entire Hanford cleanup mission encompasses the storage, retrieval, treatment, and disposal of approximately 56 million gallons of radioactive waste contained in the Hanford Site waste tanks and closure of all the tanks and associated equipment (ORP-11242, *River Protection System Plan*, Rev. 8).

percentages of radionuclides that do not end up in LLW planned to be disposed at IDF¹⁹, i.e., Non-IDF versus the tank waste contents (Best-Basis Inventory [BBI]).

Table 1-2-3. Run Case 7 Radionuclides. (2 sheets)

Radionuclide	Non-IDF	BBI	Portion of BBI Not in IDF*
106-Ru	-2.14E-03	1.20E+01	—
113m-Cd	5.04E+02	3.89E+03	13.0%
125-Sb	1.51E+00	4.13E+03	0.0%
126-Sn	1.58E-01	3.91E+02	0.0%
129-I	5.98E-01	2.94E+01	2.0%
134-Cs	7.11E+02	7.13E+02	99.7%
137-Cs	3.87E+07	3.90E+07	99.2%
137m-Ba	3.65E+07	3.68E+07	99.2%
14-C	8.24E+02	5.51E+02	149.5%**
151-Sm	3.15E+06	3.57E+06	88.2%
152-Eu	7.91E+02	9.07E+02	87.2%
154-Eu	4.82E+04	5.30E+04	90.9%
155-Eu	2.41E+04	2.55E+04	94.5%
226-Ra	1.18E-05	9.95E-03	0.1%
227-Ac	-9.32E+00	4.14E+00	—
228-Ra	-2.89E+02	6.77E+00	—
229-Th	1.42E+00	1.48E+00	95.9%
231-Pa	4.73E+00	5.16E+00	91.7%
232-Th	6.61E+00	6.77E+00	97.6%
232-U	8.17E+00	8.87E+00	92.1%
233-U	6.37E+02	6.82E+02	93.4%
234-U	2.14E+02	2.37E+02	90.3%
235-U	8.75E+00	9.71E+00	90.1%
236-U	6.05E+00	6.50E+00	93.1%
237-Np	9.02E+01	1.15E+02	78.4%
238-Pu	2.25E+03	2.63E+03	85.6%

¹⁹ LLW planned to be disposed at IDF includes Fast Flux Test Facility (FFTF) decommissioning waste, waste management facility-generated (secondary) waste, and onsite non-CERCLA non-tank waste, as mentioned in DOE/EIS-0391, *Final Tank Closure and Waste Management Environmental Impact Statement for the Hanford Site, Richland, Washington*.

Table 1-2-3. Run Case 7 Radionuclides. (2 sheets)

Radionuclide	Non-IDF	BBI	Portion of BBI Not in IDF*
238-U	1.94E+02	2.15E+02	90.2%
239-Pu	4.30E+04	4.94E+04	87.0%
240-Pu	9.10E+03	1.08E+04	84.3%
241-Am	1.42E+05	1.57E+05	90.4%
241-Pu	7.15E+04	8.38E+04	85.3%
242-Cm	8.22E-02	1.22E+02	0.1%
242-Pu	6.78E-01	8.26E-01	82.1%
243-Am	6.38E+01	7.23E+01	88.2%
243-Cm	5.04E-03	1.35E+01	0.0%
244-Cm	1.07E-01	2.98E+02	0.0%
3-H	2.81E+03	2.82E+03	99.6%
59-Ni	1.41E+03	1.62E+03	87.0%
60-Co	3.71E+03	4.10E+03	90.5%
63-Ni	1.26E+05	1.44E+05	87.5%
79-Se	4.51E-02	1.44E+02	0.0%
90-Sr	4.27E+07	4.76E+07	89.7%
90-Y	4.27E+07	4.76E+07	89.7%
93-Zr	3.37E+03	3.73E+03	90.3%
93m-Nb	2.85E+03	3.17E+03	89.9%
99-Tc	2.14E+01	2.65E+04	0.1%
Totals	1.64E+08	1.75E+08	93.7%

Adapted from Table A-1. Run Case 7 Radionuclides. of RPP-ENV-58562, *Inventory Data Package for the Integrated Disposal Facility Performance Assessment*, Rev. 3. Table data was drawn from the 2014 Best-Basis Inventory (BBI) which was the basis of the Integrated Disposal Facility (IDF) Performance Assessment (RPP-RPT-59958, *Performance Assessment for the Integrated Disposal Facility, Hanford Site*).

*Column added.

**Includes 222S laboratory sources -, i.e. sources are not in the BBI.

The Hanford Tank Waste Operations Simulator (HTWOS) reports certain radionuclides (i.e., ²²⁷Ac, ²²⁸Ra, ^{93m}Nb) as negative inventory values, which is due to the fact that HTWOS has four second-order decay chains; parent to daughter to granddaughter isotope. None of the radionuclides reporting negative inventories are considered major risk drivers and therefore will have a negligible impact on the overall performance of the IDF (see Section 2.7.7 in RPP-17152, *Hanford Tank Waste Operations Simulator (HTWOS) Version 8.1 Model Design Document*).

References

- DOE/EIS-0391, 2012, *Final Tank Closure and Waste Management Environmental Impact Statement for the Hanford Site, Richland, Washington*, U.S. Department of Energy, Washington, D.C.
- DOE/ORP-2020-01, 2020, *Draft Waste Incidental to Reprocessing Evaluation for Vitrified Low-Activity Waste Disposed Onsite at the Hanford Site, Washington*, U.S. Department of Energy, Office of River Protection, Richland, Washington.
- ORP-11242, 2017, *River Protection System Plan*, Rev. 8, U.S. Department of Energy, Office of River Protection, Richland, Washington.
- PNNL-28783, 2019, *Dead-End Filtration and Crystalline Silicotitanate Cesium Ion Exchange with Hanford Tank Waste AW-102*, RPT-TCT-003, Rev. 0, Pacific Northwest National Laboratory, Richland, Washington.
- RPP-13489, 2002, *Activity of Fuel Batches Processed Through Hanford Separations Plants, 1944 Through 1989*, Rev. 0, Fluor Hanford, Inc., Richland, Washington.
- RPP-17152, 2015, *Hanford Tank Waste Operations Simulator (HTWOS) Version 8.1 Model Design Document*, Rev. 12, Washington River Protection Solutions, LLC/AEM Consulting, LLC, Richland, Washington.
- RPP-CALC-63643, in process, *Sum of Fractions Calculations for DFLAW Immobilized LAW Glass*, Rev. 4, Washington River Protection Solutions, LLC, Richland, Washington.
- RPP-ENV-58562, 2016, *Inventory Data Package for the Integrated Disposal Facility Performance Assessment*, Rev. 3, Washington River Protection Solutions, LLC, Richland, Washington.
- RPP-RPT-59958, 2019, *Performance Assessment for the Integrated Disposal Facility, Hanford Site, Washington*, Rev. 1A, Washington River Protection Solutions, LLC, Richland, Washington.

RAI 1-3 (Percentage of ⁹⁹Tc and ¹²⁹I Recycled versus Removed)**Comment**

Additional information is needed on the percent of the ⁹⁹Tc and ¹²⁹I that could potentially be removed from the waste versus remaining in either the VLAW or the SSW. (See also RAI 2-10).

Basis

In the draft WIR evaluation, DOE stated on page 4-12 that, “with respect to ⁹⁹Tc and ¹²⁹I, the LAW Vitrification Facility is designed to maximize the capture of these radionuclides in the vitrified waste form. The LAW Vitrification Facility off gas system is designed to recycle and/or capture that portion of volatile radionuclides (including ⁹⁹Tc and ¹²⁹I) which are not vitrified (see Section 2.5.3).” During the LAW vitrification process, the volatile components will be drawn off through the melter offgas treatment system, will go through a submerged bed scrubber (SBS) and Wet Electrostatic Precipitator (WESP), two stages of high-efficiency particulate air (HEPA) filters, as well as two carbon adsorber beds, which remove the ¹²⁹I.

The draft WIR evaluation states that the ⁹⁹Tc and ¹²⁹I in the liquid condensate resulting from the offgas system (from the SBS and WESP) can potentially be routed in three ways:

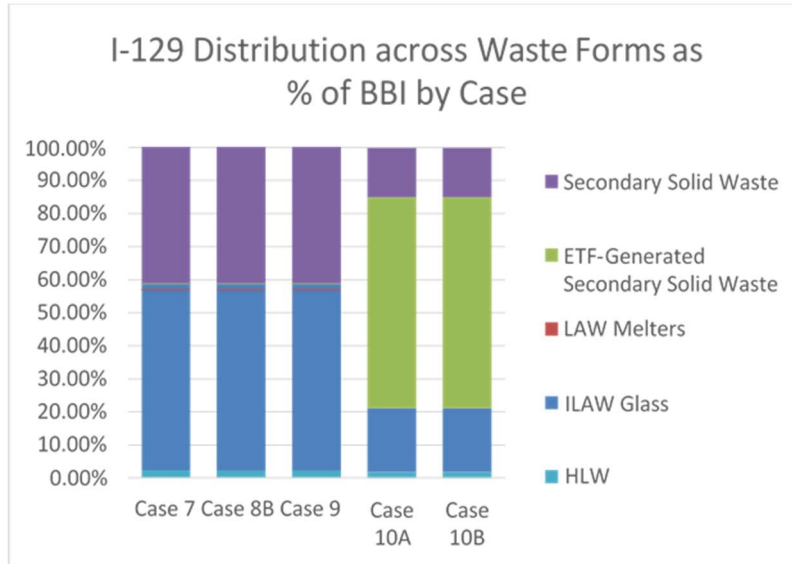
1. recycle back to the LAW Vitrification Facility for blending with incoming DFLAW feed;
2. return back to the Hanford tank farms; and
3. purge via a tanker truck load-out station ((RPP-RPT-58971, Effluent Management Facility Evaporator Concentrate – Purge Alternatives Evaluation).

Table 3-29 in the PA document provides the summary of radionuclide inventories and wastefrom distributions for five cases. As shown below, the majority of the ⁹⁹Tc and ¹²⁹I does not remain in the HLW tanks. In Case 7, Case 8B, and Case 9, about 40% of the Best Basis Inventory (BBI) of ¹²⁹I ends up in the Secondary Solid Waste (SSW). In Case 10A and Case 10B, nearly 80% of the ¹²⁹I ends up in either the Effluent Treatment Facility-Generated (ETF- Generated) SSW or the SSW. A negligible amount of the ¹²⁹I remains in the HLW in any of cases.

In Case 7, over 99% of the ⁹⁹Tc is assumed to end up in the Immobilized Low-Activity Waste (ILAW) glass. In Case 8B, as a result of removing ⁹⁹Tc from the LAW off-gas stream, 16,500 Ci of ⁹⁹Tc accumulates over the course of the waste treatment and immobilization plant mission.

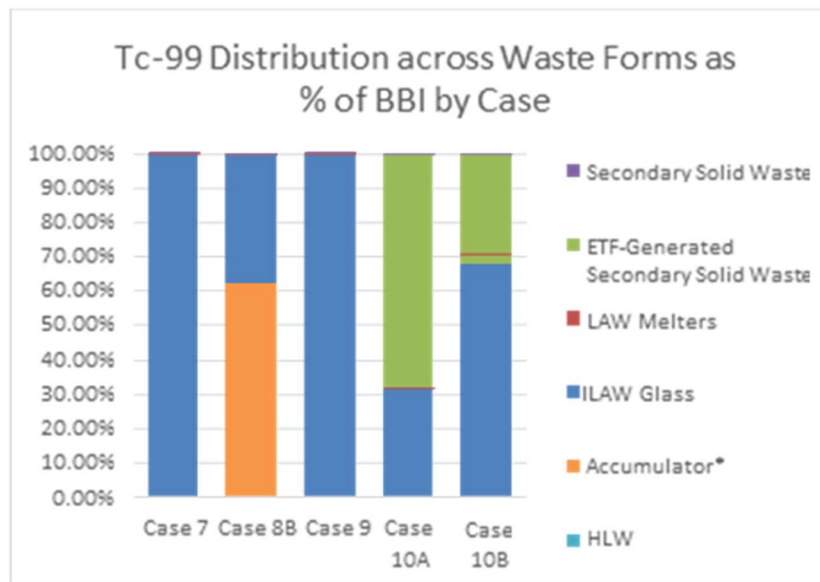
The footnote on Table 3-29 states that “these curies would likely be processed in High-Level Waste and would not end up at the IDF”. In the PA document, DOE further describes Case 8B as follows: “a ⁹⁹Tc removal unit operation has been added after the submerged bed scrubber (SBS) wet electrostatic precipitator (WESP) to remove ⁹⁹Tc at an efficiency of 99% from the LAW liquid off-gas steam prior to being recycled back to pretreatment. This inventory would not be disposed of at IDF and represents the lower range of ⁹⁹Tc inventory in glass and grout waste forms.”

Figure 1-3-1. Iodine-129 Distribution across Waste Forms as Percent of Best-Basis Inventory by Case.



Adapted from data in Table 3-29 of RPP-RPT-59958, *Performance Assessment for the Integrated Disposal Facility, Hanford Site, Washington*.

Figure 1-3-2. Technetium-99 Distribution across Waste Forms as Percent of Best-Basis Inventory by Case.



Adapted from data in Table 3-29 of RPP-RPT-59958, 2019, *Performance Assessment for the Integrated Disposal Facility, Hanford Site, Washington*.

Path Forward

Please provide additional information on the percentage of ^{99}Tc and ^{129}I that is expected to be recycled back to the DFLAW feed, percent returned to the tank farm to be disposed of as HLW, and percent purged via the Effluent Management Facility (EMF) evaporator concentrate.

Please provide additional information about the accumulator mentioned in Table 3-29 of the PA document. Please specify if the ^{99}Tc is assumed to be accumulating in one component or in multiple parts of the waste treatment plant (WTP). Please provide the hypothetical plan for disposal of the accumulator waste under this scenario.

DOE Response

In the time since the IDF PA study was performed, the DFLAW flowsheet has matured and the EMF design (used only during DFLAW) has been finalized. In the current flowsheet configuration (RPP-RPT-57991), all ^{99}Tc and ^{129}I in the liquid concentrate resulting from the off-gas system (from the SBS and WESP) will be recycled internally back to the concentrate receipt vessels of the LAW Vitrification Facility. By recycling the liquid concentrate internally, it is estimated that 98.4% of the ^{99}Tc and 96.2% of the ^{129}I that is sent to the LAW Vitrification Facility as feed will be incorporated into the VLAW during DFLAW (RPP-CALC-63643; see also Table 1-2-1 of the response to RAI 1-2). No ^{99}Tc or ^{129}I will be returned to the tank farm to be disposed of as HLW, or purged via the EMF evaporator concentrate. The Final WIR Evaluation will be updated to reflect the current flowsheet configuration. Cases 10A and 10B were hypothetical scenarios that investigated alternatives to recycling all EMF concentrate back to the concentrate receipt vessels in the LAW Vitrification Facility. With finalization of the DFLAW flowsheet, Cases 10A and 10B are no longer potential scenarios and will be withdrawn from the analyses performed for the IDF PA for its next revision, as part of PA maintenance. In the event of an extended outage of the EMF evaporator and continued tank waste treatment through the LAW melters, the dilute EMF evaporator feed will be returned to the tank farms. If that were to occur, the ^{99}Tc and ^{129}I would eventually be fed back to the LAW Vitrification Facility in a larger recycle loop, due to the soluble nature of both isotopes.

The accumulator²⁰ mentioned in Table 3-29 of the IDF PA document for Case 8B is a modeling tool used to symbolize an undefined ^{99}Tc removal operation for mass balance purposes. Case 8B was developed for the IDF PA to align with a hypothetical scenario that removed 99% of ^{99}Tc in the LAW Vitrification Facility liquid off-gas system for incorporation into HLW. In Case 8B this removal process is a hypothetical process to align with the conditions of the scenario. Case 8B is no longer a potential scenario and will be withdrawn from the analyses performed for the IDF PA for its next revision as part of PA maintenance. Due to the volatility and soluble nature of ^{99}Tc , if it were to be collected and fed to the HLW Vitrification Facility (which is not possible during DFLAW operations since the HLW Vitrification Facility is under construction and not available), only a fraction of it would be retained in the immobilized high-level waste glass. The remaining ^{99}Tc would be collected in HLW off-gas condensates, returned to the Pretreatment Facility and routed to the LAW Vitrification Facility to be incorporated into the VLAW glass. The much larger recycle loop and technical challenges that this situation would create make this scenario not technically feasible.

²⁰ No accumulator is included as part of the draft VLAW WIR. The accumulator was included in the IDF PA as a hypothetical scenario.

The inventory sensitivity cases (Cases 8B, 10A, and 10B) were deterministic cases used to demonstrate dose impacts for different LAW Vitrification Facility operating scenarios. The cases were hypothetical, but confirmed a strong correlation between waste stream inventory and waste stream dose using the PA models. Subsequent to the completion of the IDF PA, a spreadsheet was developed to track inventories and forecast the impacts to groundwater due to changes in inventory. This spreadsheet is referred to as the Risk Budget Tool and was developed in RPP-CALC-63176, *Integrated Disposal Facility Risk Budget Tool Analysis*. The calculations demonstrate that changes to the groundwater concentrations and dose to a member of the public in the future from a specific waste stream are proportional to a change in the inventory in that waste stream. Inventory changes or “what if” scenarios can be rapidly evaluated using the Risk Budget Tool and these evaluations are consistent with equivalent analyses that could be conducted with the IDF PA system model. In future revisions of the IDF PA, DOE will consider using probabilistic methods to evaluate inventory uncertainty instead of deterministic sensitivity studies.

References

- DOE/ORP-2020-01, 2020, *Draft Waste Incidental to Reprocessing Evaluation for Vitrified Low-Activity Waste Disposed Onsite at the Hanford Site, Washington*, U.S. Department of Energy, Office of River Protection, Richland, Washington.
- RPP-CALC-63176, 2020, *Integrated Disposal Facility Risk Budget Tool Analysis*, Rev. 0A, Washington River Protection Solutions, LLC, Richland, Washington.
- RPP-CALC-63643, in process, *Sum of Fractions Calculations for DFLAW Immobilized LAW Glass*, Rev. 4, Washington River Protection Solutions, LLC, Richland, Washington.
- RPP-RPT-57991, 2019, *River Protection Project Integrated Flowsheet*, 24590-WTP-RPT-MGT-14-023, Rev. 3, Washington River Protection Solutions, LLC, Richland, Washington.
- RPP-RPT-58971, 2020, *Effluent Management Facility Evaporator Concentrate – Purge Alternatives Evaluation*, Rev. 1, Washington River Protection Solutions, LLC, Richland, Washington.

RAI 1-4 (Alternative Technology Evaluation Impacting ⁹⁹Tc and ¹²⁹I)**Comment**

Additional information is needed on the alternative technologies considered for removal of ¹²⁹I and ⁹⁹Tc.

Basis

Depending on the processes used and separation that may occur, a moderate to significant amount of ¹²⁹I and ⁹⁹Tc may end up in the SSW (See the previous figures in RAI 1-3). If these key radionuclides in the SSW ultimately are disposed of in IDF, the NRC staff considers those secondary waste streams within the scope of the draft WIR evaluation and therefore considers the impact of the secondary waste and the alternative technologies considered for the wasteforms. The NRC staff note that in discussions with the DOE, the DOE has stated that the scope of the draft WIR evaluation is limited to the vitrified waste. DOE has stated that the SSW is a newly generated waste stream and will include a wide variety of waste (HEPA filters, or carbon filters) that will be generated after the low activity waste has been vitrified. Therefore, DOE considers SSW to be outside the scope of the WIR evaluation, but DOE has included the SSW as part of IDF PA analysis and the SSW will be classified to ensure it meets the Waste Acceptance Criteria (WAC) for IDF.

DOE has conducted previous studies to compare alternative technologies for removal of radionuclides from the Hanford tank wastes. These studies are summarized in the Technical Basis Summary Report (WHC-SD-WM-TI-699) completed in 1996. In the draft WIR evaluation DOE summarized the findings of the report, but DOE did not discuss alternative technologies considered for the SSW waste forms or technologies that would selectively drive the ⁹⁹Tc and ¹²⁹I back into the HLW.

Path Forward

As a result of high operating temperatures, the vitrification process appears to selectively partition the ⁹⁹Tc and ¹²⁹I to the SSW waste stream during processing of the waste. Given that ⁹⁹Tc and ¹²⁹I are key risk drivers, please provide information regarding potential technologies that may have been considered to connect the offgas system to other waste treatments that would result in those key radionuclides being incorporated into HLW compared to the VLAW or SSW.

DOE Response

The Draft WIR Evaluation focuses on the WIR criteria for separated and pretreated VLAW using the DFLAW approach. Other wastes, including secondary waste such as the carbon adsorber beds (CABs), are outside the scope of the Draft WIR Evaluation, as explained in the Draft WIR Evaluation and DOE's Response to NRC's Introductory Statement Related to Secondary Waste. To bound the analysis, the IDF PA correctly includes all wastes potentially disposed of in the IDF, including the CABs and other secondary wastes, for demonstrating compliance with performance objectives and performance measures. The following is being provided for additional information and completeness, although it is outside the scope of the Draft WIR Evaluation.

As a result of high operating temperatures in the LAW melter, volatile constituents present in the LAW feed (including ^{99}Tc and ^{129}I) will non-selectively partition to the melter off-gas system. The LAW vitrification melter off-gas system has operations (i.e., an SBS and a WESP) to recover volatile constituents. These constituents are incorporated back into the LAW vitrification feed stream via the EMF for eventual incorporation into VLAW.²¹

As provided in more detail in the answers to RAI 1-2 and RAI 1-3, approximately 98% of the ^{99}Tc , 96% of the ^{129}I , and 99% of all radionuclides from the pretreated LAW are now projected to be incorporated into the VLAW during the DFLAW approach.²² Revisions of the IDF PA will incorporate changes per required PA maintenance activities as required in DOE M 435.1-1 Chapter IV Section (P) (4).

DOE will monitor all waste as it is disposed to ensure that the IDF WAC is met and that the IDF PA is maintained.

References

- 78 FR 75913, 2013, “Record of Decision: Final Tank Closure and Waste Management Environmental Impact Statement for the Hanford Site, Richland, Washington,” *Federal Register*, Vol. 78, pp. 75913–75919 (December 13).
- DOE M 435.1-1, 2011, *Radioactive Waste Management Manual*, Change 2, U.S. Department of Energy, Washington, D.C.
- DOE/ORP-2020-01, 2020, *Draft Waste Incidental to Reprocessing Evaluation for Vitrified Low-Activity Waste Disposed Onsite at the Hanford Site, Washington*, U.S. Department of Energy, Office of River Protection, Richland, Washington.
- RPT-RPT-59958, 2018, *Performance Assessment for the Integrated Disposal Facility, Hanford Site*, Rev. 1, Washington, Department of Energy, Richland, Washington.
- WHC-SD-WM-TI-699, 1996, *Technical Basis for Classification of Low-Activity Waste Fraction from Hanford Site Tanks*, Rev. 2, Westinghouse Hanford Company, Richland, Washington.

²¹ The EMF is planned to be used only during the DFLAW approach.

²² DOE is not pursuing other potential processes that would divert volatilized Tc and I to non-VLAW (non-ILAW) waste streams (see 78 FR 75913, “Record of Decision: Final Tank Closure and Waste Management Environmental Impact Statement for the Hanford Site, Richland, Washington”).

RAI 1-5 (Removal and Disposal of Separated 129I)**Comment**

In the draft WIR evaluation, DOE indicated that they did not identify a technology that could practically remove ^{129}I from tank wastes. It isn't clear why the ^{129}I that is separated very efficiently by the vitrification process could not be disposed as HLW.

Basis

DOE identified ^{129}I as a key radionuclide with respect to protection of an offsite member of the public. Iodine-129 is present in tank waste in very low concentrations and therefore it is difficult to remove. Iodine-129 is very long-lived and mobile in the environment. The vitrification process operates at very high temperatures and volatilizes nearly all of the ^{129}I present in the waste streams. This ^{129}I then goes into the offgas system and is captured or recycled back to the glass melter. Even with recycling the capture of ^{129}I in the glass is less than 50%.

Section 4.2.2.6 of the draft WIR evaluation states that “DOE has also explored whether there is an available technology to remove ^{129}I . However, the ^{129}I concentration in the tank wastes is typically 1,000 to 10,000 times lower than would exist in commercial fuel dissolver solutions for which an available iodine removal technology was developed. Iodine-129 removal is not considered to be technically practical because no technology has been demonstrated for the relatively low concentrations in the Hanford Site tank waste (WHC-SD-WM-TI-699, Technical Basis for Classification of Low-Activity Waste Fraction from Hanford Site Tanks).”

In section 2.5.3 of the draft WIR evaluation DOE stated that the “The volatile components will be drawn off through the melter offgas treatment system, go through a submerged bed scrubber (SBS) and Wet Electrostatic Precipitator (WESP). The LAW melter offgas system consists of two stages of high-efficiency particulate air (HEPA) filters for the purpose of removing radioactive particulates from the offgas, in order to achieve compliance with both environmental and occupational dose limits. Downstream of the HEPA filters are two carbon adsorber beds filled with granular activated carbon media. By design, the purpose of these beds is to remove mercury, halides, and acid gases as well as ^{129}I .” It was not clear whether DOE evaluated the disposal of the ^{129}I separated by the vitrification process as HLW.

Path Forward

Please provide information as to whether DOE evaluated the disposal of the ^{129}I that would be adsorbed by the two carbon adsorber beds filled with granular activated carbon media as HLW. Please also describe what percentage of the ^{129}I can technically and practically be removed using the carbon adsorber beds.

DOE Response

The Draft WIR Evaluation focuses on the WIR criteria for separated and pretreated VLOW using the DFLAW approach. Other wastes, including secondary waste such as the CABs, are outside the scope of the Draft WIR Evaluation, as explained in the Draft WIR Evaluation and DOE's Response to NRC's Introductory Statement Related to Secondary Waste. To bound the analysis, the IDF PA²³ correctly includes all wastes potentially disposed of in the IDF, including the CABs

²³ The IDF PA is titled *Performance Assessment for the Integrated Disposal Facility, Hanford Site, Washington*.

and other secondary wastes, for compliance with performance objectives and performance measures. The following is being provided for additional information and completeness, although it is outside the scope of the Draft WIR Evaluation.

The LAW Vitrification Facility's melter off-gas system has a primary system and a secondary system. The primary system consists of the SBS to remove particulates and cool the off-gas, an SBS Condensate Vessel to maintain SBS liquid level, and a WESP to remove aerosols and micron-sized particulates. The secondary system consists of the Vessel Ventilation Subsystem, Off-Gas HEPA Preheaters, HEPA Filters, Activated CABs, Catalyst Skid, Catalytic Oxidizer Heat Recovery Exchanger, Catalytic Oxidizer Electric Heater, Thermal Catalytic Oxidizers, Selective Catalytic Reducer (SCR), Caustic Collection Tank, Caustic Scrubber, and Exhausters.

The CABs are used to remove mercury, halides, and acid gases, including iodine, for the control of air emissions to meet EPA air discharge limits and reduce occupational doses. The CABs are not designed or relied upon in the Draft WIR Evaluation as a treatment process for removing ¹²⁹I to meet the first WIR criterion under DOE M 435.1-1 (concerning removal of key radionuclides to the maximum extent technically and economically practical).

The CABs will be properly characterized and classified, and if characterized as LLW, treated, and disposed of in the IDF in accordance with IDF-00002. The CABs are identified as a future newly-generated LLW in the LAW Vitrification Facility Radioactive Waste Management Basis (RWMB).²⁴

The LAW Vitrification Facility off-gas system in combination with the EMF and recycling the EMF bottoms back to the LAW Vitrification facility will, by design, maximize the capture of the volatilized ¹²⁹I in the VLAW glass. Approximately 96% of the ¹²⁹I will be captured in the VLAW as explained in the response to RAI 1-2, compared to 57.51% assumed in the IDF PA²⁵.

²⁴ In addition, the CABs will be replaced periodically. The CABs are expected to be below 10 CFR 61.55 Class C concentration limits.

²⁵ Since the time of the preparation of DOE/EIS-0391, *Final Tank Closure and Waste Management Environmental Impact Statement for the Hanford Site, Richland, Washington* and the IDF PA, there have been two major changes in modeling assumptions: 1) It is no longer assumed that the EMF bottoms will be recycled to the Tank Farms, and 2) Single-pass iodine incorporation is increased from 20% to 58.33%. These are more fully explained as follows. When the modeling was performed for the IDF PA, the flowsheet assumption was that some of the EMF bottoms would be returned to Tank Farms. At that time, it was assumed that only 67% of the bottoms would be recycled back to the WTP LAW Vitrification Facility, and the other 33% would be returned to Tank Farms to be processed again through the WTP LAW Vitrification Facility at a later time. There is no return to the Tank Farms in the latest flowsheet modeling. Additionally, to be consistent with DOE/EIS-0391, the single-pass iodine incorporation rate was originally set at 20% (RPP-ENV-58562 Rev. 3, page 49) per State of Washington Department of Ecology direction (*Mass Balance Revision, 17546 Revision of PCAL 17284-2 Mass Balance, WT-ST-056 Rev. 2 Attachment 4*). This resulted in about 56.64% of the iodine being incorporated in the VLAW. Latest modeling (RPP-RPT-57991 Rev. 3) is now consistent with the WTP *Flowsheet Bases, Assumptions, and Requirements* (24590-WTP-RPT-PT-02-005 Rev, 8), which has 58.33% single pass incorporation. The combination of no returns to the Tank Farms and higher first pass incorporation now projects 96.2% of the iodine will be incorporated into VLAW. See Responses to RAI 1-2 and RAI 2-17 (which incorporates the updated modeling assumptions).

References

- 24590-WTP-RPT-PT-02-005, 2016, *Flowsheet Bases, Assumptions, and Requirements*, Rev. 8, Bechtel, River Protection Project, Waste Treatment Plant, Richland, Washington.
- DOE/ORP-2020-01, 2020, *Draft Waste Incidental to Reprocessing Evaluation for Vitrified Low-Activity Waste Disposed Onsite at the Hanford Site*, Washington, U.S. Department of Energy, Office of River Protection, Richland, Washington.
- IDF-00002, 2019, *Waste Acceptance Criteria for the Integrated Disposal Facility*, Rev. 0, CH2M HILL Plateau Remediation Company, Richland, Washington.
- RPP-ENV-58562, 2016, *Inventory Data Package for the Integrated Disposal Facility Performance Assessment*, Rev. 3, Washington River Protection Solutions, LLC, Richland, Washington.
- RPP-RPT-57991, 2019, *River Protection Project Integrated Flowsheet*, 24590-WTP-RPT-MGT-14-023, Rev. 3, Washington River Protection Solutions, LLC, Richland, Washington.
- WHC-SD-WM-TI-699, 1996, *Technical Basis for Classification of Low-Activity Waste Fraction from Hanford Site Tanks*, Rev. 2, Westinghouse Hanford Company, Richland, Washington.
- WT-ST-056, 2007, *Mass Balance Revision, 17546 Revision of PCAL 17284-2 Mass Balance*, Rev. 2, Columbia Energy & Environmental Services, Inc., Richland, Washington.

4.0 RADIONUCLIDE INVENTORY AND RELEASE RATES

RAI 2-1 (Scope of PA Compared to Scope of Draft WIR Evaluation)

Comment

The results from the PA that are directly applicable to the scope of the draft WIR evaluation are not clear. One factor could have been the timing of the completion of the PA and draft WIR evaluation.

Basis

The performance assessment was completed before the draft WIR evaluation. The performance assessment was completed in 2018 while the draft WIR evaluation was completed in 2020. Although DOE evaluated a number of different scenarios associated with waste volumes and the fraction of key radionuclides that would end up in different waste streams, the translation of the PA results to the scope of the draft waste evaluation is not clear. The inventory in the PA was larger and encompasses the smaller inventory associated with DFLAW. For example, in the PA, DOE evaluated disposal of 130,000 canisters of vitrified waste whereas the DFLAW approach is estimated to generate 13,500 canisters. The impacts associated with some wastes do not scale linearly with volume or radioactivity. Intruder impacts generally scale linearly with activity whereas impacts to an offsite intruder through all-pathways generally scale linearly with volume. In order to properly risk-inform the review process, the baseline results are needed consistent with assumptions in the draft waste evaluation.

DOE did not include secondary wastes generated as part of waste processing within the scope of the draft waste evaluation. However, as discussed previously, if significant fractions of key radionuclides are separated or partitioned as a result of waste processing (e.g. volatilization) and those radionuclides are ultimately disposed as non-HLW then those waste streams would be within the scope of the evaluation according to NRC practice and regulation. The cumulative impact of all radioactive material disposed of at IDF needs to be considered when evaluating the performance objectives of 10 CFR Part 61.

Path Forward

Please ensure that the cumulative impact of all radioactive material disposed of at IDF is considered when evaluating the performance objectives of 10 CFR Part 61, including the doses resulting from the DFLAW inventory and the associated secondary wastes generated from processing the DFLAW inventory. If significant portions of key radionuclides end up in processing components, such as the off-gas system and those components are disposed as non-HLW, then they should be included in the results. Please also provide the waste classification results for all relevant waste streams and a demonstration that those streams will be incorporated into a solid physical form.

DOE Response

The Draft WIR Evaluation focuses on the separated and pretreated LAW that has been pretreated using the DFLAW approach and vitrified (VLAW), as explained in the Draft WIR Evaluation and DOE's Response to NRC's Introductory Statement Related to Secondary Waste. The

following information is provided for additional information and completeness, outside the scope of the Draft WIR Evaluation.

To bound the analysis and provide the “cumulative impact” of all waste potentially disposed in the IDF, the IDF PA correctly analyzes all LLW that potentially may be disposed of at the IDF, including VLAW and secondary waste, for compliance with performance objectives and performance measures, as discussed in the IDF PA.

It bears emphasizing that the IDF is planned to receive LLW generated from a variety of sources as analyzed in the IDF PA, including: DFLAW approach-generated VLAW, additional VLAW from continued Hanford Waste Treatment and Immobilization Plant (WTP) LAW Vitrification Facility operation, assumed potential supplemental VLAW²⁶, VLAW glass melters, and solid secondary waste (SSW) generated by routine WTP operations and other site operations. Additional waste streams would be generated that are not a result of the WTP process, including encapsulated Fast Flux Test Facility (FFTF) decommissioning debris waste, encapsulated secondary waste management waste, and encapsulated onsite non-CERCLA²⁷ non-tank debris LLW. WTP processing components are not planned to be disposed in the IDF other than maintenance-related items.²⁸

The secondary waste that will be generated by, or derived from, the off-gas system associated with the vitrification of the pretreated LAW using the DFLAW approach will not contain significant quantities of key radionuclides. Per RPP-CALC-63643 Rev. 4, approximately 1% of the total key radionuclides after pretreatment during the DFLAW approach will be in such secondary waste, with approximately 4% of the ¹²⁹I and approximately 2% of the ⁹⁹Tc in SSW. See also RAI 1-2 response.

All LLW, including secondary waste, disposed at the IDF will be properly characterized and classified, will undergo applicable treatment, and must be compliant with IDF-00002, which requires solid waste forms for disposal. Additionally, wastes emplaced in the IDF must meet the *Washington Administrative Code* 173-303-140, “Land Disposal Restrictions,” which only allows wastes not containing free liquids in a landfill.

²⁶ Information concerning potential supplemental LAW treatment is provided in the IDF PA and, by reference, in this RAI response for additional information and completeness, and is outside the scope of both the Draft WIR Evaluation and DOE decisions concerning supplemental LAW treatment. DOE has not made decisions concerning the potential path forward for supplemental LAW treatment, as explained in footnote 7 of the Draft WIR Evaluation and 78 FR 75913, “Record of Decision: Final Tank Closure and Waste Management Environmental Impact Statement for the Hanford Site, Richland, Washington”. As explained in section 1.2 of the Draft WIR Evaluation, the Draft WIR Evaluation does not address or include in its scope supplemental LAW. To bound the IDF PA analysis, the IDF PA assumed that supplemental LAW may potentially be vitrified and disposed of in the IDF, although, as explained above, DOE has made no decisions concerning the potential path forward for supplemental LAW treatment. Changes to the actual disposed inventory of LLW assumed in the IDF PA will be appropriately evaluated through PA revisions or Supplemental Analysis per the PA maintenance and change control program.

²⁷ *Comprehensive Environmental Response, Compensation, and Liability Act of 1980*, 42 USC 9601 et seq.

²⁸ No decision has been made as to where WTP equipment will be disposed upon its mission completion and are not included in the IDF PA.

Radionuclides will be identified as required in 24590-WTP-ICD-MG-01-003, *ICD 03 - Interface Control Document for Radioactive Solid Waste*, Section 3.3.1.2, which states:

“The WTP Contractor shall characterize RSW²⁹ streams to:

1. Determine the physical characteristics and chemical characterization of the waste with sufficient accuracy and detail to properly designate and manage waste in accordance with state and federal regulations, and
2. Ensure the requirements for major radionuclides and the concentration of each major radionuclide are established with sufficient sensitivity and accuracy to properly classify and manage the waste as required by DOE M 435.1-1.
3. Ensure all RSW streams being transported to applicable Treatment, Storage, and Disposal (TSD) facility(s) are certified in accordance with DOE M 435.1-1.”

References

10 CFR 61, “Licensing Requirements for Land Disposal of Radioactive Waste,” *Code of Federal Regulations*, as amended.

24590-WTP-ICD-MG-01-003, 2019, *ICD 03 - Interface Control Document for Radioactive Solid Waste*, Rev. 7, Bechtel, River Protection Project, Waste Treatment Plant, Richland, Washington.

78 FR 75913, 2013, “Record of Decision: Final Tank Closure and Waste Management Environmental Impact Statement for the Hanford Site, Richland, Washington,” *Federal Register*, Vol. 78, pp. 75913–75919 (December 13).

Comprehensive Environmental Response, Compensation, and Liability Act of 1980, 42 USC 9601 et seq.

DOE M 435.1-1, 2011, *Radioactive Waste Management Manual*, Change 2, U.S. Department of Energy, Washington, D.C.

DOE/ORP-2020-01, 2020, *Draft Waste Incidental to Reprocessing Evaluation for Vitriified Low-Activity Waste Disposed Onsite at the Hanford Site, Washington*, U.S. Department of Energy, Office of River Protection, Richland, Washington.

IDF-00002, 2019, *Waste Acceptance Criteria for the Integrated Disposal Facility*, Rev. 0, CH2M HILL Plateau Remediation Company, Richland, Washington.

RPP-CALC-63643, in process, *Sum of Fractions Calculations for DFLAW Immobilized LAW Glass*, Rev. 4, Washington River Protection Solutions, LLC, Richland, Washington.

WAC 173-303-140, “Land Disposal Restrictions,” *Washington Administrative Code*, as amended.

²⁹ Radioactive Solid Waste (RSW).

RAI 2-2 (Model Support for the Performance Assessment)**Comment**

Additional information is needed related to demonstrate whether the conceptual and numerical models used in the performance assessment (PA) were adequately supported over the range of projected future conditions.

Basis

DOE used performance assessment modeling to integrate the results of process models and other numerical representations. The resultant system-level model was developed with the GoldSim software package. The system model was used to transfer information between models, to propagate uncertainties, and to integrate the results. The performance assessment modeling represented the present-day IDF and was used to estimate the releases of radioactivity to the environment for thousands of years into the future. Though performance assessment models cannot be validated in the traditional manner of other numerical models, performance assessment models must have adequate support of the results for the models intended purpose.

DOE presented the information used to develop the modeling in the PA report (RPP-RPT-59958, Rev. 1, 2018). The PA report was very extensive. Technical studies have been completed for decades at the Hanford site on a wide range of topics (e.g., infiltration, waste release, hydrology). Though studies have been completed to evaluate the performance of systems (e.g., engineered cover performance, unsaturated zone hydrology) and other studies are planned (e.g., glass lysimeter studies), most of the technical work has been used to develop parameter values for input to the various models, rather than to develop confirmatory information supporting the results of the PA models or the underlying conceptual models. DOE provided limited support that the conceptual models were implemented appropriately with the numerical models in the PA or that the model projections would likely bound anticipated impacts.

The IDF in its current configuration has been in existence for almost 15 years, with initial construction completed much earlier. DOE has completed numerous iterations of performance assessment calculations over the years, with the current calculations being performed prior (2018) to the recent WMA-C performance assessment that NRC reviewed (2019). In the IDF PA, DOE could not incorporate lessons learned or address recommendations made by NRC on WMA-C, one of which was for increased model support. Model support is an essential element of numerical modeling, especially of complex systems. Key intermediate results of the PA modeling include, but are not limited to, the secondary minerals that form during glass corrosion, the amount of water that contacts the wasteforms (capillary effects included), the transport time of radionuclides to the underlying aquifer, and the amount of dilution in the aquifer. Support should be provided for the key intermediate results of the numerical modeling. For example, on page 3-170 of the PA document a discussion of groundwater contaminants on the Central Plateau is provided. One of those contaminants listed is ^{90}Sr . The PA model, with appropriate changes to inputs to represent operating conditions, should be able to produce a travel time of ^{90}Sr to the water table in the approximately 40 years that was observed. It isn't clear that the existing model could generate the observed result, suggesting some aspect of infiltration, geology and properties of the unsaturated zone, unsaturated zone hydrology, or unsaturated zone geochemistry may not

be appropriate. The potential non-uniqueness of calibrated inputs places greater importance on confidence-building activities.

Because of the importance of model support to the decision-making process, a dedicated plan, strategy, and document summarizing model support for the VLAW PA could enhance confidence that the numerical models adequately project or bound future impacts.

Path Forward

Please provide a summary of model confidence-building activities for the VLAW PA model or provide DOE's strategy and plan for future verification activities that are anticipated to be completed. Describe activities that have been included in the PA maintenance plan. Complete modeling with the PA model used for the VLAW PA that shows that transport of ⁹⁰Sr to the aquifer can be generated in the modeling results under reasonable historical operating conditions.

DOE Response

Response will be provided in Revision 1 of this document.

References

RPP-RPT-59958, 2018, *Performance Assessment for the Integrated Disposal Facility, Hanford Site*, Rev. 1, Washington, Department of Energy, Richland, Washington.

RAI 2-3 (PA Modeling Discretization)**Comment**

From the information provided, it isn't clear that the numerical model utilized had a discretization sufficient to ensure acceptable accuracy.

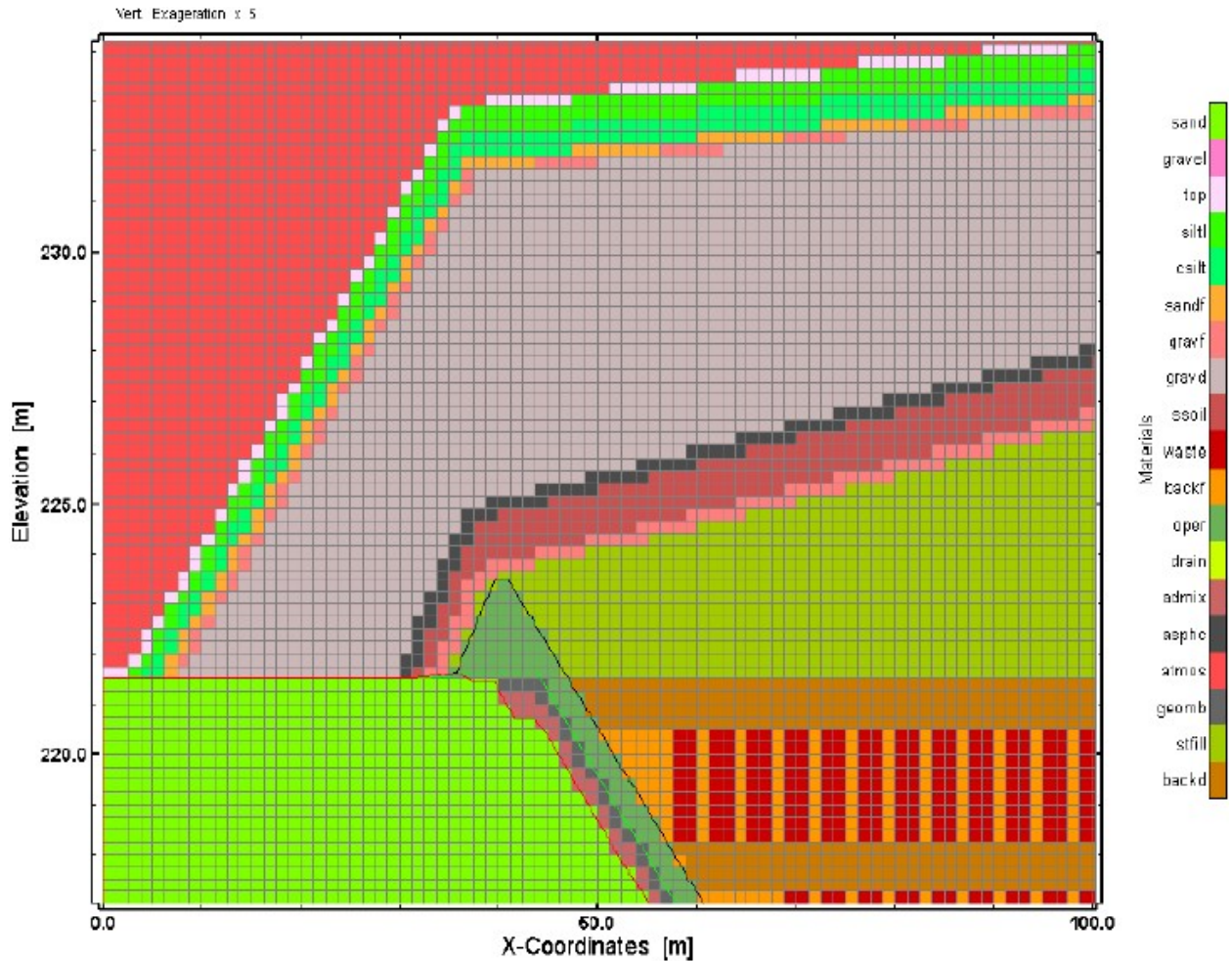
Basis

STOMP modeling was used to estimate the flow of water through the different materials in the system (e.g., engineered cover, wasteforms, unsaturated zone) and to calculate the flux rates of radionuclides from the wasteforms to the unsaturated zone. Numerical modeling of materials with very different properties, especially moisture characteristic curves which describe the unsaturated flow processes, must use a discretization of the model that is fine enough such that the numerical modeling results have converged and are sufficiently precise.

Figure 4-22 from the PA document (shown below), provided the numerical grid and material properties assigned for near-field flow. It appears that some layers are not continuous in the model. It is not clear how the discretization was fine enough to ensure proper precision. The text of the PA document describes the stair-stepped discretization but does not explain how it was determined that the model discretization was sufficient. The potential impact is shown in Figure 5-11 from the PA document (partial figure provided below) where the saturation values and liquid flux rates appear to have large variations as a result of the numerical grid selection.

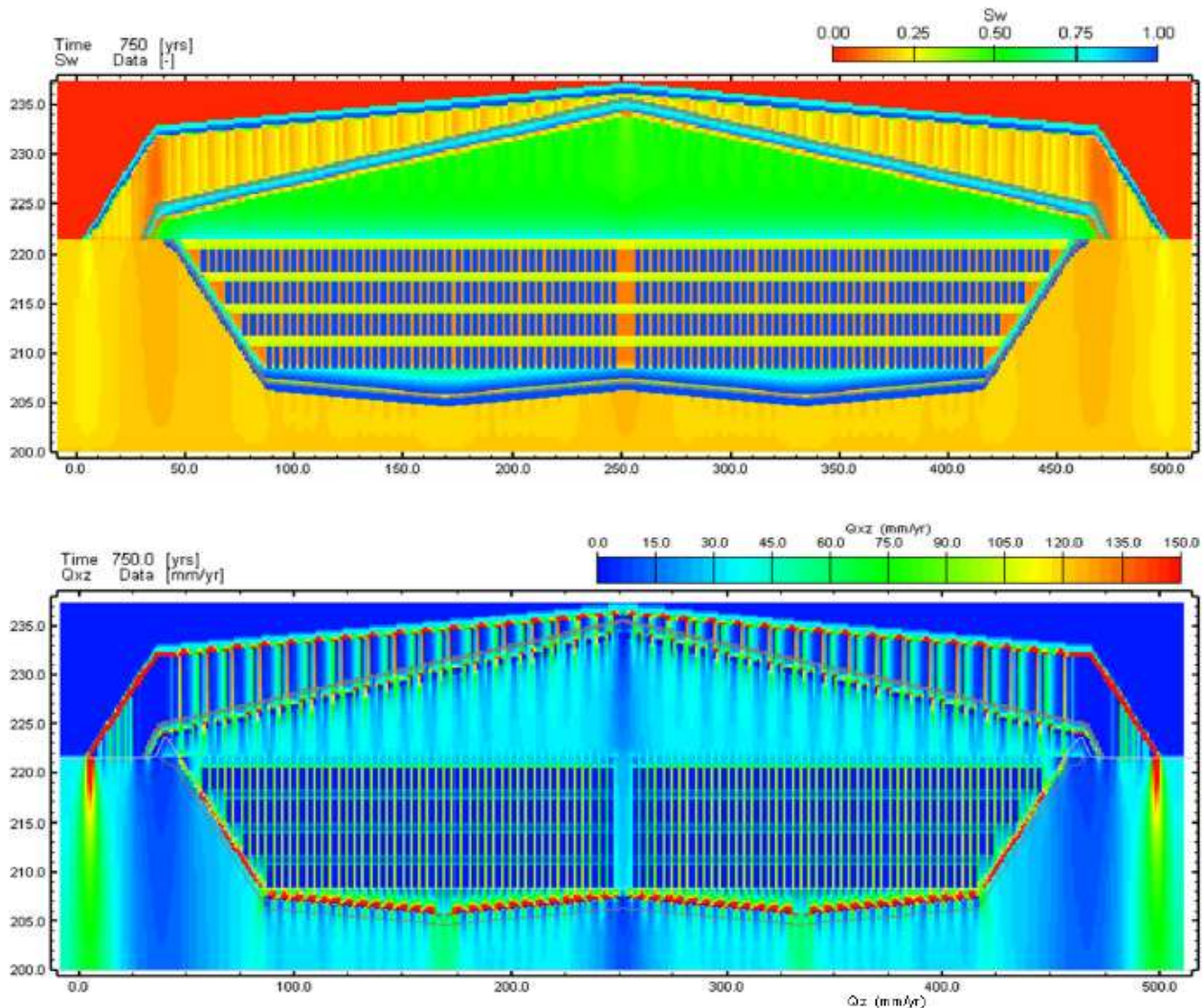
DOE described the discretization of the model for glass degradation on page 5-49 of the PA document. An attempt was made to strike a balance between computational time and accuracy. Modeling with a 2 cm by 2 cm grid spacing resulted in execution times of over a month per simulation. The resultant fractional release rate (FRR) from the glass was 26% higher than the coarser grid, which DOE did not believe was significant in the context of performance assessment uncertainties. A 2 cm grid spacing is extremely coarse to represent the processes occurring at the glass/engineered system interface. Layers that are tens of microns thick can significantly influence the ingress and egress of species at the interface. With only two data points with respect to the influence of grid discretization, it is unknown how much the FRR's will increase as the grid spacing is further refined and at what point further refinement will have a minimal impact.

Figure 2-3-1. Two-Dimensional Vertical Cross-Section Model of Integrated Disposal Facility Showing Numerical Grid and Surface Barrier Materials.



Source: Figure 4-22 of RPP-RPT-59958, *Performance Assessment for the Integrated Disposal Facility, Hanford Site, Washington*.

Figure 2-3-2. CLD3-Infiltration: 33.0 mm/yr Spatial Distribution of Saturation (Top) and Magnitude of Water Fluxes (Middle), and Vertical Fluxes (Bottom) at 750 years [After Cover/Liner Degradation].



Source: Figure 5-11 of RPP-RPT-59958, *Performance Assessment for the Integrated Disposal Facility, Hanford Site, Washington*.

Path Forward

Please provide additional basis for the discretization of the numerical models used in the PA to simulate near-field flow, release, and transport. Demonstrate that the simulated releases were not artificially biased by the stair-stepped grid representation of the slopes of the engineered cover and liner system. Provide a basis for the amount of increase, at the limit, on the FRR's from the glass as a function of refined numerical grids for release, and how the model should appropriately account for the uncertainty of a coarser numerical grid.

DOE Response

Grid Discretization in the Two-Dimensional Near-Field Flow Model:

DOE acknowledges that the discontinuous layers of the engineered surface barrier in the two-dimensional (2D) near-field flow model depicted in RPP-RPT-59958, Figure 4-22 do not physically represent the continuous layers that would be constructed in the barrier above the IDF. The discontinuous nature of the model layers in the surface barrier are a result of the selected grid size used to represent the engineered surface barrier, but DOE believes that the grid size was adequate for the intended purpose of the model, which was to investigate moisture distribution in the vicinity of the waste containers and through the IDF liner system. The simulation results were then used to develop boundary conditions for radionuclide fate and transport simulations; the near-field flow model was not used to simulate radionuclide fate and transport.

The numerical grid in the near-field flow model of the IDF simulates flow in the surface barrier, through and around the IDF waste region, and through the liner system into the vadose zone beneath the IDF. The model was used to verify a flow boundary condition for the waste form release models; the model was not used to simulate radionuclide release and transport from the waste forms to the bottom of the IDF. Similarly, the near-field flow model was also used to develop a flow boundary condition for the vadose zone flow and transport model that simulated flow and radionuclide transport from the top of the vadose zone just below the liner system down to the groundwater. The near-field flow model was not used to simulate transport of radionuclides to the groundwater.

The 2D representation of the Modified *Resource Conservation and Recovery Act of 1976* (RCRA) Subtitle C barriers focused on the capillary barrier effect of the different layers having different hydraulic and unsaturated flow properties. Simplifications in terms of discretization and assigned hydraulic properties based on the data package report PNNL-23711, *Physical, Hydraulic, and Transport Properties of Sediments and Engineered Materials Associated with Hanford Immobilized Low-Activity Waste* were biased toward conservative properties with regard to vertical flow through the different layers. This was done by increasing the hydraulic conductivity of the asphalt layer and decreasing the hydraulic conductivity of the gravel drain layers compared to the values given in the data package report (Table 4-7 in RPP-RPT-59958). The simplified discretization using a rectangular finite difference grid resulted in discontinuous sand- and gravel-filter layers overlying the gravel drain layer, resulting in non-uniform vertical flow. The capillary barrier effect of the gravel drain layer and associated lateral flow in the overlying layers is somewhat diminished, due to the reduced hydraulic and unsaturated flow properties of the gravel drain.

Except where additional resolution was a priori believed to be necessary, the vertical thickness of each node in the near-field flow model is predominantly 0.25 m. Near the apex of the asphalt layer of the surface barrier, the node thickness reduces to 0.15 m for three node layers; the thicknesses of the nodes containing the liner system are 0.125 m; and the top of the vadose zone below two 0.25-m thick grid cells at the bottom of the liner system has a node thickness of 0.5 m. A single 0.15-m thick node is also included at the elevation for the top of the berm used to raise the liner above present-day ground surface.

The discontinuous appearance of the engineered layers in the model of the cover system occurs because the thickness of the engineered layers may be less than the thickness of the nodes representing each layer (0.25 m). For instance, the design basis for the Modified RCRA Subtitle C cover (described in the IDF Facility Data package RPP-20691, *Facility Data for the Hanford Integrated Disposal Facility Performance Assessment*, Section 5.0) includes a 10-cm thick asphalt base layer, a 15-cm thick asphalt layer, a gravel drainage layer with a variable thickness that has a minimum value of 15-cm, a 15-cm thick gravel filter layer, and a 15-cm thick sand filter layer. Each of these layers is angled with a 2° to 5° slope to promote drainage while minimizing erosion. Due to the slope of the layers, multiple node layers smaller than 15-cm thickness would have been needed to form a continuous layer across the width of the barrier or a complex gridding scheme would have been necessary. DOE decided to forego this refinement because the engineered surface barrier was not being modeled to predict its performance to reduce precipitation to net infiltration. Net infiltration rates have been negotiated between DOE and the Washington State Department of Ecology. The prescribed net infiltration rates (0.5 mm/yr under an intact surface barrier and 3.5 mm/yr under a degraded surface barrier) are used as a boundary condition for the waste form release models, not the rates simulated using the near-field flow model.

The near-field flow model was also used to develop estimates of saturations in the backfill and waste forms in the absence of long-term data and evaluate the distribution of moisture into the vadose zone in the presence of an intact and a degraded liner system.

The near-field flow modeling was limited to unsaturated flow through the IDF including the preliminary design of the surface barrier above the IDF waste area and the existing liner system at the base of the trench. Moreover, the representation of the different components of the surface barrier and liner system was simplified to evaluate moisture distribution throughout the IDF and the potential for the liner system to distribute flow into the top of the vadose zone below the IDF. The examination of the model results distributing flow into the vadose zone was used to identify distinct zones associated with the IDF footprint, where the recharge rates are enhanced or reduced compared to the ambient recharge rate at land surface. This redistribution of moisture provided the flow boundary condition at the top of the vadose zone for far-field flow and transport modeling. This was done for different ambient recharge rates, and for different time periods, as described in detail in Section 4.4.2.1.4 in RPP-RPT-59958. A key finding of the near-field flow model was that even with degraded properties of the liner system, the liner system caused moisture to flow laterally towards the sumps. Eventually, saturations above the sumps would result in a head pressure that was sufficient to cause flow through the liner system into the vadose zone. This resulted in a vadose zone flow profile that is much different than if the liner system were not present. This observation also reduces the potential flow consequences of the stair stepping imposed by the coarse gridding in the engineered surface cover layers.

In addition to the distributed infiltration scenario, which was considered as the base case, a uniform infiltration scenario that distributed all the flow into the IDF across the top of the vadose zone below the IDF was used as the other end-member scenario. The mapping of the simulated flow rates computed using the 2D near-field flow model to the top of the three-dimensional (3D) model required averaging over the different grid sizes between the detailed 2D cross section grid for the near-field flow model and the coarser 3D surface grid for the vadose zone flow and

transport model. The resulting distributed infiltration rates are mapped in a simplified manner as prescribed recharge rate distribution in the 3D vadose zone model as described in Section 5.1.1.5 in RPP-RPT-59958. This resulted in distributed infiltration cases with net infiltration rates of 1.7 mm/yr, 3.5 mm/yr, and 5 mm/yr. These three net infiltration rates were also used as flow boundary conditions for the advective-diffusive transport models simulating release of constituents of potential concern (COPCs) from the cementitious waste forms and VLAW in RPP-CALC-61030, *Cementitious Waste Form Release Calculations for the Integrated Disposal Facility Performance Assessment* and RPP-CALC-61031, *Low-Activity Waste Glass Release Calculations for the Integrated Disposal Facility Performance Assessment*. No distributed infiltration scenario was considered for sensitivity cases that applied ambient infiltration rates of 0.9 mm/yr and 33 mm/yr; near-field flow models for these conditions indicated reduced or negligible variations in the distribution of flow into the top of the vadose zone across the footprint of the IDF.

Simplifications in the near-field model in representing the different components of the surface barrier and liner combined with limited sensitivity cases in terms of material properties were based on the fact that the cover represented a preliminary design concept. The maintenance plan (CHPRC-03348, *Performance Assessment Maintenance Plan for the Integrated Disposal Facility*) includes future studies on barrier performance based on information learned from historical and current studies on surface barrier concepts at other Hanford sites, including the Prototype Hanford Barrier (DOE/RL-2016-37, *Prototype Hanford Barrier 1994 to 2015*). The hydraulic properties and flow through the surface barrier are listed as a key assumption in the IDF PA (Table 8-6 in RPP-RPT-59958) and potential maintenance approaches include review of as-constructed information from similar barriers at other closed facilities at Hanford (i.e., Environmental Restoration Disposal Facility [ERDF] or Waste Management Area [WMA] C). As performance data is collected on similarly constructed barriers, DOE will evaluate these key assumptions included in the IDF PA.

Grid Discretization in the Vitrified Waste Release Model:

Simulating corrosion of vitrified waste did not investigate grid spacing finer than 2 cm. As indicated in the IDF PA (RPP-RPT-59958 Section 5.1.2.2), simulations of LAWA44 glass using a 2-cm grid spacing required one and a half months to run to completion. The resultant fractional release rate ($2.04\text{E-}07 \text{ yr-}1$) was 51% higher than a simulation with 15-cm grid spacing ($1.35\text{E-}07 \text{ yr-}1$). By the time the 2-cm run was complete and the results were evaluated, there was not enough time and computational resources to both investigate finer grid spacing and complete the suite of analyses planned for the IDF PA. Additional evaluations around the grid spacing were not performed. Instead, the simulated corrosion rate used in the PA base case was fixed at a value, $2.5\text{E-}07 \text{ yr-}1$, that is 40% higher than the highest corrosion rate calculated for a single waste package using the 15-cm spacing for either LAWA44 glass ($1.35\text{E-}07 \text{ yr-}1$), LAWB45 glass ($8.27\text{E-}09 \text{ yr-}1$) or LAWC22 glass ($1.78\text{E-}07 \text{ yr-}1$) (RPP-CALC-61031 Tables 6-2, 6-3, and 6-4) and 22.5% higher than calculated for a single LAWA44 waste package using the 2-cm spacing. The result is comparable to the highest corrosion rate calculated for four stacked waste containers using a 15-cm grid spacing [LAWC22 STOMP(c)³⁰ rate was $2.52\text{E-}07 \text{ yr-}1$].

³⁰ Subsurface Transport Over Multiple Phases (STOMP) is developed and distributed by Battelle Memorial Institute.

In the release calculations for the 2005 PA (PNNL-15198, *Waste Form Release Calculations for the 2005 Integrated Disposal Facility Performance Assessment*), the investigators used a 2-cm grid spacing to simulate vitrified waste corrosion with the STORM³¹ code (Subsurface Transport Over Reactive Multiphases) and compared the results to a simulation that used 1-cm grid spacing. They concluded that the results were not significantly different from each other (PNNL-15198 Section 2.2.2). Similar conclusions were made for the 2001 PA when grid spacing at 5 cm and 2.5 cm were compared (PNNL-13369, *Waste Form Release Calculations for the 2001 Immobilized Low-Activity Waste Performance Assessment*, page 5). No additional uncertainty was applied to the $2.5\text{E-}07\text{ yr}^{-1}$ corrosion rate applied in the PA to account for grid size resolution. The vitrified waste corrosion rate is applied to all containers of vitrified waste, even those whose corrosion rate based on the glass type is expected to be lower than the corrosion rate for Envelope C glass. Therefore, there is already some pessimism included in the vitrified waste releases in the base case. Furthermore, the uncertainty analysis includes multiple sources of uncertainty that increase the vitrified waste corrosion rate by up to a factor of 30 times higher than the base case rate (additional discussion is presented in response to RAI 2-7). In the uncertainty analysis, DOE's limit on dose was not exceeded in 1,000 or 10,000 years.

³¹ Subsurface Transport Over Reactive Multiphases was developed by Pacific Northwest National Laboratory, Richland, Washington.

References

- CHPRC-03348, 2019, *Performance Assessment Maintenance Plan for the Integrated Disposal Facility*, Rev. 1, INTERA, Inc./CH2M HILL Plateau Remediation Company, Richland, Washington.
- DOE/RL-2016-37, 2016, *Prototype Hanford Barrier 1994 to 2015*, Rev. 0, U.S. Department of Energy, Office of River Protection, Richland, Washington.
- PNNL-13369, 2001, *Waste Form Release Calculations for the 2001 Immobilized Low-Activity Waste Performance Assessment*, Pacific Northwest National Laboratory, Richland, Washington.
- PNNL-15198, 2005, *Waste Form Release Calculations for the 2005 Integrated Disposal Facility Performance Assessment*, Pacific Northwest National Laboratory, Richland, Washington.
- PNNL-23711, 2015, *Physical, Hydraulic, and Transport Properties of Sediments and Engineered Materials Associated with Hanford Immobilized Low-Activity Waste*, RPT-IGTP-004, Rev. 0, Pacific Northwest National Laboratory, Richland, Washington.
- Resource Conservation and Recovery Act of 1976*, 42 USC 6901, et seq.
- RPP-20691, 2015, *Facility Data for the Hanford Integrated Disposal Facility Performance Assessment*, Rev. 1, CH2M HILL Plateau Remediation Company, Richland, Washington.
- RPP-CALC-61030, 2017, *Cementitious Waste Form Release Calculations for the Integrated Disposal Facility Performance Assessment*, Rev. 0, INTERA, Inc. for Washington River Protection Solutions, LLC, Richland, Washington.
- RPP-CALC-61031, 2017, *Low-Activity Waste Glass Release Calculations for the Integrated Disposal Facility Performance Assessment*, Rev. 0, INTERA, Inc. for Washington River Protection Solutions, LLC, Richland, Washington.
- RPP-RPT-59958, 2019, *Performance Assessment for the Integrated Disposal Facility, Hanford Site, Washington*, Rev. 1A, Washington River Protection Solutions, LLC, Richland, Washington.

RAI 2-4 (Near-field and UZ Modeling Approach)**Comment**

Use of uniform properties and discrete layers may not yield accurate contaminant flux rates primarily for near-field flow.

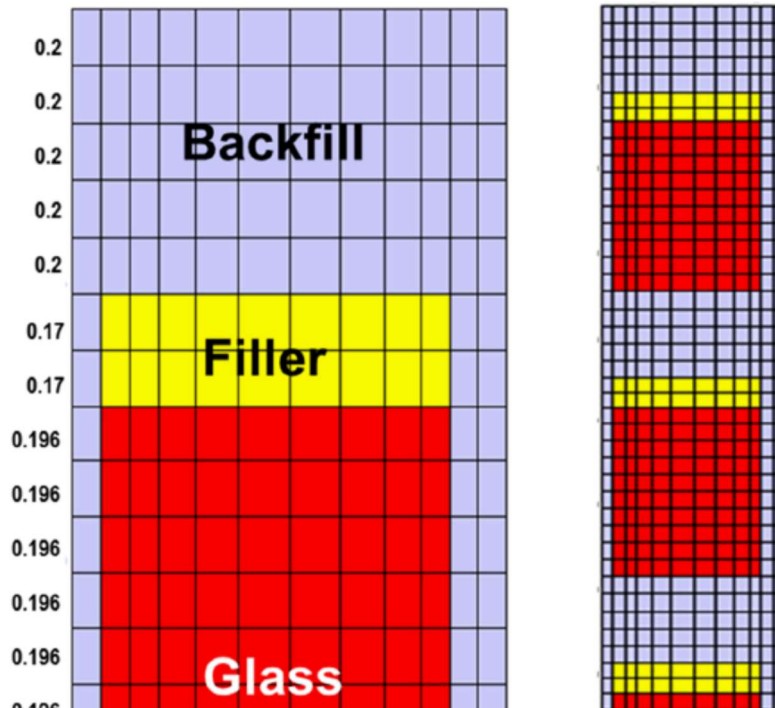
Basis

DOE assigned uniform hydrologic properties for different material layers in the simulation domain. Moisture characteristic curves (MCC's) are used to describe the relationships between saturations, pore pressures, and hydraulic conductivity. MCC's can take different forms, with some of the most common being Van Genuchten and Brooks/Corey. These relationships are derived by the fitting of empirical data to mathematical expressions. The data are generally uncertain and therefore the derived parameters are also uncertain. DOE recognized this uncertainty. For the unsaturated zone, a number of measurements were available to derive the parameters. Data on particle-size distribution, moisture retention, and saturated hydraulic conductivity (Ks) were cataloged for over 284 samples from throughout the Hanford Site, including locations in the 200 East and West Areas (PNNL-13672, "A Catalog of Vadose Zone Hydraulic Properties for the Hanford Site"). By comparison, very limited samples were available to define MCC's for the hydrologic layers within the boundaries of the engineered disposal facility.

Throughout the PA document (for example page 5-19), DOE indicated that highly permeable layers, such as the drainage layers, act as capillary barriers under most conditions. In addition, Table 5-14 showed that the simulated flux of water through the wastefrom is approximately ten times less than the infiltration rate. Adequate model support was not provided for the simulated capillary barrier effects provided by the modeling. The figure below (Figure 5-1 from RPPCALC-61031) shows the coarse discretization and discrete layers used in the near-field modeling. It isn't clear how much of the observed reduction in flow through the wastefrom is a result of the modeling approach selected.

In the real system, a fractured glass surrounded by soil will have some of the fine-grained soil that infills the fractures at the boundary of the glass (NRC notes that the glass is contained in a stainless steel canister and DOE has elected to ignore the effects of the canister). When finer scale modeling is used, water that flows along the surface of the unfractured glass will enter the fractures and saturations can build up locally resulting in dynamic rivulets of flow which otherwise would not be observed in the coarse-scale modeling with large timesteps. In addition, the MCC parameters have natural variability which is not represented in the DOE modeling approach where uniform properties are prescribed for every cell of a given material type. Modeling of the capillary barrier effect using heterogeneous properties showed much earlier breakthrough of moisture than would be estimated using homogeneous properties (Ho and Webb, 1998).

Figure 2-4-1. Grids for Alternative Disposal Configurations Involving One Waste Package or Four Vertically Stacked Waste Packages.



Source: Figure 5-1 of RPP-CALC-61031, *Low-Activity Waste Glass Release Calculations for the Integrated Disposal Facility Performance Assessment*.

Path Forward

Please provide information that demonstrates that the numerical grids used for near-field flow were sufficient to evaluate performance. This could include performing numerical modeling of near-field flow and transport using refined spatial and temporal representations with natural heterogeneity. Please provide additional support for the numerical model results.

DOE Response

Response will be provided in Revision 1 of this document.

References

PNNL-13672, 2001, *A Catalog of Vadose Zone Hydraulic Properties for the Hanford Site*, Pacific Northwest National Laboratory, Richland, Washington.

RPP-CALC-61031, 2017, *Low-Activity Waste Glass Release Calculations for the Integrated Disposal Facility Performance Assessment*, Rev. 0, INTERA, Inc. for Washington River Protection Solutions, LLC, Richland, Washington.

RPP-RPT-59958, 2019, *Performance Assessment for the Integrated Disposal Facility, Hanford Site, Washington*, Rev. 1A, Washington River Protection Solutions, LLC, Richland, Washington.

RAI 2-5 (Disposition of Nitrate)**Comment**

Previous evaluations by DOE had a large amount of nitrate (9×10^6 kg) that would be disposed of in IDF. The current inventory cases have values ranging from 1.6×10^5 kg to 2.2×10^6 kg. It is not clear how the nitrate is being removed or where it will be disposed.

Basis

Previous studies identified high nitrate feed as a potential problem for the productions of high performance glass (RPP-54130, 2012). The Environmental Impact Statement (EIS) had about nine million kilograms of nitrate in the waste feed whereas the present PA for IDF has about 1.6×10^5 to 2.2×10^6 kg depending on the inventory case (DOE/EIS-0391, 2012). It wasn't clear to the staff how the nitrate is being removed or where and how it will be disposed.

Path Forward

Please describe the removal and disposition of nitrate from the waste feed for VLAW.

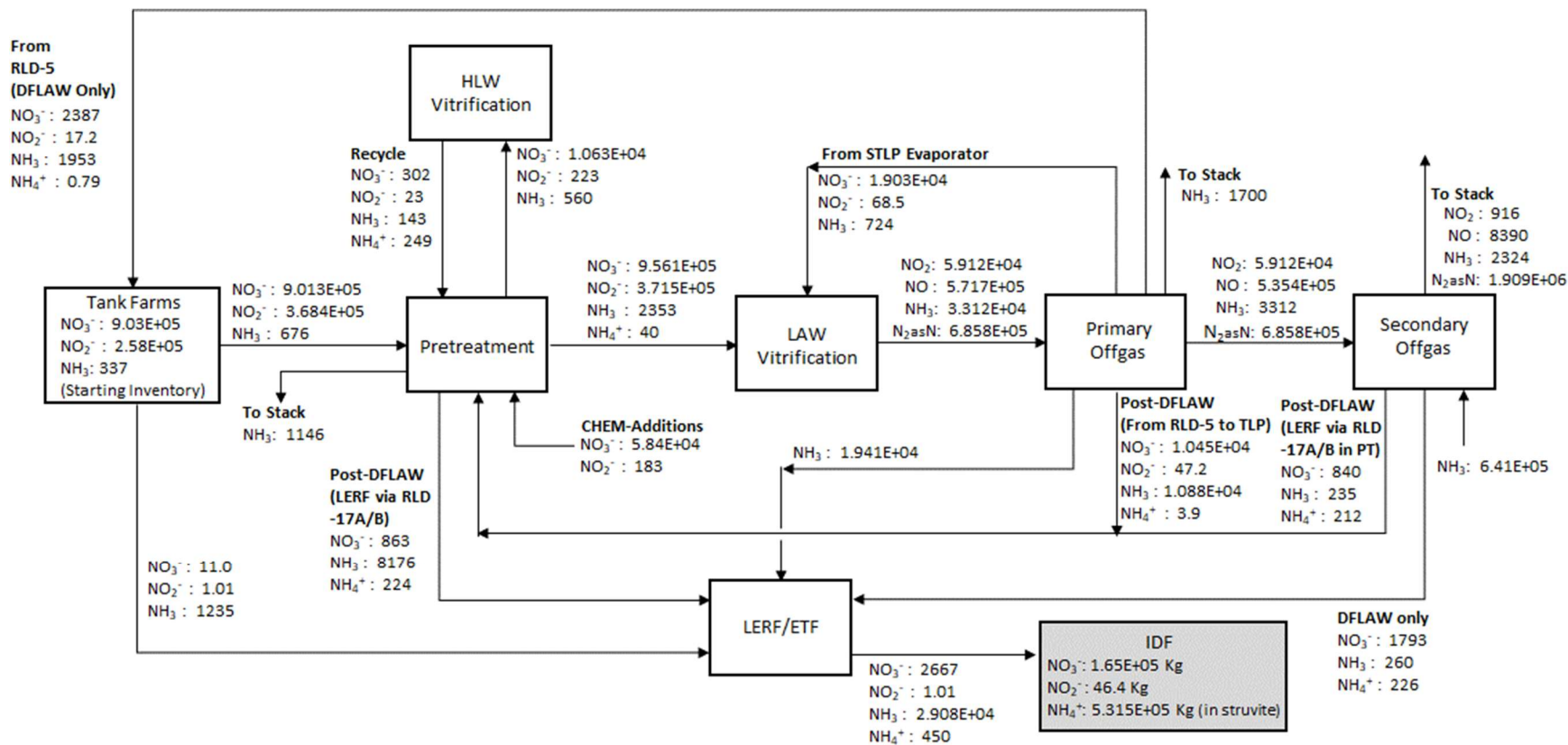
DOE Response

Nitrate is the most prominent anion present in LAW feed. Nitrite is also present but typically at lower concentrations. There is a total of 9.6×10^5 kilogram-moles (kmol) (5.9×10^7 kg) of nitrate and 3.7×10^5 kmol (1.7×10^7 kg) of nitrite in the pretreated LAW, which will be vitrified in the Hanford LAW Vitrification Facility. The majority of nitrates (nitrate + nitrite) fed to LAW vitrification are converted to nitrogen gas and ammonia in the melter and the melter off-gas system. A small fraction of the nitrates accumulate in the off-gas condensate evaporator overheads and caustic scrubber liquid effluent. Those streams are routed to the Liquid Effluent Retention Facility (LERF)/Effluent Treatment Facility (ETF) where they are incorporated into the liquid secondary waste (LSW) and immobilized in grout for disposal in the IDF.

Nitrates can cause deleterious effects during vitrification. Of greatest concern, as noted in RPP-54130, *Technetium Retention in WTP LAW Glass with Recycle Flow-Sheet: DM10 Melter Testing, VSL-12R2640-1, Rev. 0*, is the potential for foaming in the melt. This will be controlled by adding sucrose as a reductant to react with the nitrates ($\text{NO}_3^-/\text{NO}_2^-$) as described in Section 2.3 of RPP-54130. The exothermic reactions of sucrose with nitrates also provide heat, which enhances conversion of feed and glass formers to oxides in the cold cap and increases melt rate. The amount of sucrose added is less than what would be needed to convert all of the nitrate/nitrite to nitrogen gas to avoid over-reducing the melt. Too much reductant can lead to formation of sulfides and molten metals.

A summary material balance for nitrates and nitrogen compounds across the LAW Vitrification system, expressed in kmol, for the IDF PA (RPP-RPT-59958) base case is presented in Figure 2-5-1. The material balance is from the HTWOS model run performed to support the IDF PA (RPP-RPT-23412, *Hanford Tank Waste Operations Simulator Model Data Package for the Development Run for the Refined Target Case*). The material balance calculations are based on reactions described in 24590-WTP-RPT-PT-02-005, *Flowsheet Bases, Assumptions, and Requirements*, Rev. 7, which in turn are based on data from melter runs with simulants performed at the Vitreous State Laboratory (VSL).

Figure 2-5-1. Low-Activity Waste/Supplemental Low-Activity Waste Nitrogen Balance in Kmol by Contributor.



CHEM = Chemical
 DFLAW = Direct-Feed Low-Activity Waste
 ETF = Effluent Treatment Facility
 HLW = high-level radioactive waste

IDF = Integrated Disposal Facility
 LAW = low-activity waste
 LERF = Liquid Effluent Retention Facility
 PT = Pretreatment

RLD = Radioactive Liquid Waste Disposal
 STLP = Supplemental Treated LAW Evaporation Process
 TLP = Treated LAW Evaporation Process

Pretreated LAW is fed to the melters where nitrate/nitrite are converted to NO₂, NO, N₂, and NH₃ gases by reduction with sucrose. Approximately 50% of the nitrate/nitrite in the LAW feed is converted to N₂ gas (reported as kmol N in Figure 2-5-1) in the melter. Small amounts of the NO₂ and NO that remain in the melter off-gas are removed, converted to NO₃⁻ in the primary off-gas system, and recycled for blending with LAW feed. The secondary off-gas system includes an SCR designed to reduce most of the remaining NO₂ and NO to N₂ gas in order to minimize airborne emissions of regulated NO_x compounds. The SCR is followed by a caustic scrubber that captures about 20% of the residual NO₂/NO exiting the SCR as aqueous NO₃⁻. During DFLAW the liquid effluent from the caustic scrubber is routed directly to the LERF/ETF. All streams entering the LERF/ETF are summed to determine the total nitrate/nitrite for disposal in the IDF. The main contribution to the IDF inventory will be secondary waste from the caustic scrubber during DFLAW. Following DFLAW operations, the main contribution will be condensate from evaporation of liquid effluents from both the LAW and supplemental LAW vitrification off-gas treatment systems.³² The total nitrate, to be disposed of in the IDF from LSW streams as a result of treating LAW waste both during and post-DFLAW, is estimated to be about 1.6E+05 kg for the IDF PA base case.

The estimated inventory of nitrate present in the grouted ETF SSW used for the Tank Closure and Waste Management Environmental Impact Statement (TC&WM EIS)³³ analysis is based on an HTWOS model run that was performed in 2005 (RPP-RPT-23412) which predates the model runs performed to support the IDF PA by a decade. The model results were further interpreted by the EIS analysts and preparers and the nitrate inventory may have been chosen to represent a bounding case for impact analysis purposes. The inventory of 9E+06 kg of nitrates (NO₃⁻ + NO₂⁻ expressed as NO₃⁻ to simplify the analysis) represents about 13% of the tank waste inventory used for the EIS analysis. Since that time the understanding of the technology and the waste treatment flowsheet have matured substantially, and it is reasonable to project that only a small fraction of nitrate will survive the LAW vitrification and off-gas treatment processes and be incorporated in the grouted ETF LSW assumed to be disposed of in the IDF.

³² Information concerning the secondary waste associated with the supplemental LAW is provided in this RAI response for additional information and completeness only, and is outside the scope of both the Draft WIR Evaluation and DOE decisions concerning supplemental LAW treatment. DOE has not made decisions concerning the potential path forward for supplemental LAW treatment, as explained in footnote 7 of the Draft WIR Evaluation and 78 FR 75913, "Record of Decision: Final Tank Closure and Waste Management Environmental Impact Statement for the Hanford Site, Richland, Washington." As explained in Section 1.2 of the Draft WIR Evaluation, the Draft WIR Evaluation does not address or include in its scope supplemental LAW. To bound the IDF PA analysis, the IDF PA assumed that supplemental LAW may potentially be vitrified and disposed of in the IDF, although, as explained above, DOE has made no decisions concerning the potential path forward for supplemental LAW treatment.

³³ DOE/EIS-0391, *Final Tank Closure and Waste Management Environmental Impact Statement for the Hanford Site, Richland, Washington*.

References

- 24590-WTP-RPT-PT-02-005, 2013, *Flowsheet Bases, Assumptions, and Requirements*, Rev. 7, Bechtel, River Protection Project, Waste Treatment Plant, Richland, Washington.
- 78 FR 75913, 2013, “Record of Decision: Final Tank Closure and Waste Management Environmental Impact Statement for the Hanford Site, Richland, Washington,” *Federal Register*, Vol. 78, pp. 75913–75919 (December 13).
- DOE/EIS-0391, 2012, *Final Tank Closure and Waste Management Environmental Impact Statement for the Hanford Site, Richland, Washington*, U.S. Department of Energy, Washington, D.C.
- RPP-54130, 2012, *Technetium Retention in WTP LAW Glass with Recycle Flow-Sheet: DM10 Melter Testing, VSL-12R2640-1, Rev. 0*, Vitreous State Laboratory, The Catholic University of America/EnergySolutions, Federal EPC, Inc./Washington River Protection Solutions LLC, Richland, Washington.
- RPP-RPT-23412, 2005, *Hanford Tank Waste Operations Simulator Model Data Package for the Development Run for the Refined Target Case*, Rev. 1, CH2M HILL Hanford Group, Inc., Richland, Washington.
- RPP-RPT-59958, 2019, *Performance Assessment for the Integrated Disposal Facility, Hanford Site, Washington*, Rev. 1A, Washington River Protection Solutions, LLC and INTERA, Inc., Richland, Washington.

RAI 2-6 (Glass Wasteform and Volatile Species Distribution)**Comment**

Additional information is necessary to demonstrate that volatile species would be uniformly distributed in the glass inside a canister after cooling.

Basis

Volatilization of certain radionuclides (^{99}Tc , ^{129}I , ^{137}Cs) during glass production is well-known but also presents a challenge. DOE's assessment of glass performance in the VLOW PA assumed that volatile species retained in the glass will be uniformly distributed throughout the glass matrix. Volatilization and subsequent deposition of certain radionuclides during the cooling process may result in a non-uniform distribution of activity (e.g., ^{99}Tc) within the waste canister. Deposited radionuclides at the surface of the glass or on the walls of the canister would be available for more rapid release than the 1×10^{-7} to 1×10^{-8} 1/yr fractional release rates calculated in the PA.

The volatilization temperature of ^{99}Tc is well below the glass melting point (Tc_2O_7 boils at 311C) such that after production and prior to solidification, ^{99}Tc may be volatilized during the cooling of the glass wasteform. In addition, the glass may have a significant temperature gradient from the centerline to the walls of the canister for production-scale canisters creating complex dynamics in terms of gas and liquid flows. Experiments on the laboratory-scale demonstrated that up to 20% of volatile species were deposited on the walls of crucibles and ampules during testing (Kim, 2017). Experiments completed to examine the impact of a fire on a solidified glass canister showed that not only could cesium that had been immobilized in a glass matrix be volatilized but that it ended up as a gas in the head space of the canister (PNNL-11052, 1996).

In RPP-54130, the distribution of Tc was estimated throughout a glass production system with recycle of the off-gas. Sulfate salt phases were observed on the melt pool surfaces. The salt phases showed an approximate fifty-fold enrichment in concentrations of Tc compared to the concentration in the glass suggesting that the distribution of Tc throughout the solidified glass may not be uniform.

Path Forward

Please provide additional basis that ^{99}Tc will be uniformly distributed in the glass of production scale canisters and that deposition on the canister surfaces will not occur. If information is not available, provide plans that describe how the assumed distribution of ^{99}Tc will be verified prior to full-scale production, or show that the results of the performance assessment, including uncertainties, are not sensitive to the distribution of ^{99}Tc within the glass wasteform.

DOE Response

Response will be provided in Revision 1 of this document.

References

Kim, D. and A. A. Kruger, 2017, *Volatile Species of Technetium and Rhenium During Waste*

PNNL-11052, 1996, *Volatility Literature of Chlorine, Iodine, Cesium, Strontium, Technetium, and Rhenium; Technetium and Rhenium Volatility Testing*, Pacific Northwest National Laboratory, Richland, Washington.

RPP-54130, 2012, *Technetium Retention in WTP LAW Glass with Recycle Flow-Sheet: DM10 Melter Testing, VSL-12R2640-1, Rev. 0*, Vitreous State Laboratory, The Catholic University of America/EnergySolutions, Federal EPC, Inc./Washington River Protection Solutions LLC, Richland, Washington.

RAI 2-7 (Glass Wasteform Fractional Release Rate)**Comment**

The development of the fractional release rate expressions to represent glass degradation may not adequately reflect all significant sources of uncertainty.

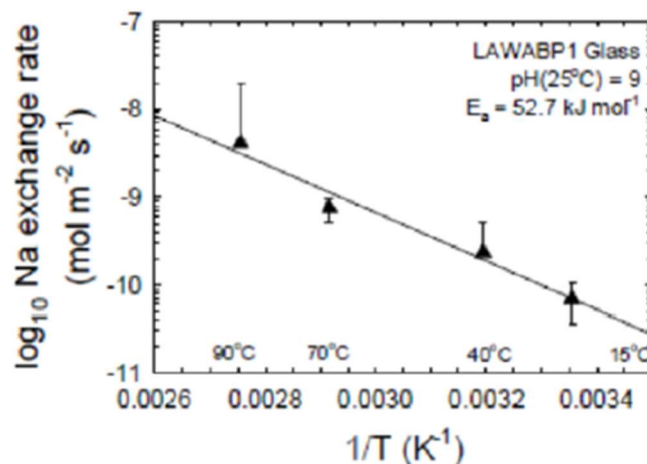
Basis

DOE developed expressions to represent the fractional release rate from glass as a function of different variables for different glass compositions. The expressions were based on the results of reactive transport calculations using process-level models (RPP-CALC-61031 and RPP-CALC-61192). Uncertainties were then represented in the expressions by performing regression on glass-type-specific kinetic dissolution parameters.

It isn't clear that the derived expressions reflect all important sources of uncertainty. The process for developing the expressions derived parameters from experimental data to then parameterize glass degradation expressions. However, the experimental data was in some cases highly uncertain and the uncertainty associated with fitting curves to the experimental data was not carried forward or was more limited than suggested by the data. In addition, some parameters, arguably the most important parameters, were set constant when the data do not suggest they should be fixed.

The figure below from PNNL-24615 shows the empirical data for determining the sodium ion exchange rate for LAWABP1 glass. The value was estimated to be 5.3×10^{-11} mol/m² s by extrapolating the data to 15 °C and assuming the value was constant in the PA (draw a line horizontally from the best fit slope at 15 °C to the y-axis). The fractional release rates are sensitive to this parameter and based on the four data points, their uncertainty, and the extrapolation of the data the basis provided by DOE was not adequate for fixing this value as a constant.

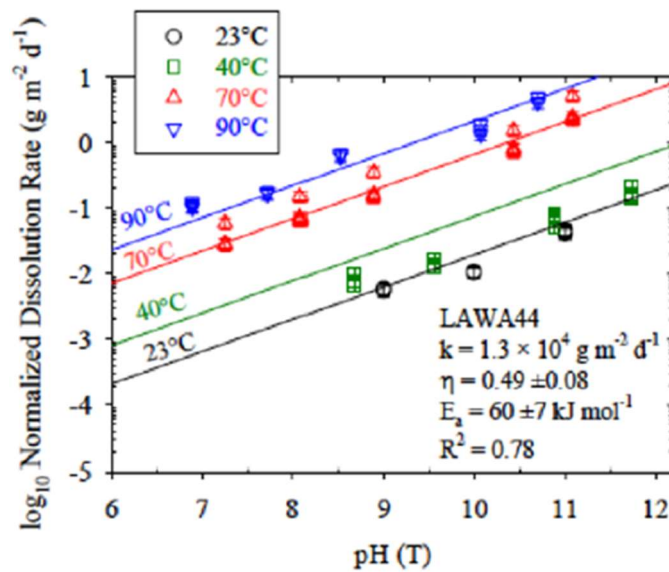
Figure 2-7-1. Sodium Ion Exchange Rate vs. Reciprocal Temperature for LAWABP1 Glass.



Source: Figure 4.6 of PNNL-24615, *Immobilized Low-Activity Waste Glass Release Data Package for the Integrated Disposal Facility Performance Assessment*.

Figure 4-7 from PNNL-24615 has a relatively poor fit of the data at 40 °C, which impacts the uncertainty assigned to the coefficients. When NRC staff attempted to use a broader range for activation energy in the FRR regression equations in order to understand the significance of the uncertainty the expression yielded non-physical results. Table 4-1 from PNNL shows the derived parameters for the different glass compositions. As implemented in the PA, the three most important parameters (the forward rate constant (k_o), the glass apparent equilibrium constant (a), the Na ion-exchange rate (r_{IEX})) were all fixed as constants. Even if the previously discussed shortcomings are dismissed, some of the derived parameters have R^2 of only 0.78 on a logarithmic scale.

Figure 2-7-2. Normalized Glass Dissolution Rate, Based on Boron, as a Function of pH(T) for LAWA44.



Source: Figure 4.7 of PNNL-24615, *Immobilized Low-Activity Waste Glass Release Data Package for the Integrated Disposal Facility Performance Assessment*.

Table 2-7-1. Summary of Rate Law Parameters for LD6-5412, LAWABP1, LAWA44, LAWB45, and LAWC22 at 15 °C.**Table 4.1.** Summary of Rate Law Parameters for LD6-5412, LAWABP1, LAWA44, LAWB45, and LAWC22 at 15 °C

Glass	Parameters							Refer
	\bar{k}_0	$K_e^{(a)}$	η	E_a	σ	I_{EX}		
	Reported Forward Rate Constant (g/[m ² d])	Converted ^(b) Forward Rate Constant (mol/[m ² s])	Glass Apparent Equilibrium Constant Based on Activity Product $a[\text{SiO}_2(\text{aq})]$	pH Power Law Coefficient	Glass Dissolution Activation Energy (kJ/mol)	Temkin Coefficient	Na Ion-Exchange Rate (mol/[m ² s])	
LD6-5412	9.7×10^9	1.8×10^0	1.14×10^{-4}	0.40 ± 0.03	74.8 ± 1.0	1	$1.74 \times 10^{-11(c)}$	McGrail et
LAWABP1	3.4×10^6	5.7×10^{-1}	4.90×10^{-4}	0.35 ± 0.03	68 ± 3.0	1	3.4×10^{-11}	McGra (200
LAWA44	1.3×10^4 ($R^2 = 0.78$)	2.2×10^{-3}	1.87×10^{-3} ($R^2 = 0.95$)	0.49 ± 0.08	60 ± 7	1	5.3×10^{-11}	Pierce et
LAWB45	1.6×10^4 ($R^2 = 0.96$)	3.0×10^{-3}	1.79×10^{-3} ($R^2 = 0.78$)	0.34 ± 0.03	53 ± 3	1	$0.0 \times 10^{0(d)}$	Pierce et
LAWC22	1.0×10^5 ($R^2 = 0.96$)	1.8×10^{-2}	1.80×10^{-3} ($R^2 = 0.94$)	0.42 ± 0.02	64 ± 2	1	1.2×10^{-10}	Pierce et

Source: Table 4.1 of PNNL-24615, *Immobilized Low-Activity Waste Glass Release Data Package for the Integrated Disposal Facility Performance Assessment*.

Additional uncertainties not reflected in the empirical FRR expressions include the assumption that the properties of laboratory-scale produced glass will be identical to production-scale glass, the Temkin coefficient was assumed to be one without empirical data to justify the selection, and the uncertainties associated with assumed secondary mineral formation in the process modeling (i.e., the need to assume Chalcedony formation without it being empirically observed).

In the PA, DOE properly took the information from the underlying technical reports, however it is not clear that in the underlying technical reports DOE properly characterized and reflected the uncertainties in the empirical data and the assumed theoretical degradation expressions.

Path Forward

Please address the treatment of the uncertainties described in the basis portion of this comment with respect to development of glass fractional release rate expressions for the PA. If necessary, revise the expressions and generate new PA results that reflect the full range of uncertainty in the glass degradation rates. NRC staff understands that a variety of sensitivity cases were examined by DOE for various uncertainties associated with glass degradation. However, most of those examinations were one-at-a-time evaluations that can be mathematically compounded but may not yield a fair assessment of the importance of these uncertainties combined with other uncertainties raised by this RAI package. If appropriate, the expressions used in the system model uncertainty analyses should be revised.

The uncertainty associated with the performance of production-scale glass may be addressed by providing DOE's performance verification plan to assure the quality and performance of production-scale glass.

DOE Response

Technical Validity of the Glass Dissolution Model Framework – In 1998, PNNL-11834, *A Strategy to Conduct an Analysis of the Long-Term Performance of Low-Activity Waste Glass in a Shallow Subsurface Disposal System at Hanford* asserted the following statement in the strategy document that has served as the basis for Hanford ILAW glass dissolution modeling for the past 22 years:

“...of all the models that have been developed to describe glass dissolution behavior, the general kinetic rate law proposed by Aagaard and Helgeson (Aagaard and Helgeson 1982) and later adapted by Grambow (Grambow 1985), best describes the majority of the experimental data that has been gathered over 35 years of studying glass/water reaction processes.”

The current relevance of the choice in PNNL-11834 to model the dissolution of Hanford LAW glass using Grambow’s transition state theory-based model coupled with alkali ion-exchange and the formation of secondary minerals is evident in the opening statement made by Fournier et al. in their 2018 paper titled “Application of GRAAL model to the resumption of International Simple Glass alteration”:

“The methodology developed for predicting nuclear waste behavior under disposal conditions combines experimental approaches and modeling. A waste glass canister placed in contact with water undergoes irreversible chemical processes leading to its degradation into more stable phases. This transformation occurs in three kinetic stages: the initial alteration rate (stage I), the residual rate (stage II), and, in some cases, a resumption of alteration (stage III) related to zeolites precipitation. Affinity effects based on the transition state theory are used to account for the rate drop from stage I to stage II.”

Note that Fournier et al. are asserting that, in 2018, the state of the art for predicting glass dissolution was consistent with rapid alteration which slows based on affinity effects according to transition state theory (as predicted by the Grambow model). Again, this is the model framework for glass dissolution identified in PNNL-11834 and currently used in the IDF PA (RPP-RPT-59341, *Integrated Disposal Facility Model Package Report: ILAW Glass Release*; PNNL-20781, *Integrated Disposal Facility FY 2011 Glass Testing Summary Report*).

Glass Dissolution Model Parameterization for the 2017 PA – Laboratory testing was used to assess the temperature and pH dependency of the rate-controlling parameters detailed in PNNL-11834. This assessment was completed on a set of prototypic ILAW glasses based on projections of glass compositions that could be produced at the WTP. Glasses were formulated for each of the original A, B, and C operating envelopes. The dissolution rate parameters measured in these tests were, excluding the Temkin coefficient (σ) which is assumed to be 1:

k_o = Dilute rate coefficient
 η = pH power law coefficient
 E_a = Dilute rate dissolution activation energy
 K_g = Pseudo-equilibrium constant
 r_{iex} = Ion exchange rate

As the NRC reviewer correctly noted, there is uncertainty associated with estimating model parameters from individual tests and this uncertainty was represented in the IDF PA modeling process by evaluating PA response over a range of properties larger than those observed experimentally (see the discussion in the next section). Since the 2017 IDF PA, a more robust uncertainty assessment using principal component analysis has been developed where instead of extracting uncertainties on individual parameters, the uncertainties of the correlated parameters are determined simultaneously, which allows for a more realistic analysis of uncertainty space.

The NRC reviewer also questioned the assumption of using a Temkin coefficient equal to one in the chemical affinity term. A Temkin coefficient not equal to unity would be used to account for non-ideal behavior in ionic solutions. McGrail originally proposed a method to measure both K_g and σ using single-pass flow-through (SPFT) tests with varying flow rates (DOE/RL-97-69, *Hanford Immobilized Low-Activity Tank Waste Performance Assessment* [see page G-10]; PNNL-11834). However, attempts to implement the method to measure both K_g and σ proved to be inadequate and it was decided to use the approach of others and assume $\sigma=1$ and determine K_g empirically (“Measurement of kinetic rate law parameters on a Na–Ca–Al borosilicate glass for low-activity waste” [McGrail et al. 1997]). It has also been argued that σ must equal to one for the transition-state theory (TST)-based model to be fundamentally valid (“Chemical Weathering Rates of Silicate Minerals,” Chapter 2. Fundamental approaches in describing mineral dissolution and precipitation rates [Lasaga 1995]). It should be noted that work subsequent to completing the 2017 IDF PA has assessed K_g values for a much wider range of glasses and the range represented by new values will be incorporated into the PA through the PA maintenance process.

Another issue raised by the NRC reviewer was that there are “...uncertainties associated with assumed secondary mineral formation in the process modeling (i.e., the need to assume Chalcedony formation without it being empirically observed).” There are many different mineral phases observed when water is allowed to contact ILAW glass for extended periods (c.f. VSL-20R4820-1, *Final Report FY 2020, Long-Term PCT of ILAW Glasses* and the references cited in this document). For the 2017 IDF PA, because the suite of weathering products that will form as a consequence of the glass-water reactions cannot be determined a priori, results from existing (The Catholic University of America/VSL and Pacific Northwest National Laboratory [PNNL]) long-term product consistency tests (PCTs) conducted at 90 °C

were compared to thermodynamic equilibrium predictions (PNNL-20781). Modeling of PCT results for the 128 glass samples was conducted using the secondary-phase reaction network reported in PNNL-14805, *Waste Form Release Data Package for the 2005 Integrated Disposal Facility Performance* for LAWA44. Comparison between measured and predicted results for the concentrations of major glass-forming components in solution for the 128 PCTs were in agreement (PNNL-20781). As noted by the NRC reviewer, the secondary reaction product network used in PNNL-20781 (and subsequently in the IDF PA) were not all observed experimentally, and some that were observed were excluded (compare Tables 5.1, 5.2, and 5.3 in PNNL-20781). These substitutions were done to match temporal trends in dissolved species data using species for which thermodynamic data were available (PNNL-20781). Chalcedony is used as a generalized representation of amorphous silica species that are observed experimentally and known to be more soluble than the corresponding crystalline species. Thus, it facilitates better fit of empirical results in the TST model framework.

Current work is collecting data on secondary mineral reaction networks (SMRNs) formed by dissolution of a wide range of ILAW glasses and this information will be used to update the SMRN used in the IDF PA to account for differences that may arise from the enhanced waste loading glass compositions. This work will follow the approach detailed in PNNL-20781, but more emphasis will be given to including frequently-measured compounds and providing a quantitative assessment of fitting quality for the phases selected.

Efforts to Bound Uncertainty in the 2017 IDF PA – The IDF PA uncertainty analysis (evaluated using the IDF PA system model implemented in GoldSim³⁴) included assessment of the uncertainty in the glass dissolution rate. The included uncertainties resulted in simulated fractional dissolution rates that spanned three orders of magnitude from $5.77\text{E-}09 \text{ yr}^{-1}$ to $1.78\text{E-}05 \text{ yr}^{-1}$. At these fractional dissolution rates, the VLAW lifetimes (corresponding to VLAW that is ~99.9% corroded) range from 400,000 years to more than 10 million years, with a range of 0.2% to 18% corroding in 10,000 years.

Although the compliance case simulates vitrified waste corrosion using a fixed dissolution rate without variability or uncertainty, the system model includes multiple aspects of uncertainty (but not variability). The system model includes the capability to include uncertainty in the glass type (as a surrogate for evaluating glass variability), kinetic dissolution rate parameters, and dissolution model regression coefficients.

The system model does not simulate the physical processes involved in glass dissolution but instead uses a regression model to calculate an applied dissolution rate. The system model abstraction includes the capability to simulate glass type uncertainty. With this capability, all vitrified waste could be simulated using the dissolution rate parameters developed in the laboratory for representative glasses from envelopes A (LAWA44), B (LAWB45), and C (LAWC22).

The system model abstraction also includes the capability to evaluate uncertainty in the dissolution rate model parameters for each glass type. Uncertainties in these parameters were

³⁴ GoldSim[®] simulation software is copyrighted by GoldSim Technology Group LLC of Issaquah, Washington (see <http://www.goldsim.com>).

developed from laboratory experiments for the four parameters used in the rate model (η - the pH power law coefficient, E_a - the glass dissolution activation energy, K_g - the glass apparent equilibrium constant, and R_{IEX} - the sodium ion exchange rate constant). Uncertainties for η and E_a were developed by the principal investigators that used laboratory experiments to develop the parameter values. However, uncertainties for K_g and R_{IEX} were not reported. The lead PA modeler evaluated the data and determined that a factor of 3 for K_g and a factor of 10 for R_{IEX} were appropriate to represent error or uncertainty that could be introduced by the parameter development process (RPP-CALC-61194, *System Model Calculations for the Integrated Disposal Facility Performance Assessment*, Section 4.3.1.2). More recent evaluations of glasses studied after the 2017 PA provide uncertainties based on experimental data for K_g and R_{IEX} (PNNL-26169, *FY2016 ILAW Glass Corrosion Testing with the Single-Pass Flow-Through Method* and PNNL-27098, *FY2017 ILAW Glass Corrosion Testing with the Single-Pass Flow-Through Method*).

These parameters, including uncertainty, are applied to a regression model that was developed from multiple process model runs simulating glass dissolution for the four glass types using different values for the rate parameters. The different values for K_g in the simulations used to develop the abstraction ranged from 1E-04 to 5E-03, which is a factor of 4.9 lower than the lowest value for the four included glass types and a factor of 2.7 higher than the highest value for the four included glass types. The different values for R_{IEX} in the modeling used to develop the abstraction ranged from 5E-16 mol/cm²/s to 1E-12 mol/cm²/s, which is a factor of 6.8 lower than the lowest rate value for the four included glass types and a factor of 83 higher than the highest rate value for the four included glass types. The range for the pH power law coefficient ranged from 0.25 to 0.55, which does not extend across the full range of values in the data package (0.31 to 0.57) when uncertainty is included in the laboratory-developed parameters. The range of values for the rate constant, which accounts for the intrinsic forward rate constant and the activation energy, ranged from 1E-19 mol/cm²/s to 5E-15 mol/cm²/s. This range extends across the full range of values for the four glass types when uncertainty in the activation energy is included, which extends from 1.6E-19 mol/cm²/s to 2.6E-16 mol/cm²/s. Up to 126 rate parameter combinations were simulated with the process model for each glass. A regression model was fit to the process model output to generate a representative equation that could be used to calculate the dissolution rate in the PA model without incorporating the process model simulations into the system model. The system model abstraction included uncertainty in the estimates of the regression coefficients when calculating the applied dissolution rate.

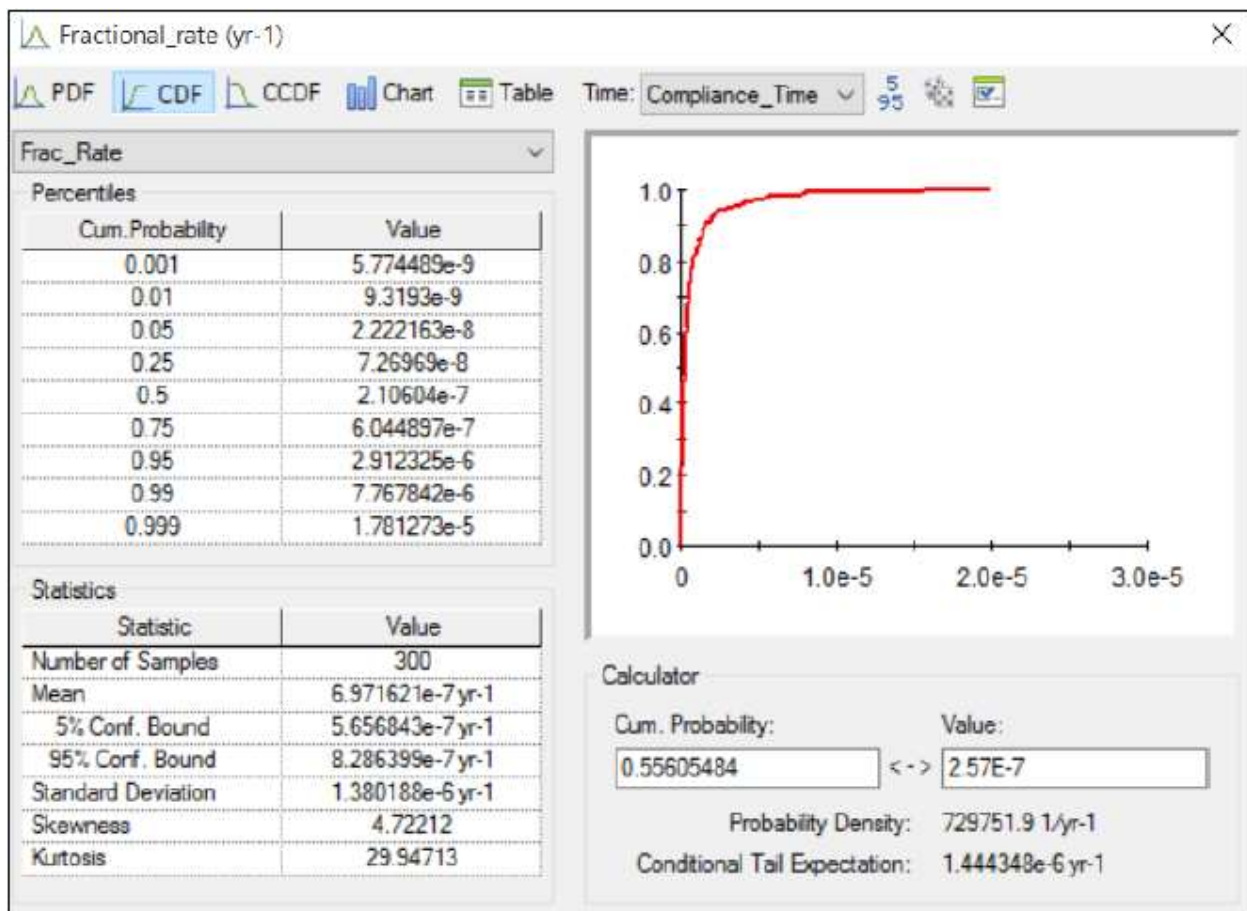
These uncertainties in the regression model coefficients and estimates of the parameter values were included in the IDF PA uncertainty evaluation. Uncertainty in the glass type was not included in the PA uncertainty analysis. Only rate parameters for the envelope A glass were included in the uncertainty analysis; simulating LAWABP1 glass was excluded because it is no longer a glass formulation planned for production at the WTP. In addition, LAW45 was not simulated because it tended to have lower dissolution rates than envelope A and envelope C glass types. Envelope C was not simulated because the dissolution rates for envelope A and envelope C glasses are similar so that simulating one is representative of the other.

Figures 2-7-3 and 2-7-4 below show the distribution of fractional dissolution rates from the applied uncertainties for LAWA44 glass and LAWC22 glass. The ratio of the 99.9-percentile

value to the 0.1-percentile value is about 3,000 for LAWA44 glass and about 1,600 for LAWC22 glass, illustrating that either type would provide an uncertainty range that spans three orders of magnitude.

In summary, to account for different uncertainties in both the dissolution model and the parameter values, the corrosion rates evaluated in the PA uncertainty analysis spanned a three-order-of-magnitude range. This range was from 44x below to 70x above the rate used in the compliance case for LAWA44. None of the realizations in the uncertainty analysis exceeded the 25 mrem/yr dose limit in 1,000 years or in 10,000 years.

Figure 2-7-3. Distribution of Fractional Dissolution Rates from the Applied Uncertainties for LAWA44 Glass.

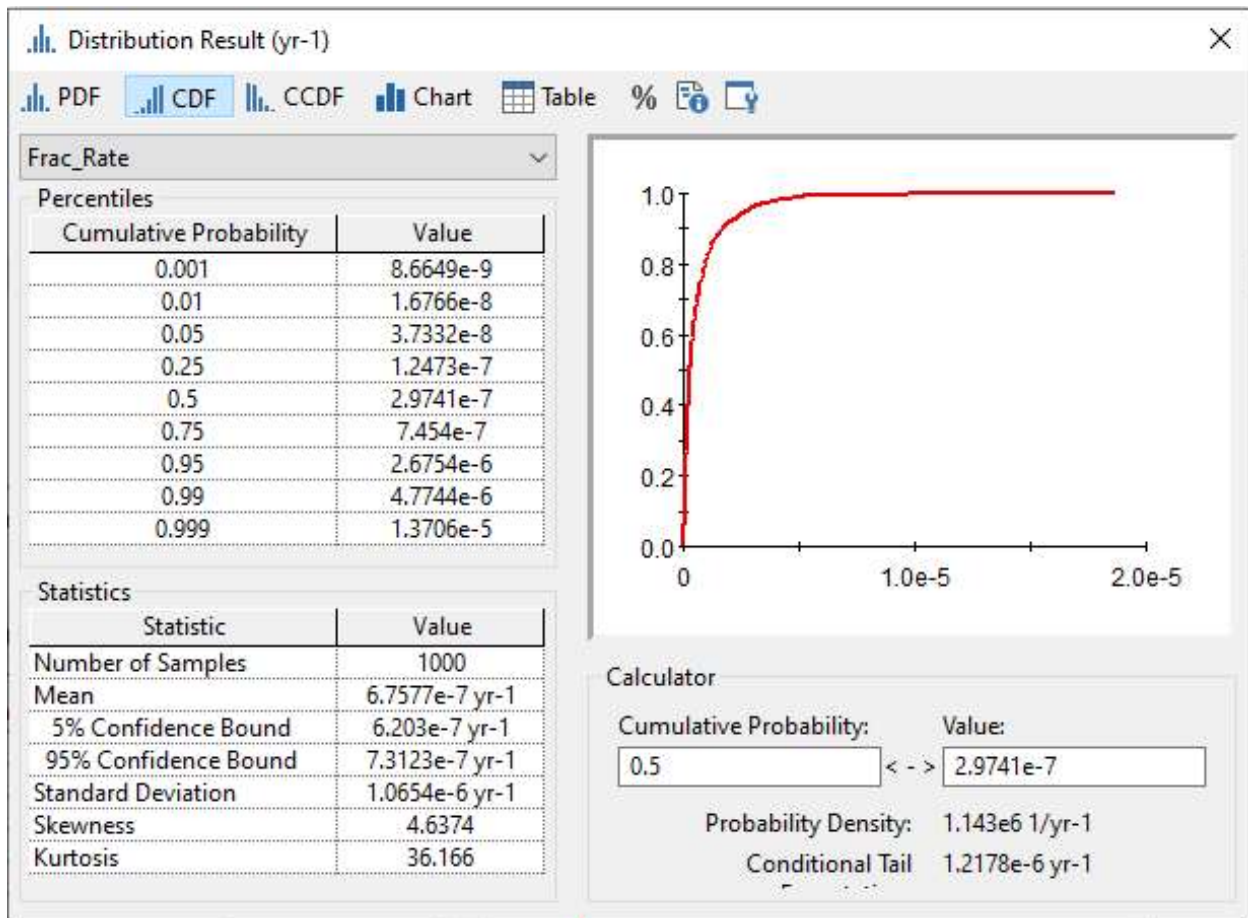


Source: RPP-CALC-61194, *System Model Calculations for the Integrated Disposal Facility Performance Assessment*, Rev. 1A, Figure 7.3-45(a).

Correlating Laboratory-Scale and Production-Scale Glass Performance – It is not practical or necessary to verify the performance characteristics of VLAW glass made from real waste at the production scale through laboratory-scale testing of actual VLAW glass samples. Glass durability as determined via methods such as the Product Consistency Test (ASTM C1285) and Vapor-phase Hydration Test (ASTM C1663) for nuclear waste glasses has been correlated with glass composition to demonstrate compliance with Waste Acceptance Product Specifications for

high-level waste and WTP contract specifications for VLAW glass (PNNL-22631, *Glass Property Models and Constraints for Estimating the Glass to be Produced at Hanford by Implementing Current Advanced Glass Formulation Efforts*; PNNL-25835, *2016 Update of Hanford Glass Property Models and Constraints for Use in Estimating the Glass Mass to be Produced at Hanford by Implementing Current Enhanced Glass Formulation Efforts*). The detailed strategies for demonstrating compliance with glass durability requirements for all DOE vitrification facilities are described in the waste form compliance plans for those facilities, and the data and test results demonstrating compliance are found in the waste form qualification reports for those facilities. All rely on laboratory-scale testing of glasses made from simulated waste to cover a range of compositions of glasses to be made from real waste. The composition of nuclear waste glass during actual production operations is then controlled within the pre-qualified glass composition region and the performance of any glass produced can be predicted from models that correlate glass performance with glass composition, after accounting for uncertainties in composition and performance (PNNL-22631, PNNL-25835).

Figure 2-7-4. Distribution of Fractional Dissolution Rates from the Applied Uncertainties for LAWC22 Glass.



This same approach is utilized to determine the projected long-term performance of VLAW glass under IDF disposal conditions. As described in the section below titled “**Ongoing and Future to Improve Representation of Uncertainty in Glass Dissolution Rates,**” glass dissolution

parameters are being correlated, where possible, with glass composition. Conservative or bounding values will be implemented for parameters that do not show definitive correlation with glass composition. Statistical analyses of the data will provide the basis for establishing ranges of variation and uncertainty.

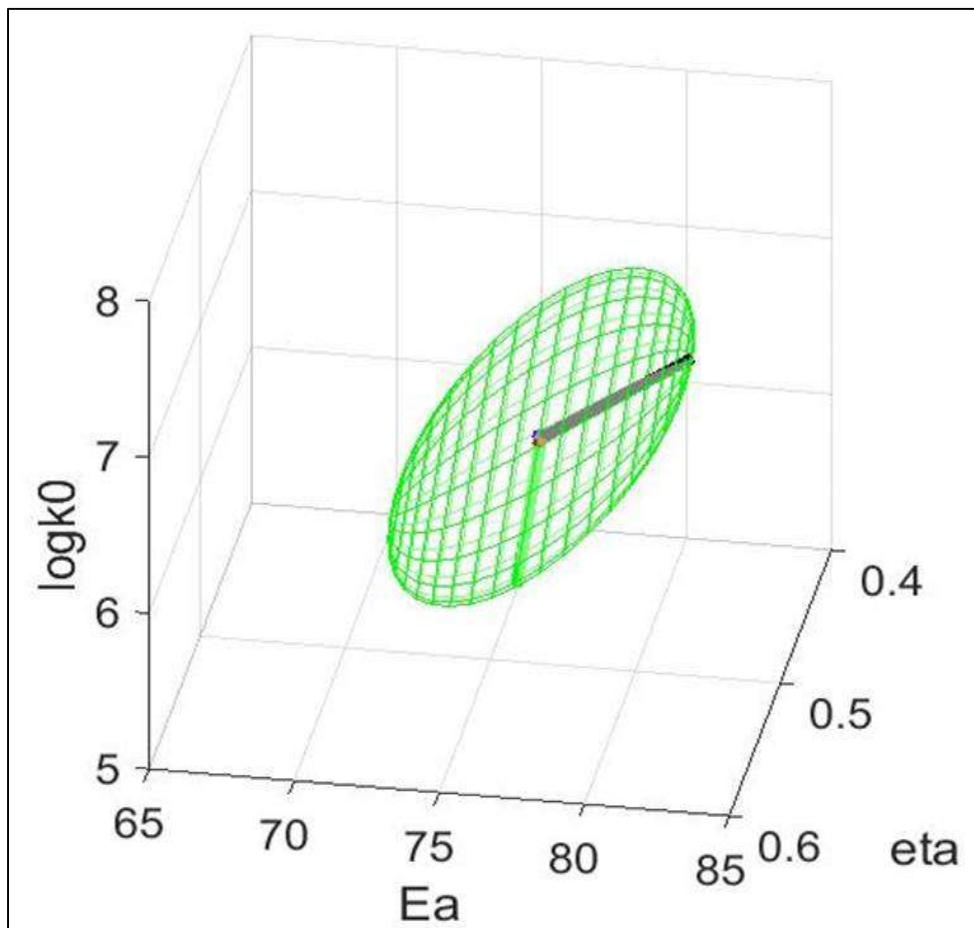
There is a large body of data collected over decades demonstrating the relationships between glass composition and glass properties and performance for nuclear waste borosilicate glasses. There are numerous reports of tests and demonstrations of VLOW glass production with simulated waste at scales ranging from crucible scale (hundreds of grams) to a 1/3 scale pilot melter system producing greater than 5 metric tons of glass per day. Excellent agreement in glass properties was observed across the full range of scales (c.f. VSL-07R1130-1, *Final Report – Enhanced LAW Glass Formulation Testing* [also referenced as ORP-56293, *Final Report – Enhanced LAW Glass Formulation Testing, VSL-07R1130-1, Rev. 0, dated 10/05/07*]; VSL-06R6480-1 [also referenced as ORP-56324, *Final Report – DuraMelter 100 Tests to Support LAW Glass Formulation Correlation Development, VSL-06R6480-1, Rev. 0*]; VSL-01R3501-2, *Final Report – Melter Tests with LAW Envelope A and C Simulants to Support Enhanced Sulfate Incorporation* [also referenced as ORP-63503, *Final Report – Melter Tests with LAW Envelope A and C Simulants to Support Enhanced Sulfate Incorporation, VSL-01R3501-2, Rev. 0*]). Finally, properties of glass made from real waste at crucible scale were found to be in excellent agreement with VLOW glass made from simulated waste in melter runs at a range of scales (PNNL-13372, *Vitrification and Product Testing of AW-101 and AN-107 Pretreated Waste*).

Ongoing and Future Work to Improve Representation of Uncertainty in Glass Dissolution Rates – The IDF PA is updated annually as relevant new information is made available. There are on-going efforts funded by DOE to address several areas of uncertainty associated with ILAW glass dissolution, including the issues raised by the NRC reviewer. The details of the testing approach can be found in RPP-PLAN-60520, *Program Plan for Immobilized Low Activity Waste (ILAW) Glass Testing*. The following is a brief description of the items relevant to the reviewer’s comments on the need to better define uncertainty.

- **Dilute Rate Parameters (η , E_a , k_0):** The reviewer specifically identified uncertainty in dilute rate parameters reported for LAWA44 in PNNL-14805. Since the time of issuance of the ILAW data package, further insight has been gained into the uncertainty and relationship of the dilute rate model parameters. In recent years, analyses have been carried out that have shown that the three dilute rate model parameters are correlated with one another (“The dissolution behavior of borosilicate glasses in far-from equilibrium conditions” [Neeway et al. 2018]). Principal component analysis showed that, as a result of this correlation, the 95% confidence interval volume on the magnitude of the three dilute rate model parameters adopts a flattened ellipsoidal shape in the 3D space defined by the three model parameters (Figure 2-7-5). Therefore, independently varying the three parameters in sensitivity analyses can result in highly inaccurate estimates and appropriate uncertainties for the three parameters should be determined from this ellipsoid representation instead. This observation was first made using glass dissolution data collected using the SPFT technique, including data on the glasses used in the 2017 IDF PA.

More recently this correlation was confirmed based on data collected using a novel technique termed the Stirred Reactor Coupon Analysis (SRCA). This technique was applied to a statistically designed matrix of glasses that were designed to represent the enhanced waste glass (EWG) composition space, which in itself covers a majority of the composition ranges allowed in the baseline models (Figure 2-7-6). SRCA relies on the use of a physical measurement of the amount of glass removed from the surface of a coupon sample relative to an area that was protected (masked) from dissolution. The difference between corroded and protected portions of the glass coupon generates a “step” that can be measured (e.g., using optical profilometry). Multiple measurements of this step provide experimental uncertainty that is applied to the corrosion rate. The traditional SPFT method uses crushed glass and analysis of glass components in the leachate solution (e.g., boron) to determine corrosion rates with error derived from analytical uncertainty and test variables (e.g., assumed glass surface area). The SRCA technique enables high test throughput resulting in 24 new glass compositions being analyzed in a single year, compared to only 2 to 4 per year with traditional SPFT testing.

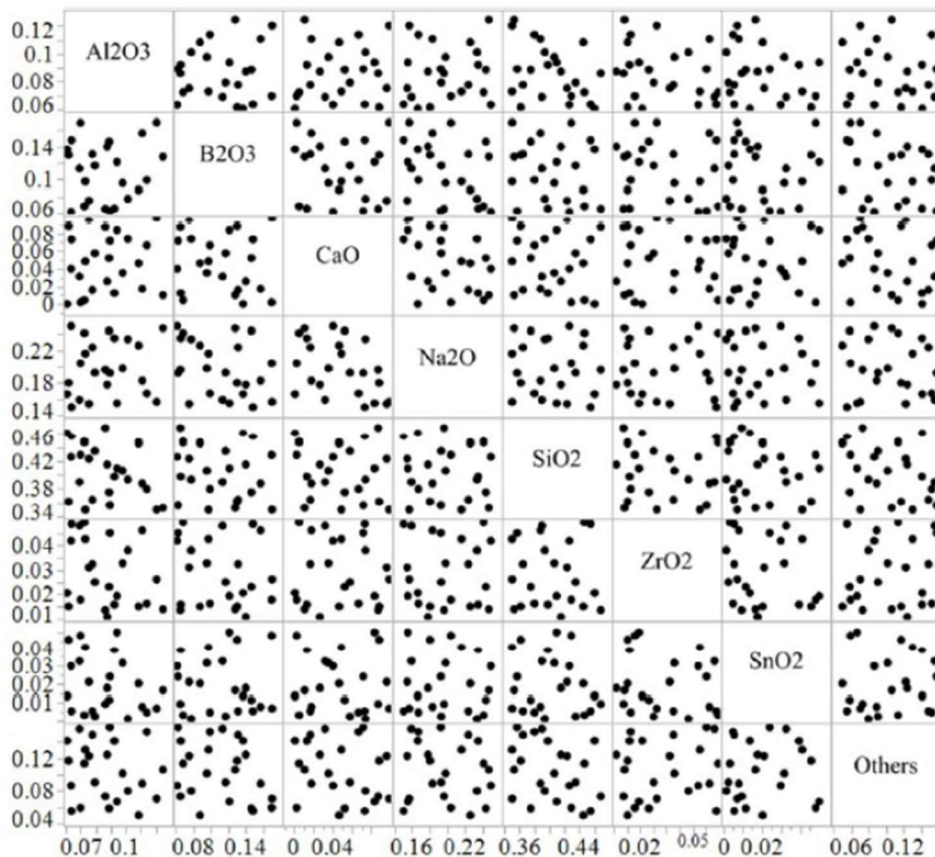
Figure 2-7-5. Example of Principal Component Analysis of the Dilute Rate Model Parameters for a Borosilicate Glass.



Note: The measured dilute rate model parameters are the center point and the flattened ellipsoid space (Green mesh) represents the 95% confidence interval around the correlated parameters.

Dilute rate parameters (k_0 , E_a , η) results for the 24 glasses tested in FY 2020 are expected to provide a statistically valid representation of the range for these parameters for all ILAW glasses to be produced at the WTP using current process flowsheet algorithms. In addition, composition-parameter correlation modeling is being completed to determine if individual constituents, or combinations of glass constituents, dictate the magnitude and uncertainty of the dilute rate model parameters or if a range of valid values of the dilute rate model parameters can be represented by a single ellipsoid. Final results are expected to be made available to the IDF PA maintenance effort in FY 2022.

Figure 2-7-6. Scatter Plot of Individually Varied Glass Components (in mass fractions) in the Statistically-Designed Glass Formulations Representative of the Enhanced Immobilized Low-Activity Waste Glass Compositional Region.



- Pseudo-equilibrium Coefficient:** Data mining and experimental efforts have been ongoing since FY 2019 to assess K_g values for EWGs. In testing of enhanced waste loading glasses, irregularities were observed in SPFT tests used to determine K_g where the glass dissolution rate did not slow with increased silicon addition to solution as one

would expect from the TST rate model. A data mining effort was initiated to assess the source of this irregularity using a plethora of SPFT and PCT data sets on ILAW glass available at both PNNL and the VSL and other borosilicate glass data available in the ALTGlass database from SRNL and PNNL. The data mining effort concluded that the irregularity arose from the application of test method to determine K_g and was not a characteristic of the glass type or composition.

An alternate test method, termed the q/S sweep method, where the expected response of the glasses to increasing silicon concentrations was observed, was identified to measure K_g using existing data. Unlike tests where silicon is added to the reactor feed to suppress glass dissolution, the q/S sweep method relies on adjusting the flowrate and glass surface area to increase the solution concentration of silicon and other glass components. Additionally, unlike the baseline method where only the influence of orthosilicic acid is used to determine K_g , in the q/S sweep method all glass components are dissolved in solution so the effect of orthosilicic acid on the rate is not isolated. Experimental testing was also carried out on the alternate test method and K_g values were obtained successfully. This data set of K_g values will be subjected to statistical analysis to determine if there are primary and secondary glass composition dependencies. These dependencies can then be used to determine how to represent K_g for the expected range of EWG glass compositions. Due to the nature of the K_g value a single, conservative bounding value may be used to represent all EWG compositions or the magnitude of K_g may be tied to glass composition.

In addition, a rate model verification effort is being executed in which the K_g values determined for individual glasses are being combined with independently-measured dilute rate parameters and used to model theoretical response of the glass in a PCT. These responses are then being compared to experimental data sets to determine how well the independently-measured parameters describe the complete time dependence response as a validation of the rate model. The impact of the K_g value used in the validation model on the degree of deviation between the predicted and actual response is being explored to support the definition of K_g values selected for IDF PA uncertainty analysis. Final results are expected to be available to the IDF PA maintenance effort in FY 2022.

- **Alkali Ion Exchange:** The NRC reviewer noted the uncertainty associated with estimates of alkali ion exchange rates as demonstrated in Figure 4.6 from PNNL-13043, *Waste Form Release Data Package for the 2001 Immobilized Low-Activity Waste Performance Assessment*. The alkali ion exchange process within borosilicate glass has long been recognized as being a diffusion-based process that involves the exchange of hydronium ions with alkali ions within the glass matrix (“A glass dissolution model for the effects of S/V on leachate pH” [Feng and Pegg 1994], “The ion exchange phase in corrosion of nuclear waste glasses” [Ojovan et al. 2006]). However, until recently testing methods have not focused on extracting the time and pH dependency that results from these mechanistic phenomena. Not accounting for these effects may be one of the reasons for variation in experimentally-derived ion exchange rates.

To circumvent this limitation, work at VSL and PNNL has been ongoing since FY 2017 to gather information on the time, temperature, and pH dependence of alkali ion exchange in ILAW glasses to better represent the ion exchange process in the rate model (PNNL-26594, *A Critical Review of Ion Exchange in Nuclear Waste Glasses to Support the Immobilized Low-Activity Waste Integrated Disposal Facility Rate Model*). Initial results indicate the time-dependent ion exchange rates rapidly fall below the time-invariant constant rate values utilized for the 2017 PA analysis. This program includes work using an alternate test method to measure time-dependent ion exchange rates, the Pulse Flow Tests developed by VSL (VSL-19R4620-2, *Final Report FY 2019 ILAW Glass Ion Exchange Rate Testing*) and analysis of data from surface area:volume variable (known as q/S) SPFT tests at PNNL in FY 2021. The equation being parameterized is:

$$r_{IEX} = \frac{1}{2} k_{d0} \exp\left(-\frac{E_{ad}}{RT}\right) \left(\frac{[H^+]}{[H^+]_0}\right)^\alpha t^{-\gamma}$$

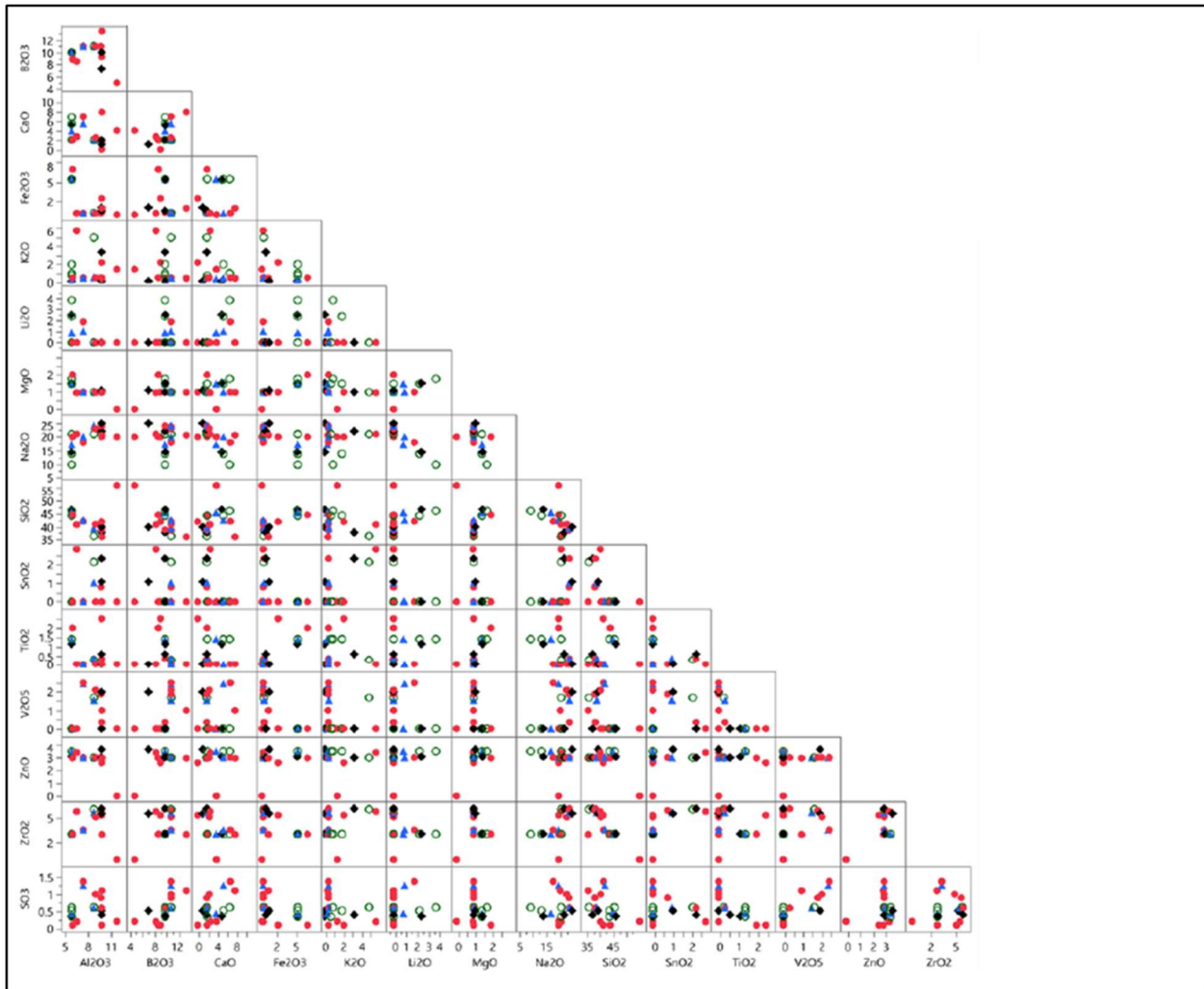
Note: γ is a positive number (theoretically 0.5) and the model conceptually accounts for ion exchange rate diminishing with time as the outer layer of glass becomes depleted of alkali ions. To date, data has been collected and analyzed for 17 glasses and data for at least 4 more glasses will be available in FY 2021. These 21 glasses represent a large portion of the compositional region for both baseline and enhanced waste loading glasses, especially for the alkali and alkali-earth species that are pertinent to the ion exchange process (Figure 2-7-7). Results for the ion exchange time-dependent rate parameters are being evaluated for correlations with glass composition (as individual constituents, or combinations of constituents). This approach will define how best to represent the parameters for the time-dependent ion exchange rate equation for the full ILAW glass compositions and the associated uncertainty (e.g., a single set of conservative parameters, or parameters whose magnitude are tied to glass composition). Initial results indicate that once a glass starts to corrode in the disposal environment, within a year, the predicted time-dependent ion exchange rates fall below the time-invariant constant rate values utilized for the 2017 PA analysis. Finally, data from long-term dissolution tests are being evaluated to determine whether the ion exchange rates eventually reach steady state as the glass dissolution front recedes at the same rate as the ion exchange front is receding into the glass. Final results are expected to be available to the IDF PA maintenance effort in FY 2022.

- **Potential for, and Effect of, Stage III Behavior:** This topic is more fully addressed in the response to RAI 2-09. The following discussion is a summary of the recent work being conducted for the IDF PA maintenance program to address the potential impacts of Stage III behavior.

The potential uncertainty in the glass dissolution rate that results from Stage III dissolution behavior is being addressed through zeolite seeding experiments using 24 statistically-designed glasses that span the possible composition space for the enhanced waste loading glasses, which in itself covers a majority of the composition

ranges of components included in the baseline models. In summary, samples of the 24 glasses are being incubated in aqueous solutions, at multiple temperatures, both with and without zeolite seeding. In the static test, zeolite seeds can initiate an acceleration of glass dissolution (Stage III) (PNNL-28898, *FY2019 Status Report: Seeded ILAW Glass Stage III Static Dissolution Rate Measurements*; “In-situ monitoring of seeded and unseeded stage III corrosion using Raman spectroscopy” [Ryan et al. 2019]). Initial results indicate that the magnitude and onset of Stage III behavior can vary with composition with some glasses showing no evidence of rate increase. Dissolved glass component concentrations are being measured in periodically-collected liquid samples to assess the dissolution rate with time. At the conclusion of the tests, the secondary solid phases that are formed are also being analyzed and the results used to compare to phases identified in unseeded static tests of the same glasses. The unseeded test data will support defining the secondary mineral network to be used in the IDF PA. The glasses being tested provide statistical coverage of the ILAW glass composition region (see the next section). The seeded test solids analysis will provide comparison of changes to the phases upon Stage III occurrence and in the artificial presence of zeolite phases.

Figure 2-7-7. Scatterplot of 15 Glass Compositions for Which Sodium Ion Exchange Was Measured by Single-Pass Flow-Through (12 red full circles), by Single-Pass Flow-Through and Pulse Flow Test (3 black diamonds), and by Pulse Flow Test Only (3 blue triangles).



Note: Glasses to be measured by Pulse Flow Test in fiscal year 2021 are shown in the green open circles.

The dissolution rates in seeded tests (Stage III rates) are also being correlated with glass composition to determine if individual constituents, or combinations of constituents, dictate the magnitude of the Stage III rates and subsequent behavior. The range of the measured Stage III rates will be evaluated as part of the IDF PA uncertainty evaluation to determine: 1) if the occurrence of Stage III in the IDF using a conservative Stage III rate can still meet performance objectives, or 2) if compositional constraints could be imposed to assure Stage III rates for the full ILAW glass inventory would fall within performance objective limits. Final results are expected to be available for the IDF PA maintenance effort in FY 2022.

- **Secondary Mineral Reaction Network:** The SMRN employed in the IDF PA requires an update to encompass the EWG composition region, to provide technical defense in

depth for the mineral phases used in the PA, and to evaluate any potential correlation between the secondary mineral phases formed and the glass composition. Thus far, efforts on secondary minerals for EWGs have only focused on their impact on Stage III behavior. However, additional relevant secondary phases, which are instrumental in predicting long-term glass dissolution rates in the IDF PA, have not been fully identified for EWG glasses. The SMRN used in IDF PA modeling is being revised in FY 2021 and FY 2022 based on solids analysis conducted at VSL in long-term PCTs (c.f. VSL-20R4820-1) and at PNNL for the unseeded and seeded Stage III tests. Geochemical modeling will be used to assess the ability of the SMRN to match glass dissolution data using the existing SMRN, any updated SMRN for EWG, and phases observed in the long-term tests. This work will follow the approach detailed in PNNL-20781, but more emphasis will be given to including frequently measured compounds and those with greatest potential to influence dissolution behavior in the IDF environment. This information will be available to the IDF PA maintenance effort in FY 2022.

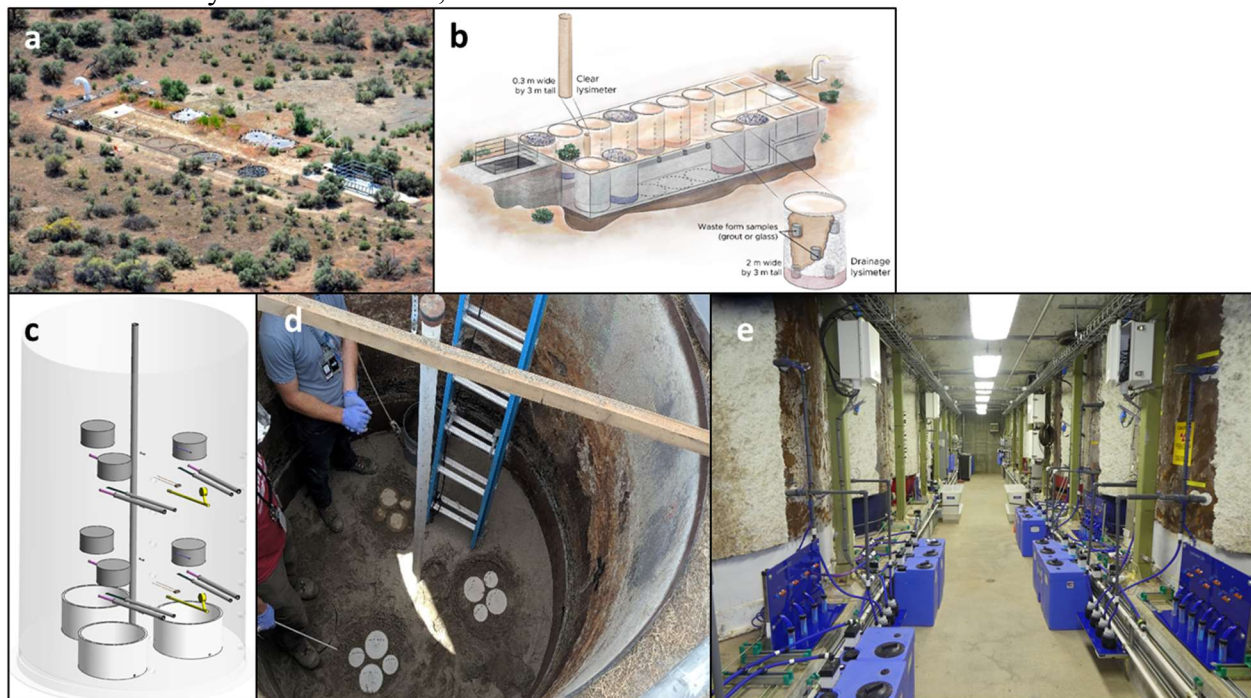
- **Corroboration of IDF PA Prediction and Field Lysimeter Results:** Work is being conducted to validate predictions of ILAW glass dissolution rates in the Hanford Site IDF using the Field Lysimeter Test Facility (FLTF). As shown in Figure 2-7-8, the FLTF has a series of field lysimeter tubes (most extend to a depth of 3 m) that can be filled with various waste forms, including glass and cementitious materials, and back filled with IDF soils. Water infiltration rate is controlled within each lysimeter tube. Water samples will be collected at various depths within the lysimeters over the next several years, along with measurements of the *in situ* distribution of moisture.

Prior to initiation of the lysimeter test, a modeling effort was performed using the same simulation style as the IDF PA to predict the behavior of the emplaced waste forms and corresponding contaminant release, using ^{99}Tc and ^{127}I as tracers for the cementitious waste forms and molybdenum and rhenium as tracers for the glass waste forms (PNNL-27394, *Field-Scale Lysimeter Studies of Low-Activity Waste Form Degradation Implementation Plan*). As data are collected from the tests, comparisons will be made against the initial modeling that will serve as validation of the model and determine the extent to which the laboratory-based parameters are applicable to waste form behavior in the field. Water analysis and *in situ* soil moisture data from these tests will start to be available in FY 2021 but data from solids analysis will not be available until the tests conclude, which depending on the test may be 5 years to 25 years in the future.

With the two glass formulations selected, Stage III behavior may not be observed over the duration of the lysimeter test. However, post-experimental characterization of the excavated waste forms and backfill will also be completed at the test conclusion to evaluate the evolution of mineral phases and to determine if any zeolite phases have been formed. Note that the presence of zeolites does not indicate that Stage III behavior is inevitable, but their presence does suggest Stage III may occur. As stated under the discussion of Stage III (above), data is also being collected in laboratory tests to assess the magnitude of the impact of Stage III rate behavior on contaminant release from the IDF to the surrounding environment.

Figure 2-7-8. Images of the Field Lysimeter Test Facility a) Aerial Photograph of the Facility, b) Artist Three-Dimensional Drawing of the Facility, c) Depiction of the Layout of Buried Waste Forms and Sampling Devices Within a Single Lysimeter Tube, d) Photograph of the Lower Level of Buried Cementitious Waste Forms, and e) Photograph of the Underground Sampling Bay Showing the Two Rows of Lysimeter Tubes.

Images of the Field Lysimeter Test Facility a) Aerial Photograph of the Facility, b) Artist Three-Dimensional Drawing of the Facility, c) Depiction of the Layout of Buried Waste Forms and Sampling Devices Within a Single Lysimeter Tube, d) Photograph of the Lower Level of Buried Cementitious Waste Form and e) Photograph of the Underground Sampling Bay Showing the Two Rows of Lysimeter Tubes,



Conclusion – The IDF PA model used an abstraction of a rate model that has a development history that has been documented in peer-reviewed literature for decades. The IDF PA model includes uncertainty in the parameters that are associated with the rate model and accounts for additional uncertainties in the development of an abstraction of that rate model. The IDF PA model also includes multiple conservatisms about the propensity of the dissolution rate to be a continuous process despite recent observations that the ion exchange process (which controls glass dissolution at long time frames) might not be constant and is expected to decrease with time. DOE continues to evaluate the mechanisms associated with borosilicate glass dissolution, which includes the development of additional glass formulations, models to correlate dissolution rate parameters with glass composition, and additional processes that may accelerate (Stage III) or reduce (diffusion of sodium ions across an expanding layer of alteration products) the VLAW dissolution rate.

In accordance with the PA maintenance plan, advancements in borosilicate glass science are evaluated in the PA on an annual basis as new information is gained.

References

- Aagaard, P. and H. C. Helgeson, 1982, "Thermodynamic and kinetic constraints on reaction rates among minerals and aqueous solutions I. Theoretical considerations," *American Journal of Science*, vol. 282, pp. 237–285.
- DOE/RL-97-69, 1998, *Hanford Immobilized Low-Activity Tank Waste Performance Assessment*, Rev. 0, U.S. Department of Energy, Richland, Washington.
- Feng, X. and I. L. Pegg, 1994, "A glass dissolution model for the effects of S/V on leachate pH," *Journal of Non-Crystalline Solids*, vol. 175, Issues 2–3, pp. 281–293.
- Fournier, M., P. Frugier, and S. Gin, 2018, "Application of GRAAL model to the resumption of International Simple Glass alteration," *npj Materials Degradation*, vol. 2, Article number 21, pp. 1–9.
- Grambow, B., 1985, "A General Rate Equation for Nuclear Waste Glass Corrosion" in *Materials Research Society Symposium Proceedings 44*, pp. 15–27, Cambridge University Press, Cambridge, United Kingdom.
- Lasaga A. C., 1995, "Chemical Weathering Rates of Silicate Minerals," Chapter 2. Fundamental approaches in describing mineral dissolution and precipitation rates, in *Reviews in Mineralogy and Geochemistry*, vol. 31, No. 1, pp. 23–86.
- McGrail, B. P., W. L. Ebert, A. J. Bakel, and D. K. Peeler, 1997, "Measurement of kinetic rate law parameters on a Na–Ca–Al borosilicate glass for low-activity waste," *Journal of Nuclear Materials*, vol. 249, pp. 175–189.
- Neeway, J. J., P. C. Rieke, B. P. Parruzot, J. V. Ryan, and M. R. Asmussen, 2018, "The dissolution behavior of borosilicate glasses in far-from equilibrium conditions," *Geochimica et Cosmochimica Acta*, vol. 226, pp. 132–148.
- Ojovan, M. I., A. Pankov, and W. E. Lee, 2006, "The ion exchange phase in corrosion of nuclear waste glasses," *Journal of Nuclear Materials*, vol. 358, pp. 57–68.
- PNNL-11834, 2000, *A Strategy to Conduct an Analysis of the Long-Term Performance of Low-Activity Waste Glass in a Shallow Subsurface Disposal System at Hanford*, Rev. 1, Pacific Northwest National Laboratory, Richland, Washington.
- PNNL-13043, 2001, *Waste Form Release Data Package for the 2001 Immobilized Low-Activity Waste Performance Assessment*, Rev. 2, Pacific Northwest National Laboratory, Richland, Washington.

- PNNL-13372, 2000, *Vitrification and Product Testing of AW-101 and AN-107 Pretreated Waste*, WTP-RPT-003, Rev. 0, Pacific Northwest National Laboratory, Richland, Washington.
- PNNL-14805, 2004, *Waste Form Release Data Package for the 2005 Integrated Disposal Facility Performance*, Pacific Northwest National Laboratory, Richland, Washington.
- PNNL-20781, 2011, *Integrated Disposal Facility FY 2011 Glass Testing Summary Report*, Pacific Northwest National Laboratory, Richland, Washington.
- PNNL-22631, 2013, *Glass Property Models and Constraints for Estimating the Glass to be Produced at Hanford by Implementing Current Advanced Glass Formulation Efforts*, Rev. 1, ORP-58289, Pacific Northwest National Laboratory, Richland, Washington.
- PNNL-24615, 2015, *Immobilized Low-Activity Waste Glass Release Data Package for the Integrated Disposal Facility Performance Assessment*, RPT-IGTP-005, Pacific Northwest National Laboratory, Richland, Washington.
- PNNL-25835, 2016, *2016 Update of Hanford Glass Property Models and Constraints for Use in Estimating the Glass Mass to be Produced at Hanford by Implementing Current Enhanced Glass Formulation Efforts*, Pacific Northwest National Laboratory, Richland, Washington.
- PNNL-26169, 2017, *FY2016 ILAW Glass Corrosion Testing with the Single-Pass Flow-Through Method*, RPT-IGTP-013, Rev. 0.0, Pacific Northwest National Laboratory, Richland, Washington.
- PNNL-26594, 2017, *A Critical Review of Ion Exchange in Nuclear Waste Glasses to Support the Immobilized Low-Activity Waste Integrated Disposal Facility Rate Model*, RPT-IGTP-018, Rev 0.0, Pacific Northwest National Laboratory, Richland, Washington.
- PNNL-27098, 2018, *FY2017 ILAW Glass Corrosion Testing with the Single-Pass Flow-Through Method*, RPT-IGTP-015, Rev. 0, Pacific Northwest National Laboratory, Richland, Washington.
- PNNL-27394, 2018, *Field-Scale Lysimeter Studies of Low-Activity Waste Form Degradation Implementation Plan*, RPT-IGTP-017, Rev 0.0, Pacific Northwest National Laboratory, Richland, Washington.
- PNNL-28898, 2019, *FY2019 Status Report: Seeded ILAW Glass Stage III Static Dissolution Rate Measurements*, Pacific Northwest National Laboratory, Richland, Washington.
- RPP-CALC-61031, 2017, *Low-Activity Waste Glass Release Calculations for the Integrated Disposal Facility Performance Assessment*, INTERA, Inc. for Washington River Protection Solutions LLC, Richland, Washington.
- RPP-CALC-61192, 2017, *Integrated Disposal Facility Performance Assessment: Sensitivity Calculations for ILAW Glass Dissolution Rate Parameters*, AEM Consulting, LLC for Washington River Protection Solutions LLC, Richland, Washington.

- RPP-CALC-61194, 2018, *System Model Calculations for the Integrated Disposal Facility Performance Assessment*, Rev. 1A, INTERA, Inc. for Washington River Protection Solutions, LLC, Richland, Washington.
- RPP-PLAN-60520, 2020, *Program Plan for Immobilized Low Activity Waste (ILAW) Glass Testing*, Rev. 1, Washington River Protection Solutions, LLC, Richland, Washington.
- RPP-RPT-59341, 2016, *Integrated Disposal Facility Model Package Report: ILAW Glass Release*, Rev. 0A, Washington River Protection Solutions, LLC, Richland, Washington.
- RPP-RPT-59958, 2019, *Performance Assessment for the Integrated Disposal Facility, Hanford Site, Washington*, Rev. 1A, Washington River Protection Solutions, LLC, Richland, Washington.
- Ryan, J. V., B. Parruzot, A. M. Lines, S. A. Bryan, L. M. Seymour, J. F. Bonnett, and R. K. Motkuri, 2019, "In-situ monitoring of seeded and unseeded stage III corrosion using Raman spectroscopy," *npj Materials Degradation*, vol. 3, Article number 34, pp. 1–7.
- VSL-01R3501-2, 2001, *Final Report – Melter Tests with LAW Envelope A and C Simulants to Support Enhanced Sulfate Incorporation*, Vitreous State Laboratory, The Catholic University of America, Washington, D.C. (ORP-63503, 2001, *Final Report – Melter Tests with LAW Envelope A and C Simulants to Support Enhanced Sulfate Incorporation*, VSL-01R3501-2, Rev. 0, Rev. 0, U.S. Department of Energy, Office of River Protection, Richland, Washington).
- VSL-06R6480-1, 2006, *Final Report – DuraMelter 100 Tests to Support LAW Glass Formulation Correlation Development*, Vitreous State Laboratory, The Catholic University of America, Washington, D.C. (ORP-56324, 2006, *Final Report – DuraMelter 100 Tests to Support LAW Glass Formulation Correlation Development*, VSL-06R6480-1, Rev. 0, Rev. 0, U.S. Department of Energy, Office of River Protection, Richland, Washington).
- VSL-07R1130-1, 2007, *Final Report – Enhanced LAW Glass Formulation Testing*, Vitreous State Laboratory, The Catholic University of America, Washington, D.C. (ORP-56293, 2007, *Final Report – Enhanced LAW Glass Formulation Testing*, VSL-07R1130-1, Rev. 0, dated 10/05/07, Rev. 0, U.S. Department of Energy, Office of River Protection, Richland, Washington).
- VSL-19R4620-2, 2019, *Final Report FY 2019 ILAW Glass Ion Exchange Rate Testing*, Vitreous State Laboratory, The Catholic University of America, Washington, D.C.
- VSL-20R4820-1, 2020, *Final Report FY2020, Long-Term PCT of ILAW Glasses*, Vitreous State Laboratory, The Catholic University of America, Washington, D.C.

RAI 2-8 (Glass Cracking)

Comment

Additional information is needed on the basis for the assumed factor of 10 increase in specific surface area of the glass to account for cracking.

Basis

Glass release rates for many glass formulations, although not all, are directly proportional to the specific surface area (m²/g). To account for potential cracking of the glass during cooling and handling, DOE increase the geometric surface area of the glass by a factor of 10. In sensitivity cases (termed RSA) examined in the PA document, DOE further increased the specific surface area by a factor of 10 and showed a proportional increase in the fractional release rate for two do not address what the value will be for production-scale glass canisters which will have different glass compositions.

Many of the reports dealing with cracking of glass are older (e.g., PNL-5947) but do have useful information to try to evaluate the DOE assumed value of 10. PNL-5947 had a maximum adjusted relative surface area of 65 with many of the reported values greater than 10. Table 1 show below (from ML040130177) provides some observed values from the literature (including values from PNL-5947).

Table 2-8-1. Summary of Studies Examining Surface Area Increases Due to Thermal Fracturing.

Glass Composition	Glass block size (relative)	Surface Area Increase (relative to unfractured glass)	Reference
SRL211	large-scale	2 - 40	Smith and Baxter 1981
SRL211, SRL131	large-scale	7 - 18	Peters and Slate 1981
SRL211, SRL131	small-scale	0 - 18	Peters and Slate 1981
borosilicate	large-scale	9.0 - 16.3	Laude et al. 1982
SRL165	large-scale	25 - 35	Bickford and Pellarin 1987
borosilicate	small- to large scale	1.1 - 86	Faletti and Ethridge 1988
borosilicate	medium-scale	2.0 - 10	Lutze et al. 1986
R7T7	small-scale, 1:10	10 - 12	Vernaz and Godon 1991
PNL76-375	large-scale	8 - 45	Martin 1985
PNL76-375	small-scale	1.1 - 12	Martin 1985
borosilicate	medium-scale	not measured	Keinzler 1989
BRETHLW borosilicate glass	medium-scale	not measured	Farnsworth et al. 1985

Source: Table 1 of Section 2.2.1.5 of UCRL-ID-108314, *Preliminary Waste Form Characteristics Report Version 1.0*, Rev. 1.

NRC staff were not able to determine the canister filling and cooling procedures that DOE would use to determine the appropriateness of the assumed factor of 10. Rapid cooling can contribute to more significant crack formation, however slow cooling can impact the quality and performance of glass that is produced. NRC staff were also not able to identify verification plans for the specific surface area in production-scale glass canisters.

Path Forward

Please provide additional technical basis for the assumed effect of cracking on glass specific surface area, utilize a bounding value, or provide plans to verify the assumed value in production-scale glass canisters. Please describe the cooling cycles anticipated to be used during glass production.

DOE Response

Response will be provided in Revision 1 of this document.

References

ML040130177, 1991, *Preliminary Waste Form Characteristics Report Version 1.0*, Lawrence Livermore National Laboratory, Livermore, CA (UCRL-ID-108314, 1994, *Preliminary Waste Form Characteristics Report Version 1.0*, Rev. 1, Lawrence Livermore National Laboratory, Livermore, California).

RAI 2-9 (Glass Stage III)**Comment**

Additional information is needed to support the basis that Stage III glass corrosion will not occur for disposal of vitrified waste at IDF.

Basis

Stage III behavior in glass corrosion or degradation is believed to occur late in the reaction sequence as a result of the formation of zeolites and other phases which deplete silicon and other species in solution faster than which those species are added to solution. The phenomenon is not well-understood but has been associated with higher temperatures and closed systems. DOE indicated that Stage III conditions are not likely at IDF because it will be low temperature (150C) and an open system. The temperature of the system is fairly certain unless degrading organic matter or heat-generating waste were to be disposed in the facility. The openness of the system is more uncertain. The impermeable asphalt layer combined with the Geosynthetic Composite Layer (GCL) liner under the facility can result in very low flow rates and conditions that could approximate a closed system. In addition, the fluid that reacts with the glass in the simulations was not a fluid that had reacted with the overlying engineered barriers but was a Hanford groundwater composition.

The modeling of glass degradation used Chalcedony as a kinetic control because the results of chemical reaction progress modeling were found to agree reasonably well with experimental results involving several different glass types at 90°C if chalcedony was assumed to form (PNNL-20781, 2011); however, chalcedony has not been directly detected as an alteration product of glass corrosion (PNNL-24615, 2015). In other words, Chalcedony and the assumed kinetic controls is a calibration parameter used by DOE to fit the empirical data. That does not justify the assumption of the absence of Stage III behavior. In the assessment of different secondary mineral formation, DOE didn't consider minerals that could conceivably generate Stage III glass corrosion because such behavior was considered unlikely under IDF-relevant conditions (PNNL-24615, 2015).

Path forward

Please demonstrate Stage III behavior is unlikely taking into consideration the potential temperature ranges and degrees of openness of the disposal system. This may be done by performing geochemical modeling or generating experimental data using relevant fluid compositions and appropriate minerals. PA calculations could be used to address the significance of the formation of Stage III behavior.

DOE Response (Tim New Section)

DOE maintains that Stage III conditions are not likely at the IDF because it will be low temperature (15 °C) and an open system. However, DOE recognizes the point raised by the NRC review:

“The openness of the system is more uncertain. The impermeable asphalt layer combined with the Geosynthetic Composite Layer (GCL) liner under

the facility can result in very low flow rates and conditions that could approximate a closed system.”

Hence, work to assess the potential impacts of Stage III rate acceleration in Hanford VLOW glasses is an ongoing part of the IDF PA Maintenance Program. Laboratory-based efforts are addressing two questions: 1) If the IDF acts more like a closed system, then is there experimental evidence that Stage III behavior, or the formation of zeolites, occurs at the IDF temperature (approximately 15 °C)?, and 2) Are induced Stage III glass dissolution rates high enough at the IDF temperature to cause contaminant releases to exceed IDF performance objectives? As the NRC reviewer noted, the temperature of the IDF system is fairly certain since no significant sources of heat will be part of the waste buried in the facility. In addition to the laboratory efforts, a long-term field study in the Hanford Site FLTF is underway to observe the behavior of glass waste forms under conditions that more closely represent those of waste buried in the IDF.

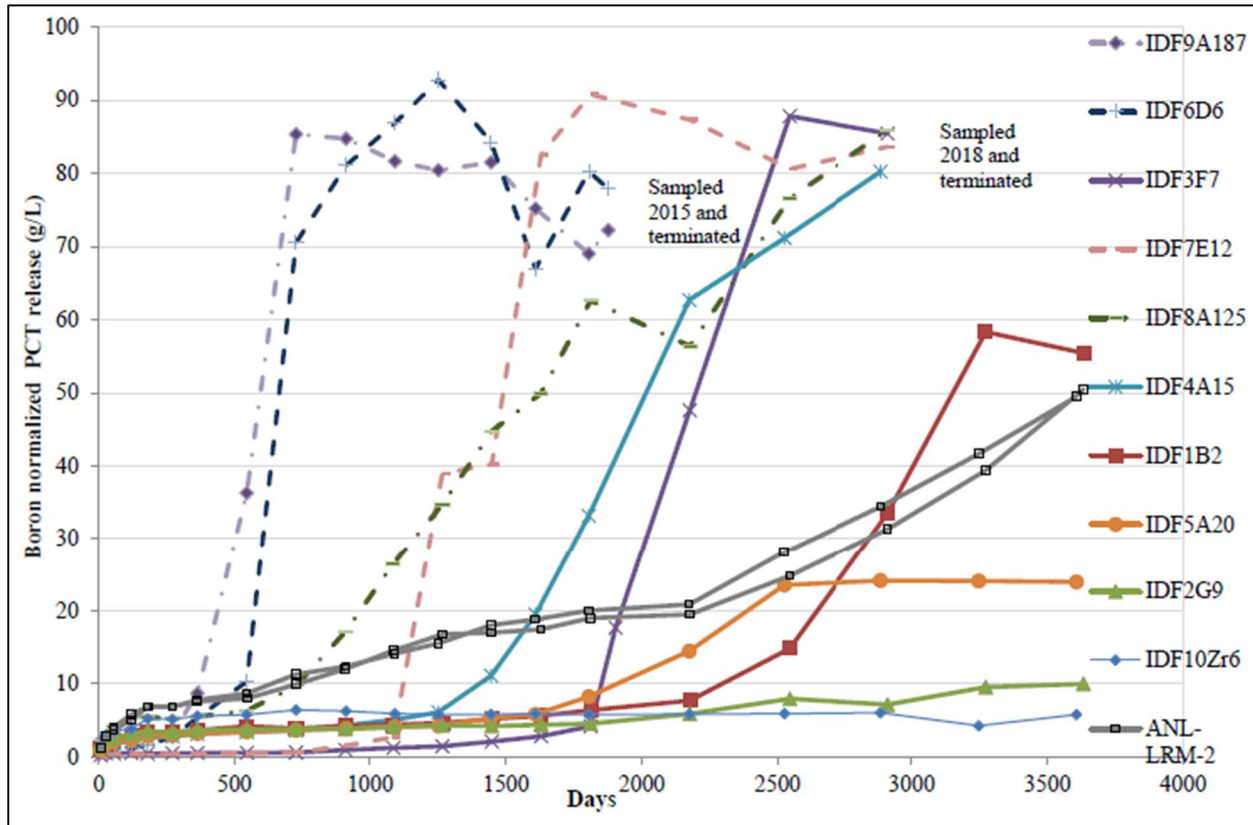
Laboratory Testing to Address Question 1

Long-term testing at the VSL has been observing the dissolution behavior of numerous ILAW glass samples in a closed system containing glass in an aqueous solution. These glass samples have been incubating for as long as ten years. As has been reported by numerous authors, Stage III rate acceleration is observed at temperatures at, or above, 90 °C for samples with high surface area-to-liquid volume ratios (i.e., conditions that promote concentrated aqueous solutions) (VSL-20R4820-1; “Resumption of alteration at high temperature and pH: rates measurements and comparison with initial rates” [Fournier et al. 2014]). It should be noted that a vast majority of the historical glass corrosion data available, as a whole, has been obtained from tests performed at 90 °C. Figure 2-9-1 (extracted from VSL-20R4820-1) shows results for ten Hanford ILAW glasses (and a reference glass ANL-LRM-2) incubated in water for 10 years. Clearly, several of the glasses have accelerated from a low rate to a high rate indicating Stage III behavior (c.f. IDF9A187, IDF6D6, IDF3F7, IDF7E12, IDF8A125, IDF4A15, IDF1B2, IDF5A20, ANL-LRM-2). Similar behavior is also observed in glasses in the ALTGlass database (“Accelerated Leach Testing of GLASS (ALTGLASS): I. Informatics approach to high level waste glass gel formation and aging” [Jantzen et al. 2017]).

In contrast, the glasses represented in Figure 2-9-1 showed much less alteration when tested at 40 °C (see Figure 2-9-2) than at 90 °C, and rate resumption is not as evident. Note that in both figures the data are presented as the normalized *cumulative* release of boron so the slope of each curve approximates the dissolution rate for that glass³⁵. VSL asserts that none of the glasses tested at 40 °C have reached an accelerated Stage III rate over the 10-year testing period (VSL-20R4820-1). The highest initial rate was for IDF8A125, with 11% of the glass reacted at 900 days with little alteration occurring since then. PNNL evaluated the data represented in Figure 2-9-2 and suggested that four glasses (IDF8A125, IDF9A187, IDF5A20, and IDF2G9) may show onset times of Stage III glass dissolution (PNNL-28898). However, as the data shows, if Stage III behavior is occurring, it is not sustained in all glasses.

³⁵ Note that the data shown in these figures represents tests where 4% of the liquid volume is removed and replaced with deionized water at each sampling interval so any estimates of reaction rates should account for this slight departure from purely static test conditions.

Figure 2-9-1. PCT-B (static dissolution) Results (90 °C and S/V of 2,000 m⁻¹) for the Ten Integrated Disposal Facility Glasses (Total available normalized boron release is 100 g/L at S/V of 2,000 m⁻¹).



Source: VSL-20R4820-1, *Final Report FY2020, Long-Term PCT of ILAW Glasses*.

Evidence for Stage III rate increase in ILAW glasses at temperatures below 90 °C has been reported by Ryan et al. (2019). These researchers observed dissolution rate increase in an ILAW glass (LAWA76) in tests at 70 °C. LAWA76 was chosen since it exhibited a rapid transition to Stage III at 90 °C, and it was thought that this system may be susceptible to the same processes at lower temperatures. After approximately 75 days, Stage III behavior was observed and continued in a constant fashion for the remainder of the test period (approximately 4 months).

Laboratory Testing to Address Question 2

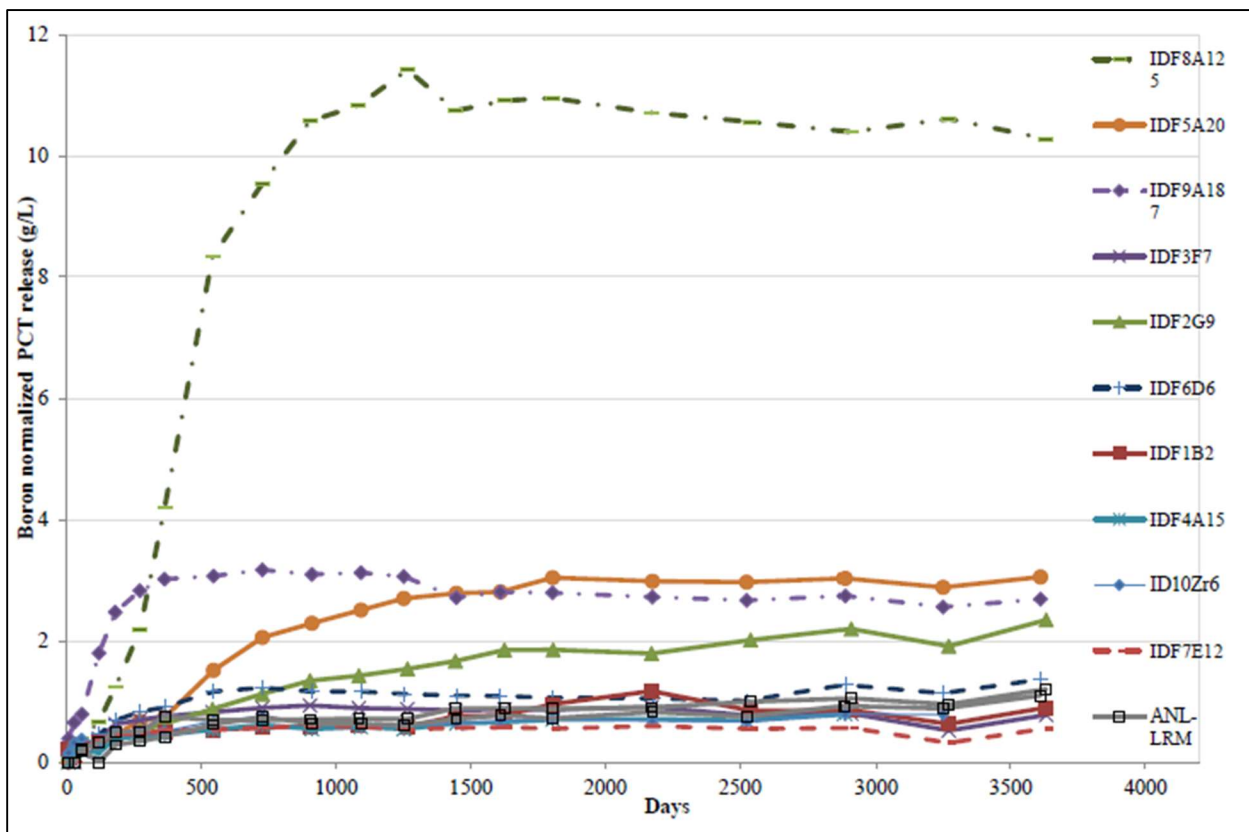
It is difficult to show through testing that ILAW glass would not undergo Stage III rate acceleration at IDF conditions due to the slow dissolution rates at lower temperatures and uncertainty regarding nucleation time of zeolite phases that can promote Stage III. Testing has been undertaken at PNNL to determine the range of dissolution rates that could be expected if Stage III were to occur by seeding with zeolites known to promote Stage III (PNNL-28898). The logic associated with these tests is as follows:

- If Stage III rates are experimentally measured at multiple temperatures for a glass, an apparent activation energy can be used to determine a Stage III rate at the IDF

temperature of 15 °C (Note: experimental data are available at 22 °C, which is only a 7 °C difference)

- This Stage III rate can then be used in a sensitivity case in a PA calculation to assess the impact of Stage III behavior in the IDF PA
- If the result of the PA calculation where Stage III is assumed to occur is below compliance limits, it would provide technical defensibility for a minimal risk of Stage III adversely impacting IDF performance objectives.

Figure 2-9-2. PCT-B Results (40 °C and S/V of 2,000 m⁻¹) for the Ten Integrated Disposal Facility Glasses (Total available normalized boron release is 100 g/L at S/V of 2,000 m⁻¹).



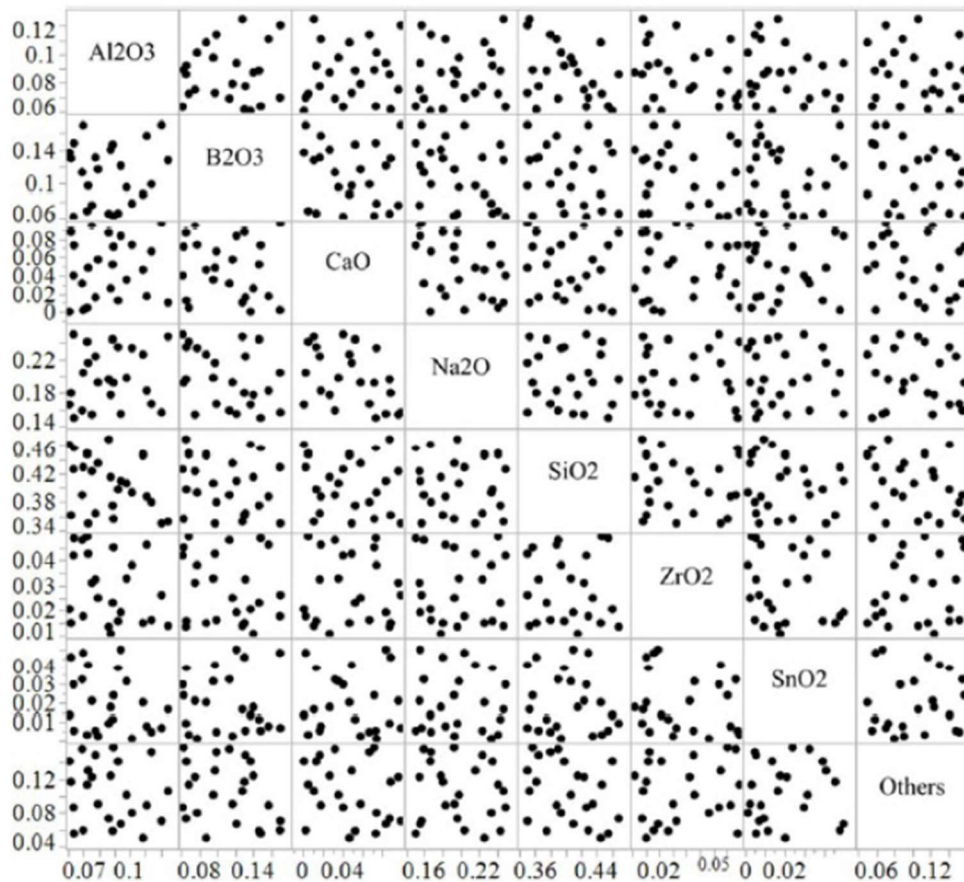
Note the 8x difference in the Y-axis scales between Figures 1 and 2.

Source: VSL-20R4820-1, *Final Report FY2020, Long-Term PCT of ILAW Glasses*.

To support this analysis, Stage III data on glasses that cover the full range of ILAW glass compositions is needed. A method has been developed at PNNL wherein long-term PCTs are seeded with zeolites once the glasses have reached the Stage II residual rate, then monitored for onset and magnitude of Stage III behavior. This work at PNNL is being conducted on 24 statistically-designed glasses (Figure 2-9-3) that span the possible composition space for enhanced waste loading ILAW glasses. This composition space also covers a majority of the processible baseline glasses (“Acceleration of glass alteration rates induced by zeolite seeds at

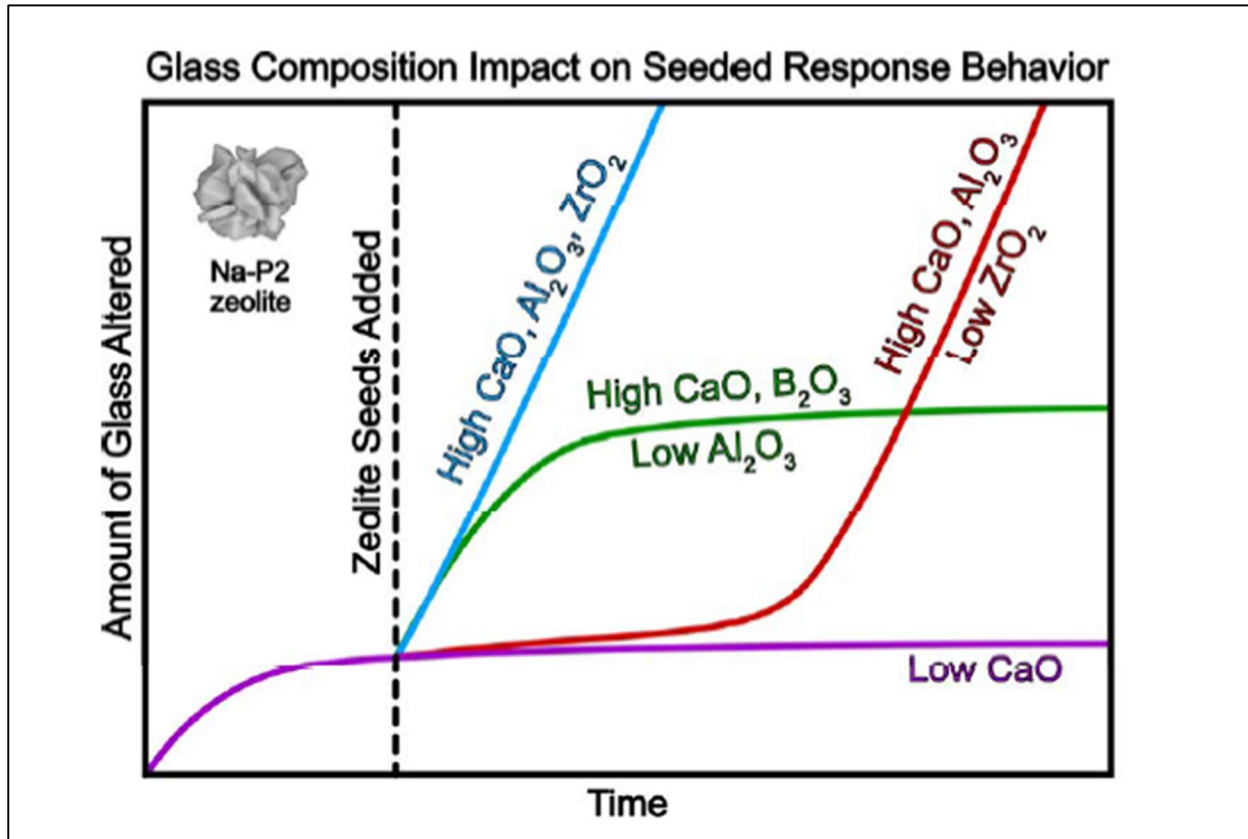
controlled pH” [Neeway et al. 2020]; “Multi-glass investigation of Stage III glass dissolution behavior from 22 to 90 °C triggered by the addition of zeolite phases” [Parruzot et al. 2019]; Ryan et al. 2019; PNNL-28898).

Figure 2-9-3. Scatter Plot of Individually Varied Glass Components (in mass fractions) in the Statistically-Designed Glass Formulations Representative of the Enhanced Immobilized Low-Activity Waste Glass Compositional Region.



In these tests at PNNL, samples of the 24 glasses are being incubated in aqueous solutions at multiple temperatures (90 °C, 70 °C, 40 °C, and room temperature, ~22 °C), both with and without zeolite seeding. Dissolved glass components are measured in periodically-collected liquid samples to assess dissolution rate with time. At the conclusion of the tests the secondary solid phases that are formed are also being analyzed and the results used to reassess the SMRN to be used in the IDF PA glass dissolution model. Results to date have shown that most of the 24 glasses have shown an increase in rate (Stage III) after zeolite seeds were added to the system at all four temperatures. The responses to the introduction of seeds can be binned into four different behavior types. Figure 2-9-4 summarizes these four types of responses to zeolite seeding for the test duration along with the apparent relationship between the response and the composition of certain elements in the glass. It should be noted that these observations are primarily based on data from tests at 90 °C (“Seeded Stage III Glass Dissolution Behavior of a Statistically Designed Glass Matrix” [Crum et al. *Under Review*]).

Figure 2-9-4. Graphical Depiction of the Four Types of Responses Measured for Hanford Immobilized Low-Activity Waste Glasses Exposed to an Aqueous Solution and Seeded with Zeolite P2.



Note: The observed relationship to composition for each of the four responses is also indicated.

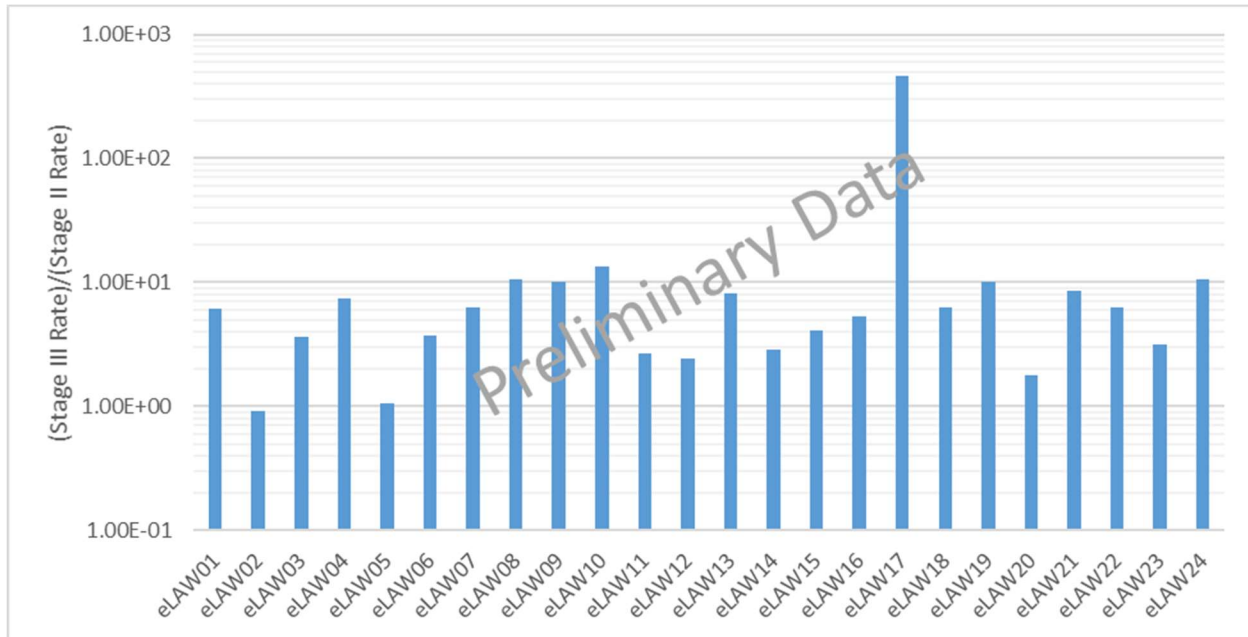
Source: "Seeded Stage III Glass Dissolution Behavior of a Statistically Designed Glass Matrix" (Crum et al. *Under Review*).

The ratio of the preliminary predicted dissolution rates for seeded to unseeded tests (i.e., [seeded Stage III rate]/[rate prior to seeding]) at 15 °C reported in PNNL-28898 ranges from 0.9 to 470 with a geometric mean³⁶ of 5.7. IDF PA predictions indicate that a glass dissolution rate increase of less than approximately 9X over the nominal Stage II glass dissolution rate would not result in contaminant releases exceeding regulatory limits at the point of compliance (RPP-CALC-63176). Eighteen of the 24 glasses tested had ratios at, or below, 9X and only one glass had a ratio greater than 11 (eLAW 17) as shown in Figure 2-9-5, which summarizes the rate ratio based on data extracted from Tables 5-4 and 5-5 in PNNL-28898. It should be noted that these results are based predominantly on data collected at 90 °C and 70 °C and will be updated with data collected at lower temperatures in FY 2021. While the Stage III/Stage II ratio may be a useful metric for demonstrating compliance, the ultimate criterion will be whether the potential Stage III rate for any specific glass composition would exceed the IDF PA performance

³⁶ The geometric mean is used rather than the arithmetic mean since the data spans two orders of magnitude with one possible outlier (see Figure 2-9-5, below). Use of the arithmetic mean would produce a result heavily weighed by the high value measured for eLAW17.

objective. As a defense-in-depth measure, it is expected that glass composition constraints could be implemented to ensure potential Stage III dissolution rates at IDF conditions would be well below a rate that would exceed IDF performance objectives.

Figure 2-9-5. Ratio of Predicted Stage III Rates (from seeded tests) to Stage II Rates (using the rate prior to seeding) at 15 °C.



Note: This data is marked as preliminary since it is based on estimates of the Stage II rate that will be updated in fiscal year 2021.

Data in this figure were extracted from Tables 5-4 and 5-5 in PNNL-28898, *FY2019 Status Report: Seeded ILAW Glass Stage III Static Dissolution Rate Measurements*.

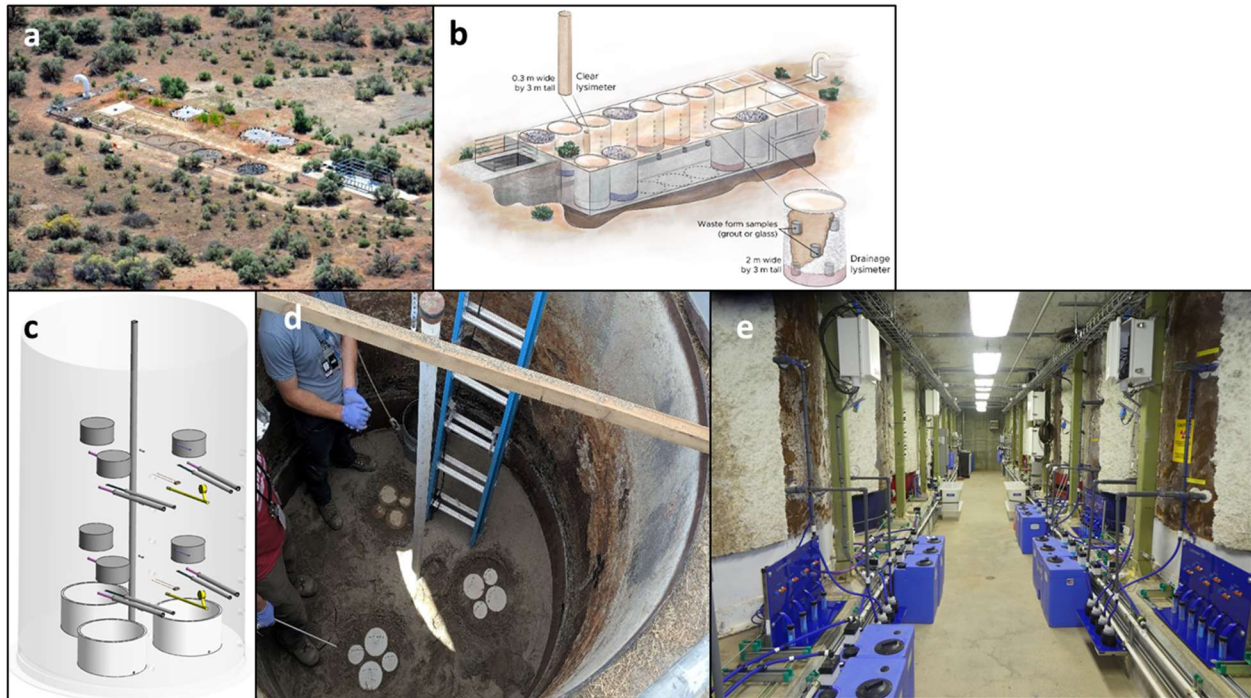
Assessing Waste Form Degradation Under Field Conditions

The final area of work being conducted to support validating predictions of ILAW glass dissolution rates within the IDF is a lysimeter field demonstration in the Hanford Site FLTF. As shown in Figure 2-9-6, the FLTF has a series of field lysimeter tubes (most extend to a depth of 3 m) that can be filled with various waste forms, including glass and cementitious materials, and back filled with IDF soils. Water infiltration rate is controlled within each lysimeter tube. Water samples will be collected at various depths within the lysimeters over the next several years, along with measurements of the *in situ* distribution of moisture.

Prior to initiation of the lysimeter test, a modeling effort was performed using the same simulation methods as the IDF PA to predict the behavior of the emplaced waste forms and corresponding contaminant releases, using ^{99}Tc and ^{127}I as tracers for the cementitious waste forms and molybdenum and rhenium as tracers for the glass waste forms (PNNL-27394). As data are collected from the test, comparisons will be made against the initial modeling that will serve as a validation of the model and determine the extent to which the laboratory-based parameters are applicable to waste form behavior in the field. Water analysis and *in situ* soil moisture data from these tests will start to be available in FY 2021 but data from solids analysis

will not be available until the tests conclude, which depending on the test may be 5 years to 25 years in the future.

Figure 2-9-6. Images of the Field Lysimeter Test Facility a) Aerial Photograph of the Facility, b) Artist Three-Dimensional Drawing of the Facility, c) Depiction of the Layout of Buried Waste Forms and Sampling Devices Within a Single Lysimeter Tube, d) Photograph of the Lower Level of Buried Cementitious Waste Forms, and e) Photograph of the Underground Sampling Bay Showing the Two Rows of Lysimeter Tubes.



With the two glass formulations selected, Stage III behavior may not be observed over the duration of the lysimeter test. However, post-experimental characterization of the excavated waste forms and backfill will also be completed at the test conclusion to evaluate the evolution of mineral phases and to determine if any zeolite phases have been formed. Note that the presence of zeolites does not indicate that Stage III behavior is inevitable, but the presence of zeolites has been correlated to Stage III behavior in laboratory testing. As stated under the discussion of Stage III (above), data is also being collected in laboratory tests to assess the magnitude of the impact of Stage III rate behavior on contaminant release from the IDF to the surrounding environment.

References

- Crum, J. V., T. J. Reiser, B. P. Parruzot, J. J. Neeway, J. F. Bonnett, S. N. Kerisit, S. K. Cooley, J. V. Ryan, G. L. Smith, R. M. Asmussen, *Under Review*, “Seeded Stage III Glass Dissolution Behavior of a Statistically Designed Glass Matrix,” *Journal of the American Ceramic Society*.
- Fournier, M., P. Fruiger, and S. Gin, 2014, “Resumption of alteration at high temperature and pH: rates measurements and comparison with initial rates,” *Procedia Materials Science*, vol. 7, Issue 14, pp. 202–208.
- Jantzen, C. M., C. L. Trivelpiece, C. L. Crawford, J. M. Pareizs, and J. B. Pickett, 2017, “Accelerated Leach Testing of GLASS (ALTGLASS): I. Informatics approach to high level waste glass gel formation and aging,” *International Journal of Applied Glass Science*, vol. 8, Issue 1, pp. 69–83.
- Neeway, J. J., B. P. Parruzot, J. F. Bonnett, J. T. Reiser, S. N. Kerisit, J. V. Ryan, and J. V. Crum, 2020, “Acceleration of glass alteration rates induced by zeolite seeds at controlled pH,” *Applied Geochemistry*, vol. 113, PNNL-SA-148595.
- Parruzot, B., J. V. Ryan, J. L. George, R. K. Motkuri, J. F. Bonnett, L. M. Seymour, and M. A. Derewinski, 2019, “Multi-glass investigation of Stage III glass dissolution behavior from 22 to 90 °C triggered by the addition of zeolite phases,” *Journal of Nuclear Materials*, vol. 523, pp. 490–501, PNNL-SA-138413.
- PNNL-20781, 2011, *Integrated Disposal Facility FY 2011 Glass Testing Summary Report*, Pacific Northwest National Laboratory, Richland, Washington.
- PNNL-24615, 2015, *Immobilized Low-Activity Waste Glass Release Data Package for the Integrated Disposal Facility Performance Assessment*, RPT-IGTP-005, Pacific Northwest National Laboratory, Richland, Washington.
- PNNL-27394, 2018, *Field-Scale Lysimeter Studies of Low-Activity Waste Form Degradation Implementation Plan*, RPT-IGTP-017, Rev 0.0, Pacific Northwest National Laboratory, Richland, Washington.
- PNNL-28898, 2019, *FY2019 Status Report: Seeded ILAW Glass Stage III Static Dissolution Rate Measurements*, RTP-IGTP-021, Rev 0.0, Pacific Northwest National Laboratory, Richland, Washington.
- RPP-CALC-63176, 2020, *Integrated Disposal Facility Risk Budget Tool Analysis*, Rev. 0A, Washington River Protection Solutions, LLC, Richland, Washington.
- Ryan, J. V., B. Parruzot, A. M. Lines, S. A. Bryan, L. M. Seymour, J. F. Bonnett, and R. K. Motkuri, 2019, “In-situ monitoring of seeded and unseeded stage III corrosion using Raman spectroscopy,” *npj Materials Degradation*, vol. 3, Article number 34, pp. 1–7.
- VSL-20R4820-1, 2020, *Final Report FY2020 Long-Term PCT of ILAW Glasses*, Vitreous State Laboratory, The Catholic University of America, Washington, D.C.

RAI 2-10 (Volatile Species and Glass)**Comment**

One of the most important aspects of uncertainty associated with the VLAW PA appears to be the assumed partitioning of various species, especially volatile species, between different waste types. Additional information is needed to support the amount of volatile species that will be retained in glass (Case 7 – the base case).

Basis

Initial testing of glass production determined a low retention rate of volatile species (Tc, I, Cs). The glass process was modified to recycle the off gas back into the glass feed to increase the loading of volatile species in the glass. The modifications were effective in increasing Tc retention percentages from generally less than 50% to approximately 75% (Pegg, 2015). The Tc retention in the glass assumption in the base case PA is approximately 99.9% - essentially all of the Tc ultimately is disposed in the glass waste form.

Detailed evaluation of Tc recycle was completed by Catholic University's Vitreous State Laboratory (RPP-54130, 2012). The glass production system uses a wet electrostatic precipitator (WESP) among other components. By measuring the amount of Tc in the WESP effluents, DOE estimated that the Tc retention was 99.8%. The Case 7 inventory partitioning of Tc is consistent with the WESP emissions. The amount of Tc observed in the glass was 68%. In addition, the mass balance of Tc across all tests averaged approximately 90%. DOE indicated that a significant amount of technetium was held up in the system during testing, particularly in the WESP internals, the film cooler, and the transition line. This material was therefore not available for recycle and incorporation into the glass. All of the Tc that gets deposited and retained in the various processing equipment eventually has to be disposed and those components are not going to be disposed as glass. Sulfate salt phases were observed on the melt pool surface after two of the tests. The salt phase showed an approximate fifty-fold enrichment in technetium over the glass; rhenium and halides also showed significant enrichments. These phases may be considered as being "retained" by the glass but would not likely have the same release properties as the glass.

DOE's assumed retention of Tc in glass for Case 7 would appear to be unrealistically optimistic. Case 10A had approximately 32% of the Tc in the glass reflecting no recycling of the off gas, which is likely to be unrealistically pessimistic if recycling is used. As discussed above, the mass balance was limited to approximately 90% and the amount of Tc observed to be in the glass was approximately 70%. Appropriate base case values for Tc retention in glass would appear to be in the 70 to 95% range.

The design, operation, and especially the reliability of the off-gas system with recycle would appear to be extremely important to justify the assumed Tc retention in the glass. Staff did not identify information to support the assumed 100% reliability of the off-gas system. System downtime would significantly contribute to not being able to achieve extremely high Tc retention in the glass.

Path forward

Please provide additional basis for the base case inventory or revise the base case inventory to be consistent with the observed testing data. For the base case inventory, DOE should observe mass balance, glass concentrations of volatile species, concentration of species in salt phases, and reliability of the off-gas system. For the base case inventory DOE should also account for the disposal of volatile species that build up in the system components and in what form they will be disposed.

DOE Response

Nuclear chemical processing systems are designed utilizing the principles of redundant capabilities and defense in depth for nuclear safety and environmental protection purposes. Therefore, 100% reliability is the ultimate goal of the design and operating procedures for such systems. The LAW Vitrification Facility off-gas system is designed with multiple unit operations, each having a specific function for controlling the quantities and composition of gaseous, liquid, and solid effluents from the process. The fundamental engineering concept of recycling is employed within the off-gas system design to control emissions of hazardous and radioactive constituents.

The NRC reviewers cited results from scaled melter tests with simulants as indicative of the efficiency and effectiveness that could be expected from the full-scale production system. Those studies provide valuable insight into specific aspects of volatile constituent behavior and performance of the off-gas system and its components. With proper consideration of the test system's limitations and realistic interpretation of the results, the data support the expectation that the full-scale production system will function as designed and will be capable of achieving very high recycle efficiency and incorporation of volatile constituents into the glass.

The NRC reviewers noted the extensive evaluation of technetium recycle in small-scale melter tests by the VSL (RPP-54130). The melter system included several of the major components of a prototypic LAW vitrification off-gas system (e.g., SBS, WESP, and vacuum evaporator) to facilitate simulating full off-gas condensate recycle. Nine separate melter runs were performed with different simulated feed compositions spiked with ^{99m}Tc . The authors reported 68% of technetium observed in the glass with an average mass balance closure of about 90%. In a subsequent analysis of the analytical technique used (VSL-13R2800-1, *Final Report Wet Electrostatic Precipitator Performance and Technetium-Rhenium Behavior in LAW Recycle Flow-Sheet*), VSL determined that the results of solid sample analyses for those tests were biased low by about 8.2%. Applying a correction to the melter test results would raise the average technetium in glass to about 74% and average mass balance closure to 95%.

In 2016, modifications were made to the VSL DM-10 melter system to further investigate the retention of ^{99}Tc and other volatile species in the LAW glass with recycling of the off-gas condensate. Specifically, modifications were made to decrease the hold-up of constituents in the off-gas system and reduce the time required to reach steady-state concentrations in the glass. In particular, reduction of the evaporator sump volume and periodic rinses of the WESP and evaporator head space combined to achieve 100% closure of the technetium mass balance and

near 100%³⁷ incorporation into the glass (VSL-16R3840-1, *Tracking the Key Constituents of Concern of the WTP LAW Stream*). These results confirmed the effectiveness of recycle and the ability to achieve a high percentage of incorporation of technetium in the glass product. The results also show the base case inventory is consistent with observed testing data.

In tests conducted with ^{99m}Tc, the interpretation of the results is constrained by the short 6-hour half-life of this isotope. Testing with actual ⁹⁹Tc is not economically practical as the entire melter system would be irreversibly contaminated and all the products generated would need to be managed as radioactive waste. Technetium-99m is readily available from nuclear pharmacies at reasonable cost but due to the rapid decay, the maximum melter run time that can be achieved with reasonable isotope detection limits is about 72 hours. A significant fraction of the run time is required for the system to reach steady state, so the time available for data collection at steady-state operations is limited to between 24 and 48 hours.

It is largely for this reason that the results from these melter tests should be carefully analyzed to determine their applicability to sustained steady-state operations in a production environment. A particularly valuable use of the results is to collect data on the partitioning of key constituents across the melter and off-gas system components and the performance of those components relative to their design specifications and operating parameters. In this regard, it is useful to evaluate performance of the off-gas system at points where key radionuclides and hazardous constituents will be purged from the system and therefore not recycled for incorporation into the glass product.

Major purge points in the off-gas system during DFLAW operations include components located downstream from the WESP (HEPA filters, Carbon Absorber Beds, and the Caustic Scrubber) and overhead condensate from the primary off-gas system evaporator. For example, analysis of the data from DM-10 melter runs showed that only a small fraction of feed technetium, 0.02 to 0.04%, exited the off-gas system through the WESP exhaust (VSL-13R2800-1). Results also showed that virtually all of this remaining small fraction technetium exiting the WESP will accumulate on HEPA filters downstream of the WESP during DFLAW operations. Quantities of technetium in the evaporator overhead condensates ranged from <0.0001 to 0.0004% in DM-10 melter runs conducted in 2016 (VSL-16R3840-1). During DFLAW, the evaporator overhead stream will be directed to LERF/ETF for treatment and solidification in grout for disposal at the IDF.

The NRC reviewers correctly noted that significant percentages of ^{99m}Tc accumulated in off-gas system components during DM-10 melter tests with off-gas recycle. Certain accumulations are expected due to hold-up of process liquids and residual solids at the end of a melter run. This

³⁷ Actual incorporation of technetium into the glass during the third run of this series of tests was 95%. This value represents the average composition over the entire run which included glass produced at the beginning of the run that contained very little technetium. There is no technetium in the glass pool at the start of a run and the technetium increases gradually as technetium in the fresh feed and recycle streams are fed to the melter and the system approaches steady state. After accounting for small amounts of technetium held up in lines and sumps at the end of the test, essentially 100% of the technetium not exiting the system via the WESP exhaust and evaporator overhead condensate during steady-state operation was accounted for in the glass product. The authors also noted in their conclusions that the results helped explain the lower technetium concentrations measured in product glasses in previous tests with recycle reported in RPP-54130/VSL-12R2640-1.

can be considered essentially a snapshot of the system configuration at any given point in time. Such data are useful for comparison to process model predictions as described in Section 9 of VSL-12R2640-1 (RPP-54130) which provide a more realistic representation of steady-state operations. For example, significant accumulations of ^{99m}Tc in the WESP, film cooler, and transition line during the DM-10 melter tests were measured for the primary purpose of closing the technetium mass balance. During steady-state operations, these components will be periodically rinsed or deluged to flush accumulated solids and residuals into the off-gas liquids to be recycled back to LAW vitrification for incorporation into the glass.

The appearance of sulfate salt phases on the surface of the melt pool after two of the tests reported in RPP-54130 was unexpected but could be attributed to sulfate content in the melter feed that was ~10% higher than in previous tests and at or near the sulfate solubility limit for those specific glass compositions. LAW glasses are formulated to be below the sulfate solubility limit and the data are incorporated in glass formulation algorithms to minimize the potential for sulfate salt phase formation (PNNL-25835). It is of particular concern during operations to avoid the formation of a sulfate salt layer as this would be highly corrosive to the melter refractory liner as well as Inconel[®] (a registered trademark of Special Metals Corporation, New Hartford, New York) components such as bubblers. It is of lesser concern for glass poured from the melter because the glass pour spout is fed from a location near the bottom of the melt pool and would not draw off material from the salt phase floating on top of the melt pool. Despite the fact that a salt phase on the surface of the melt pool would be unlikely to affect the quality of the glass product, the potential for salt phase formation is of considerable concern for sustained melter operations, so the information from these tests – along with other considerations such as melter scale, melt pool temperature, cold cap coverage, etc. – is used to evaluate whether adjustments to sulfate solubility models and/or glass formulation model constraints would be warranted during DFLAW operations.

References

- Pegg, I. L., 2015, "Behavior of technetium in nuclear waste vitrification processes," *Journal of Radioanalytical and Nuclear Chemistry*, Vol. 305, No. 1, pp. 287–292.
- PNL-5947, 1986, *A Method for Predicting Cracking in Waste Glass Canisters*, Pacific Northwest Laboratory, Richland, Washington.
- PNNL-25835, 2016, *Update of Hanford Glass Property Models and Constraints for Use in Estimating the Glass mass to be Produced at Hanford by Implementing Current Enhanced Glass Formulation Efforts*, Pacific Northwest National Laboratory, Richland, Washington.
- RPP-54130, 2012, *Technetium Retention in WTP LAW Glass with Recycle Flow-Sheet: DM10 Melter Testing, VSL-12R2640-1, Rev. 0*, Vitreous State Laboratory, The Catholic University of America/EnergySolutions, Federal EPC, Inc./Washington River Protection Solutions LLC, Richland, Washington.
- VSL-13R2800-1, 2013, *Final Report Wet Electrostatic Precipitator Performance and Technetium-Rhenium Behavior in LAW Recycle Flow-Sheet, Rev. 0*, Vitreous State Laboratory, Catholic University of America, Washington, D.C.
- VSL-16R3840-1, 2016, *Final Report Tracking the Key Constituents of Concern of the WTP LAW Stream, Rev. 0*, Vitreous State Laboratory, Catholic University of America, Washington, D.C.

RAI 2-11 (Comparison of STOMP and GWB)

Comment

Additional information is needed to support why some comparison cases for glass release rates generated with STOMP and Geochemist's Workbench (GWB) have not applicable (NA) entries.

Basis

In the evaluation of sensitivity cases for release from the glass wastefrom, DOE used both STOMP and GWB to estimate fractional release rates. In most cases the agreement between the two programs was reasonable (see Table 5-4 and Table 5-9 of the PA document). However, in a number of entries in the table results were only provided for one model. Because these types of calculations can have large uncertainties it is good practice to calculate results with two models. Additional information should be provided to provide the basis for only using one model for certain entries.

Path Forward

In the evaluation of sensitivity cases for release from the glass wastefrom, DOE used both STOMP and GWB to estimate fractional release rates. In most cases the agreement between the two programs was reasonable (see Table 5-4 and Table 5-9 of the PA document).

DOE Response

DOE used reactive transport models in two different software applications, STOMP and The GeoChemists Workbench³⁸ (GWB), to evaluate releases from vitrified LAW disposed of in the IDF. Models in both software applications were used to simulate glass corrosion under the expected conditions in the IDF for each simulated glass type (Envelops A, B, and C). The STOMP model is a dynamic model that starts with initial conditions and evolves over time to represent the long-term, steady-state corrosion rate associated with Stage II glass corrosion. The GWB model is an equilibrium model used only to estimate the Stage II corrosion rate. One or both software applications were used to evaluate the sensitivity of the developed models to alternative conditions and parameter values. The reference case conditions were simulated for the three glass types using models for both software applications and the results from the model runs were compared to each other to build confidence that the models developed in each application produced long-term corrosion rates that were comparable. Subsequently, the models in each application were used to investigate corrosion rates under different conditions. In many cases, the alternative conditions were run in both applications, but in others only one or the other model was used. The decision to simulate a prescribed alternative condition using just one software application or both software applications considered model capability and availability of computational resources³⁹ and time available to perform the simulations before the results were needed in a downstream calculation to support the IDF PA. None of the instances when only a single model was used for a sensitivity case were attributable to a lack of numerical convergence or similar modeling issues.

³⁸ The Geochemist's Workbench[®] is a registered trademark of Aqueous Solutions LLC, Champaign, Illinois.

³⁹ The available resources capable of running STOMP simulations were simultaneously doing simulations for near-field flow, vitrified waste releases, cementitious waste form releases, and far-field (vadose and saturated zone) flow and transport modeling as well as performing similar calculations for the Hanford WMA C performance assessment.

The EIS case (RPP-RPT-59958 Table 5-3) used STOMP to replicate as closely as possible STORM simulations that supported the Tank Closure and Waste Management Environmental Impact Statement (TC&WM EIS) (DOE/EIS-0391, *Final Tank Closure and Waste Management Environmental Impact Statement for the Hanford Site, Richland, Washington*). Additional evaluations using GWB were considered unnecessary because this calculation case involved only a comparison of STOMP and STORM results.

Calculation cases that were evaluated using only STOMP (VFLUX, HYDRL, BACK, COMB4) (RPP-RPT-59958 Table 5-3) involved changes in hydraulic properties (porosity, hydraulic conductivity, permeability) of the glass waste form and/or backfill. These properties were not explicitly accounted for in GWB models. The GWB models were instead constrained by STOMP results at steady/stationary state pertaining to the volumetric flow rate, moisture content, and residence time of water infiltrating the waste form.

Calculation cases that were evaluated using only GWB (RSA, SMRN, ICHEM, COMB2, COMB3) (RPP-RPT-59958 Table 5-3) were intended to illustrate the sensitivity of model results to alternative assumptions and/or model parameter values. GWB was considered adequate for this purpose and was also preferred because run times were expected to be much shorter than for comparable STOMP models. The opportunity to run more than 100 STOMP simulations was constrained by the very long run times required to simulate corrosion and the finite amount of time available to perform the simulations, document the analysis, and provide the inputs to downstream modeling projects, such as development of the IDF PA system model. The long STOMP model runs times were discovered once the model was up and running. It became apparent that computational time and required resources would limit the opportunity to perform all of the sensitivity cases that were planned to demonstrate how the corrosion model responds to each parameter. For this reason, the GWB model was developed to complement and augment the limited number of STOMP analyses that could be performed. Whenever possible, both models were used and compared to enhance the confidence in the results reported by the GWB model.

The “N/A” entries in RPP-RPT-59958 Table 5-9 (see also RPP-RPT-59958 Tables 5-4 and 5-6) refer to two STOMP models for the IEX case that could not be evaluated because run times were excessively long. These models were based on assumed upper bounds on the ion-exchange rate constant for LAWA44 and LAWC22 glass. Time steps, which were adjusted automatically in the STOMP simulations, were reduced significantly in these models causing run times to become excessively long. Although these simulations were started, the runs were terminated before completion because it was evident that waiting for the models to complete would delay the completion of the calculation report and jeopardize the completion of the work that used results of the glass release modeling as input. For the runs shown in Table 5-9 that were simulated with both GWB and STOMP, the two models both showed proportional changes to the corrosion rate when the ion exchange rate was changed. Since the GWB runs for LAWA44 with an ion exchange rate of $5.3\text{E-}10$ mol/m²/s and for LAWC22 with an ion exchange rate of $1.2\text{E-}9$ mol/m²/s showed the same trends as the other cases that were run with both models, it is not believed that stopping the STOMP simulations for these conditions affects the technical validity of PA results.

References

DOE/EIS-0391, 2012, *Final Tank Closure and Waste Management Environmental Impact Statement for the Hanford Site, Richland, Washington*, U.S. Department of Energy, Washington, D.C.

RPP-RPT-59958, 2019, *Performance Assessment for the Integrated Disposal Facility, Hanford Site, Washington*, Rev. 1A, Washington, Department of Energy, Richland, Washington.

RAI 2-12 (Sensitivity and Uncertainty Analyses)**Comment**

The sensitivity and uncertainty analyses presented by DOE did not include some aspects that may be important to risk-inform the review process and to determine if the relevant criteria are likely to be met.

Basis

In section 5.2.3 of the PA document, DOE described the uncertainty and sensitivity analyses completed for the draft waste evaluation for VLAW (disposal in the near surface at IDF). Key uncertainties identified by DOE included release rates, recharge rates, vadose zone hydraulic properties, vadose zone transport properties, saturated zone hydraulic properties, and waste loading configuration in the disposal facility. Sensitivity and uncertainty analyses were completed with the deterministic process models as well as the probabilistic system model. The types of uncertainties examined were reasonable and consistent with NRC's understanding of the system. However, there were some uncertainties that were not included within the scope of the evaluation that may be important to understand in order to risk-inform the review and determine if the criteria will be met with reasonable expectation (DOE) or reasonable assurance (NRC).

In section 5.1 of the PA document, DOE described a number of different analyses cases completed to evaluate near-field flow and source-term release. The computational results were presented in RPP-CALC-61029. DOE examined the timing of engineered layer "failures" by examining a case where the surface cover and liner had a step change in properties at 500 years post-closure. While this is an appropriate case to examine, given the uncertainties being addressed, the evaluation is incomplete. The performance of the engineered cover is reliant to a large extent on an asphalt layer whereas the performance of the liner is reliant on a GCL. Because of numerical difficulties, the hydraulic conductivity of the asphalt layer was only increased an order of magnitude in a step manner. The properties of fresh, intact asphalt compared to aged, cracked asphalt would be expected to differ by much more than an order of magnitude. In addition, because of the different materials involved, there is limited expectation that the different layers would "fail" at the same time or same rate. In general, engineered layers closer to the land surface experience a more diverse set of processes and events that lead to more rapid alteration by nature. It would be reasonable to examine a case with a degraded cover and an indefinitely performing liner system. NRC was not able to find information describing the drain and sump systems to evaluate their propensity for plugging or decrease in performance.

In section 5.1.2 of the PA document, DOE examined sensitivity of glass release rates to various parameters. One case, termed HYDRL, examined the effect of changes to hydraulic properties of the glass wastefrom. Moisture characteristic curves (MCC's) can have a significant impact on release rates if differing materials are present and simulation of capillary barrier effects occurs. The HYDRL and combined cases should be expanded to include the impact of uncertainties in MCC's. There may be reduced sensitivity of the results to changes in some inputs, such as recharge, due to the masking effect of the asphalt layer performance and the MCC's assigned. The SRMN cases evaluated the impact of the secondary mineral formation network. The SRMN cases showed a large impact from uncertainty in what minerals form and therefore their thermodynamic properties. The SRMN cases should be expanded and, if possible, supported by

information from experiments and the literature. The discussion in the PA indicates that selection of chalcedony (see RAI 2-7) was essentially a calibration as it was used to match empirical results, and actual phases observed in experiments were not used because acceptable glass degradation rates could not be achieved. This is a source of uncertainty within the modeling and the simulated degradation rates in the PA are essentially an extrapolation of short-term empirical observations. This type of uncertainty should be reflected in the base case results, or the potential impact on the base case results communicated to decisionmakers, otherwise a false sense of confidence may be assigned to the assurance as to whether the regulatory criteria will be achieved.

DOE indicated that when considered together, multiple sources of conceptual and parameter uncertainty with respect to glass release modeling may thus have a cancelling effect in predictive models of glass corrosion. The overall impact of these uncertainties on fractional releases may consequently be relatively small. It is unclear how this conclusion was arrived at unless inverse correlations between the relevant uncertainties were observed (and this is not common). Uncertainties will propagate and expand the potential range of outcomes. A probabilistic assessment of glass release rate uncertainties would help better define the range of uncertainty in glass release rates.

A large source of uncertainty in the performance of the IDF is from the inventory splits, or the fraction of key radionuclides that end up in different waste streams. DOE's base case (Case 7) has a very high percentage of the ^{99}Tc that ends up in the glass wasteform because of recycling. By comparison, cases 10A and 10B have a low percentage of ^{99}Tc that ends up in the glass wasteform as a result of volatilization during processing. This uncertainty is the only uncertainty discussed that by itself that can swing the results from compliance to noncompliance. This uncertainty was not included in the global uncertainty analyses completed with the system model. The significance of an individual uncertainty depends on all other uncertainties, how they impact the results, and how close the results are to the regulatory standards. If a key uncertainty is identified but left out of the comprehensive uncertainty analyses the importance of individual uncertainties may be misinterpreted.

DOE examined some types of inventory uncertainties through special cases. The magnitude of the inventory in the base case did not reflect the uncertainty in the inventory that would be generated and processed into the various waste types. NRC had made various comments on the development of inventory values for WMA-C, some of which are also relevant to this draft WIR evaluation (ML20128J832). While it is true that this type of uncertainty has a relatively linear impact on the dose results and can be easily projected, this type of uncertainty directly compounds with other types of uncertainties in the PA and increases the range of potential outcomes thereby decreasing the certainty with which demonstration of compliance with the criteria can be achieved.

Path Forward

Please expand the sensitivity and uncertainty analyses to include the items discussed above in the basis part of this comment (e.g., additional glass release uncertainties, inventory splits, inventory uncertainties).

DOE Response

Response will be provided in Revision 1 of this document.

References

ML20128J832, 2020, *Technical Evaluation Report, Draft Waste Incidental to Reprocessing Evaluation for Closure of Waste Management Area C, Hanford Site, Washington*, U.S. Nuclear Regulatory Commission, Rockville, Maryland.

RPP-CALC-61029, 2017, *Two-Dimensional, Two-Phase Flow Model Calculations for the Integrated Disposal Facility Performance Assessment*, Rev. 0, INTERA, Inc. for Washington River Protection Solutions, LLC, Richland, Washington.

RAI 2-13 (Quality Assurance)

Comment

Some aspects of the quality assurance program were not clear from the documentation provided.

Basis

DOE provided detailed information on most aspects of the quality assurance program applied to the development of the analyses supporting the draft waste evaluation for VLAW. However, a few aspects of the quality assurance program were not clear. The quality assurance status and controlled use of the major software or computer programs was demonstrated (e.g., GoldSim, STOMP). The quality assurance status or verification activities for ancillary software was not provided in all instances. For example, the Hanford Defined Waste model (HDW) was used as part of the inventory development process. Some components of the HDW were previously assessed and found to contain significant errors, but other components of the HDW were not verified (ML20128J832). The thermodynamic database used in the geochemical modeling for glass degradation (thermo.com.V8.R6+.tdat) came from Lawrence Livermore National Laboratory. The qualification status of that database was not clear.

Verification information was provided for STOMP verification and test cases that demonstrated select aspects of the software. However, it wasn't clear from the documentation provided how those verification activities demonstrate or verify the correct functioning of the software for the key aspects of the performance assessment, namely the glass degradation and release rate calculations and the unsaturated flow phenomena especially the capillary barrier effects. Verification of unsaturated flow phenomena in general is not the same as verifying that STOMP correctly produces results for very dissimilar materials using a coarse numerical grid.

Path Forward

Please provide the qualification status of software and databases that supply information to the performance assessment calculations, or the plans to determine the qualification status of the referenced software and databases. Please provide the verification results or plans for verification of the release rate and unsaturated flow phenomena simulated by STOMP for glass degradation as applicable to the performance assessment.

DOE Response

Response will be provided in Revision 1 of this document.

References

ML20128J832, 2020, *Technical Evaluation Report, Draft Waste Incidental to Reprocessing Evaluation for Closure of Waste Management Area C, Hanford Site, Washington*, U.S. Nuclear Regulatory Commission, Rockville, Maryland.

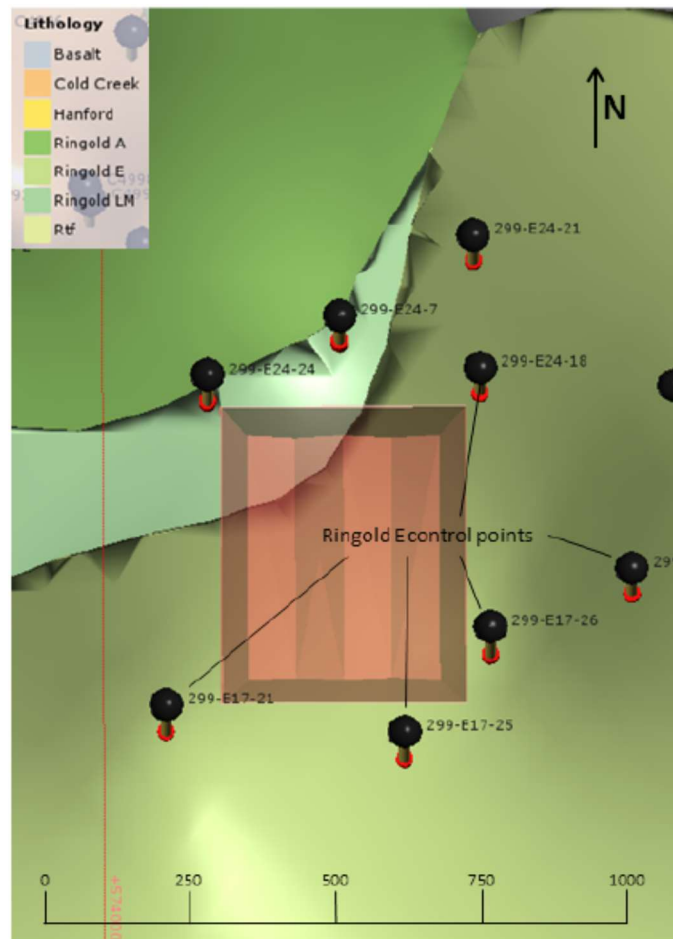
RAI 2-14 (Geologic Uncertainty)**Comment**

The basis for the interpretation of the geology underlying the footprint of the IDF that removed the Ringold E formation is not clear.

Basis

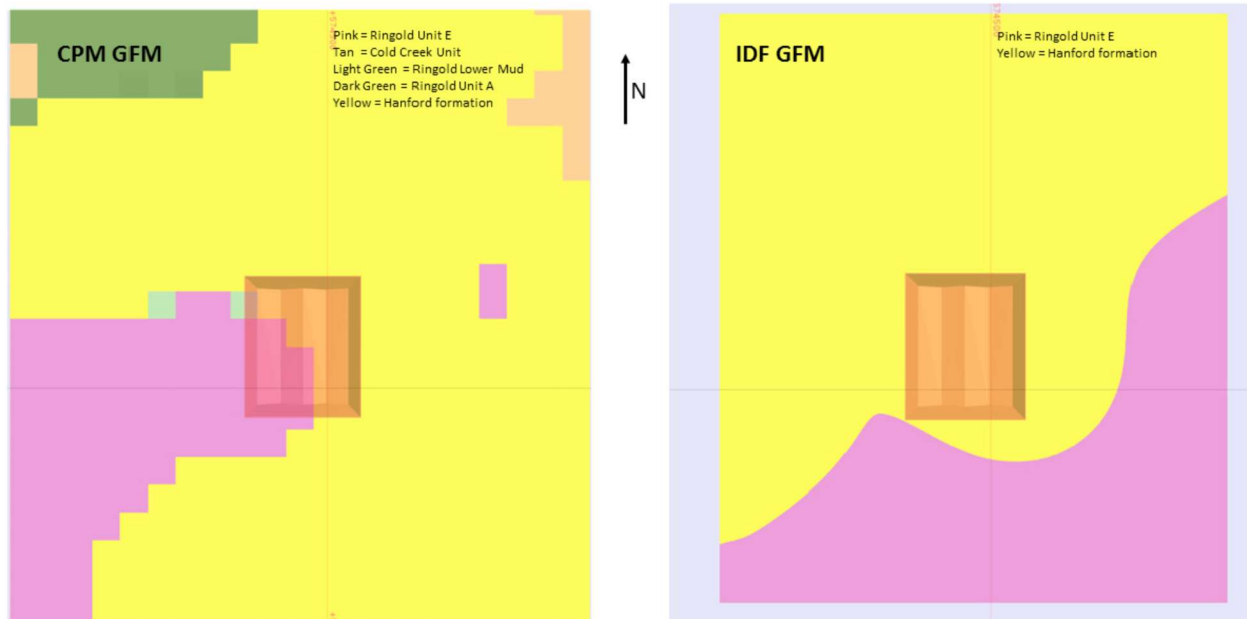
DOE's previous interpretation of the geology underlying the IDF had a layer termed the Ringold E present in the northwest corner of the footprint of the facility (see the figures below). DOE explained that some geologic information was reinterpreted, and the geologic framework model was revised. The data shows quantitative information to suggest the boundary of the layer is somewhere between the boreholes (see first figure below). If the modeling was revised, it isn't clear how the change in the boundary of the unit was validated in the absence of additional data. The significance of the unit is that the Ringold E is much less permeable than the Hanford unit such that fluxes of contaminants into the unit experience lower dilution and therefore result in higher concentrations. If groundwater protection standards apply to all geologic units, then it may be more difficult to demonstrate that groundwater protection standards have been met.

Figure 2-14-1. Hanford South Geologic Framework Model Ringold E Well Control.



Source: Figure 3-53 of RPP-RPT-59958, *Performance Assessment for the Integrated Disposal Facility, Hanford Site, Washington*.

Figure 2-14-2. Plan View Comparison of Central Plateau and Integrated Disposal Facility Geologic Framework Models at 114.5 Meters.



Source: Figure 3-63 of RPP-RPT-59958, *Performance Assessment for the Integrated Disposal Facility, Hanford Site, Washington*.

Path Forward

Please provide additional basis for the reinterpretation of the location of the Ringold E and indicate whether groundwater protection standards apply to this unit.

DOE Response

DOE acknowledges that there is uncertainty in the geologic framework model (GFM) describing the sediments underneath the IDF. Borehole characterization is the main technique that is used to delineate the contact locations between different hydrostratigraphic layers across the Hanford Site. The geologic framework models built from borehole logs are subject to re-interpretation each time a new borehole is drilled into the subsurface and each time a groundwater model is calibrated to existing conditions. Often times the professional staff developing the refinements to the GFMs are different, which can lead to the use of different techniques to interpret contact points away from boreholes and can also result in alternative contact points being developed from borehole logs based on professional judgement. Working groups are utilized to minimize the changes that can be made by a single individual.

Interpretation of the location of the contact between the Ringold Unit E (Rwie) and Hanford formation hydrostratigraphic units (HSUs) near the IDF has evolved over time as additional boreholes have been drilled and logged. According to well construction and soil boring records in the Hanford Environmental Information System (HEIS) database, between 2000 and the end

of 2020 more than 1,000 groundwater wells and 1,600 soil borings have been drilled on the Hanford Site. Since 2014, nearly 300 groundwater wells and 100 soil borings have been drilled. Geologic framework models are coupled to a database of HSU contact points that is regularly updated with new boring information. The interpretations have been included in the GFMs of the area of the Central Plateau that include the area near the IDF. As noted in the RAI, the location of that contact can make a significant difference in the dilution afforded by the saturated zone beneath the IDF depending on the hydraulic conductivity of the two HSUs beneath the IDF (see RAI 2-16 for additional discussion of the basis for the base case hydraulic conductivity for the Hanford and Rwie HSUs beneath the IDF).⁴⁰

The groundwater protection standards apply to the point-of-compliance, which is defined as the point of maximum predicted groundwater concentration along the groundwater flow path at a boundary located 100 m from the disposed of waste, which is approximated as the edge of the IDF. The groundwater specific discharge between the edge of the IDF and the 100-m boundary controls the amount of dilution contributed by the saturated zone in the IDF PA and therefore controls the predicted groundwater concentration that is compared to the groundwater protection standards. The groundwater specific discharge is determined by the hydraulic conductivity and hydraulic gradient in the HSU beneath and downgradient of the edge of the IDF. Therefore, the groundwater specific discharge is dependent on the hydraulic characteristics of the HSU beneath and within 100 m of the edge of the IDF.

To address the RAI, the response is organized into the following sections:

- Evolution of the Location of the Ringold Unit E in GFMs near the IDF
- Current Interpretation of the Location of the Ringold Unit E near the IDF
- Current Interpretation of the Hydraulic Conductivity of HSUs near the IDF.

Evolution of Location of the Ringold Unit E in GFMs near the IDF

The interpreted location of the Rwie near the IDF has evolved over time as additional boreholes have been drilled and characterized and additional data sources have been interpreted by different subject matter experts to distinguish between the poorly-cemented gravels of the Hanford formation and the Cold Creek Unit (CCU), which comprise the paleochannel deposits in the high-conductivity zone beneath the 200 East Area, and the cemented gravels of the Rwie.

The history of the different interpreted GFMs developed for the area is summarized in

Table 2-14-1.

At the time of the initial ILAW PA⁴¹ completed in 1998 (DOE/RL-97-69, *Hanford Immobilized Low-Activity Tank Waste Performance Assessment*), it was assumed that the water table beneath the ILAW site was in the Rwie (equivalent to the mapped Ringold Unit 5). This assumption was made given the lack of site-specific information on the lateral extent of the Hanford formation

⁴⁰ The importance of the characteristics of the HSUs beneath the IDF, in particular the location of the Rwie/Hanford contact, was noted as a key assumption in Section 8.4.3 of the IDF PA (RPP-RPT-59958). Additional characterization of the hydrostratigraphy in the saturated zone beneath the IDF was identified as maintenance activity in Section 4.7 of the IDF Maintenance Plan (CHPRC-03348).

⁴¹ The Immobilized Low-Activity Waste (ILAW) disposal facility was renamed the Integrated Disposal Facility (IDF).

gravel and uncertainty in the location of the Hanford paleochannel near the location of the ILAW site. Prior to 1998, very few boreholes were drilled near the IDF. As a result of this assumption, the dilution of radionuclides released from the ILAW facility and transported to the saturated aquifer beneath the ILAW site was limited by the lower specific discharge in the Rwie (due to the lower hydraulic conductivity of the Rwie compared to the Hanford formation gravels).

Table 2-14-1. Evolution of Geologic Framework Models in the Vicinity of the Integrated Disposal Facility. (5 sheets)

GFM Document ID (Date)	Basis for Interpretation of Hydrostratigraphic Unit Contacts
TC&WM EIS DOE/EIS-0391 (December 2012)	<p>DOE/EIS-0391 Appendix L: The TC&WM EIS groundwater flow model has been encoded with hydrogeologic data for the entire model domain developed from Hanford well borings completed as of September 2009. Approximately 5,000 boring logs from Hanford and its surroundings were reviewed to determine whether the geologic units and discrete hydrostratigraphic layers could be recognized from the geologic descriptions. When multiple logs existed for a borehole, higher credibility was given to those descriptions recorded by a professional geologist. Logs were reviewed for specific identification of the Elephant Mountain basalt, Hanford and Ringold Formations, and Cold Creek and Plio-Pleistocene Units. The logs were further examined to discern textural types among the sedimentary units: mud, silt, sand, and gravel. Each of the resulting hydrogeologic units is encoded with unique properties (see DOE/EIS-0391 Section L.4.4).</p> <p>DOE/EIS-0391 Appendix N: Subsurface geology for the set of STOMP models was determined using field data from over 5,000 boring logs. Soil types for each model domain were assigned based on individual borehole interpretations. Examination of single or multiple cross sections were used to specify the three-dimensional (3D) spatial distribution of soil types in row/column views.</p>
Hanford South GFM ECF-HANFORD-13-0029, Rev. 0 (July 2014)	<p>To define and construct geologic unit layers within the Hanford South Model, two primary data sets were utilized, 1) best-estimate depth to geologic unit contacts (in feet below ground surface), and 2) ground surface elevations (at the time of drilling in meters above mean sea level). These data are selected based on professional judgment by professional or registered geologists and hydrogeologists, reviewed and approved by general technical consensus for model input. Anomalies in the geologic model and the related borehole data (e.g., elevations) with high variability for specific unit contacts were reevaluated to verify or revise best-estimate geologic unit contacts or ground surface elevations relative to raw and interpreted borehole or other related data. For the Hanford South Model, best estimates of geologic unit contacts were compiled for 1,396 wells and boreholes within, and adjacent to, the Hanford South Model domain.</p> <p>In summary, the technical approach for this work was to assemble a regional stratigraphic model of the southern Hanford Site using previously published interpretations of the geologic units. These geologic units are managed, periodically updated as new well data become available, and maintained in an Excel® spreadsheet at CH2M HILL Plateau Remediation Company (CHPRC) (GeoContacts Hanford revision date). The GeoContacts_Hanford_2014-06-26 data set used for this model is located on the internal link maintained by CHPRC.</p>
Hanford South GFM	This revision provides the 2014 updated 3D model results which utilized the GeoContacts_Hanford_2015-02-24 data set. This data set includes the addition of

Table 2-14-1. Evolution of Geologic Framework Models in the Vicinity of the Integrated Disposal Facility. (5 sheets)

GFM Document ID (Date)	Basis for Interpretation of Hydrostratigraphic Unit Contacts
ECF-HANFORD-13-0029, Rev. 1 (May 2015)	nine new boreholes to the model (none of which are in the 200 East area) and refinements to the surfaces based on input from project staff.
Central Plateau GFM, Version 6.3.3 CP-47631, Rev. 2 (July 2015)	<p>Freestone Environmental Services, Inc. provided borehole data for the entire model domain in the form of a geodatabase (NearFieldGeoElevations_7_16_09.mdb) as described in ECF-200PO1-09-2074, <i>200-PO-1 Groundwater Operable Unit Remedial Investigation Report - Geologic Cross Sections</i>.</p> <p>A total of 56 wells in the 200-BP-5 Groundwater operable unit (OU) area have undergone elevation adjustments after receiving the hydrostratigraphic unit (HSU) database from Freestone Environmental Services, Inc. Most of these involve the bottom elevation of the Hanford formation. A number of issues led to the reevaluation of HSU elevations in the 200-BP-5 Groundwater OU area including:</p> <ul style="list-style-type: none"> • Discrepancies in the Pacific Northwest National Laboratory (PNNL) tops database (Geologic Contact Depths_2009_12_03.xls) identified by inspection and review of specific well logs by a geologist • Discrepancies in entries in the database compiled by Freestone Environmental Services, Inc. identified by comparison to the PNNL tops database • Gaps of missing elevations between units identified by inspection • Errors/reinterpretation based on review of well logs. <p>The Hanford formation bottom elevations were lowered to the top of basalt for 49 wells located in the paleochannel area extending from 200 East and through the Gable Gap (between Gable Mountain and Gable Butte). This modification was justified based on the review of well logs that reported the Cold Creek unit beneath the Hanford formation in 200-BP-5 Groundwater OU area to be of large grain size, indicating that it may behave hydraulically much like the Hanford formation. Furthermore, a subset of wells had information gaps where no units were specified below the Hanford formation, and the gap between the bottom of the Hanford unit and the basalt surface needed to be filled for developing a 3D model.</p>
Hanford South GFM ECF-HANFORD-13-0029, Rev. 2 (December 2015)	<p>This revision provides the 2014 updated 3D model results which utilized the Leapfrog Geo® modeling software and used the most current GeoContacts_Hanford_2015-02-24 data set. This data set includes the nine 2014 boreholes added in Revision 1 of this environmental calculation file (ECF) and refinements to the surfaces based on input from subject matter experts and project staff.</p> <p>For this version of the Hanford South Geologic Framework Model, best estimates of geologic unit contacts were compiled for 1,405 wells and boreholes within, and adjacent to the Hanford South Geologic Framework Model domain.</p>
Integrated Disposal Facility (IDF) GFM RPP-RPT-59343 (July 2016)	Interpretations for Hanford formation sub-unit lithology were made by examining borehole geologic and geophysical logs obtained from the Hanford Environmental Information System (HEIS). HEIS is a quality-controlled database maintained by CHPRC and was accessed for the geologic and geophysical borehole logs needed for interpretation. GeoContacts_Hanford_2015-02-24.xlsx was also accessed for existing interpretations and is the best estimate at the time of drilling for the geologic contact depths for the sedimentary units underlying the Hanford Site.

Table 2-14-1. Evolution of Geologic Framework Models in the Vicinity of the Integrated Disposal Facility. (5 sheets)

GFM Document ID (Date)	Basis for Interpretation of Hydrostratigraphic Unit Contacts
	<p>All boreholes identified to exist within the IDF GFM domain were considered for interpretation. However, log information for some of the boreholes existing within the IDF GFM domain was insufficient for use in a high-confidence interpretation and therefore these boreholes were omitted from the facies model. This decision is based on the professional judgment of experienced geologists; when a contact location could be determined it was entered into the database, when there was insufficient information or the quality of the records were poor no contact elevation was determined for that location.</p> <p>It should be noted that saturated flow and transport simulation for IDF utilizes the established Central Plateau Groundwater Model (CPGWM), which incorporated a GFM developed independently of any Hanford South GFM version (CP-47631, <i>Model Package Report: Central Plateau Groundwater Model, Version 6.3.3</i>). Therefore, a comparison of the IDF and CPGWM GFM's was needed in order to gauge any possible effects that differences between the two models would have on flow and transport simulations.</p> <p>Data sources include:</p> <ul style="list-style-type: none"> • PNNL-14586, <i>Geologic Data Package for 2005 Integrated Disposal Facility Performance Assessment</i> • PNNL-15237, <i>Geology of the Integrated Disposal Facility Trench</i> • PNNL-17913, <i>Hydrogeology of the Hanford Site Central Plateau – A Status Report for the 200 West Area, Rev. 1</i> • ECF-Hanford-13-0029, <i>Development of the Hanford South Geologic Framework Model, Hanford Site Washington</i> • HEIS is a controlled database from which borehole geologic and geophysical logs used in IDF GFM geologic interpretations were accessed.
Hanford South GFM ECF-HANFORD-13-0029, Rev. 3 (January 2017)	<p>This revision provides the 2015 updated 3D model that utilizes the Leapfrog Geo[®] modeling software and uses the most current GeoContacts_Hanford_2016-05-10.xlsx data set. This data set includes the addition of 64 boreholes drilled or interpreted in fiscal year 2015 and six boreholes with recently revised stratigraphic contacts to the model. After borehole data is input, there are refinements made to the stratigraphic surfaces based on input from subject matter experts and project staff.</p> <p>This version of the Hanford South GFM (HS_051016_EXP.lfw) has been updated to expand the outer boundary of the model. The expanded domain boundaries are to the expanded to the west, east and south by 7,312, 2,183 and 7,197 meters, respectively, from the previous versions. This expansion was made to accommodate numerical modeling needs.</p>
Hanford South GFM ECF-HANFORD-13-0029, Rev. 4 (January 2017)	<p>This revision provides a 2016 update to the Hanford South GFM, which utilizes the Leapfrog Geo[®] modeling software and uses the most current GeoContact_Hanford_2017-01-12.xlsx data set. This data set includes the boreholes utilized in Revision 3 and 17 boreholes drilled or interpreted in fiscal year 2016. One older borehole (699-38-70) was removed from the 2016 input file because a new borehole (299-W 19-116) was drilled immediately adjacent and has higher data quality available. After borehole data is</p>

Table 2-14-1. Evolution of Geologic Framework Models in the Vicinity of the Integrated Disposal Facility. (5 sheets)

GFM Document ID (Date)	Basis for Interpretation of Hydrostratigraphic Unit Contacts
	input, there are refinements made to the stratigraphic surfaces based on input from subject matter experts and project staff.
Central Plateau Vadose Zone (CPVZ) GFM, Rev. 0 CP-60925, Rev. 0 (March 2018)	The technical approach for creating the CPVZ GFM included using the existing Hanford South GFM (ECF-HANFORD-13-0029, Rev. 4) and previously-published interpretations of the major geologic units to refine and update a database of major vadose zone stratigraphic contacts. In addition, an evaluation of available and applicable borehole data was included to interpret vadose contacts where none were previously recorded. During this process, comparisons to the existing GeoContacts data set and area-specific type logs were made to guide, verify, and ultimately select the best-estimate contacts for use in the model. The best-estimate contacts and ground surface elevations were then selected, based on professional judgment and general consensus, to develop two-dimensional (2D) interpretations, structure and isopach maps, and geologic cross sections. These interpretations were used to further evaluate vadose zone stratigraphic continuity, boundary extents and conditions, and correlation of the units between boreholes across the Composite Analysis domain. Data anomalies identified in the geologic interpretations and boreholes were re-evaluated to verify the best-estimate GeoContacts relative to the raw borehole data and type logs. Changes were made as necessary; the corrected and updated contacts data were defined, through an iterative process, and the final best-estimate contacts data set was used to complete the 2D interpretations.
Hanford South GFM ECF-HANFORD-13-0029, Rev. 5 (May 2018)	In this revision of this ECF (Revision 5), 96 boreholes were added, seven boreholes were deleted, and the stratigraphy of 16 existing boreholes was revised. Other changes to the model – adjustments in control data and slight changes in model extent – are discussed. The deleted boreholes either contradicted other nearby data or belonged in the 100-Area GFM north of Gable Mountain and Gable Butte.
CPVZ GFM, Rev. 1 ECF-HANFORD-18-0035, Rev. 0 (March 2020)	<p>The purpose of this revision includes the following:</p> <ul style="list-style-type: none"> – Integrate updated saturated zone surfaces from the Hanford South GFM (ECF-HANFORD-13-0029) – Include new geologic data from boreholes drilled after 2016 – Utilize numerical grain-size distribution data stored in the Hanford Virtual Library’s ROCSAN database to evaluate existing interpretations based on geologic modified Folk-Wentworth classification and geophysics – Expand the model domain to encompass the Treated Effluent Disposal Facility – Add a light detection and ranging topography surface as the top of the GFM – Correct inconsistencies in the original revision of the CPVZ Rev. 0 (CP-60925) <p>This current revision of the CPVZ GFM contains tops from 1,216 boreholes within the domain boundary compared to the 1,092 boreholes utilized in CP-60925. Twenty-four of the wells from the original 1,092 were removed while 148 boreholes were added in this revision. New boreholes were added in this revision of the CPVZ GFM for the following reasons:</p> <ol style="list-style-type: none"> a. Recent drilling b. Changes in the model domain boundary c. Site-specific models within the GFM domain providing new information

Table 2-14-1. Evolution of Geologic Framework Models in the Vicinity of the Integrated Disposal Facility. (5 sheets)

GFM Document ID (Date)	Basis for Interpretation of Hydrostratigraphic Unit Contacts
	d. New interpretations of older borehole data <ul style="list-style-type: none"> – Information that makes the hydrostratigraphic interpretation more consistent with the rest of the GFM.

GFM = Geologic Framework Model

TC&WM EIS = Tank Closure and Waste Management Environmental Impact Statement

References:

CP-47631, *Model Package Report: Central Plateau Groundwater Model Version 6.3.3, Rev. 2.*

CP-60925, *Model Package Report: Central Plateau Vadose Zone Geoframework Version 1.0, Rev. 0.*

DOE/EIS-0391, *Final Tank Closure and Waste Management Environmental Impact Statement for the Hanford Site, Richland, Washington.*

ECF-HANFORD-13-0029, *Development of the Hanford South Geologic Framework Model, Hanford Site Washington, Rev. 0.*

ECF-HANFORD-13-0029, *Development of the Hanford South Geologic Framework Model, Hanford Site, Washington, Rev. 1.*

ECF-HANFORD-13-0029, *Development of the Hanford South Geologic Framework Model, Hanford Site, Washington, Rev. 2.*

ECF-HANFORD-13-0029, *Development of the Hanford South Geologic Framework Model, Hanford Site, Washington, Rev. 3.*

ECF-HANFORD-13-0029, *Development of the Hanford South Geologic Framework Model, Hanford Site, Washington Fiscal Year 2016 Update, Rev. 4.*

ECF-HANFORD-13-0029, *Development of the Hanford South Geologic Framework Model, Hanford Site, Washington, Rev. 5.*

ECF-HANFORD-18-0035, *Central Plateau Vadose Zone Geoframework, Rev. 0.*

RPP-RPT-59343, *Integrated Disposal Facility Model Package Report: Geologic Framework, Rev. 0.*

Excel® is a registered trademark of Microsoft Corporation in the U.S. and other countries.

Leapfrog Geo® is a registered trademark of ARANZ Geo Limited, LLC of Christchurch, New Zealand.

Subsurface Transport Over Multiple Phases (STOMP) is developed and distributed by Battelle Memorial Institute.

Between the initial ILAW PA in 1998 and the 2001 version completed in 2001 (DOE/ORP-2000-24, *Hanford Immobilized Low-Activity Waste Performance Assessment: 2001 Version*), additional boreholes were drilled (e.g., 299-E17-21 was constructed in April 1998 and 299-E24-21 was constructed in March 2001) and characterized near the IDF. The new information resulted in a reinterpretation of the location and thickness of the gravels in the Hanford paleochannel and the contact between the Rwie and Hanford gravel. This reinterpretation resulted in there being an increase in the lateral extent of the Hanford gravel beneath the IDF which resulted in an increase in the assumed dilution afforded by the higher specific discharge in the Hanford gravel of about a factor of 7 and a corresponding reduction in peak concentration by a factor of 0.14 (Table ES-8 of DOE/ORP-2000-24). Hydraulic properties of the Rwie and Hanford formation gravels were still based on measurements made from locations throughout the footprint of the Hanford Site.

The basis for the location of the contact of the Rwie and Hanford gravel used to develop the GFM used in the IDF PA is taken from the Hanford South GFM, which uses an HSU contact points database dated in February 24, 2015. By comparison, the Central Plateau Groundwater

Model (CPGWM) was based on a contact database developed by PNNL in 2009 (Geologic Contact Depths_2009_12_03.xls) and refined to correct discrepancies identified during a data review before the data were used. No new wells in the vicinity of the IDF were installed to groundwater between December 2009 and February 2015. Therefore, the differences between contact points between the Rwie and Hanford gravel are attributed to grid scale and the technique and rules used to assign HSUs to each grid node.

The HSU contact points away from the well control points for the GFM in CPGWM Version 6.3.3 are interpolated using 100-m grid blocks with varying thicknesses near the water table. The upper and lower HSU surfaces between adjacent layers were developed independently of each other using standard kriging (CP-47631, *Model Package Report: Central Plateau Groundwater Model, Version 6.3.3, Rev. 2, Section 4.2.6*). When the bottom of an upper HSU overlapped with the top of an underlying HSU, preferential assignment was given to the upper HSU in the GFM because the upper units tend to be more permeable and more important to the modeling representation of flow in the aquifer. This decision would tend to substitute Hanford formation gravel where Rwie might be present away from a characterized borehole. The newer Hanford South GFM was developed by another team using different techniques to assign HSU contact points. The Hanford South GFM developed in ECF-HANFORD-13-0029, *Development of the Hanford South Geologic Framework Model, Hanford Site, Washington, Rev. 2*, which is the basis of the IDF GFM, used a different kriging algorithm (the proprietary radial basis interpolation function built into Leapfrog Geo^{®42}) that considered the HSU elevation in the nearby boreholes when assigning a grid block to a specific HSU. Because of the different grid scales and interpolation techniques away from borehole control points, the GFMs from two representations near the IDF have different HSU contact points between the Hanford formation and Rwie. The most recent version of the CPGWM (CP-47631, *Model Package Report: Central Plateau Groundwater Model, Version 8.4.5, Rev. 4*) uses the Hanford South GFM.

The cited figure in the RAI (Figure 3-62 of RPP-RPT-59958), compares the location of the contact of the Rwie and Hanford gravel as interpreted in the CPGWM GFM (documented in CP-47631, Rev. 2) current at the time the IDF PA model was completed and the interpreted contact in the IDF GFM (documented in RPP-RPT-59343, *Integrated Disposal Facility Model Package Report: Geologic Framework*) at an elevation of 119.5 m above sea level (asl) (corresponding to the elevation of the long-term steady-state water table near the IDF). The difference in interpreted surfaces was ascribed to the different GFMs used, with the GFM used in the CPGWM GFM (CP-47631, Rev. 2) based on a predecessor to the Hanford South GFM (see **Table 2-14-1**) while the interpreted surface in the IDF GFM (RPP-RPT-59343) was based on a more recent version of the Hanford South GFM (ECF-HANFORD-13-0029, Rev. 2). The boreholes used to define the location of the Rwie/Hanford contact are illustrated in Figure 3-53 of RPP-RPT-59958 (which is included in the RAI; see Figure 2-14-1).

The reason for the changing interpretation is that the physical and compositional differences between the Hanford, CCU gravel unit (CCUg) and Rwie are subtle. Traditionally, the key difference used to distinguish the Rwie and the Hanford gravels has been the composition of the gravel. At the time of Ringold deposition the basalt highlands such as Rattlesnake Mountain did

⁴² Leapfrog Geo[®] is a registered trademark of ARANZ Geo Limited, LLC of Christchurch, New Zealand.

not exist, so there were fewer basalt clasts in the gravel. In addition, at that time the ancestral Columbia River was flowing through mountain ranges in Canada that provided abundant quartzite and micas to the sediments. As a result, the Ringold gravels are generally characterized by an increase in quartzite pebbles and a decrease in basalt pebbles compared to the Hanford gravels, with the CCUg gravels having intermediate quartzite and basalt pebble fractions between the Rwie and Hanford end members. In addition, because the Ringold sediments are older, they are characterized by having greater cementation and lithification than the younger CCUg and Hanford formation gravel unit (H3) gravels. The identification of the presence of and contact elevation between HSUs of similar physical and compositional appearance many years after a borehole is drilled is dependent on the quality of the characterization reported in the borehole log and a subjective judgement made by the interpreter(s). In some areas of 200 East, like WMA C, trying to separate these units is very challenging because lower gravel units have been reworked in the main channel areas and interpretations in some local areas have treated these gravel units as a combined undifferentiated H3, CCUg and Rwie unit.

Current Interpretation of the Location of the Ringold Unit E near the IDF

As summarized in **Table 2-14-1**, the GFM's in the area near the IDF have continued to be updated as new information has been developed and interpreted. The most current version of the Central Plateau Vadose Zone (CPVZ) GFM is documented in ECF-HANFORD-18-0035, *Central Plateau Vadose Zone Geoframework*. **Table 2-14-2** summarizes the HSU contacts for the key HSUs (H3 gravel, CCUg and Rwie) that define the location and thickness of these HSUs near the IDF. Figures illustrating the most recent interpretation of the contact are included as **Figure 2-14-3** based on the boreholes with interpreted contacts of the Rwie illustrated in **Figure 2-14-4** (derived from ECF-HANFORD-18-0035).

Table 2-14-2. Formation Tops and Elevations in Boreholes near the Integrated Disposal Facility. (2 sheets)

Well Name	Hanford ID	Depth (m)	Elevation (m)	H3 Depth (m)	CCU Depth (m)	CCU Elevation (m asl)	CCUg Depth (m)	CCUg Elevation (m asl)	Rtf Depth (m)	Rwie Depth (m)	Rwie Elevation (m asl)	Comment
299-E17-21	B8500	146.3	224.3	75.3	96.7	127.6	97.2	127.1	97.8	98.5	125.8	These boreholes are located to the south or southeast of the Integrated Disposal Facility (IDF). The long-term steady-state water table, assumed to be at an elevation of 119.5 m asl, is in the Rwie for these boreholes consistent with the interpretation in the IDF geologic framework model (RPP-RPT-59343).
299-E17-22	C3826	109.3	220.6	65.9	77.8	142.8	86.5	134.1	—	93.2	127.4	
299-E17-23	C3827	112.8	223.8	77.3	99.5	124.3	99.5	124.3	99.6	99.7	124.1	
299-E17-24	C3828	116.7	224.8	84.6	98.5	126.3	99.3	125.5	—	100.2	124.6	
299-E17-25	C3926	113.9	225.0	83.8	98.8	126.2	99.5	125.5	—	100.1	124.9	
299-E17-26	C4648	115.5	224.4	77.7	85.7	138.7	86.9	137.5	—	97.9	126.5	
299-E24-18	A4753	100.6	219.4	67.4	90.3	129.1	90.9	128.5	—	—	<118.8	These boreholes are located to the north or northeast of the IDF. The long-term steady-state water table, assumed to be at an elevation of 119.5 m asl, is in the CCUg for these boreholes (with the exception of 299-E17-57) in contrast to the interpretation in the IDF geologic framework model (RPP-RPT-59343) which has the water table in the H3 gravel. The CCUg has hydraulic properties equivalent to the H3.
299-E24-21	C3177	101.8	217.8	80.9	82.6	135.2	83.0	134.8	—	—	<116.0	
299-E24-24	C4647	110.9	220.5	67.1	91.2	129.3	91.7	128.8	—	—	<109.6	
299-E24-7	A4757	137.2	218.7	65.1	89.0	129.7	89.9	128.8	—	115.2	103.5	
299-E17-56	D0038	111.2	220.0	—	88.4	131.6	89.9	130.1	—	103.6	116.4	
299-E17-57	D0041	108.4	220.8	—	—	—	—	—	—	—	<112.4	
299-E24-164	D0040	106.7	219.1	—	85.3	133.8	89.9	129.2	—	—	<112.4	

Table 2-14-2. Formation Tops and Elevations in Boreholes near the Integrated Disposal Facility. (2 sheets)

Well Name	Hanford ID	Depth (m)	Elevation (m)	H3 Depth (m)	CCU Depth (m)	CCU Elevation (m asl)	CCUg Depth (m)	CCUg Elevation (m asl)	Rtf Depth (m)	Rwie Depth (m)	Rwie Elevation (m asl)	Comment
-----------	------------	-----------	---------------	--------------	---------------	-----------------------	----------------	------------------------	---------------	----------------	------------------------	---------

Source: Modified from ECF-HANFORD-18-0035, *Central Plateau Vadose Zone Geoframework*, Rev. 0, Table C-1.

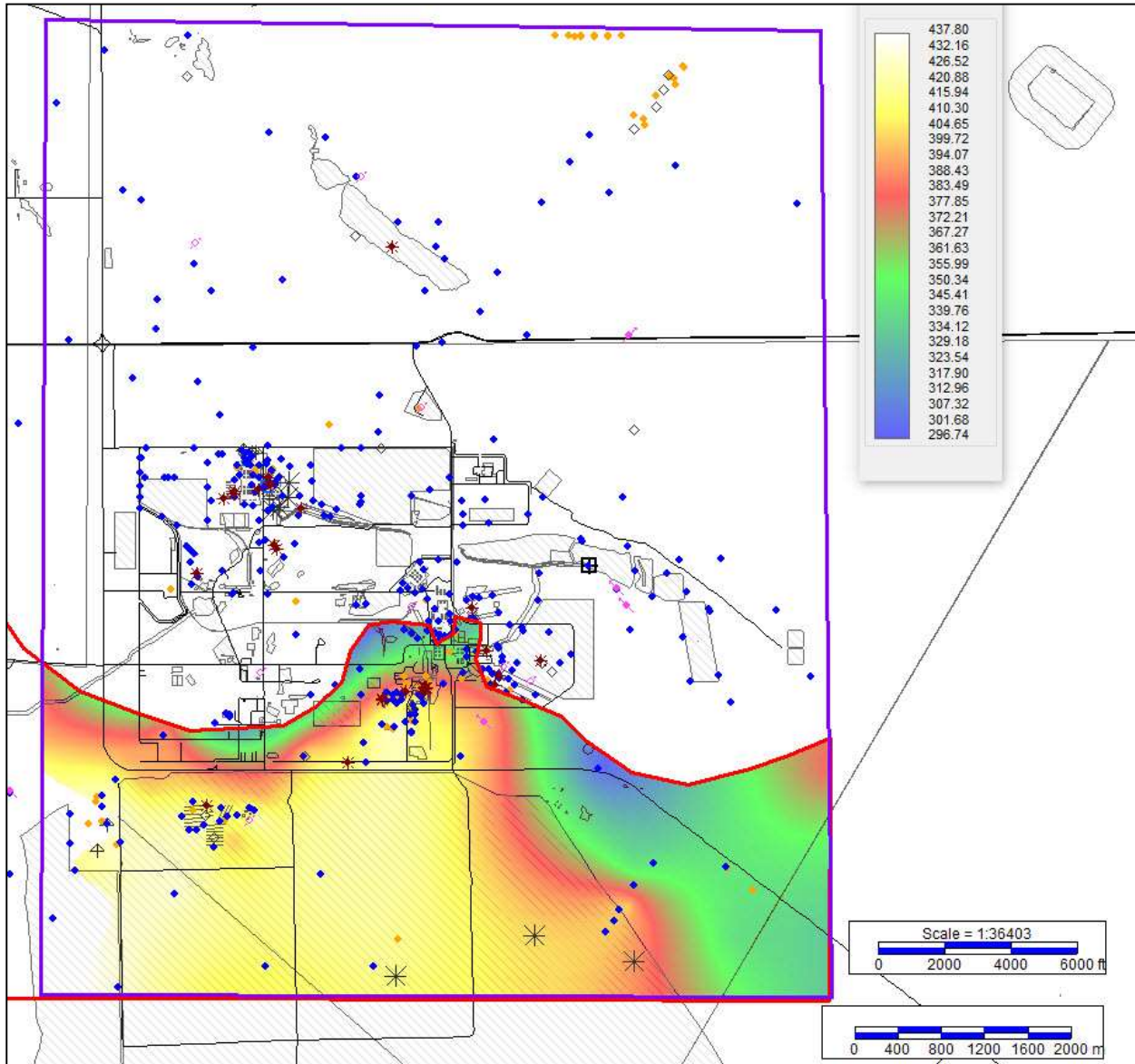
Reference: RPP-RPT-59343, *Integrated Disposal Facility Model Package Report: Geologic Framework*, Rev. 0.

Note: Blank cells indicate that the stratigraphic unit has not been interpreted in that borehole. The borehole could either be too shallow or the stratigraphic unit itself is not present at that location. CCU depth corresponds to the base of the H3. Elevation tops for CCU, CCUg and Rwie are calculated by taking the surface elevation minus the reported depths from Table C-1 of ECF-HANFORD-18-0035. Because the Rwie is not identified as present in boreholes 299-E24-18, 299-E24-21, 299-E24-24, 299-E17-57 and 299-E24-164, the Rwie depth is greater than the total depth of the borehole and the elevation is less than the elevation of the bottom of the borehole. Geology from boreholes 299-E17-56, 299-E17-57 and 299-E24-164 is reported in SGW-63813, *Borehole Summary Report for the Installation of Six M-24 Wells in the 200-PO-1, 200-UP-1 and 300-FF-5 Operable Units, FY2019*. These interpretations were made in 2019 in parallel to the completion of ECF-HANFORD-18-0035. Borehole 29-E17-57 is noted as being in the Hanford formation for its entire depth.

CCU = Cold Creek unit
 CCUg = Cold Creek unit gravel
 H3 = Hanford formation unit 3

Rtf = Ringold Formation member of Taylor Flat
 Rwie = Ringold Formation member of Wooded Island – unit E

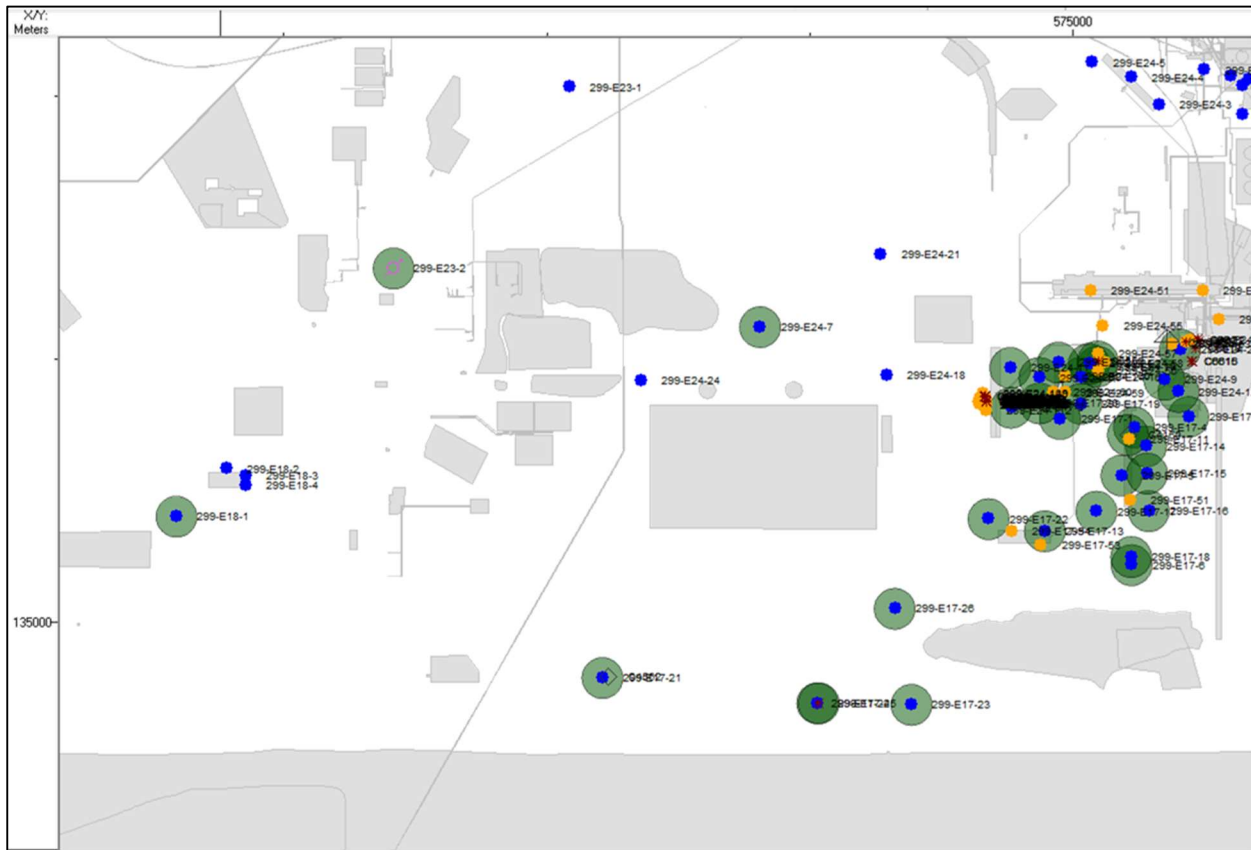
Figure 2-14-3. Ringold Formation Member of Wooded Island – Unit E Structure Elevation (feet) in 200 East Area with Extent Limiting Polygon in Orange.



Source: ECF-HANFORD-18-0035, *Central Plateau Vadose Zone Geoframework*, Rev. 0, Figure G-17.

Note: The elevation of the top of the Ringold Unit E (Rwie) varies from about 350 ft (about 107 m) above sea level (asl) in the northwest corner of the Integrated Disposal Facility (IDF) footprint to about 400 ft (about 122 m) asl in the southeast corner of the IDF footprint and averages about 375 ft (about 114 m) asl across the center of the IDF footprint from the southwest corner to the northeast corner. The long-term steady-state water table is at an elevation of about 119.5 m asl, implying that in the southeast corner of the IDF footprint, the steady-state water table is within the Rwie.

Figure 2-14-4. Boreholes near the Integrated Disposal Facility Used to Develop Structural Contours of Hydrostratigraphic Unit Tops.



Source: Derived from ECF-HANFORD-18-0035, *Central Plateau Vadose Zone Geoframework*.

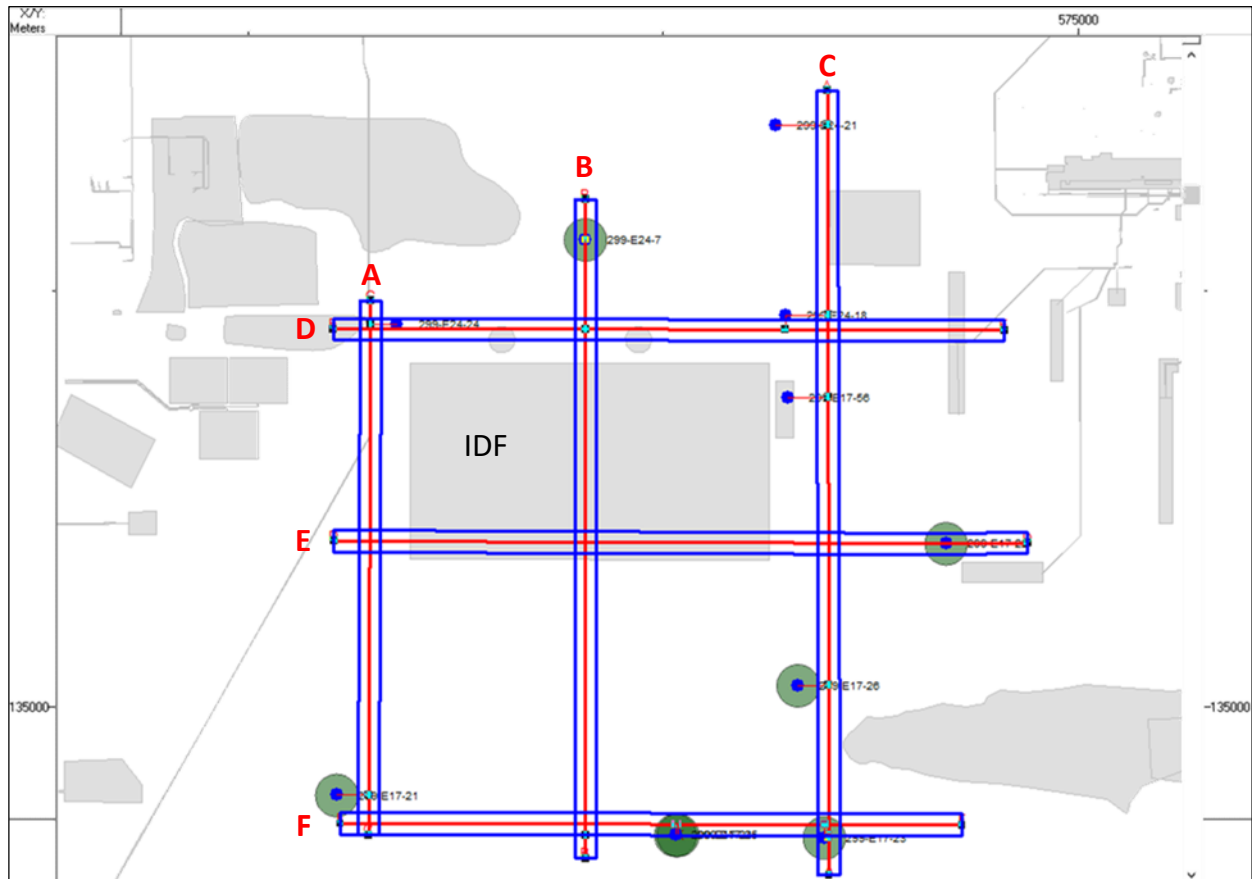
Note: Green circles indicate boreholes which intersect the Ringold Unit E (Rwie) and were used to develop the top of Rwie structural map.

To provide a more detailed examination of the hydrostratigraphy near the IDF, a series of north-south and west-east cross sections (**Figure 2-14-5**) have been developed based on the current version of the CPVZ GFM (ECF-HANFORD-18-0035) and are provided in **Figures 2-14-6** and **2-14-7**. These cross sections illustrate that the vadose zone near the IDF has been reinterpreted (again) to include a thin CCU sand unit between the H3 gravel and the CCU gravel, and that the long-term steady-state water table (at an elevation of 119.5 m asl) is in the CCU gravel instead of the H3 gravel beneath the IDF. This difference is not significant because as summarized in the most recent version of the CPGWM (Plateau to River Groundwater Model [P2R] Version 8.3, described in CP-57037, *Model Package Report: Plateau to River Groundwater Model Version 8.3*, Rev. 2), the H3 gravel and CCU gravel are both represented by the high conductivity zone making up the Hanford paleochannel (see also response to RAI 2-16) and have similar hydraulic characteristics.

The cross sections presented in **Figures 2-14-6** and **2-14-7** illustrate that the saturated thickness of the CCU gravel thins to the east and south of the IDF in a similar fashion as the saturated thickness of the H3 gravel thinned in the IDF PA GFM (see RPP-RPT-59958 Figure 3-52). To

illustrate this, an isopach of the saturated thickness of the CCU gravel near the IDF has been developed from the hydrostratigraphic contacts in the current version of the CPVZ GFM (ECF-HANFORD-18-0035, Rev. 0) by taking the difference between the long-term water table elevation (119.5 m asl) and the top of the Rwie (Figure 2-14-8). Consistent with the cross section, the CCU gravel saturated thickness decreases to the east and south of the IDF and decreases to 0.0 m where the long-term water table (at an elevation of 119.5 m asl) is below the top of the Rwie.

Figure 2-14-5. Location of Cross-Sections through the Central Plateau Vadose Zone Geologic Framework Model near the Integrated Disposal Facility.



Source: Derived from ECF-HANFORD-18-0035, *Central Plateau Vadose Zone Geoframework*.

IDF = Integrated Disposal Facility

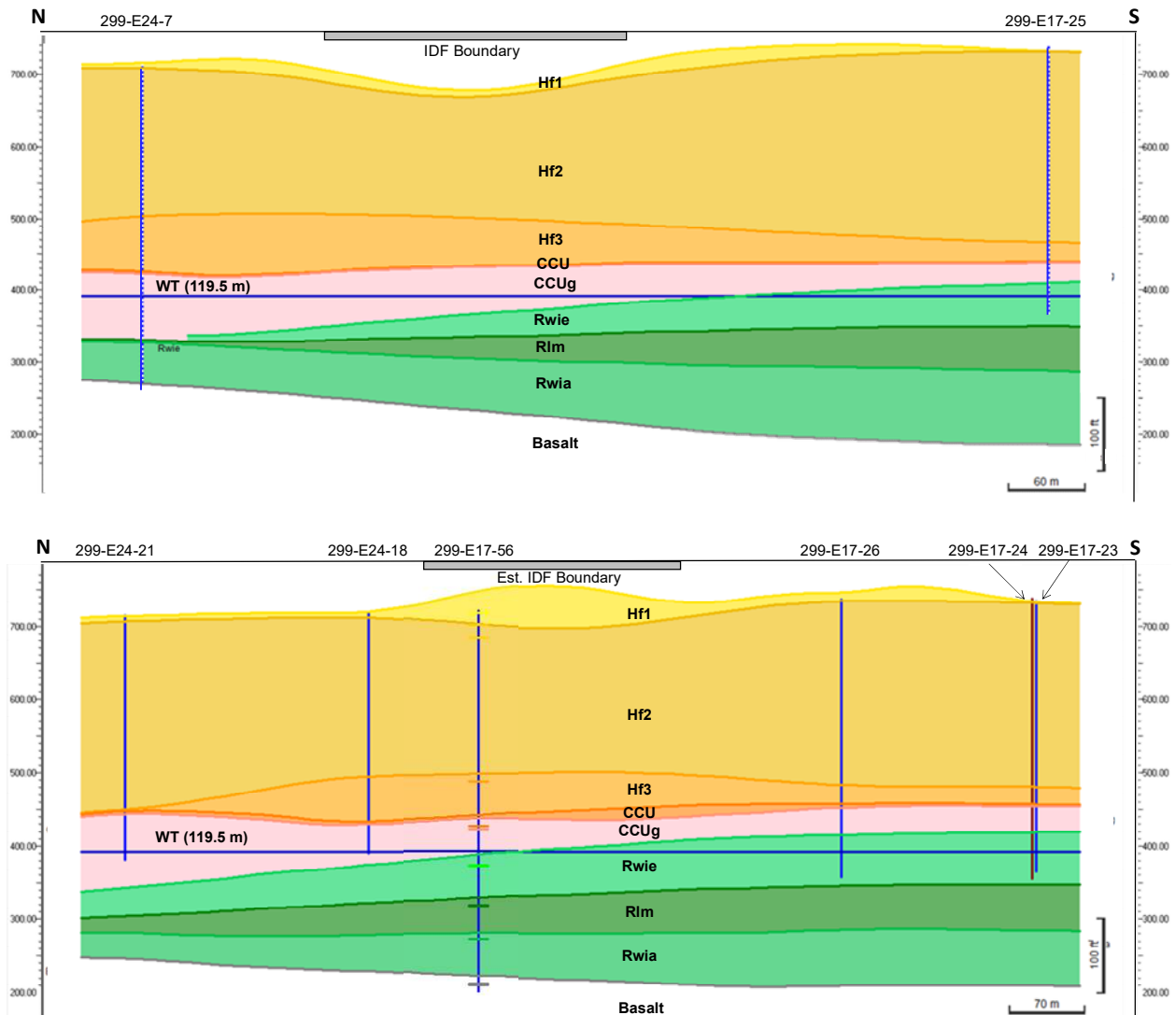
Note: Green circles indicate those boreholes that have identified the presence of Rwie. Borehole 299-E17-56 was drilled in 2019 and is not included in the current version of ECF-HANFORD-18-0035.

Current Interpretation of the Hydraulic Conductivity of HSUs near the IDF

In addition to evaluating the revised interpretation of the HSUs near the IDF documented in updates to the GFMs (both the Hanford South GFM and the CPVZ GFM) to address this RAI, it is also important to evaluate updates to the groundwater flow models of the saturated sediments near the IDF. The basis for the base case hydraulic conductivity for the sediments beneath the IDF is the subject of RAI 2-16. The response to RAI 2-16 notes that since the completion of the

IDF PA, updates to the groundwater flow models have been completed which are relevant to the response to RAI 2-16. Updates to the GFM are discussed in this RAI response, while updates to the groundwater models and hydraulic properties of the sediments beneath the IDF are discussed in the response to RAI 2-16.

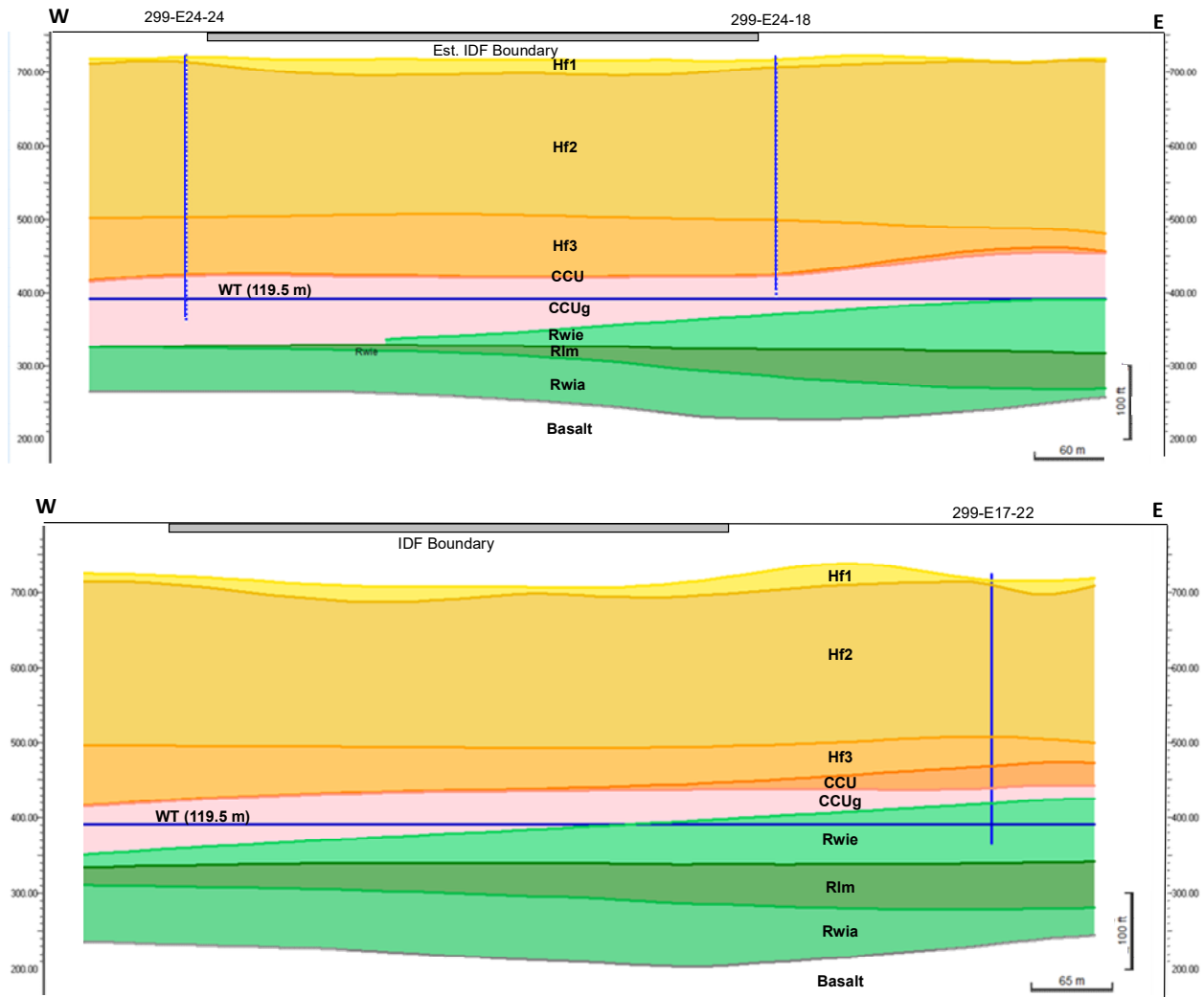
Figure 2-14-6. North-South Cross-Sections through the Central Plateau Vadose Zone Geologic Framework Model near the Integrated Disposal Facility, Section B (top) and Section C (bottom).



Source: Derived from ECF-HANFORD-18-0035, *Central Plateau Vadose Zone Geoframework*.

Note: The HSU contacts for borehole 299-E17-56 are based on SGW-63813, *Borehole Summary Report for the Installation of Six M-24 Wells in the 200-PO-1, 200-UP-1 and 300-FF-5 Operable Units, FY2019*. Borehole 299-E17-56 was drilled in 2019 and is not included in the Central Plateau Vadose Zone Geologic Framework Model Rev. 1 (ECF-HANFORD-18-0035).

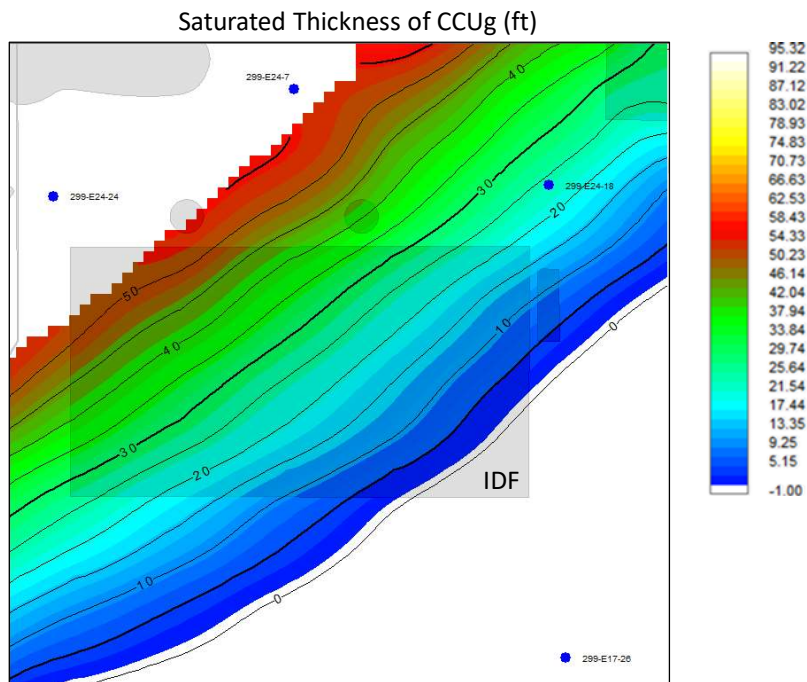
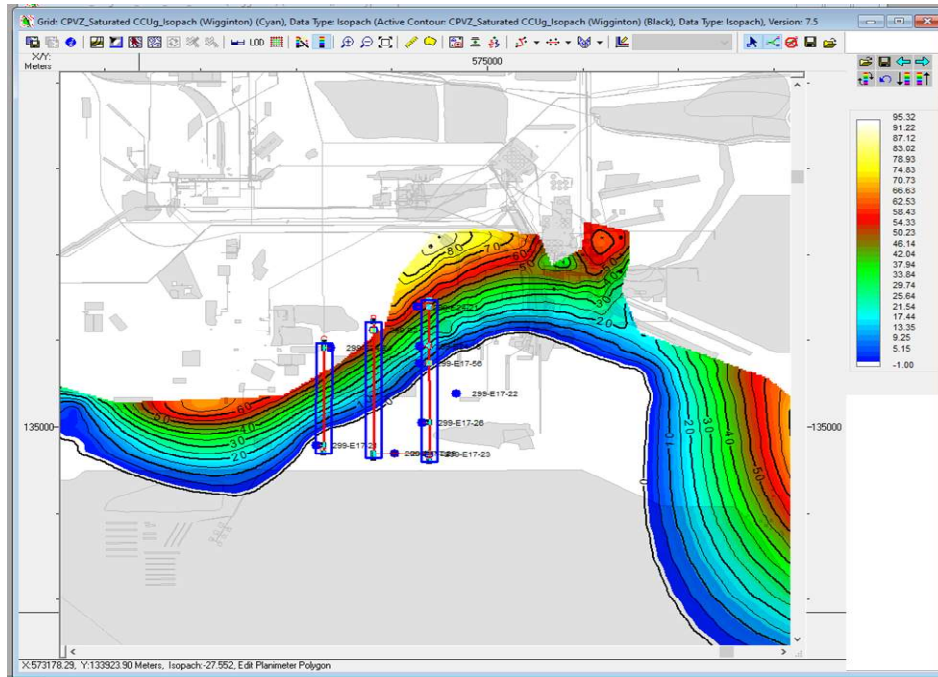
Figure 2-14-7. West-East Cross Sections of Central Plateau Vadose Zone Geologic Framework Model near the Integrated Disposal Facility, Section D (top) and Section E (bottom).



Source: Derived from ECF-HANFORD-18-0035, *Central Plateau Vadose Zone Geoframework*.

Note: The long-term average water table elevation of 119.5 m asl is in the Cold Creek unit (CCU) gravel (CCUg) over most of the Integrated Disposal Facility (IDF) footprint. In comparing these cross sections with the cross section based on the IDF geologic framework model (GFM) (Figure 3-61 of RPP-RPT-59958, *Performance Assessment for the Integrated Disposal Facility, Hanford Site, Washington*), it is apparent that Central Plateau Vadose Zone GFM Rev. 1 has included a thin CCU layer (comprised of sand) between the Hanford formation unit 3 (Hf3) gravel and the CCUg gravel while the IDF GFM interpreted the entire section above the Ringold Unit E (Rwie) as the Hf3 gravel. This revised GFM does not significantly affect the fate and transport of radionuclides in the vadose zone as the CCU sand and CCUg have hydraulic properties similar to those modeled for the Hanford sand (Hanford formation unit 2 [Hf2]) and Hanford gravel (Hf3).

Figure 2-14-8. Saturated Thickness of the Cold Creek Gravel Unit near the Integrated Disposal Facility.



Source: Derived from ECF-HANFORD-18-0035, *Central Plateau Vadose Zone Geoframework*.

Note: Contours are in feet. Saturated thickness calculated by subtracting the elevation of the top of the Ringold Unit E (Rwie) from the long-term average steady-state water table elevation of 119.5 m above sea level. Based on the cross sections, the long-term steady-state water table is in the Cold Creek unit gravel (CCUg) in all except the southeast corner of the Integrated Disposal Facility (IDF) where it is in the Rwie. The saturated thickness of the CCUg thins to the southeast similar to the thinning

of the Hanford formation unit 3 gravel in the IDF GFM (see Figure 3-52 of RPP-RPT-59958, *Performance Assessment for the Integrated Disposal Facility*).

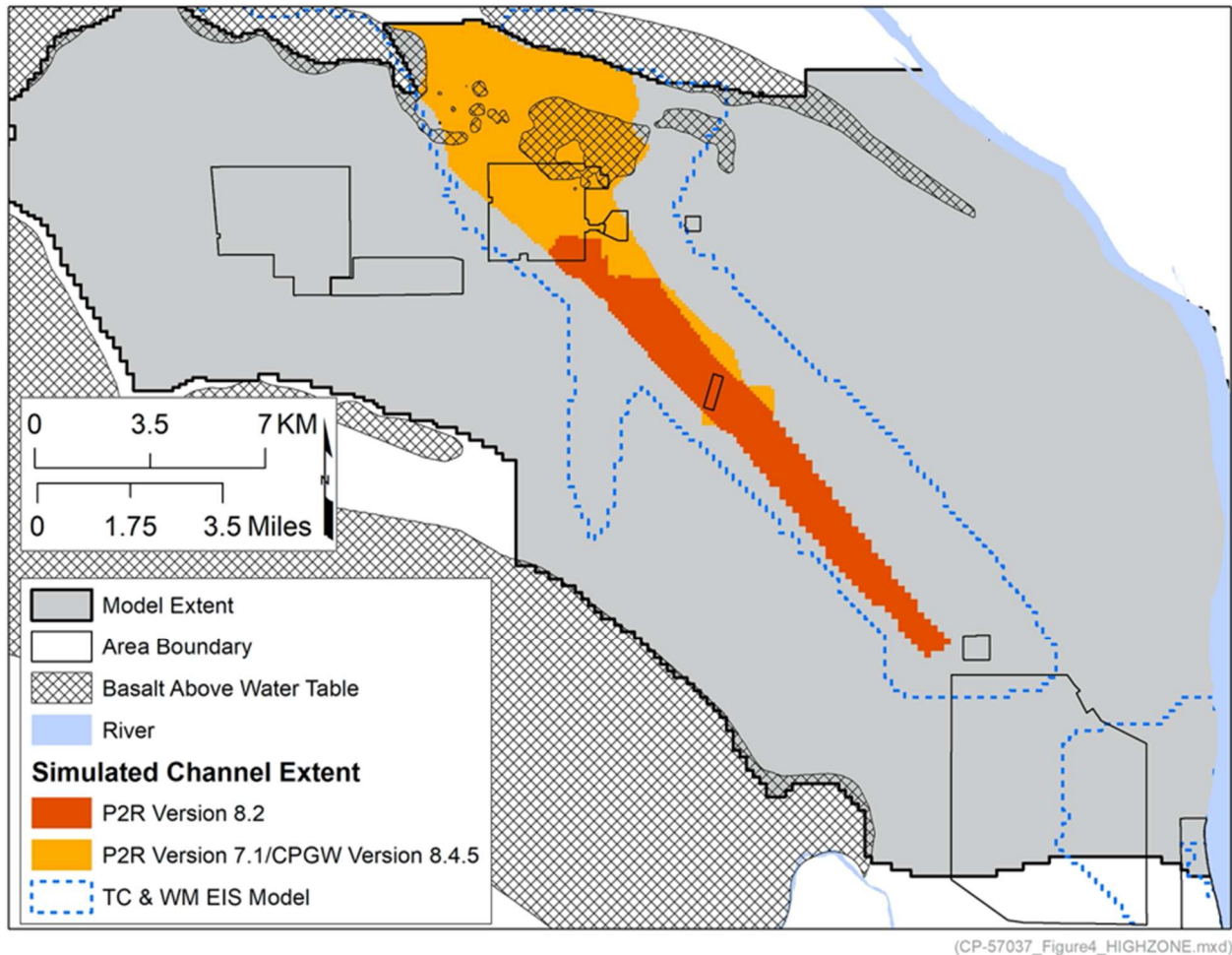
At the time of the development of the models and calculations used in the IDF PA, the available groundwater flow model was based on Central Plateau Groundwater Model (CPGWM) Version 6.3.3 documented in CP-47631, Rev. 2. The HSUs included in this groundwater flow model were based on a predecessor to the Hanford South GFM and included the Hanford formation and Rwie near the IDF. The calibrated hydraulic conductivities of the Hanford formation and the Rwie in the CPGWM Version 6.3.3 were 17,000 and 5 m/day, respectively. These values were used in the local-scale model of groundwater flow beneath the IDF as documented in RPP-CALC-61032, *Vadose Zone and Saturated Zone Flow and Transport Calculations for the Integrated Disposal Facility Performance Assessment* and summarized in RPP-RPT-59958. The calculated groundwater flow direction and flow rate in the Hanford formation beneath the IDF were controlled by the contrast in hydraulic conductivity between the Hanford formation and Rwie (defined by the results of the CPGWM Version 6.3.3) combined with the lateral continuity of the Hanford formation and Rwie defined in the Hanford South GFM and IDF GFM.

As summarized in the response to RAI 2-16, subsequent to the completion of the IDF PA updates to the groundwater flow model were completed. The most recent models are the CPGWM Version 8.4.5 (CP-47631, Rev. 4) and P2R Version 8.3 (CP-57037, Rev. 2). Both of these models modified the characteristics of the HSUs near the IDF by replacing the Hanford and Rwie HSUs directly beneath the IDF with a single HSU that represents sediments in the Hanford channel and is conceptualized as extending from Gable Gap through the 200 East Area in a northwest to southeast trend following the ancestral Columbia River channel. The extent and orientation of this Hanford channel HSU (called the high conductivity zone (HCZ) in the P2R model) is based on the low hydraulic gradients in the central and eastern portions of the 200 East Area as well as the trend of historic tritium plumes in the area. **Figure 2-14-9** illustrates the extent of the HCZ modeled in the CPGWM Version 8.4.5 and P2R Versions 7.1 and 8.2 as well as the highly conductive Hanford formation modeled in Appendix L of the TC&WM EIS (DOE/EIS-0391).⁴³

Based on the interpreted extent of the Hanford channel and the HCZ in the recent groundwater flow models (CPGWM Version 8.4.5 and P2R Version 8.3), the HSUs beneath the IDF footprint are comprised of the high-hydraulic conductivity Hanford/Cold Creek sediments and there is no evidence of the presence of the lower hydraulic conductivity Rwie. As noted in P2R Version 8.3 (CP-57037, Rev. 2), two explanations are possible for this inconsistency: either (a) the Rwie is not present as mapped in the GFMs, including the most recent CPVZ GFM (illustrated in **Figures 2-14-6 to 2-14-8**) or (b) the Rwie hydraulic properties have been significantly altered by the presence of the Hanford channel, resulting in the Rwie having a greater hydraulic conductivity in the channel area than in other areas of the model domain. In either case, the hydraulic conductivity of the sediments beneath the IDF is characterized by the Hanford channel deposits rather than the Hanford formation or Rwie away from the Hanford channel.

⁴³ As summarized in the response to RAI 2-16, the current version of the P2R model (version 8.3), did not fix the location of the HCZ but instead allowed the parameter estimation routine used in the model calibration to identify the model cells with a high-hydraulic conductivity within an area called the HCZ analysis area. The calibrated hydraulic conductivity values near the IDF are above 10,000 m/day.

Figure 2-14-9. Location of the High Conductivity Zone (Hanford Channel) Modeled in Central Plateau Groundwater Model Version 8.4.5 and Plateau to River Groundwater Model Version 8.3 and the Tank Closure and Waste Management Environmental Impact Statement.



Source: CP-57037, *Model Package Report: Plateau to River Groundwater Model Version 8.3*, Rev. 2, Figure 4-4.

References:

CP-47631, *Model Package Report: Central Plateau Groundwater Model, Version 8.4.5*, Rev. 4.

DOE/EIS-0391, *Final Tank Closure and Waste Management Environmental Impact Statement for the Hanford Site, Richland, Washington*.

Note: The simulated channel extent in these models extends beneath the Integrated Disposal Facility footprint in the southcentral part of the 200 East Area.

Summary

The presence of the Rwie and the location of the Rwie/Hanford (or Rwie/Cold Creek) contact have changed over time as additional information has been developed and interpreted (or reinterpreted) by subject matter experts. Groundwater protection standards are applied at the point of highest concentration at a distance that is at least 100 meters from the disposed-of waste. If the point of highest concentration occurs in an unit that is re-interpreted to be Rwie, then the

standards would be applied in the Rwie. In addition, the interpreted hydraulic characteristics of the sediments in the southeastern part of the 200 East Area, including the area encompassing the footprint of the IDF, have changed over time with improved groundwater flow model calibrations. The current interpretation is that the high-energy gravel deposits in the Hanford channel (the HCZ in P2R Versions 8.2 and 8.3) comprise the HSU underlying the IDF. The calibrated hydraulic conductivity of these deposits is discussed in the response to RAI 2-16.

References

- CP-47631, 2015, *Model Package Report: Central Plateau Groundwater Model Version 6.3.3*, Rev. 2, INTERA, Inc., Richland, Washington. Available at: <https://pdw.hanford.gov/document/0077133H>
- CP-47631, 2018, *Model Package Report: Central Plateau Groundwater Model, Version 8.4.5*, Rev. 4, CH2M HILL Plateau Remediation Company, Richland, Washington. Available at: <https://pdw.hanford.gov/document/0066449H>.
- CP-57037, 2020, *Model Package Report: Plateau to River Groundwater Model Version 8.3*, Rev. 2, CH2M HILL Plateau Remediation Company, Richland, Washington. Available at: <https://pdw.hanford.gov/document/AR-03674>.
- CP-60925, 2018, *Model Package Report: Central Plateau Vadose Zone Geoframework Version 1.0*, Rev. 0, CH2M HILL Plateau Remediation Company, Richland, Washington. Available at: <https://pdw.hanford.gov/arpir/index.cfm/viewDoc?accession=0065500H>.
- DOE/EIS-0391, 2012, *Final Tank Closure and Waste Management Environmental Impact Statement for the Hanford Site*, Richland, Washington, U.S. Department of Energy, Washington, D.C.
- DOE/ORP-2000-24, 2001, *Hanford Immobilized Low-Activity Waste Performance Assessment: 2001 Version*, U.S. Department of Energy, Office of River Protection, Richland, Washington. Available at: <https://www.osti.gov/servlets/purl/807263>.
- DOE/RL-97-69, 1998, *Hanford Immobilized Low-Activity Tank Waste Performance Assessment*, U.S. Department of Energy, Richland, Washington. Available at: <https://www.osti.gov/servlets/purl/10148305>.
- ECF-200PO1-09-2074, 2010, *200-PO-1 Groundwater Operable Unit Remedial Investigation Report - Geologic Cross Sections*, Rev. 0, prepared by Freestone Environmental Services for CH2M HILL Plateau Remediation Company, Richland, Washington. Available at: <https://pdw.hanford.gov/document/0084350>.
- ECF-HANFORD-13-0029, 2014, *Development of the Hanford South Geologic Framework Model, Hanford Site Washington*, Rev. 0, prepared by INTERA, Inc. for CH2M HILL Plateau Remediation Company, Richland, Washington. Available at: <https://pdw.hanford.gov/document/0072753H>.

- ECF-HANFORD-13-0029, 2015, *Development of the Hanford South Geologic Framework Model, Hanford Site, Washington*, Rev. 1, prepared by INTERA, Inc. for CH2M HILL Plateau Remediation Company, Richland, Washington. Available at: <https://pdw.hanford.gov/document/0080813H>.
- ECF-HANFORD-13-0029, 2015, *Development of the Hanford South Geologic Framework Model, Hanford Site, Washington*, Rev. 2, prepared by INTERA, Inc. for CH2M HILL Plateau Remediation Company, Richland, Washington. Available at: <https://pdw.hanford.gov/document/0072751H>.
- ECF-HANFORD-13-0029, 2017, *Development of the Hanford South Geologic Framework Model, Hanford Site, Washington*, Rev. 3, prepared by INTERA, Inc. for CH2M HILL Plateau Remediation Company, Richland, Washington. Available at: <https://pdw.hanford.gov/document/0072750H>.
- ECF-HANFORD-13-0029, 2017, *Development of the Hanford South Geologic Framework Model, Hanford Site, Washington Fiscal Year 2016 Update*, Rev. 4, prepared by INTERA, Inc. for CH2M HILL Plateau Remediation Company, Richland, Washington. Available at: <https://pdw.hanford.gov/document/0072357H>.
- ECF-HANFORD-13-0029, 2018, *Development of the Hanford South Geologic Framework Model, Hanford Site, Washington*, Rev. 5, prepared by INTERA, Inc. for CH2M HILL Plateau Remediation Company, Richland, Washington. Available at: <https://pdw.hanford.gov/document/0064943H>.
- ECF-HANFORD-18-0035, 2020, *Central Plateau Vadose Zone Geoframework*, Rev. 0, CH2M HILL Plateau Remediation Company, Richland, Washington. Available at: <https://www.osti.gov/servlets/purl/1603767>.
- PNNL-14586, 2002, *Geologic Data Package for 2005 Integrated Disposal Facility Waste Performance Assessment*, Rev. 1, Pacific Northwest National Laboratories, Richland, Washington. Available at: https://www.pnnl.gov/main/publications/external/technical_reports/PNNL-14586Rev1.pdf.
- PNNL-15237, 2005, *Geology of the Integrated Disposal Facility Trench*, Pacific Northwest National Laboratory, Richland, Washington.
- PNNL-17913, 2009, *Hydrogeology of the Hanford Site Plateau – A Status Report for the 200 West Area*, Rev. 1, Pacific Northwest National Laboratory, Richland, Washington.
- RPP-CALC-61032, 2018, *Vadose Zone and Saturated Zone Flow and Transport Calculations for the Integrated Disposal Facility Performance Assessment*, Rev. 0A, prepared by INTERA Inc. for Washington River Protection Solutions, LLC, Richland, Washington.

RPP-RPT-59343, 2016, *Integrated Disposal Facility Model Package Report: Geologic Framework*, Rev. 0, prepared by INTERA, Inc. for Washington River Protection Solutions, LLC, Richland, Washington.

RPP-RPT-59958, 2019, *Performance Assessment for the Integrated Disposal Facility, Hanford Site, Washington*, Revision 1A, Washington River Protection Solutions, LLC, Richland, Washington.

SGW-63813, 2019, *Borehole Summary Report for the Installation of Six M-24 Wells in the 200-PO-1, 200-UP-1 and 300-FF-5 Operable Units, FY2019*, prepared by Freestone Environmental, Inc. for CH2M HILL Plateau Remediation Company, Richland, Washington. Available at: <https://pdw.hanford.gov/document/AR-03916>.

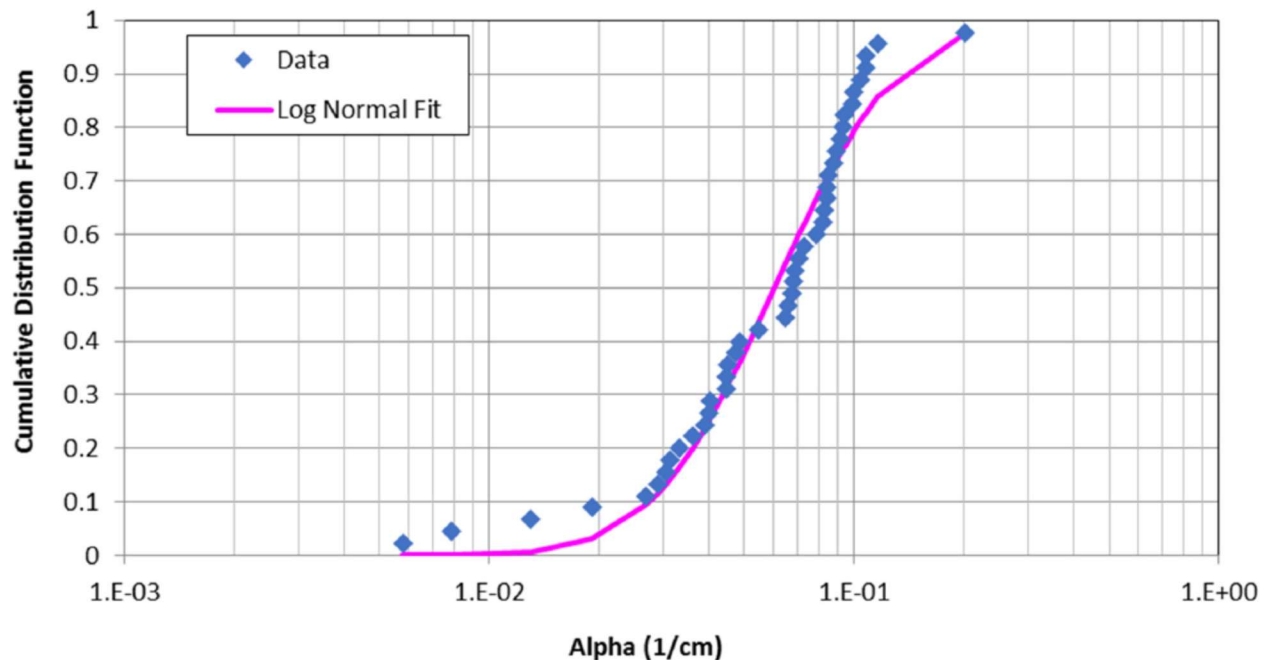
RAI 2-15 (Vadose Zone Parameters)**Comment**

The log-normal fit of the van Genuchten alpha parameter for the H2 unit does not appear to represent the data well at the tails of the distribution..

Basis

To develop uncertainty distributions of unsaturated flow parameters the empirical data were fit with statistical distributions. The van Genuchten alpha parameter for the H2 unit was assigned a log-normal distribution. The fit of the equation to the data showed deviations at the tails of the distributions (See Figure 4-56 from the PA document provided below).

Figure 2-15-1. Fitted Log-Normal Distribution to the van Genuchten “Alpha” Parameter Data Set Used for the H2 Unit.



Source: Figure 4-56 of RPP-RPT-59958, *Performance Assessment for the Integrated Disposal Facility, Hanford Site, Washington*.

Path Forward

Please discuss the implications of the deviation in the fitted distributions from the underlying data.

DOE Response

The vadose zone hydraulic (van Genuchten-Mualem) parameter values used to evaluate the fate and transport of radionuclides released from the base of the IDF to the water table are uncertain. The parameter uncertainty is represented in the range of laboratory-measured moisture retention

curves for 44 samples of the H2 sand illustrated in Figures 3-76 and 3-77 of RPP-RPT-59958⁴⁴. The range of moisture retention curves is the result of a range of values for the following van Genuchten-Mualem parameters presented in Table 3-5 of RPP-RPT-59958:

- Saturated moisture content (porosity)
- Residual moisture content
- van Genuchten parameter alpha
- van Genuchten parameter n (correlated to alpha as discussed in RPP-RPT-59958 Rev 1A Section 4.4.2.1.6)
- Saturated hydraulic conductivity (correlated to alpha as discussed in RPP-RPT-59958 Rev 1A Section 4.4.2.1.6)

Although the RAI specifically addresses the adequacy of fit for the van Genuchten parameter alpha, this RAI response discusses the adequacy of all five parameters to represent the underlying data because these parameters are used together to evaluate the uncertainty for the vadose zone hydraulic properties and the implication of this uncertainty on simulated groundwater concentrations and dose in the all-pathways exposure scenario. These five parameters and Equations 4.4.2.1-2 and 4.4.2.1-3 in RPP-RPT-59958 are used to estimate moisture content in the sediments below the IDF. This RAI response looks at how uncertainty in the underlying parameters translates to uncertainty in the predicted moisture content and then compares the predicted moisture content to observed values from boreholes near the IDF.

The response to this RAI is comprised of three parts: first, an evaluation of the impact the sampled uncertain H2 sand hydraulic parameter distributions have on the predicted moisture content in the H2 sand for a given estimate of the net infiltration rate near the IDF; second, an evaluation of the predicted moisture contents in the H2 sand using the H2 sand hydraulic parameter values compared to observed moisture contents in the H2 sand near the IDF; and third, an evaluation of the impact of using alternative vadose zone hydraulic property sets that are representative of the observed moisture contents in the H2 sand near the IDF.

Based on the result of the presented evaluations, it is concluded that: (a) the sampled distributions provide an adequate range of moisture retention parameter sets to capture the expected uncertainty in the performance of the vadose zone as a barrier on the predicted

⁴⁴ The discussion in this RAI response focuses on the vadose zone hydraulic parameter values of the H2 sand beneath the IDF and the approach used to evaluate the impact of the uncertainty in the H2 sand hydraulic parameter values in the IDF PA. A similar approach was applied to the H3 gravel; however, because the H3 gravel beneath the IDF is assumed to be analogous to the H3 gravel beneath WMA C, the range of uncertainty in the H3 gravel hydraulic parameter values is the same as that adopted for the WMA C PA (RPP-ENV-58782, *Performance Assessment of Waste Management Area C, Hanford Site, Washington*) as summarized in Section 4.4.2.1.6 of RPP-RPT-59958. Therefore, the uncertainty in the H3 gravel hydraulic parameter values is not discussed in this response.

performance, and (b) the sampled distributions provide a reasonable match to moisture contents observed in sediment samples taken from boreholes drilled near the IDF.

Evaluation of Uncertain Moisture Retention Relationships to Define the Range of Uncertain Moisture Contents and Pore Velocities

The base case value for each of these five van Genuchten-Mualem parameters (along with the parameter L and the power averaged tensorial-connectivity-tortuosity (PA-TCT) parameter p used to define the moisture-dependent anisotropy (MDA) of the vadose zone sediments) was based on an upscaling of the 44 individual laboratory measured data sets as described in PNNL-23711 and summarized in Section 4.4.2.1.5 and Table 4-24 of RPP-RPT-59958.

To evaluate the uncertainty in the vadose zone hydraulic property values, the approach taken in the IDF PA (similar to the approach adopted in the WMA C PA documented in RPP-ENV-58782, *Performance Assessment of Waste Management Area C, Hanford Site, Washington*) was to fit empirical relationships to each of the five uncertain van Genuchten-Mualem parameter values using the 44 laboratory measured data sets for the H2 sand.

As noted in the RAI, the fitted relationships truncated the distributions at the lowest and highest observed values for each of the five van Genuchten-Mualem parameters. This truncation may affect the developed fitted relationships that are used to identify discrete van Genuchten-Mualem parameter values that are used to represent predicted moisture contents and pore velocities that encompass the range of possible outcomes.

The purpose of developing the fitted distributions to the laboratory-measured van Genuchten-Mualem parameter values is to evaluate the impact that the uncertainty in the vadose zone hydraulic parameter values has on the fate and transport of radionuclides released from engineered features of the IDF through the natural system beneath the IDF. This impact is realized by a change in the predicted moisture content which in turn impacts the interstitial pore water velocity. This velocity impacts the time it takes radionuclides released from the engineered barriers to be transported through the vadose zone to the underlying water table.

Although the RAI comments on one specific distribution for the vadose zone hydraulic property set, this response takes a holistic approach to address uncertainty in all of the parameters in the hydraulic property sets. Transport rates through the vadose zone are not all correlated to the alpha parameter mentioned in the RAI.⁴⁵

The approach taken in the IDF PA was to sample the five uncertain fitted distributions (like the example of the fitted distribution for the van Genuchten alpha parameter illustrated in Figure 4-46 [included in the RAI basis]) 200 times and then to calculate the moisture content for

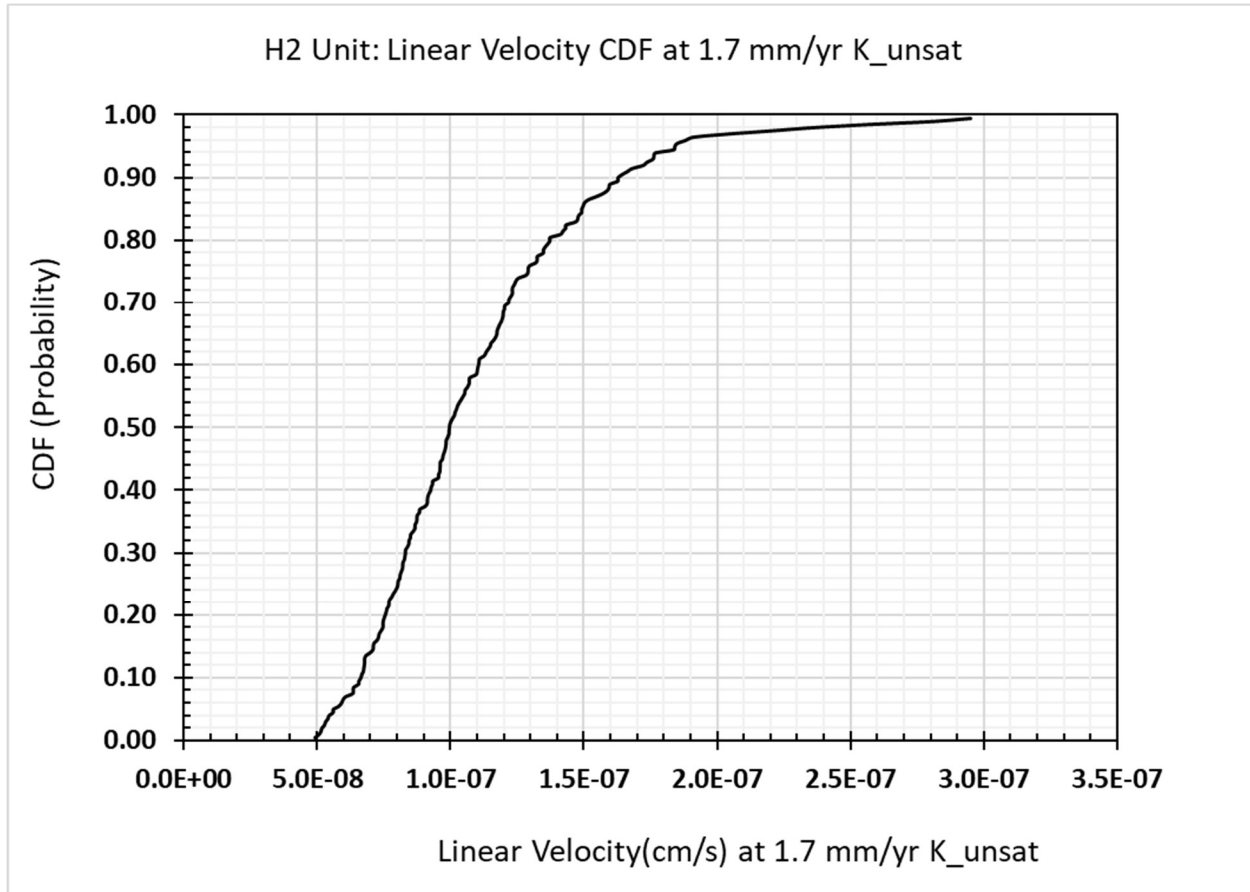
⁴⁵ Due to the relationship between alpha and the matric potential in the equations used to determine the moisture content for the assumed vertical hydraulic conductivity (RPP-RPT-59958 Equations 4.4.2.1-2 and 4.4.2.1-3), any change to the alpha value will result in a proportional but opposite change in the corresponding matric potential necessary to match the assumed vertical hydraulic conductivity. Consequently, the predicted moisture content computed using Equation 4.4.2.1-2 does not change when the estimate for alpha is overestimated in the uncertainty analysis.

an assumed vertical unsaturated hydraulic conductivity and the resulting pore velocity for each of the 200 sampled realizations. The resulting distribution of pore velocities was used to develop an abstraction to account for uncertainty in the hydraulic parameters in the uncertainty analysis. The vertical unsaturated hydraulic conductivity chosen for this calculation was 1.7 mm/yr because this is representative of the net infiltration rate in undisturbed areas near the IDF and is close to the mode of the net infiltration rate distribution in the uncertainty analysis in the IDF PA⁴⁶. After sorting the 200 realizations by the pore velocity as represented in Figure 2-15-2, it was then assumed that the uncertainty in the hydraulic property set could be represented in the uncertainty analysis by using a flow field abstraction developed from process model simulations using the parameter values used to generate the 95th, 50th and 5th percentiles of the pore velocity (which correspond to the 5th, 50th, and 95th percentiles of the predicted moisture content, respectively). These cases were called cases Vz04, Vz03 and Vz05, respectively, if the properties are assumed to be isotropic and cases Vz14, Vz13 and Vz12, respectively, if the properties are assumed to have a low anisotropy when using the PA-TCT representation of MDA. The van Genuchten-Mualem parameter values for these cases are reproduced from RPP-RPT-59958 Table 5-47 in Table 2-15-1.

The resulting pore velocity distribution for the 200 realizations developed to evaluate the impact of vadose zone hydraulic property uncertainty is illustrated in Figure 2-15-2. The predicted moisture content for these same 200 realizations is illustrated in Figure 2-15-3. The sampled values for the realizations corresponding to the 5th-, 50th, and 95th percentiles of the vertical pore velocity were used in simulations to develop the moisture profile and Darcy flux in the vadose zone that are used for fate and transport calculations.

⁴⁶ The net infiltration rate through undisturbed surface soils near the IDF is uncertain. Different values of net infiltration have been recommended by previous researchers. Net infiltration values typically used for the types of soils present near the IDF (Burbank Loamy Sand and Rupert Sand) with mature shrub-steppe vegetation are 3.0 mm/yr and 4.0 mm/yr (PNNL-14702, *Vadose Zone Hydrogeology Data Package for Hanford Assessments*), respectively, with a typical average recommended value of 3.5 mm/yr. This was the value adopted in the TC&WM EIS (DOE/EIS-0391) for the Central Plateau and the value used for the post-barrier design life net infiltration rate base case in the IDF PA (see Tables 2-9, 2-12 and 2-13 and Section 4.4.1.1 of RPP-RPT-59958). Near the IDF, PNNL-14744, *Recharge Data Package for the 2005 Integrated Disposal Facility Performance Assessment* noted that the designation of the soil type is complicated by the presence of silt layers near the surface and recommended that the soil type be classified as a combined Rupert Sand/Burbank Loamy Sand with a best-estimate net infiltration rate of 0.9 mm/yr (with a lower estimated bound of 0.16 mm/yr and an upper estimated bound of 2.1 mm/yr). The value of 0.9 mm/yr was also used for the post-barrier design life net infiltration rates through the IDF-East surface barrier in the TC&WM EIS (DOE/EIS-0391) based on agreements documented in DOE, 2005, *Technical Guidance Document for Tank Closure Environmental Impact Statement Vadose Zone and Groundwater Revised Analyses*. Based on the range of 0.9 mm/yr to 3.5 mm/yr, the IDF PA used a nominal value of 1.7 mm/yr (about a factor of 2 x greater than recommended 0.9 mm/yr value and about a factor of 2 x less than the agreed-to 3.5 mm/yr value) which is close to the mode of 1.9 mm/yr of the uncertainty distribution of post-barrier design life net infiltration rate. The value of 1.7 mm/yr also corresponds to the value used for the ERDF PA (WCH-520, *Performance Assessment for the Environmental Restoration Disposal Facility, Hanford Site, Washington*).

Figure 2-15-2. Cumulative Distribution Function of Vertical Pore Velocity Assuming a Vertical Darcy Flux of 1.7 mm/yr.



Source: RPP-RPT-59958, *Performance Assessment for the Integrated Disposal Facility, Hanford Site, Washington*, Figure 4-65.

Note: Cumulative Distribution Function (CDF) is based on 200 realizations of sampled values of H2 sand hydraulic (van Genuchten-Mualem) parameter values: (1) saturated moisture content, (2) residual moisture content, (3) van Genuchten alpha, (4) van Genuchten n and (5) saturated vertical hydraulic conductivity. Linear velocity is the vertical velocity assuming the vertical Darcy flux is 1.7 mm/yr and a unit hydraulic gradient. The 95th, 50th and 5th percentile linear pore velocity values are 1.85E-07 cm/s, 1.00E-07 cm/s and 5.62E-08 cm/s, respectively.

The numerical value labels on the x-axis have been edited to reflect two digits; these labels displayed incorrectly when just a single digit was shown.

To evaluate the impact of the sampled distributions of the uncertain van Genuchten-Mualem parameter values (i.e., the saturated moisture content, residual moisture content, van Genuchten alpha, van Genuchten n and saturated vertical hydraulic conductivity) on the predicted moisture content for an assumed vertical Darcy flux of 1.7 mm/yr (corresponding to a vertical hydraulic conductivity of 1.7 mm/yr given a unit vertical hydraulic gradient), five cross plots are presented in Figure 2-15-4. Cross plots provide an indication of how strongly each uncertain

van Genuchten-Mualem parameter influences the predicted moisture content calculated using RPP-RPT-59958 Equations 4.4.2.1-2 and 4.4.2.1-3. These plots illustrate the following.

- The predicted moisture content is most affected by the sampled values of the residual moisture content and the van Genuchten n parameter values and to a lesser extent by the saturated vertical hydraulic conductivity.
- The predicted moisture content is not significantly affected by the sampled values of the saturated moisture content or the van Genuchten alpha parameter values.
- The predicted moisture content decreases with a decrease in the sampled residual moisture content value. The minimum residual moisture content in the assumed uniform distribution is 0.0 and several realizations with values close to 0.0 were sampled from the distribution. The sampled residual moisture content value for the 95th percentile realization is 0.0077.
- The predicted moisture content decreases with an increase in the van Genuchten n parameter value. The maximum observed value in the 44 laboratory-measured samples was 3.182 but this sample also had the maximum laboratory-measured residual moisture content of 0.046 (see Sample 110U in Table 3-5 of RPP-RPT-59958). The sampled van Genuchten n parameter value for the 95th percentile realization is 2.398.

Table 2-15-1. van Genuchten-Mualem Parameter Values used for Base Case and Sensitivity Analyses.

Case or Realization	H2 Vadose Zone Hydraulic Property Sets						
	Ksat (cm/s)	Saturated Moisture Content (-)	Residual Moisture Content (-)	Alpha (1/cm)	n (-)	m (1-1/n)	L
Base Case (Vzp00)	6.20E-03	0.384	0.029	0.0642	1.698	0.411	0.5
121 (Vzp03)	1.40E-03	0.337	0.0183	0.0288	1.814	0.449	0.5
73 (Vzp04)	5.95E-04	0.320	0.00766	0.0366	2.398	0.583	0.5
(Vzp05)	4.84E-04	0.414	0.0317	0.0390	1.694	0.410	0.5

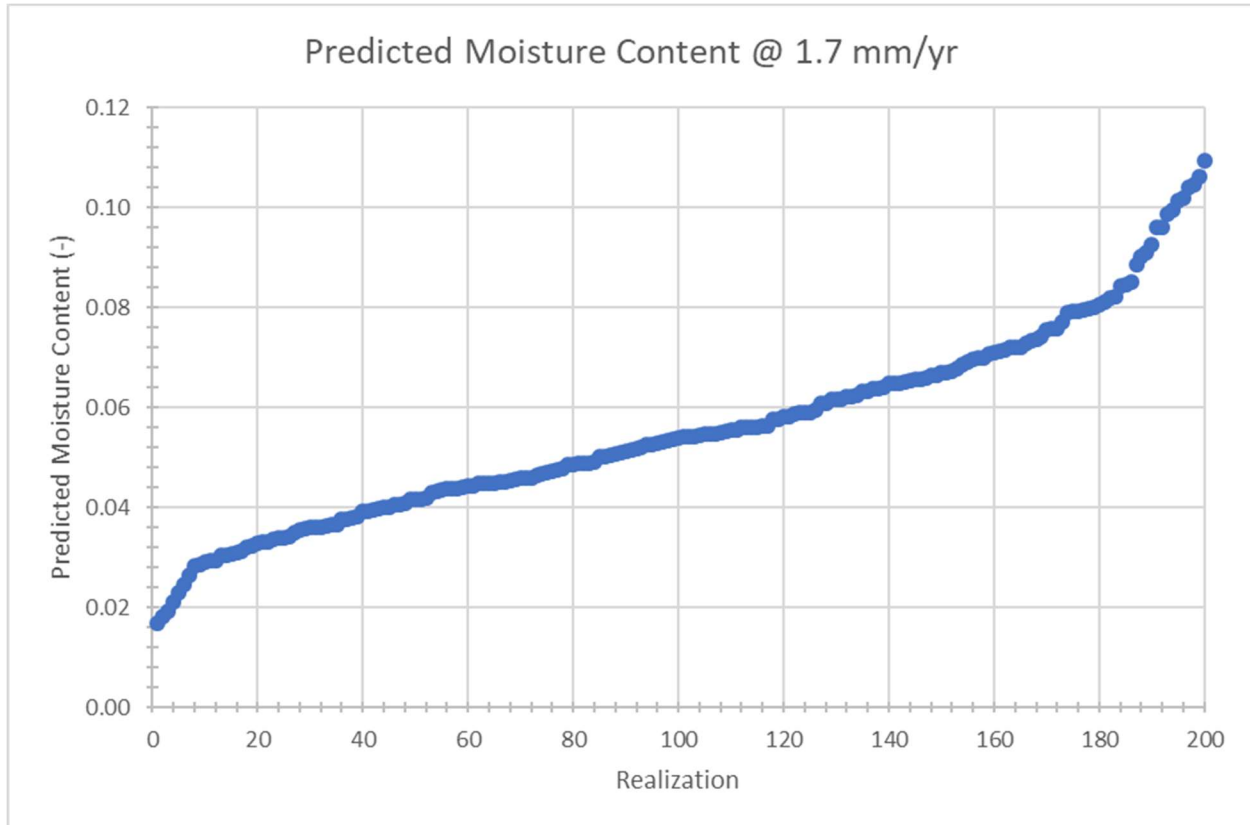
Ksat = Vertical saturated hydraulic conductivity

Case Vzp04 represents one of the 200 realizations used to evaluate the effect of uncertainty in van Genuchten-Mualem parameter values on vadose zone transport and represents the 95th percentile of the vadose zone pore velocity (equivalent to the 5th percentile of the moisture content) for a vertical Darcy flux of 1.7 mm/yr.

Case Vzp03 represents one of the 200 realizations used to evaluate the effect of uncertainty in van Genuchten-Mualem parameter values on vadose zone transport and represents the 50th percentile of the vadose zone pore velocity (equivalent to the 50th percentile of the moisture content) for a vertical Darcy flux of 1.7 mm/yr.

Case Vzp05 represents one of the 200 realizations used to evaluate the effect of uncertainty in van Genuchten-Mualem parameter values on vadose zone transport and represents the 5th percentile of the vadose zone pore velocity (equivalent to the 95th percentile of the moisture content) for a vertical Darcy flux of 1.7 mm/yr.

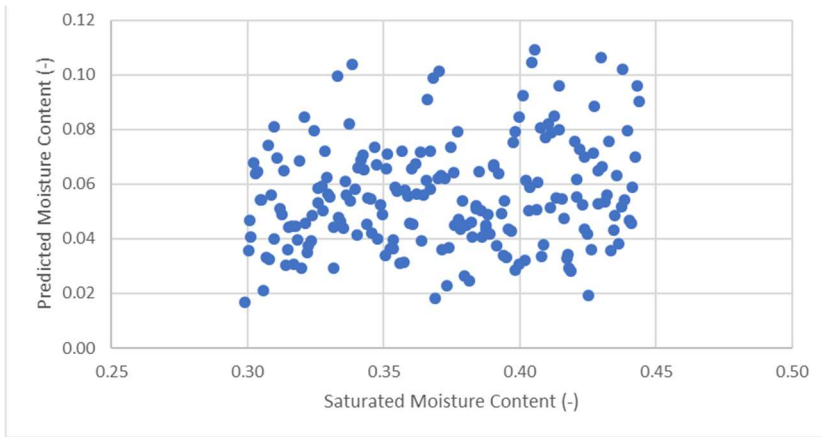
Figure 2-15-3. Distribution of Predicted H2 Sand Volumetric Moisture Content for 200 Realizations of Uncertain Vadose Zone Property Sets.



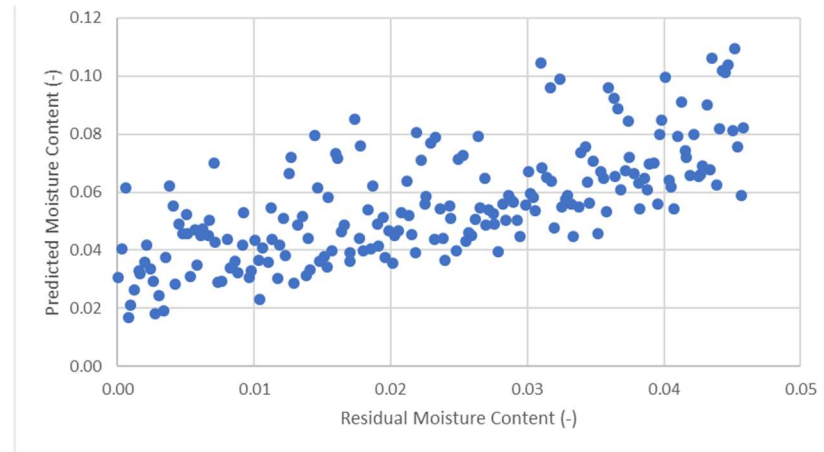
Note: Predicted moisture content distribution assuming a vertical Darcy flux of 1.7 mm/yr for the 200 realizations used to calculate the 5th, 50th and 95th percentile pore velocity distribution. The 200 realizations are sorted from the minimum moisture content of 0.0167 to the maximum value of 0.1093. The 95th percentile of pore velocity corresponds to the 5th percentile of moisture content. The 95th, 50th and 5th percentile pore velocity values are 1.85E-07 cm/s, 1.00E-07 cm/s and 5.62E-08 cm/s, respectively. The corresponding 5th, 50th and 95th percentile moisture contents are 0.0292, 0.0540 and 0.0960, respectively. For comparison purposes, the moisture content predicted for the base case parameter values (case Vzp00) for 1.7 mm/yr is 0.063.

The range of predicted moisture contents in the H2 sand from about 0.016 to 0.11 for an assumed net infiltration rate (and corresponding vertical Darcy flux and vertical unsaturated hydraulic conductivity for a unit hydraulic gradient) of 1.7 mm/yr is representative of the uncertainty in the van Genuchten-Mualem parameter values. For the purpose of identifying discrete cases that represent the range of possible moisture contents based on uncertain van Genuchten-Mualem parameter values, the selection of the 95th, 50th-, and 5th percentile pore velocity cases (i.e., cases Vzp04, Vzp03, and Vzp05 or cases Vzp14, Vzp13, and Vzp12, respectively) is appropriate.

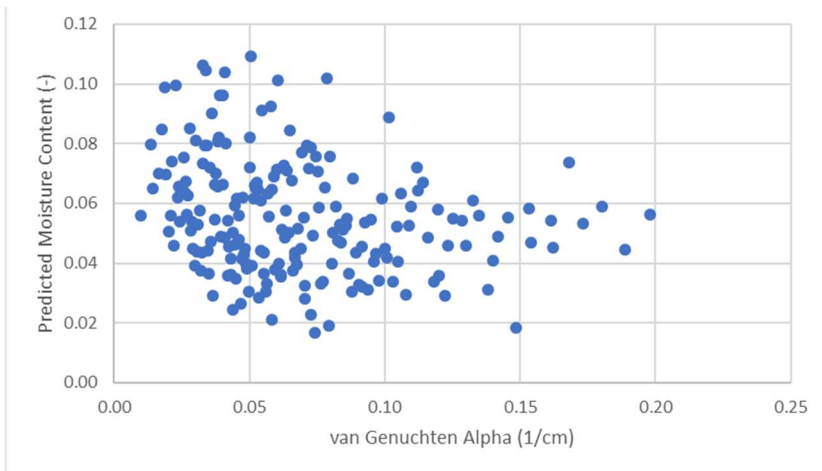
Figure 2-15-4. Cross-Plots of Predicted H2 Sand Volumetric Moisture Content versus Uncertain Vadose Zone Parameter Values for a Vertical Darcy Flux of 1.7 mm/yr. (sheet 1 of 2)



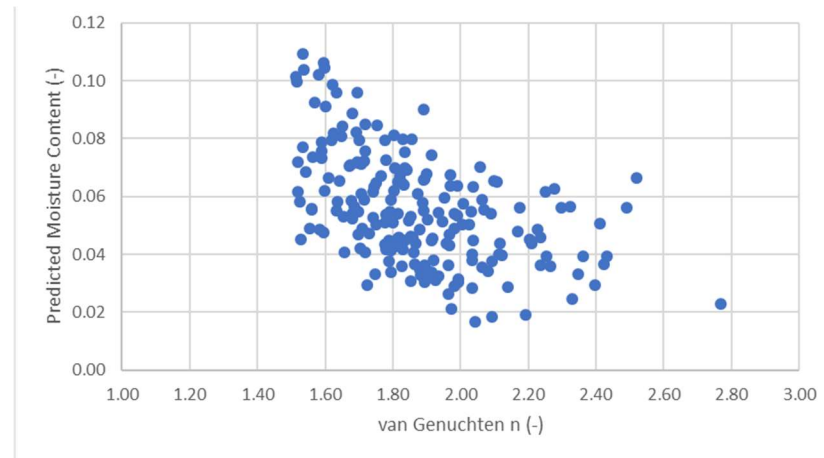
Saturated Moisture Content



Residual Moisture Content

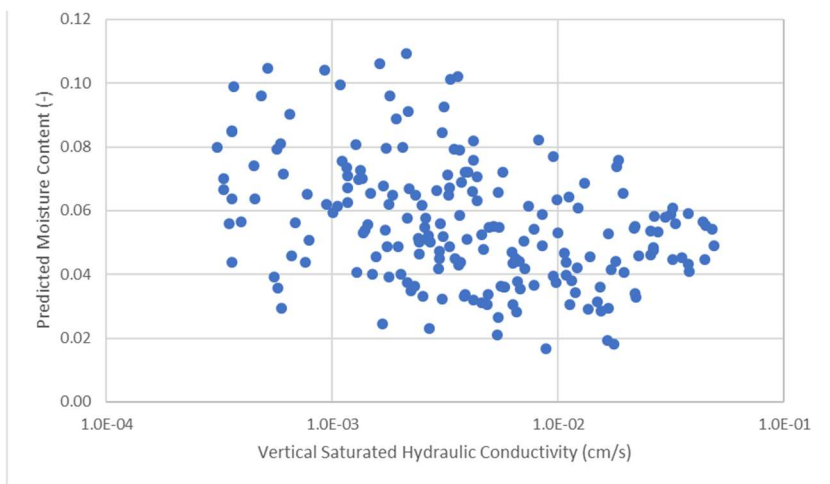


van Genuchten Alpha



van Genuchten n

Figure 2-15-4. Cross-Plots of Predicted H2 Sand Volumetric Moisture Content versus Uncertain Vadose Zone Parameter Values for a Vertical Darcy Flux of 1.7 mm/yr. (sheet 2 of 2)



Saturated Hydraulic Conductivity

Note: Derived from Excel® (a registered trademark of Microsoft Corporation in the U.S. and other countries) file used to create the distributions and results used in Figure 4-65 of RPP-RPT-59958, *Performance Assessment for the Integrated Disposal Facility, Hanford Site, Washington*.

The hydraulic property sets for the discrete cases developed to represent the uncertainty in the vadose zone hydraulic parameter values are illustrated in Figure 2-15-5 in comparison to the base case property set (Vzp00) recommended in PNNL-23711. The resulting vertical moisture content profiles calculated using STOMP for these cases are illustrated in Figure 2-15-6 for an assumed net infiltration rate of 1.7 mm/yr⁴⁷. For comparison purposes, Figure 2-15-6 also includes a case using the vadose zone hydraulic property set used in the TC&WM EIS (DOE/EIS-0391). As expected, the 50th percentile case (Vzp03) produces moisture content results that are similar to the base case (Vzp00). As will be discussed in the next section, the van Genuchten-Mualem parameter values represented by case Vzp04 or Vzp14 produce predicted moisture contents that are representative of observed moisture contents in sediment samples taken from boreholes near the IDF.

Evaluation of Alternative Moisture Retention Relationships Compared to Observed Moisture Contents in the H2 Sand near the IDF

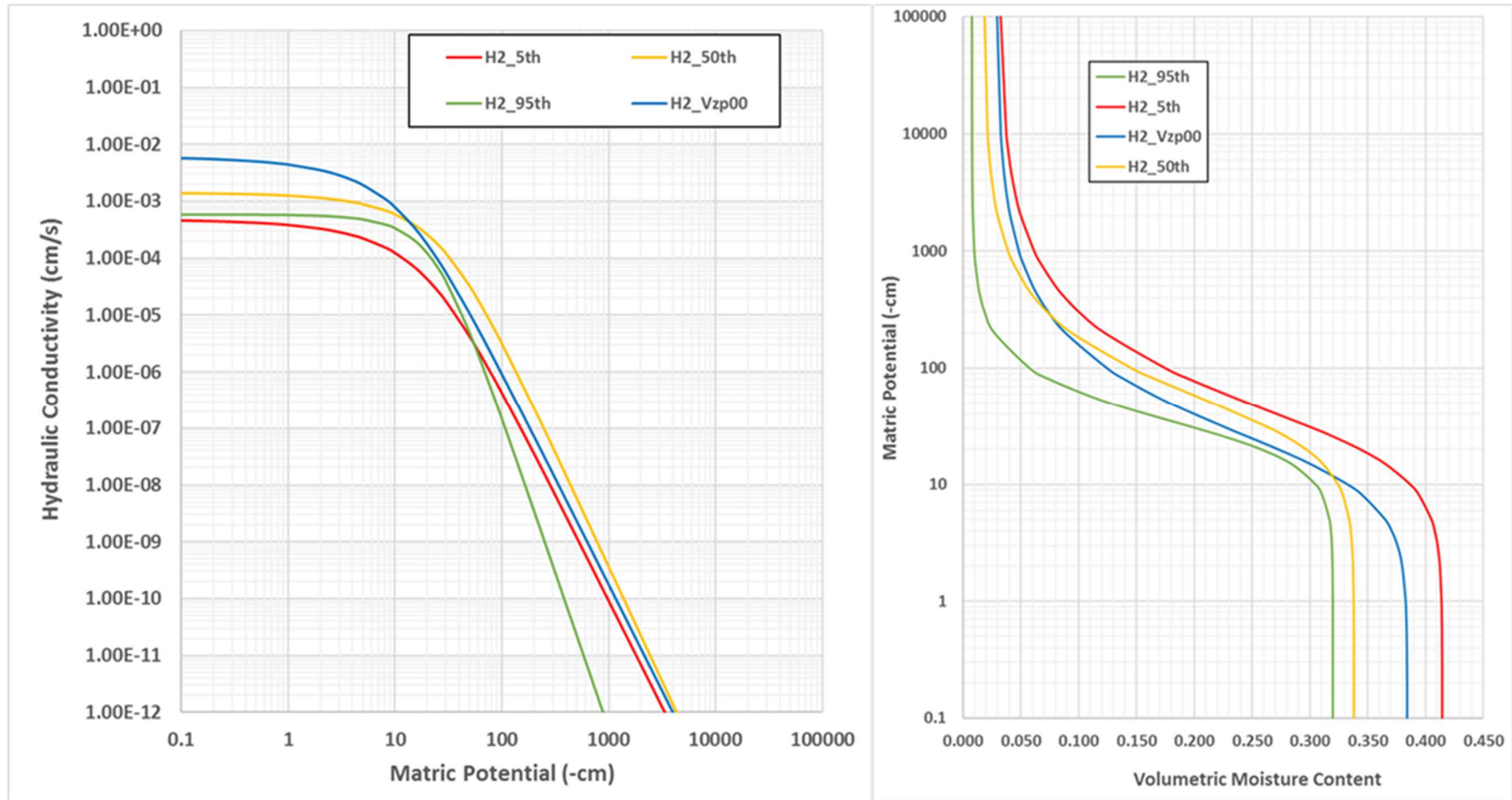
The uncertainty in vadose zone hydraulic (van Genuchten-Mualem) parameter values was evaluated using process model sensitivity cases and an abstraction developed from these sensitivity cases. The process model sensitivity cases applied parameter values that reproduced the 95th, 50th and 5th percentile of the pore velocity distribution assuming either an isotropic MDA (cases Vzp04, Vzp03 and Vzp05, respectively) or a low anisotropy MDA (cases Vzp14, Vzp13 and Vzp12, respectively). The complete range of predicted moisture contents for an assumed net infiltration rate (and corresponding vertical Darcy flux) of 1.7 mm/yr illustrated in Figure 2-15-3 is captured by using the discrete cases that supplement the calculations using the base case (Vzp00) property set recommended by PNNL-23711.

The impact of using the different vadose zone property sets was evaluated in different vadose zone sensitivity analyses summarized in Section 5.2.4.3 of RPP-RPT-59958. These vadose zone sensitivity cases were run to define the uncertainty in the predicted moisture content as summarized in Section 5.2.4.8 of RPP-RPT-59958. Additional vadose zone sensitivity cases that were not summarized in RPP-RPT-59958 were performed and documented in RPP-CALC-61032. These sensitivity analyses provide information that can be used to compare the predicted moisture content in the H2 sand for a range of vadose zone property sets and recharge (i.e., net infiltration) conditions to observed moisture content in the H2 sand near the IDF⁴⁸.

⁴⁷ The selection of 1.7 mm/yr for this comparison was based on the observation that it is about a factor of 2 x greater than the base case of 0.9 mm/yr used for most of the calculations of the IDF-East in the TC&WM EIS (DOE/EIS-0391) and about a factor of 2 x less than the base case assumed value of 3.5 mm/yr used for the IDF PA (RPP-RPT-59958). It also is close to the 1.9 mm/yr value used for the mode of the uncertainty distribution of net infiltration rate used in the uncertainty analyses (Section 6.0) of the IDF PA (RPP-RPT-59958).

⁴⁸ Observations of moisture content in the H2 sand have been reported in several PNNL reports based on laboratory analyses of sediment samples taken during drilling of nearby wells. This information is supplemented by neutron probe measurements and neutron moisture logging results of other wells. There are no observations of moisture content in the H3 gravel near the IDF due to the difficulty in retrieving samples from the H3. Therefore, this discussion focuses on comparing the observed H2 sand moisture contents with the predicted moisture contents using estimated net infiltration rates (and corresponding vertical Darcy fluxes) near the boreholes with observed moisture contents.

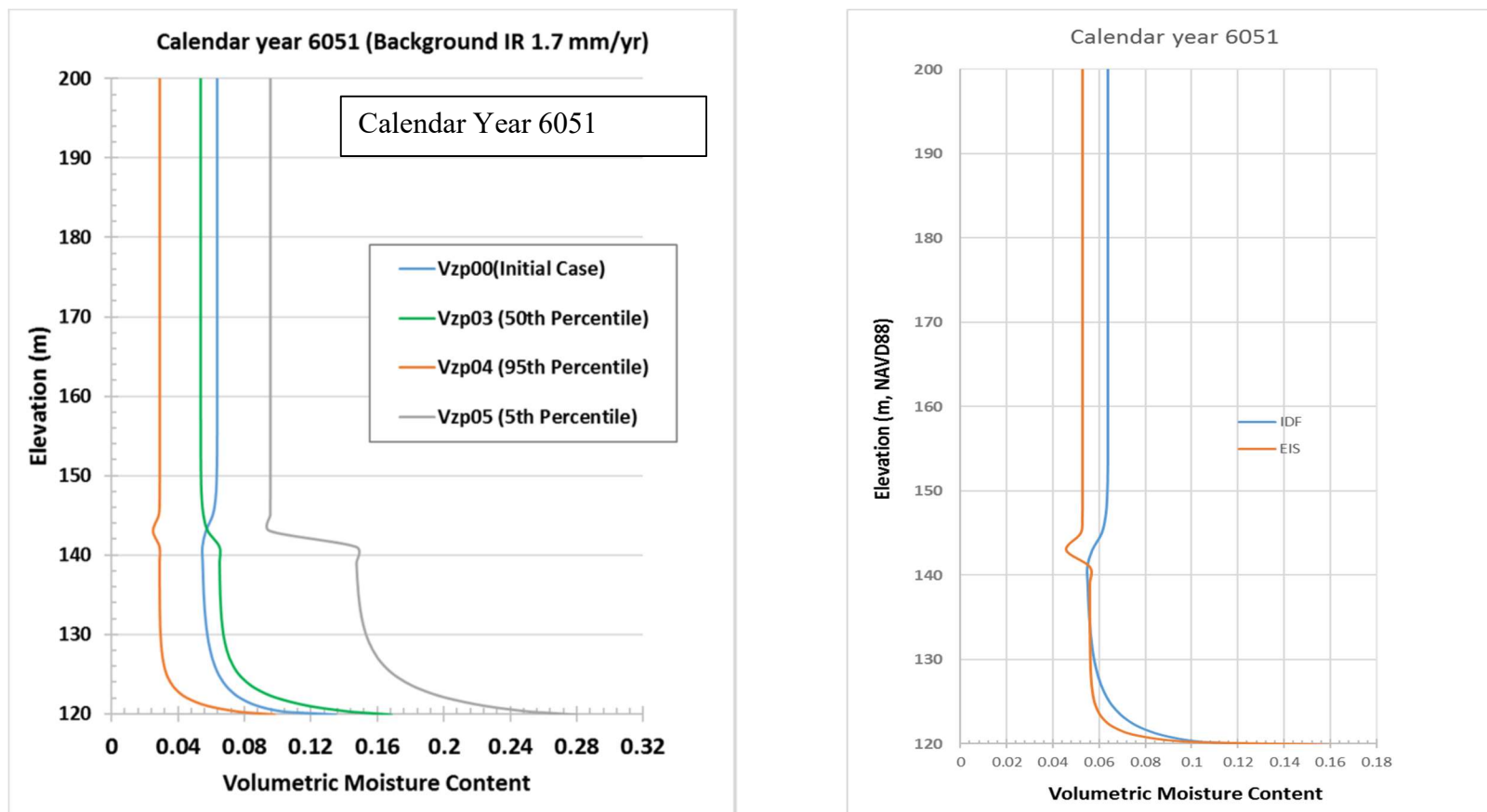
Figure 2-15-5. Comparison of Vadose Zone Hydraulic Parameter Sets for the H2 Sand.



Source: RPP-CALC-61032, *Vadose Zone and Saturated Zone Flow and Transport Calculations for the Integrated Disposal Facility Performance Assessment*, Figure B-25.

Note: Case Vzp00 corresponds to the base case vadose zone hydraulic parameter set for the H2 sand used in the Integrated Disposal Facility Performance Assessment. The 5th, 50th and 95th cases represent hydraulic parameter sets that correspond to the 5th, 50th and 95th percentiles of the pore velocity distribution assuming a vertical Darcy flux of 1.7 mm/yr. They correspond to cases Vzp05, Vzp03 and Vzp04, respectively, for the isotropic moisture-dependent anisotropy.

Figure 2-15-6. Predicted Vertical Moisture Profile Under Integrated Disposal Facility for Different Hydraulic Parameter Sets.



Source: RPP-RPT-59958, *Performance Assessment for the Integrated Disposal Facility, Hanford Site, Washington*, Figures 4-71 and 5-149, derived from RPP-CALC-61032, *Vadose Zone and Saturated Zone Flow and Transport Calculations for the Integrated Disposal Facility Performance Assessment*, Figures B-29 and 7-123.

Note: Vzp00 corresponds to the base case vadose zone hydraulic property set used in the Integrated Disposal Facility (IDF) Performance Assessment. Vzp03, Vzp04 and Vzp05 correspond to the vadose zone hydraulic property sets that result in 50th, 95th and 5th percentiles of the pore velocity (or 50th, 5th and 95th percentiles of the moisture content) assuming a 1.7 mm/yr net infiltration rate and a unit hydraulic gradient. The environmental impact statement (EIS) case corresponds to the base case vadose zone hydraulic property set used in DOE/EIS-0391, *Final Tank Closure and Waste Management Environmental Impact Statement for the Hanford Site, Richland, Washington*. The results assume a uniform net infiltration rate of 1.7 mm/yr through the surface barrier and IDF starting after the assumed 500-year design life of the surface barrier. The selected time (calendar year 6051) corresponds to a time close to the peak I-129 release rate from the vadose zone to the saturated zone.

NAVD88 = North American Vertical Datum of 1988

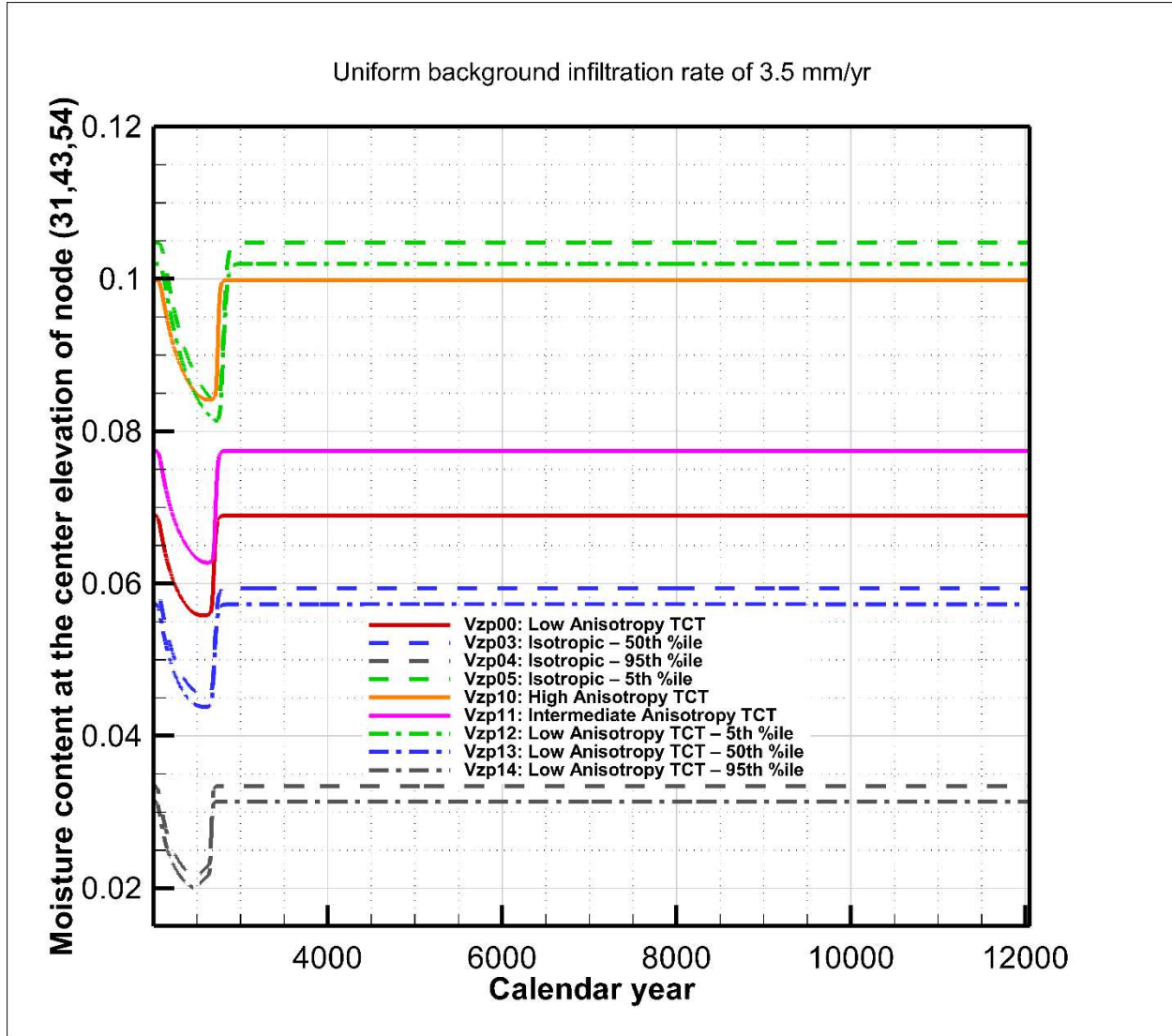
Example plots illustrating the range of predicted moisture contents for different vadose zone property sets are presented in Figure 2-15-7 for long-term average net infiltration rates of 3.5 mm/yr, 1.7 mm/yr and 0.9 mm/yr. These plots illustrate the temporal evolution of the moisture content at a point beneath the IDF liner system that is at an elevation of 169 m asl. This elevation corresponds to the middle of the H2 sand beneath the IDF as the base of the IDF liner system is about at an elevation of 204 m asl and the H2 sand is about 70 m thick beneath the base of the IDF liner system. The three different net infiltration rates are selected for the following reasons.

- 3.5 mm/yr represents the long-term steady-state net infiltration rate assumed for the post-design life of the IDF surface barrier. It represents the base case value assumed in the IDF PA. It also represents an average of the net infiltration rate in the undisturbed Burbank Loamy Sand and Rupert Sand soils with mature shrub-steppe vegetation (with best-estimate net infiltration rates of 3.0 mm/yr and 4.0 mm/yr, respectively, based on PNNL-14702) in other areas of the Central Plateau of the Hanford Site. This value was used for the net infiltration rate through surface barriers after their design life for other areas on the Central Plateau in the TC&WM EIS (DOE/EIS-0391).
- 1.7 mm/yr is the average value for Rupert Sand with mature shrub-steppe vegetation in the Central Plateau recommended in PNNL-16688, *Recharge Data Package for Hanford Single-Shell Tank Waste Management Areas*. This also represents a value about 2 x less than the 3.5 mm/yr case and 2 x greater than the 0.9 mm/yr case. This value was also used for the base case net infiltration rate in the ERDF PA (WCH-520, *Performance Assessment for the Environmental Restoration Disposal Facility, Hanford Site, Washington*). This value is also close to the 1.9 mm/yr used as the mode of the uncertainty distribution of post-design life net infiltration rates used in the IDF PA uncertainty analysis (Section 6.0 of RPP-RPT-59958).
- 0.9 mm/yr represents the best-estimate value of average net infiltration rate in undisturbed surface soils near the IDF recommended in PNNL-14744. This value was based on an average of seven discrete estimates of net infiltration rate using the chloride mass balance approach discussed in PNNL-14744 and recognizes the unique characteristics of the surface soils near IDF and the role that eolian silt deposits near the IDF can have on net infiltration in the area⁴⁹. This value was also used for the post-design life infiltration rate through the surface barrier for most of the calculations of IDF-East in the TC&WM EIS.

⁴⁹ As summarized in PNNL-14744, the range of net infiltration rates in undisturbed area near the IDF is estimated to be between 0.16 mm/yr and 2.1 mm/yr. In addition, PNNL-14744 notes that the net infiltration rate through the layered soils near IDF can be significantly affected by the contrasting textures of the sediments in nearly horizontal layers of alternating sands, gravels, and fines observed near the IDF that can create capillary breaks that impede infiltration: “The water storage capacity of the eolian material residing above the layers will influence the potential deep drainage rate. Depths of eolian material between 1.0 and 2.0 m may be ideal for storing all precipitation till it can be removed by evapotranspiration, thus significantly reducing deep drainage rates. If thinner than 1.0 m, the eolian material may not be able to store all winter precipitation. If thicker than 2.0 m, the eolian material can store the precipitation, but the water stored near the deep capillary break may be too deep to be removed by evapotranspiration. In either case, the result is an increased potential for higher drainage rates.”

Figure 2-15-7. Calculated Moisture Content in the Middle of H2 Sand at 169-meter Elevation with Different Vadose Zone Hydraulic Parameter Sets and Background Infiltration Rates. (sheet 1 of 3)

(a) Background Infiltration Rate of 3.5 mm/yr



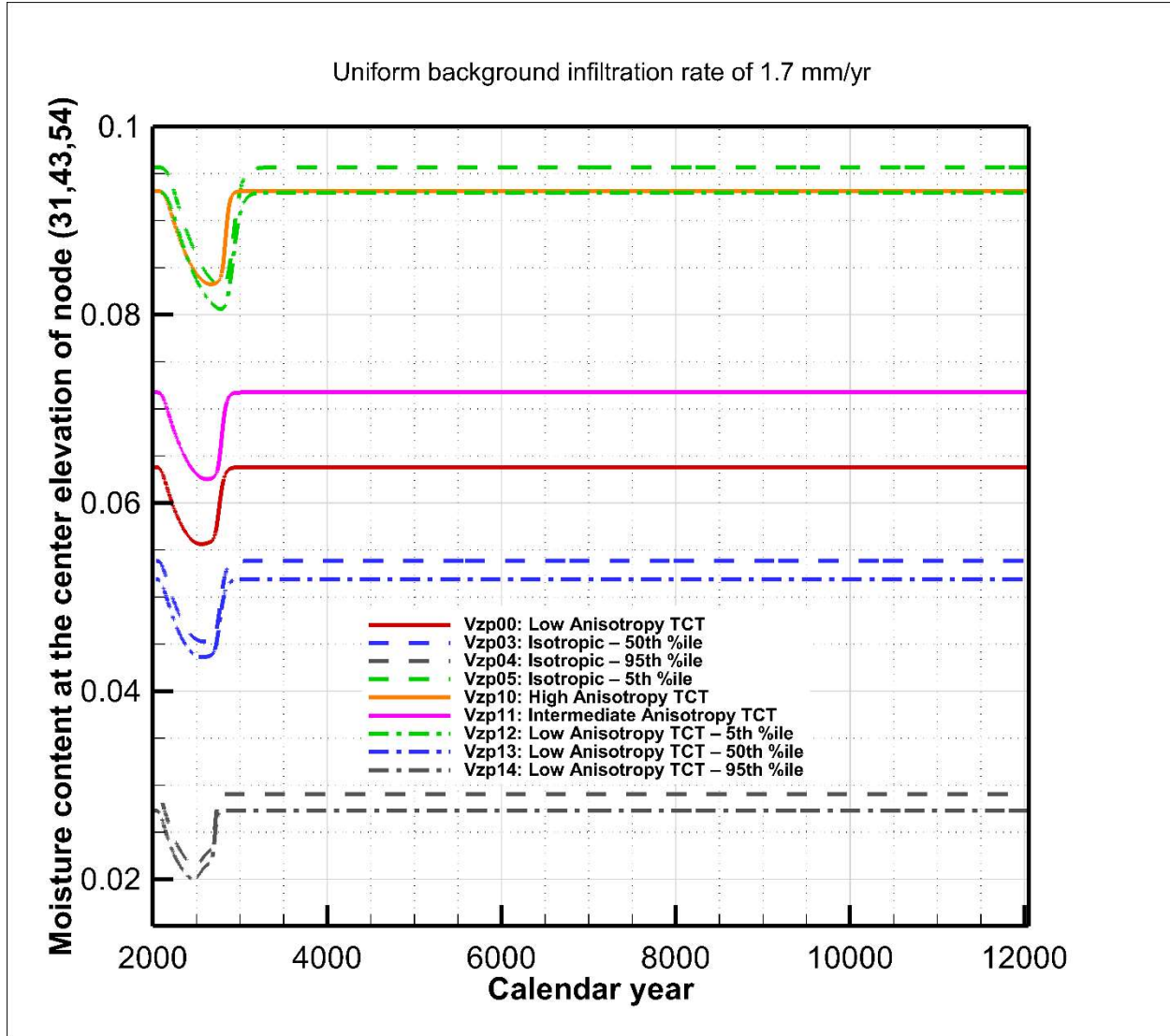
Source: RPP-CALC-61032, *Vadose Zone and Saturated Zone Flow and Transport Calculations for the Integrated Disposal Facility Performance Assessment*, Figure 7-170.

Note: The uniform background infiltration rate of 3.5 mm/yr is applied through the surface barrier after the 500-year design life of the surface barrier, i.e., starting in calendar year (CY) 2551. From CY 2005 to 2151, the vertical Darcy flux through the liner system is 0.0 mm/yr due to the operations of the leachate recovery system. From CY 2151 to 2551, the vertical Darcy flux through the liner system is assumed to be 0.5 mm/yr. The steady-state moisture content for the base case property set (Vzp00) is about 0.069. The steady-state moisture content for the 95th percentile pore velocity case (Vzp04) is about 0.034.

TCT = tensorial-connectivity-tortuosity

Figure 2-15-7. Calculated Moisture Content in the Middle of H2 Sand at 169-meter Elevation with Different Vadose Zone Hydraulic Parameter Sets and Background Infiltration Rates. (sheet 2 of 3)

(b) Background Infiltration Rate of 1.7 mm/yr



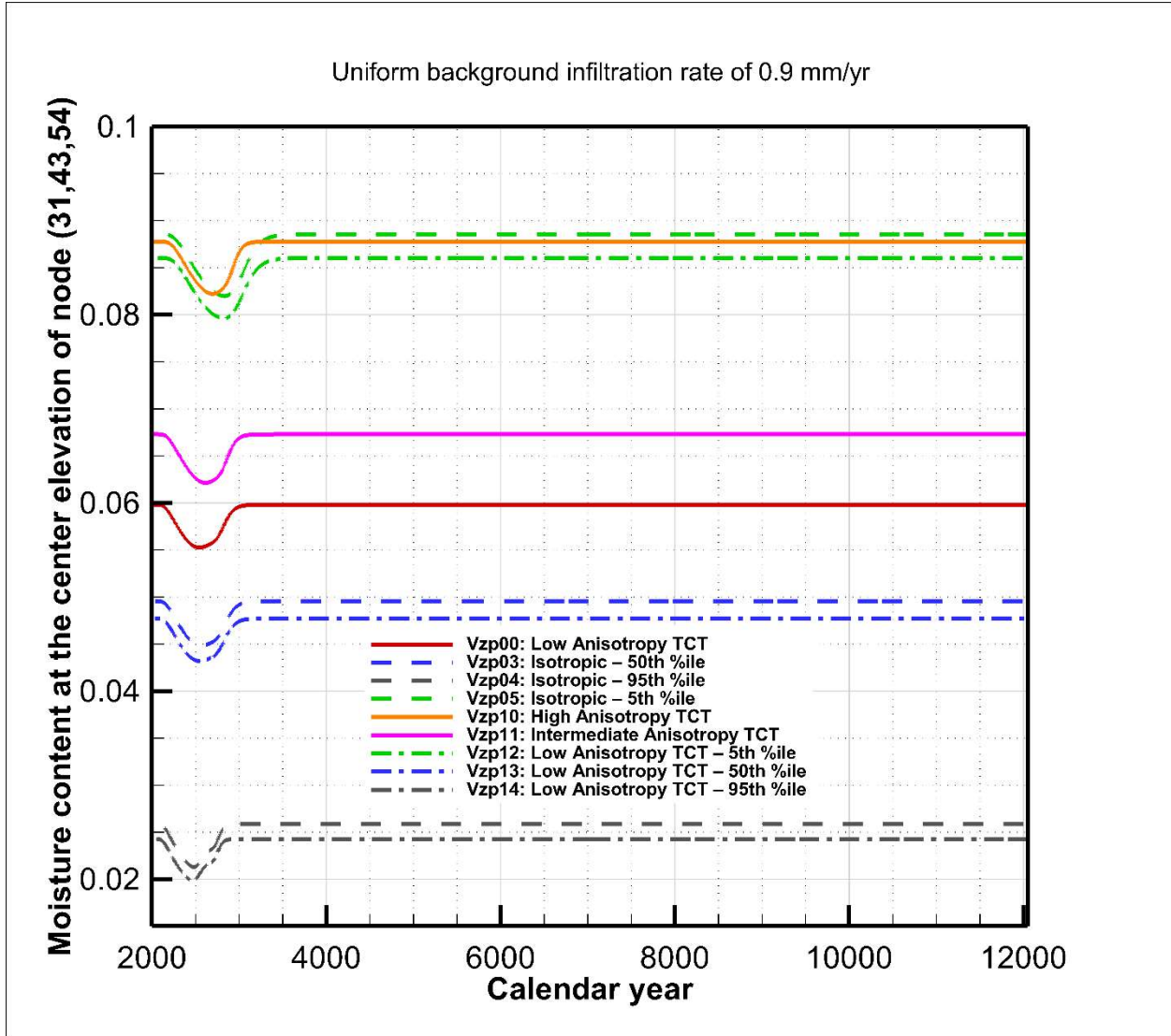
Source: RPP-CALC-61032, Figure 7-182.

Note: The uniform background infiltration rate of 1.7 mm/yr is applied through the surface barrier after the 500-year design life of the surface barrier, i.e., starting in CY 2551. From CY 2005 to 2151, the vertical Darcy flux through the liner system is 0.0 mm/yr due to the operations of the leachate recovery system. From CY 2151 to 2551, the vertical Darcy flux through the liner system is assumed to be 0.5 mm/yr. The steady-state moisture content for the base case property set (Vzp00) is about 0.063. The steady-state moisture content for the 95th percentile pore velocity case (Vzp04) is about 0.029.

TCT = tensorial-connectivity-tortuosity

Figure 2-15-7. Calculated Moisture Content in the Middle of H2 Sand at 169-meter Elevation with Different Vadose Zone Hydraulic Parameter Sets and Background Infiltration Rates. (sheet 3 of 3)

(c) Background Infiltration Rate of 0.9 mm/yr



Source: RPP-CALC-61032, Figure 7-188.

Note: The uniform background infiltration rate of 0.9 mm/yr is applied through the surface barrier after the 500-year design life of the surface barrier, i.e., starting in CY 2551. From CY 2005 to 2151, the vertical Darcy flux through the liner system is 0.0 mm/yr due to the operations of the leachate recovery system. From CY 2151 to 2551, the vertical Darcy flux through the liner system is assumed to be 0.5 mm/yr. The steady-state moisture content for the base case property set (Vzp00) is about 0.060. The steady-state moisture content for the 95th percentile pore velocity case (Vzp04) is about 0.026.

TCT = tensorial-connectivity-tortuosity

The predicted moisture contents for the three long-term average steady-state net infiltration rates modeled illustrate the following.

- As the assumed net infiltration rate increases from 0.9 to 1.7 to 3.5 mm/yr, the predicted moisture content increases from 0.060 to 0.063 to 0.069 for case Vz00, from 0.026 to 0.029 to 0.034 for case Vz04 and from 0.024 to 0.027 to 0.032 for case Vz14.
- Case Vz04 results in lower predicted moisture contents than case Vz00 by about a factor of two. This is expected because this case represents the 95th percentile pore velocity (or 5th percentile moisture content) for the 1.7 mm/yr net infiltration case.
- Case Vz14 results in a slightly lower predicted content (by about 0.002) compared to case Vz04 due to the lateral flow caused by the anisotropy in the vadose zone sediments.

The predicted moisture contents developed over the range of estimated net infiltration rates can be compared to observed moisture contents in the H2 sand.

Available moisture content information for the H2 sand developed from sediment samples and other indirect methods (neutron probes or neutron moisture logging) in undisturbed areas near the IDF is summarized in Table 2-15-2. Based on the sediment samples collected from boreholes drilled near the IDF, the average H2 sand moisture content is about 0.032. This average moisture content is representative of the steady-state vertical Darcy flux through the H2 sand near the IDF which is assumed to be equal to the long-term average net infiltration rate (and thus long-term average recharge rate) in the undisturbed surface conditions with mature shrub-steppe vegetation prior to the surface-disturbing activities resulting from the construction of the IDF⁵⁰.

The area near the IDF where boreholes have been drilled and sampled to determine the average *in situ* moisture content of about 0.032 is characterized as being an undisturbed surface (native soil with mature shrub-steppe vegetation), where the net infiltration rate is assumed to be equal to the steady-state vertical Darcy flux. At steady state, the vadose zone model and associated hydraulic (van Genuchten-Mualem) parameter values should be able to calculate moisture contents that are in the range of the observed moisture contents when using a representative net infiltration rate. However, determining what is a representative net infiltration rate is uncertain. To address this uncertainty, a range of values from 0.9 to 3.5 mm/yr have been used for most of the calculations presented in the IDF PA (RPP-RPT-59958) and the examples discussed above. However, it is possible that the net infiltration rate is as low as 0.16 mm/yr (the lower bound recommended in PNNL-14744) or even lower if one considers the possibility that the presence of

⁵⁰ This assumption may not be applicable in the area around the Sisson and Lu test site (boreholes 299-E24-76 to 299-E24-107), which is located next to an area with disturbed surface conditions which includes an unused waste disposal crib. However, the interpreted moisture content in the Sisson and Lu boreholes was not used to develop the average value of 0.032.

olian silts in the upper few meters of the vadose zone at the IDF could significantly reduce the net infiltration rate as hypothesized in PNNL-14744⁵¹.

In addition to the moisture contents measured in areas of undisturbed surface conditions, additional moisture content has been measured in areas near the IDF in the 200 East Area that have disturbed surfaces since Hanford operations began in 1944. Examples of these areas include the tank farm areas associated with WMA C and WMA A-AX located about a kilometer north of the IDF. The observed moisture content in sediment samples collected from boreholes drilled in these areas with disturbed surfaces averages about 0.052 (see Table 3-3 and Figure B-2a of RPP-ENV-58782).

The best-estimate net infiltration rate in the disturbed surface areas in the tank farm areas for the time period since the surfaces were disturbed is about 100 mm/yr (PNNL-14702). Although it would take some time for the effects of the surface disturbance and resulting increase in the net infiltration rate (from the pre-disturbance value of 0.9 to 3.5 mm/yr to the post-disturbance value of about 100 mm/yr) to propagate to the depth of the H2 sand beneath the disturbed surfaces, there has been sufficient time between the time the surfaces were disturbed (about calendar year [CY] 1944) to the time when moisture contents were measured (CY 2003 to CY 2013 for WMA C and CY 2014 for WMA A-AX) to allow the moisture regime to reach a quasi-steady state to the depth of the H2 sand. Therefore, it is possible to also use the observed moisture contents in the H2 sand in disturbed surface areas along with the best estimate of the net infiltration rate in these areas to evaluate the representativeness of the vadose zone hydraulic parameter values.

The 200 realizations of vadose zone hydraulic parameter values of the H2 sand were developed to evaluate the impact of the vadose zone hydraulic parameter uncertainty on predicted moisture contents (and thus pore velocity and vadose zone transport times) for the IDF PA. These same 200 hydraulic parameter realizations have been used to compare predicted moisture contents to observed average moisture contents.

Figure 2-15-8 presents the results of the 200 realizations of predicted moisture contents for the best-estimate net infiltration rate in undisturbed surface areas near the IDF of 0.9 mm/yr (based on PNNL-14744) and the best-estimate net infiltration rate in disturbed surface areas near the IDF of 100 mm/yr (based on PNNL-14702). Considering that the average observed H2 sand moisture content for the 0.9 mm/yr case is about 0.032 and the average observed H2 sand moisture content for the 100 mm/yr case is about 0.052, it is apparent that few realizations of the sampled vadose zone hydraulic parameter values can reproduce the observed average moisture contents.

⁵¹ The eolian silt deposits that are capable of reducing recharge in the vicinity of the IDF relative to other areas of the Hanford Site are shallow and were removed during IDF excavation. Consequently, the IDF PA base case does not account for these layers when developing the base case long-term recharge rate for the post-closure analysis.

Table 2-15-2. H2 Sand Moisture Content Data in Boreholes Drilled near the Integrated Disposal Facility. (2 sheets)

Monitoring Well ID	Borehole ID	Location	Drilling Date	Moisture Content Data (Depth Range, m bgs)	Number of Sediment Samples	Volumetric Moisture Content (-) Average (min, max)	Reference
299-E24-161	B2428	~ 35 m north of 299-E24-162	1995	Sediment cores (0 – 15 m)	30	0.023 (0.018, 0.035)	PNNL-13033, Table B.3
299-E24-162	B2429	~Northeast corner of Integrated Disposal Facility (IDF) trench	1995	Sediment cores (0 – 15 m)	30	0.024 (0.016, 0.030)	PNNL-13033, Table B.4
Not applicable	C4071	Western cell (cell 1) of IDF trench	1995	Sediment cores (0 – 4.6 m)	7	0.026 (0.020, 0.032)	PNNL-13033, Table B.5
299-E17-21	B8500	~ 400 m south of southwest corner of IDF trench	1998	Sediment cores (14 – 73 m) Sediment cores (3 – 107 m) Neutron log (0 – 100 m)	20 85	0.034 (0.020, 0.061) 0.028 (0.017, 0.065)	RPP-20621, App. A, Table 3 PNNL-13033, Table B.6 PNNL-11957, Figure D.2
Not applicable	B8501	~ 30 m north of B8500	1998	Sediment cores (0 – 14.7 m)	72	0.030 (0.010, 0.071)	PNNL-13033, Table B.7
Not applicable	B8502	~ 30 m east of B8500	1998	Sediment cores (0 – 13.3 m)	70	0.035 (0.016, 0.087)	PNNL-13033, Table B.8
Not applicable	B8503	~ 25 m northeast of B8500	1998	Sediment cores (0 – 8.4 m)	44	0.044 (0.026, 0.061)	PNNL-13033, Table B.9
299-E24-21	C3177	~ 350 m north of northeast corner of IDF trench	2001	Sediment cores (5 – 255 ft) (1.5 – 77.7 m)	37	0.036 (0.008, 0.108)	PNNL-14289, Table 4.3
299-E17-22	C3826	~ 200 m east of IDF	2002	Sediment cores (2.7 – 67.9 m)	16	0.030 (0.020, 0.041)	PNNL-14744, Table B.3

Table 2-15-2. H2 Sand Moisture Content Data in Boreholes Drilled near the Integrated Disposal Facility. (2 sheets)

Monitoring Well ID	Borehole ID	Location	Drilling Date	Moisture Content Data (Depth Range, m bgs)	Number of Sediment Samples	Volumetric Moisture Content (-) Average (min, max)	Reference
299-E24-76 to 299-E24-107	Not reported	~ 200 m east of northeast corner of IDF trench	2000-2001	Neutron probes (0 m – 18 m)	1,376	0.035 (0.016, 0.167)	PNNL-15443, Tables 2.7 - 2.8
299-E24-164	D0040	~ 120 m north of northeast corner of IDF trench	August 2019	Neutron log (0 – 97.5 m)	Not applicable	~ 0.03	SGW-63813, Appendix D

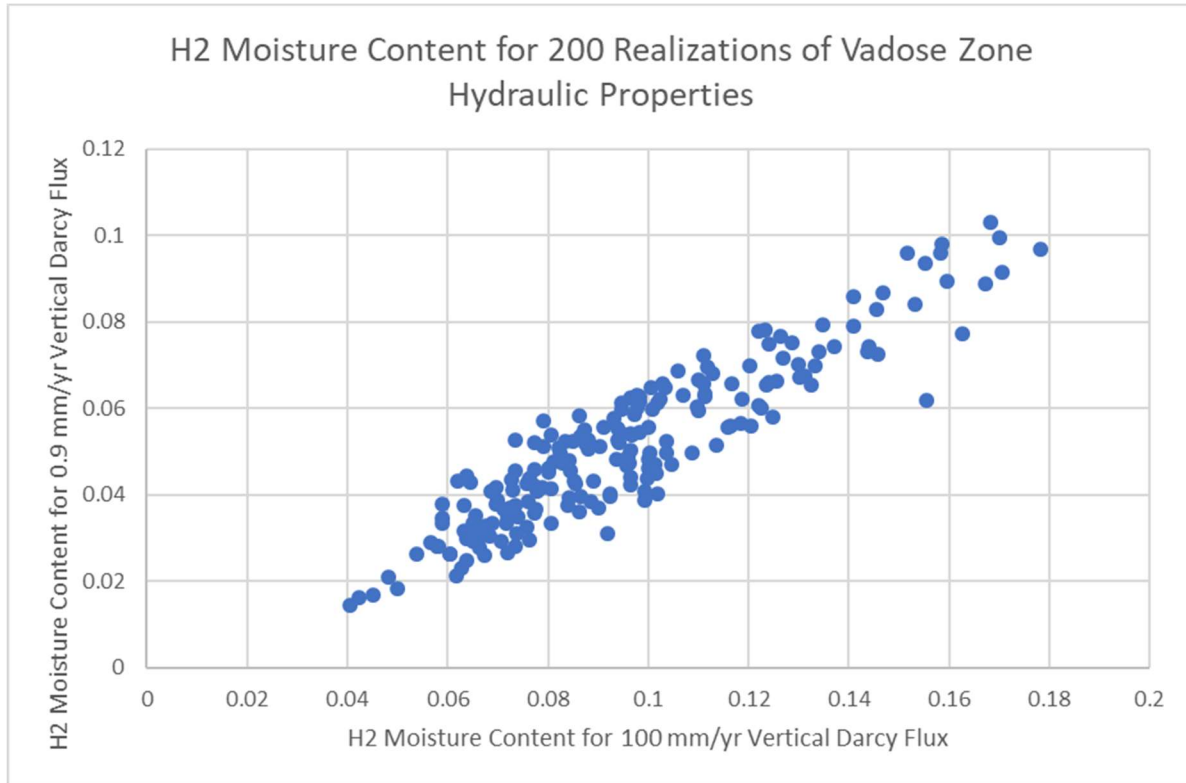
Note:

- a) The sediment samples included in the summary exclude the upper 3 m (3.5 m in the case of B8503) of samples from these boreholes because the shallow moisture contents are likely impacted by short-term transient infiltration events and finer-grained sediments that are not representative of the average *in-situ* conditions.
- b) Neutron probes of boreholes 299-E24-76 to 299-E24-107 were conducted prior to, during and after injecting water and tracers as part of the Sisson and Lu field experiment. Different neutron probes and different calibration methods were used during the course of the experiment to convert the neutron measurements (counts per second) to volumetric moisture content. The results of these tests are summarized in PNNL-15443. The moisture contents summarized here are associated with the neutron probe measurements conducted prior to injection tests performed on June 2, 2000 and March 30, 2001.
- c) Volumetric moisture contents interpreted from the neutron log conducted after drilling at borehole D0040 (299-E24-164) represent the interval between a depth of 20 and 80 ft below ground surface (bgs). The values above 20 ft bgs were impacted by infiltration from a rainfall event which occurred about 3 weeks prior to the neutron log. The values below 80 ft bgs were likely impacted by water added during drilling below depths of 80 ft bgs.

References:

PNNL-11957, *Immobilized Low-Activity Waste Site Borehole 299-E17-21*
 PNNL-13033, *Recharge Data Package for the Immobilized Low-Activity Waste 2001 Performance Assessment*
 PNNL-14289, *Geochemistry of Samples from Borehole C3177 (299-E24-21)*
 PNNL-14744, *Recharge Data Package for the 2005 Integrated Disposal Facility Performance Assessment*
 PNNL-15443, *Vadose Zone Transport Field Study Summary Report*
 RPP-20621, *Far-Field Hydrology Data Package for the Integrated Disposal Facility Performance Assessment*
 SGW-63813, *Borehole Summary Report for the Installation of Six M-24 Wells in the 200-PO-1, 200- UP-1 and 300-FF-5 Operable Units, FY2019*

Figure 2-15-8. Predicted H2 Sand Moisture Content for Uncertain Vadose Zone Hydraulic Parameter Values for Vertical Darcy Fluxes of 0.9 mm/yr and 100 mm/yr.



Source: Derived from Excel® (a registered trademark of Microsoft Corporation in the U.S. and other countries) spreadsheet used to develop vadose zone property sets corresponding to the 5th, 50th and 95th percentile of pore velocity (or 95th, 50th and 5th percentile of moisture content).

Note: The observed moisture content for a recharge rate (and corresponding vertical Darcy flux) of 0.9 mm/yr is 0.032. The observed moisture content for a recharge rate (and corresponding vertical Darcy flux) of 100 mm/yr is 0.052. Five realizations result in an under prediction of observed moisture contents for both the disturbed (100 mm/yr) and undisturbed (0.9 mm/yr) surface conditions; i.e., for these five realizations the predicted moisture contents are less than 0.032 and 0.052 for the undisturbed (0.9 mm/yr) and disturbed (100 mm/yr) surface condition, respectively. The 30 realizations with lowest predicted moisture content for both undisturbed and disturbed surface conditions are presented in Table 2-15.3.

The results for individual realizations that come closest to reproducing the observed moisture contents for both infiltration cases are summarized in Table 2-15-3. These are the realizations with the lowest predicted moisture contents for an undisturbed infiltration (and vertical Darcy flux) of 0.9 mm/yr (representative of undisturbed surface conditions near the IDF) and 100 mm/yr (representative of disturbed surface conditions in areas near the IDF such as the WMA C and WMA A-AX tank farm areas). Although there is no unique realization that matches the observed average moisture contents for both the undisturbed and disturbed surface conditions, there are several realizations that produce representative results.

Table 2-15-3. Comparison of Vadose Zone Hydraulic Parameter Realizations with Lowest Predicted Moisture Contents for Best-Estimate Undisturbed and Disturbed Recharge Rates.

Percentile	Undisturbed Surface Recharge (0.9 mm/yr)		Disturbed Surface Recharge (100 mm/yr)	
	Realization #	Predicted Moisture Content	Realization #	Predicted Moisture Content
1	59	0.0145	59	0.0405
	6	0.0161	6	0.0422
2	112	0.0170	112	0.0452
	4	0.0184	46	0.0483
3	46	0.0209	4	0.0499
	189	0.0213	43	0.0539
4	132	0.0232	55	0.0567
	80	0.0250	138	0.0578
5	73	0.0260	13	0.0581
	169	0.0263	140	0.0590
6	129	0.0263	93	0.0590
	43	0.0264	173	0.0590
7	177	0.0267	169	0.0604
	71	0.0277	129	0.0604
8	138	0.0280	189	0.0617
	13	0.0280	181	0.0619
9	168	0.0282	132	0.0627
	55	0.0290	19	0.0633
10	108	0.0294	49	0.0634
	78	0.0294	11	0.0637
11	79	0.0297	124	0.0637
	124	0.0299	80	0.0639
12	128	0.0303	35	0.0644
	192	0.0305	108	0.0651
13	29	0.0308	91	0.0651
	26	0.0310	151	0.0656
14	28	0.0312	29	0.0659
	49	0.0317	128	0.0662
15	96	0.0325	71	0.0664
	84	0.0329	73	0.0673

Note:

Realization 73 is the 95th percentile case used in the IDF PA (RPP-RPT-59958, *Performance Assessment for the Integrated Disposal Facility, Hanford Site, Washington*) (cases Vz04 or Vz14) based on an assumed recharge rate of 1.7 mm/yr.

Highlighted realizations are those that result in the lowest predicted moisture contents for both the undisturbed (best-estimate recharge rate of 0.9 mm/yr) and disturbed (best-estimate recharge rate of 100 mm/yr) surface conditions.

Realizations #43, #138, #13 and #55 are representative of cases that reproduce both the observed average moisture content of 0.032 for a best-estimate undisturbed net infiltration rate of 0.9 mm/yr as well as the observed average moisture content of 0.052 for a best-estimate disturbed net infiltration rate of 100 mm/yr.

For several realizations that yield predicted moisture contents that are representative of observed average moisture contents for both undisturbed and disturbed surface conditions, it is possible to evaluate the predicted moisture contents for other assumed net infiltration rates, including an infiltration rate of 3.5 mm/yr that is assumed to be representative of net infiltration through the surface barrier at IDF after the surface barrier's 500-yr design life. This comparison is presented in Table 2-15-4. Compared to the 95th percentile case (realization #73, case Vz04 or Vz14) used in the IDF PA (RPP-RPT-59958), the other realizations that yield representative predicted moisture contents for undisturbed and disturbed surface conditions (realizations #55, #138, #43 and #13) produce similar predicted moisture contents for the 3.5 mm/yr base case post-design-life net infiltration rate assumed in the IDF PA. Therefore, these different realizations would be expected to produce similar predicted vadose zone performance predictions to those resulting from realization #73 (cases Vz04 and Vz14) if they were implemented in the IDF vadose zone model.

Realization #73 (case Vz04 or Vz14) provides a case that is consistent with observed moisture contents in the H2 sand near the IDF when the long-term average undisturbed net infiltration rate is in the range of 0.9 to 3.5 mm/yr. If the undisturbed net infiltration rate is in the range of 0.9 to 3.5 mm/yr, then the vadose zone hydraulic parameter values used in case Vz04 or case Vz14 can reproduce the observed H2 sand average moisture content (Table 2-15-4). If the undisturbed infiltration rate is less than 0.16 mm/yr, then the base case (Vz00) property set provides a representative case that can reproduce the observed moisture contents. Based on these comparisons, it can be concluded that the range of vadose zone hydraulic parameter sets used in the IDF PA encompasses the observed moisture contents given the uncertainty in the assumed undisturbed net infiltration rate.

Impact of Alternative Moisture Retention Relationships on IDF Performance

Sensitivity analyses presented in the IDF PA (Section 5.2.4.3 and 5.2.4.8 of RPP-RPT-59958) on effects of uncertain vadose zone hydraulic parameter values can be used to examine the significance of the uncertain vadose zone hydraulic parameter values on the performance of the IDF disposal facility. Some example results are reproduced as Figure 2-15-9. The following observations can be made from these results.

- Cases Vz04 and Vz14⁵² result in earlier radionuclide arrival at the water table than the base case (Vz00) due to the lower predicted moisture content (and higher predicted pore velocity) for a given long-term average steady-state net infiltration rate. For the distributed flow case, this can result in peak arrival times for unretarded radionuclides (e.g., ⁹⁹Tc) occurring prior to 1,000 years after the facility is closed.

⁵² Cases Vz04 and Vz14 represent the 95th percentile pore velocity (equivalent to the 5th percentile moisture content) for an assumed net infiltration rate of 1.7 mm/yr for both the H2 sand and the H3 gravel. Comparisons between predicted and observed moisture contents are only possible for the H2 sand as there are no relevant observations of moisture content in the H3 gravels in undisturbed surface areas near the IDF. Observations of moisture content in H3 gravels in disturbed surface areas near WMA C and WMA A-AX are available. Cases Vz04 and Vz14 have also modified the hydraulic property values of the H3 gravel to represent the 95th percentile pore velocity.

- Cases Vz00 and Vz04 (and other vadose zone parameter sets) result in similar peak release rates to the water table, albeit at different times.

Table 2-15-4. Predicted Moisture Content in the H2 Sand for Different Vadose Zone Hydraulic Property Sets and Recharge Rates.

Recharge Rates (mm/yr)	H2 Vadose Zone Hydraulic Property Sets (Realization #)							Observed Average Moisture Content
	Base Case (Vz00)	# 121 (Vz03)	# 73 (Vz04)	# 55	# 13	# 138	# 43	
140	NC	0.106	0.072	0.060	0.062	0.061	0.057	0.052
100	0.103	0.100	0.067	0.057	0.058	0.058	0.054	
60	NC	0.092	0.060	0.052	0.053	0.053	0.049	
3.5	0.069	0.060	0.034	0.034	0.034	0.034	0.032	0.032
1.7	0.063	0.054	0.029	0.031	0.031	0.030	0.029	
0.9	0.060	0.050	0.026	0.029	0.028	0.028	0.026	
0.16	0.050	0.040	0.019	0.024	0.022	0.023	0.022	

Note:

The different vadose zone property sets are:

Case Vz00 is the base case in the IDF PA (RPP-RPT-59958, *Performance Assessment for the Integrated Disposal Facility, Hanford Site, Washington*).

Case Vz03 (realization #121 of the 200 realizations used to evaluate the effect of uncertainty in van Genuchten-Mualem parameter values on vadose zone transport) represents the 50th percentile for a vertical Darcy flux of 1.7 mm/yr.

Case Vz04 (realization #73) represents the 95th percentile for a vertical Darcy flux of 1.7 mm/yr.

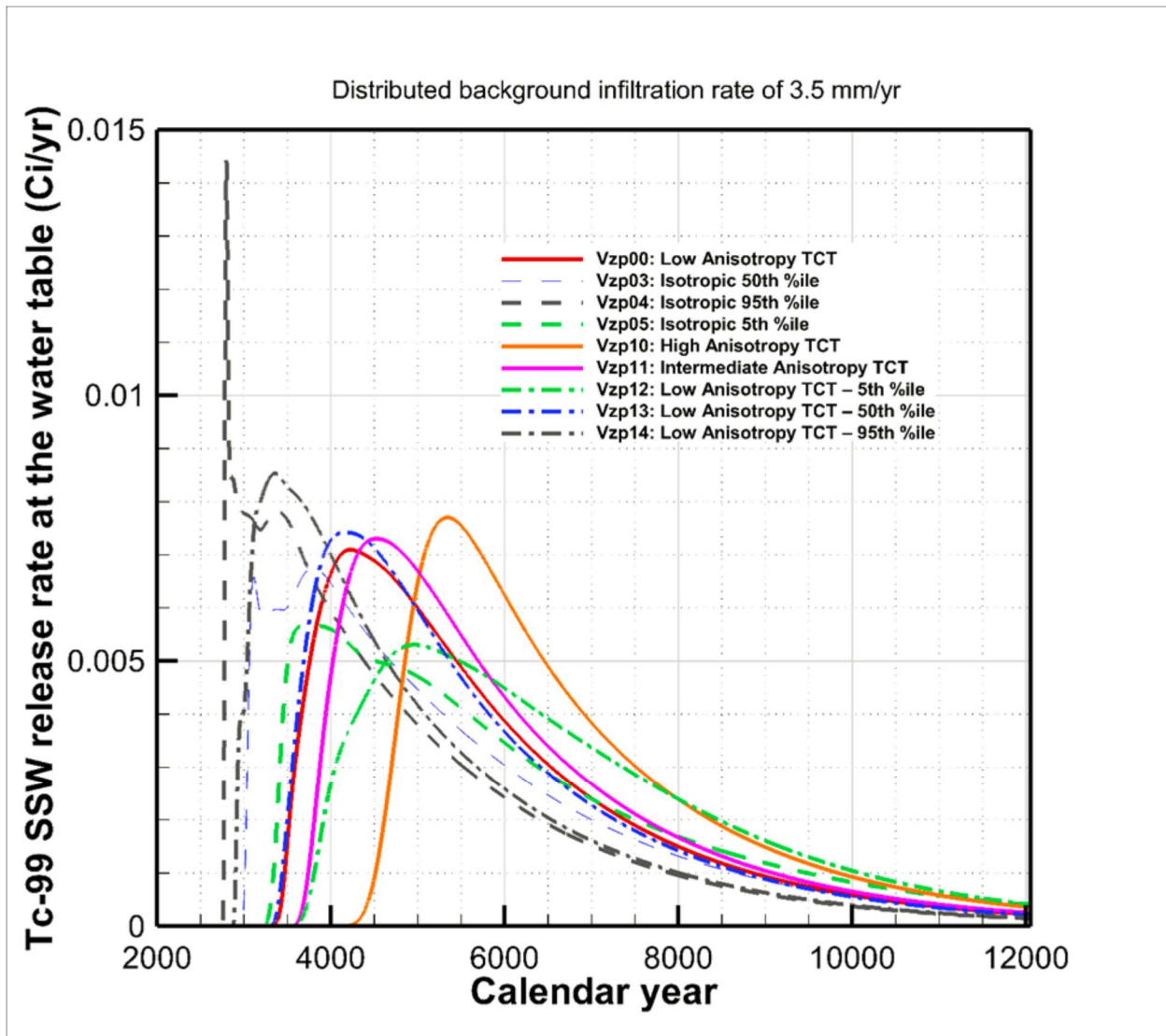
Realizations #55, #13, #138 and #43 represent cases that come closest to reproducing both the observed moisture content of 0.032 for a best-estimate undisturbed net infiltration rate of 0.9 mm/yr as well as the observed average moisture content of 0.052 for a best-estimate disturbed net infiltration rate of 100 mm/yr (see Table 2-15-3).

The different recharge rates represent the following:

- 100 mm/yr is the recharge rate in areas with disturbed surface conditions with a gravel surface and no vegetation as recommended in PNNL-14702, *Vadose Zone Hydrogeology Data Package for Hanford Assessments* and used in ECF-HANFORD-15-0019, *Hanford Site-wide Natural Recharge Boundary Condition for Groundwater Models*, Rev. 2. This includes the disturbed surfaces in the WMA C and WMA A-AX areas.
- 140 and 60 mm/yr represent the upper and lower limits of the estimated recharge rates in areas with disturbed surface conditions as recommended in PNNL-14702.
- 3.5 mm/yr is the average of the net infiltration rate into the Rupert Sand and Burbank Loamy Sand in areas with mature shrub-steppe vegetation near the IDF as reported in PNNL-14702. 3.5 mm/yr is also the long-term average flux into the IDF after the assumed 500-year design life of the surface cap.
- 1.7 mm/yr is the average value for Rupert Sand with mature shrub-steppe vegetation in the Central Plateau recommended in PNNL-16688, *Recharge Data Package for Hanford Single-Shell Tank Waste Management Areas*. This value is also close to the mode (1.9 mm/yr) of the uncertainty distribution used in the IDF PA. This value was the vertical Darcy flux value used to develop the statistics on moisture content and pore velocity used to define the 95th, 50th and 5th percentile cases in the IDF PA.
- 0.9 mm/yr is the best-estimate recharge rate for the IDF recommended in PNNL-14744, *Recharge Data Package for the 2005 Integrated Disposal Facility Performance Assessment* based on the interpreted chloride mass balance average of seven boreholes near the IDF.
- 0.16 mm/yr is the minimum bounding recharge rate recommended in PNNL-14744 based on the interpreted chloride mass balance in borehole 299-E24-161 located near the IDF.

Average observed moisture contents for the IDF undisturbed recharge conditions are based on about 400 observations in boreholes near the IDF (the same boreholes with measured chloride mass used to estimate the average net infiltration rate in PNNL-14744). Average observed moisture contents for disturbed recharge conditions are based on observations made in WMA C and WMA A-AX for disturbed surface conditions.

Figure 2-15-9. Technetium-99 Breakthrough at Water Table from Solid Secondary Waste Sources for Different Vadose Zone Conceptual Models and Property Sets – Distributed Infiltration 3.5 mm/yr.



SSW = solid secondary waste

TCT = tensorial-connectivity-tortuosity

Source: RPP-RPT-59958, *Performance Assessment for the Integrated Disposal Facility, Hanford Site, Washington*, Figure 5-147 (derived from RPP-CALC-61032, *Vadose Zone and Saturated Zone Flow and Transport Calculations for the Integrated Disposal Facility Performance Assessment*, Figure 7-154).

As noted in RPP-RPT-59958, many of the detailed process-model sensitivity analyses performed focused on only one component of the disposal system. This is a result of the long computational times for running some of the models. For example, Section 5.2.4 presents the results of sensitivity analyses using only the vadose zone feature of the combined vadose zone/saturated zone flow and transport model because the vadose zone-only STOMP model took only 12 hours to complete while the combined vadose zone/saturated zone flow and transport model took almost 2 weeks to complete.

Because there are no combined vadose zone/saturated zone model runs that correspond to case Vz04 or Vz14 with best-estimate values of radionuclide sorption, to evaluate the impact of case Vz04 and Vz14 on the predicted groundwater concentration at the 100-m point of assessment boundary, additional calculations were performed to support this RAI response that will be included in future updates to the PA according to the PA change management process. The results of these additional sensitivity analyses are presented in Figures 2-15-10 to 2-15-13. These figures include the base case results presented in Figures 5-98 and 5-99 of RPP-RPT-59958. These figures also contain a secondary axis that converts the groundwater concentration to a dose using the All-Pathways Groundwater Dose conversion factor value of 0.69 mrem/yr per pCi/L for ^{129}I and 3.76E-03 mrem/yr per pCi/L for ^{99}Tc . The following observations can be drawn from these sensitivity analyses.

- The peak concentrations for ^{129}I and ^{99}Tc in the groundwater are not significantly affected by the uncertainty in the vadose zone hydraulic parameter values. This is analogous to the observation made in comparing the peak release rates from the vadose zone to the saturated zone.
- The timing of the peak concentration arrival at the 100-m point of assessment boundary is reduced when using the alternative vadose zone property sets. This is also analogous to the observation made in comparing the time of the peak release rate from the vadose zone to the saturated zone.
- The timing of the peak concentration arrival at the 100-m point of assessment is less for the isotropic case (Vz04) than the low anisotropic case (Vz14).

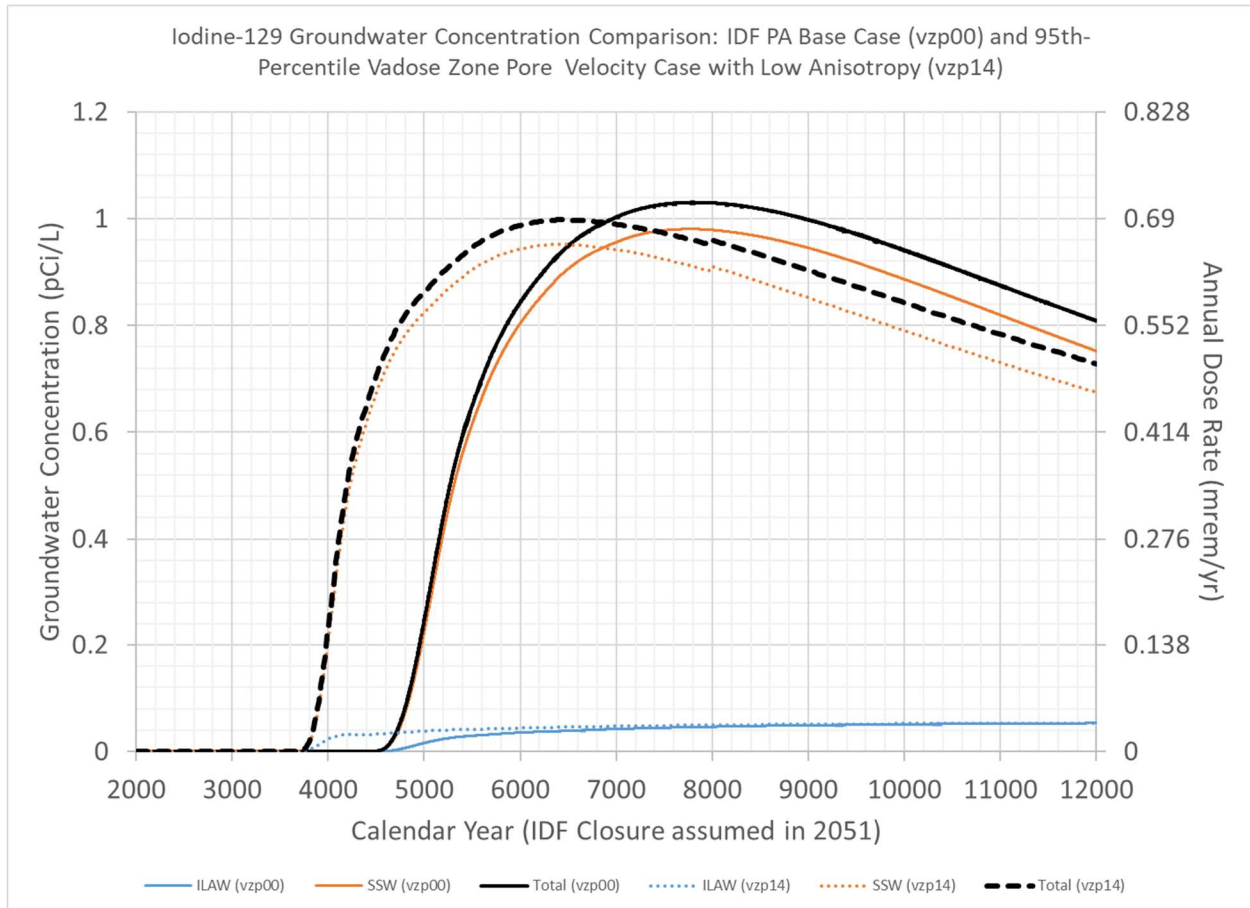
The results of the base case and alternative vadose zone hydraulic property sets are summarized in Table 2-15-5.

Summary

The vadose zone hydraulic (van Genuchten-Mualem) parameter values affect the fate of radionuclides released from the IDF as they are transported through the vadose zone to the underlying saturated zone. The uncertainty in these parameter values can affect the timing of the release of radionuclides to the underlying saturated zone and thus the timing of the radionuclide plume arrival at the point of assessment in the groundwater located 100-m from the edge of the IDF footprint. The IDF PA analyzed the effect of this uncertainty using the existing data on vadose zone hydraulic parameter values from 44 samples of the H2 sediments. Although it is possible that the parameter value uncertainty could be broader than that represented by the 44 samples, the range of values used in the analysis captures the range of predicted moisture contents and thus the expected range of predicted pore velocities and transport times.

The IDF PA noted that the vadose zone was a significant feature due to both the low net infiltration rate and the hydraulic properties of the Hanford sand and gravel units which directly determine whether radionuclides released from the IDF will reach the water table (and hence compliance boundary) within 1,000 years (RPP-RPT-59958, Table 8-6). This importance was highlighted in the discussion of key assumptions presented in RPP-RPT-59958, Section 8.4.2.

Figure 2-15-10. Iodine-129 Breakthrough Curves for Cases Vzp00 and Vzp14 at Location of Peak Impact Along the 100-meter Buffer Boundary for Release from Immobilized Low-Activity Waste Glass and Solid Secondary Waste.



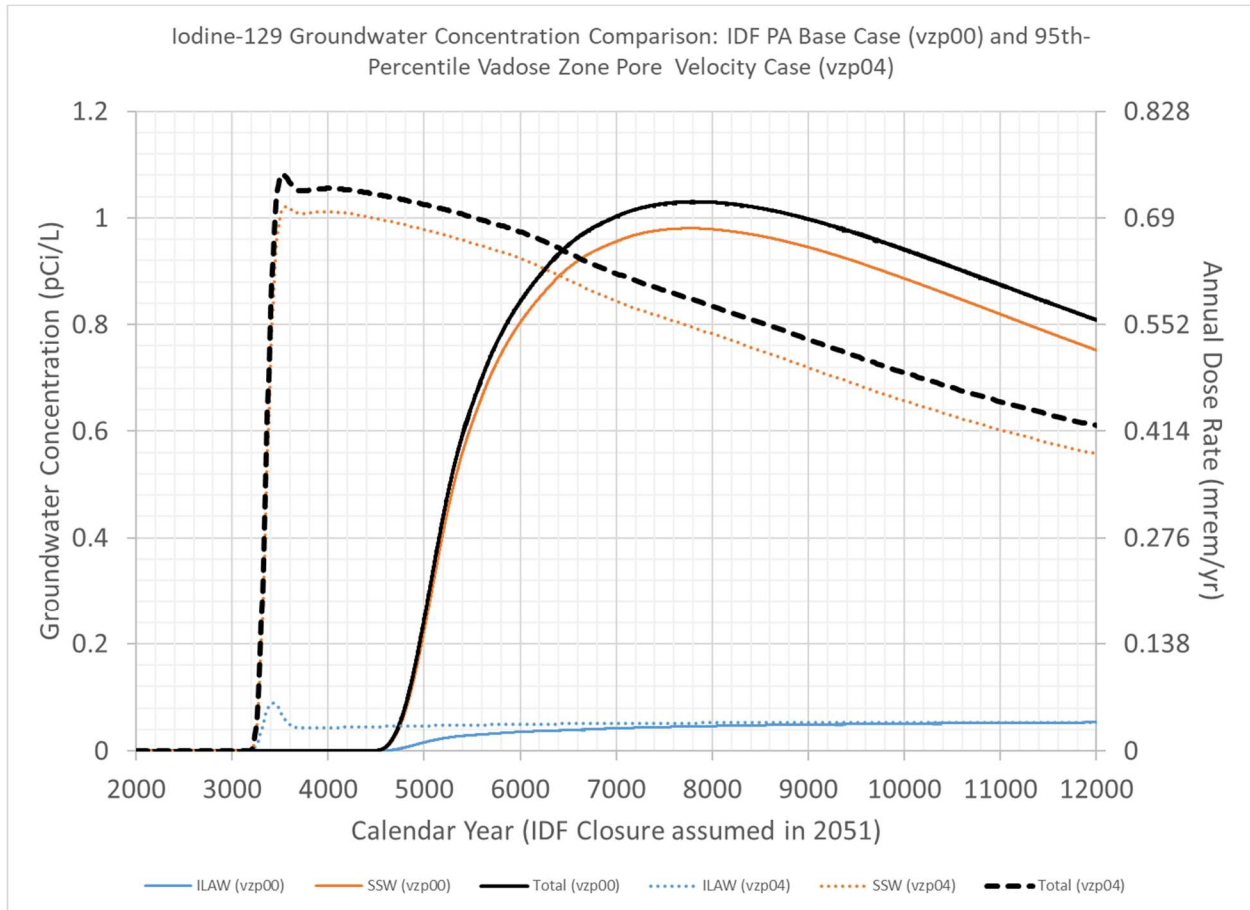
PA = Performance Assessment

Note: Time is in calendar year, the Integrated Disposal Facility (IDF) is assumed to be closed in calendar year 2051. Assumes base case distributed flow recharge rate of 3.5 mm/yr (case Inf06) and base case immobilized low-activity waste (ILAW) and solid secondary waste (SSW) release rate of RPP-RPT-59958, *Performance Assessment for the Integrated Disposal Facility, Hanford Site, Washington*. The total for vzp00 includes a small contribution from Effluent Treatment Facility liquid secondary waste (see RPP-RPT-59958 Figure 5-99), the total for VZP14 does not. The dose is converted from the groundwater concentration to a dose using the All-Pathways Groundwater Dose conversion factor value of 0.69 mrem/yr per pCi/L.

In addition to the transport velocity, and hence transport time, in the vadose zone being affected by the assumed recharge rate and recharge distribution at the top of the vadose zone (e.g., the base of the IDF liner), the transport velocity is also strongly dependent on the assumed van Genuchten-Mualem vadose zone property set and the assumed anisotropic conceptual model for flow in the vadose zone, which in turn affect the calculated moisture content in the vadose zone under future hydrologic conditions. The range of feasible moisture contents is roughly a factor of two greater than or less than the nominal or expected moisture content. This factor of two translates into a factor of two lower or higher pore velocity and therefore a factor of two longer or shorter transport times to the water table. The nominal moisture content at IDF, about 0.07, is about the same as the nominal value at WMA C under similar recharge conditions. There are limited relevant soil moisture measurements in boreholes in the IDF. Future boreholes

in the area should be considered in developing a more robust data set on expected moisture contents. It is noted that these moisture contents represent average values (i.e., the scale of meters), as local scale heterogeneities (i.e., silt lenses and paleosols) can alter the moisture content locally (at the scale of centimeters) (RPP-RPT-59958, Section 8.4.2).

Figure 2-15-11. Iodine-129 Breakthrough Curves for Cases Vzp00 and Vzp04 at Location of Peak Impact Along the 100-meter Buffer Boundary for Release from Immobilized Low-Activity Waste Glass and Solid Secondary Waste.



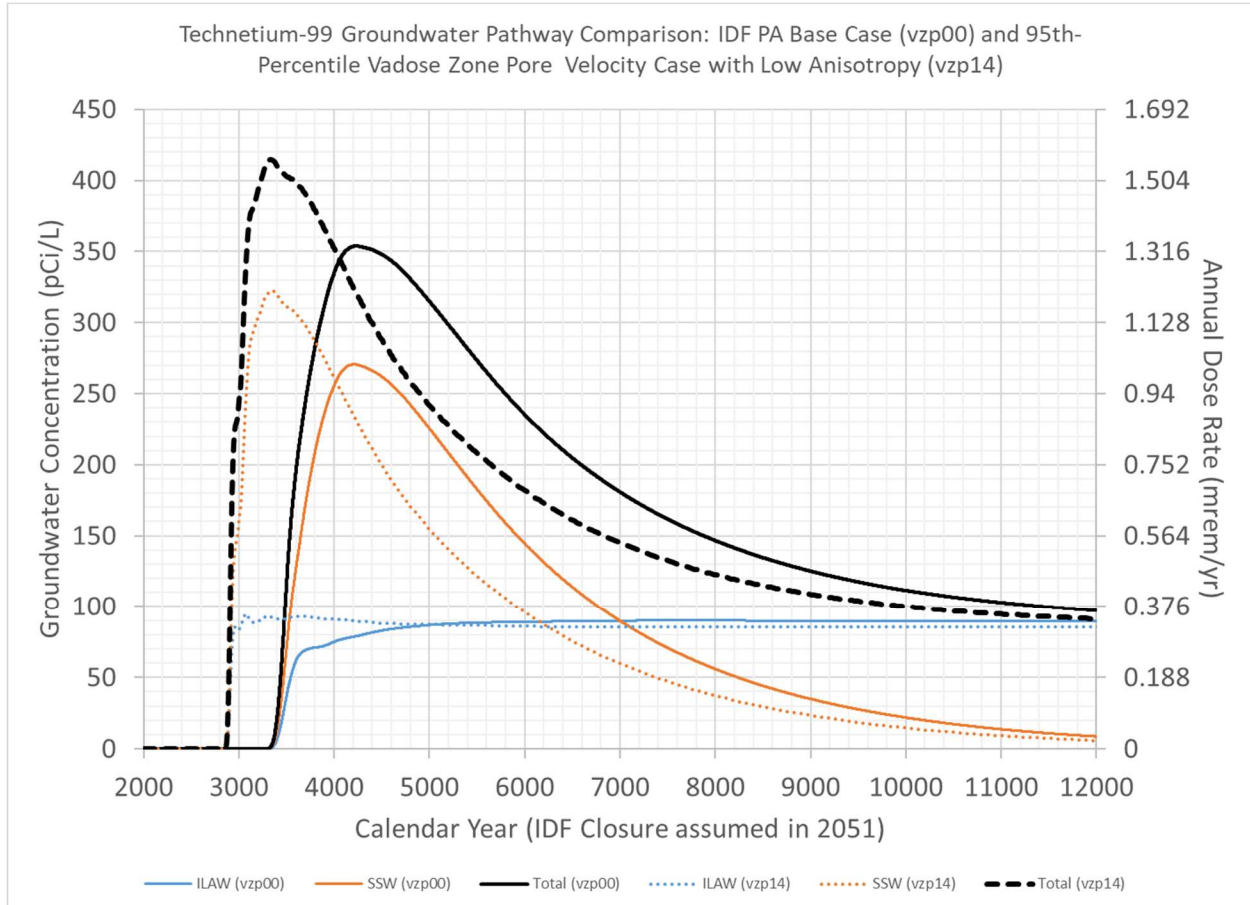
PA = Performance Assessment

Note: Time is in calendar year, the Integrated Disposal Facility (IDF) is assumed to be closed in calendar year 2051. Assumes base case distributed flow recharge rate of 3.5 mm/yr (case Inf06) and base case immobilized low-activity waste (ILAW) and solid secondary waste (SSW) release rate of RPP-RPT-59958, *Performance Assessment for the Integrated Disposal Facility, Hanford Site, Washington*. The total for vzp00 includes a small contribution from Effluent Treatment Facility liquid secondary waste (see RPP-RPT-59958 Figure 5-99), the total for VZP04 does not. The dose is converted from the groundwater concentration to a dose using the All-Pathways Groundwater Dose conversion factor value of 0.69 mrem/yr per pCi/L.

Based on the identified significance of the vadose zone hydraulic property set on the predicted performance, specifically related to the time it takes radionuclides released from the base of the IDF liner system to reach the water table and thus the point of assessment, Table 8-8 of RPP-RPT-59958 recommended including moisture profile measurements in boreholes drilled near the IDF. This recommendation was implemented in Section 4.7 of the IDF Maintenance Plan (CHPRC-03348), where the need to evaluate undisturbed present-day soil moisture profiles

for areas near the IDF was identified and it was noted that one of the few locations with ambient moisture information is at well 299-E17-21.

Figure 2-15-12. Technetium-99 Breakthrough Curves for Cases Vzp00 and Vzp14 at Location of Peak Impact along the 100-meter Buffer Boundary for Release from Immobilized Low-Activity Waste Glass and Solid Secondary Waste.

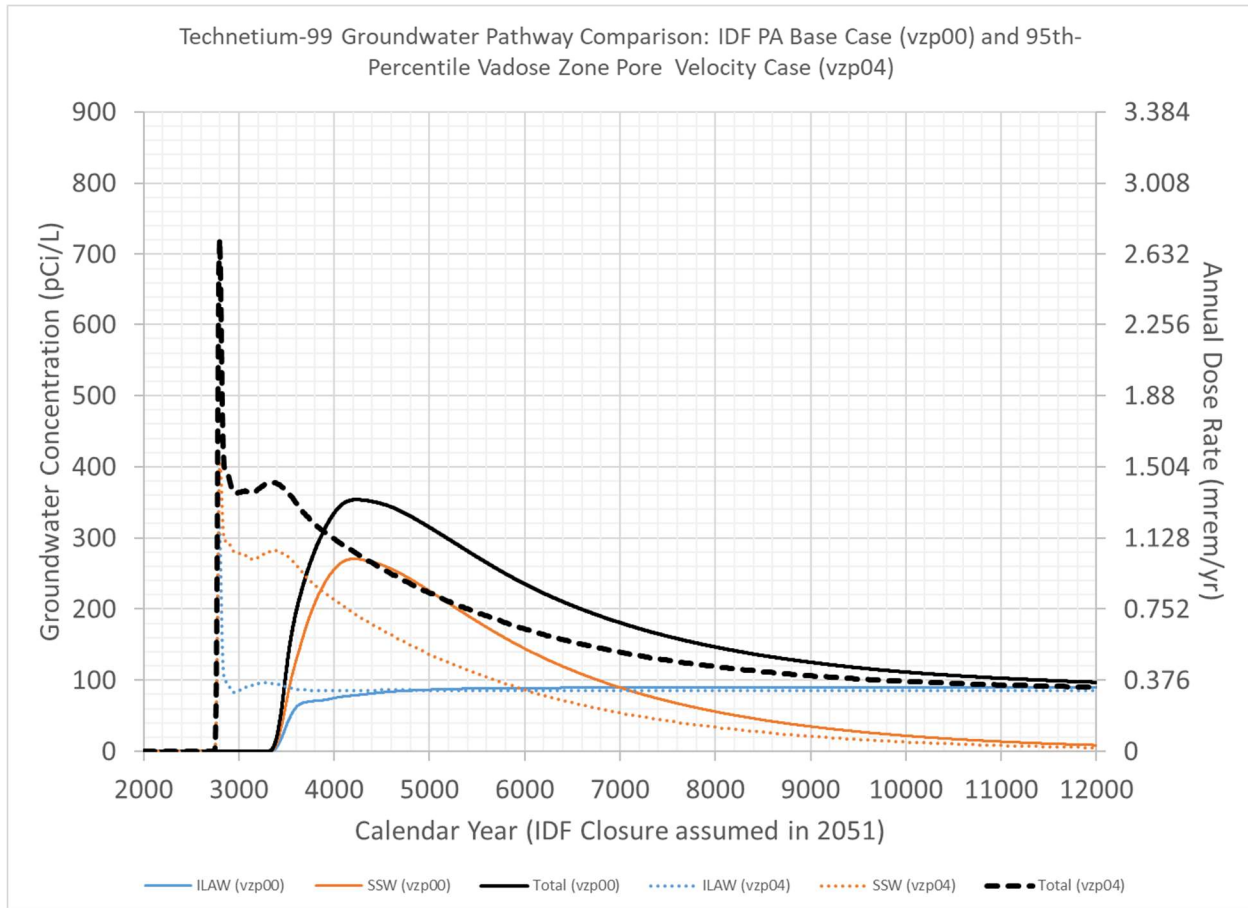


PA = Performance Assessment

Note: Time is in calendar year, the Integrated Disposal Facility (IDF) is assumed to be closed in calendar year 2051. Assumes base case distributed flow recharge rate of 3.5 mm/yr (case Infd06) and base case immobilized low-activity waste (ILAW) and solid secondary waste (SSW) release rate of RPP-RPT-59958, *Performance Assessment for the Integrated Disposal Facility, Hanford Site, Washington*. The Tc-99 release rate to the water table for this vadose zone property set (Vzp14) is illustrated in Figure 5-147 of RPP-RPT-59958. The total for vzp00 includes a small contribution from Effluent Treatment Facility liquid secondary waste (see RPP-RPT-59958 Figure 5-99), the total for VZP14 does not. The dose is converted from the groundwater concentration to a dose using the All-Pathways Groundwater Dose conversion factor value of 3.76E-03 mrem/yr per pCi/L.

Moisture contents observed in H2 sand sediment samples taken from boreholes drilled near the IDF, including new wells installed in FY 2019, have been reviewed to determine that an average value of 0.032 is representative of undisturbed surface conditions near the IDF while a value of 0.052 is representative of disturbed surface conditions near the IDF. These values are within the range of values predicted with the uncertain vadose zone hydraulic property sets used in the IDF PA, which provides confidence in the range of results presented in the IDF PA.

Figure 2-15-13. Technetium-99 Breakthrough Curves for Cases Vzp00 and Vzp04 at Location of Peak Impact along the 100-meter Buffer Boundary for Release from Immobilized Low-Activity Waste Glass and Solid Secondary Waste.



PA = Performance Assessment

Note: Time is in calendar year, the Integrated Disposal Facility (IDF) is assumed to be closed in calendar year 2051. Assumes base case distributed flow recharge rate of 3.5 mm/yr (case Infd06) and base case immobilized low-activity waste (ILAW) and solid secondary waste (SSW) release rate of RPP-RPT-59958, *Performance Assessment for the Integrated Disposal Facility, Hanford Site, Washington*. The Tc-99 release rate to the water table for this vadose zone property set (Vzp04) is illustrated in Figure 5-147 of RPP-RPT-59958. The total for vzp00 includes a small contribution from Effluent Treatment Facility liquid secondary waste (see RPP-RPT-59958 Figure 5-99), the total for VZP04 does not. The dose is converted from the groundwater concentration to a dose using the All-Pathways Groundwater Dose conversion factor value of 3.76E-03 mrem/yr per pCi/L.

Using representative vadose zone hydraulic property set cases that reproduce the observed moisture contents for disturbed and undisturbed surface conditions illustrates that the peak groundwater concentrations for risk-significant radionuclides (i.e., ^{99}Tc and ^{129}I) do not exceed groundwater protection standards or DOE's dose limit performance objectives for the All-Pathways scenario. However, the timing of the peak groundwater concentration is earlier than predicted with the base case vadose zone property set used in the IDF PA. Continued maintenance activities to confirm the observed moisture content and to develop better estimates of undisturbed infiltration rates remain as important activities within the IDF maintenance program.

Table 2-15-5. Comparison of Peak Groundwater Concentration for Base Case (Vzp00) and Alternative Vadose Zone Hydraulic Property Set (Vzp04 and Vzp14).

Radionuclide	Waste Source	Peak Concentration (pCi/L)			Time of Peak Concentration (Calendar Year)		
		Case Vzp00	Case Vzp14	Case Vzp04	Case Vzp00	Case Vzp14	Case Vzp04
Tc-99	SSW	270	322	408	4208	3346	2801
	ILAW	90	95	321	7663	3073	2794
	SSW+ILAW	350	415	721	4224	3336	2797
I-129	SSW	0.980	0.952	1.021	7727	6362	3561
	ILAW	0.053	0.054	0.089	>12051	12036	3421
	SSW+ILAW	1.0	0.998	1.082	7809	6403	3526

ILAW = immobilized low-activity waste

SSW = solid secondary waste

Note: Peak concentrations rounded to nearest pCi/L for Tc-99 and 0.001 pCi/L for I-129. Case Vzp00 represents the base case presented in RPP-RPT-59958, *Performance Assessment for the Integrated Disposal Facility, Hanford Site, Washington*, Table 5-43 and illustrated in Figures 5-98 and 5-99 of RPP-RPT-59958. Cases Vzp14 and Vzp04 represent the 95th percentile pore velocity cases developed for the low anisotropy and isotropic moisture dependent anisotropy, respectively.

Note: The *Safe Drinking Water Act of 1974* Maximum Concentration Levels yielding a drinking-water dose of 4 mrem/yr are 900 pCi/L for Tc-99 and 1.0 pCi/L for I-129. The peak drinking water dose may be calculated as the peak groundwater concentration times the unit concentration yielding 4 mrem/yr drinking water dose, i.e., 4.444E-04 mrem/yr per pCi/L of Tc-99 and 4 mrem/yr per pCi/L of I-129.

Note: The peak groundwater exposure pathway dose of the all-pathways dose may be calculated as the peak groundwater concentration times the base case unit concentration dose factors presented in Table 4-46 of RPP-RPT-59958, i.e., 3.76E-03 mrem/yr per pCi/L of Tc-99 and 0.690 mrem/yr per pCi/L of I-129.

References

- CHPRC-03348, 2019, *Performance Assessment Maintenance Plan for the Integrated Disposal Facility*, Rev. 1, INTERA, Inc./CH2M HILL Plateau Remediation Company, Richland, Washington.
- DOE, 2005, *Technical Guidance Document for Tank Closure Environmental Impact Statement Vadose Zone and Groundwater Revised Analyses*, Final Rev 0, U.S. Department of Energy, Richland, Washington.
- DOE/EIS-0391, 2012, *Final Tank Closure and Waste Management Environmental Impact Statement for the Hanford Site, Richland, Washington*, U.S. Department of Energy, Washington, D.C.
- ECF-HANFORD-15-0019, 2020, *Hanford Site-wide Natural Recharge Boundary Condition for Groundwater Models*, Rev. 2, INTERA, Inc., CH2M HILL Plateau Remediation Company, Richland, Washington.
- NAVD88, *North American Vertical Datum of 1988*, National Geodetic Survey, U.S. Department of Commerce, National Oceanic and Atmospheric Administration, Silver Spring, Maryland.
- PNNL-11957, 1998, *Immobilized Low-Activity Waste Site Borehole 299-E17-21*, Pacific Northwest National Laboratories, Richland, Washington. Available at: <https://www.osti.gov/servlets/purl/665973>.
- PNNL-13033, 1999, *Recharge Data Package for the Immobilized Low-Activity Waste 2001 Performance Assessment*, Pacific Northwest National Laboratories, Richland, Washington. Available at: https://www.pnnl.gov/main/publications/external/technical_reports/13033.pdf
- PNNL-14289, 2003, *Geochemistry of Samples from Borehole C3177 (299-E24-21)*, Pacific Northwest National Laboratories, Richland, Washington. Available at: https://www.pnnl.gov/main/publications/external/technical_reports/PNNL-14289.pdf.
- PNNL-14702, 2006, *Vadose Zone Hydrogeology Data Package for Hanford Assessments*, Rev. 1, Pacific Northwest Laboratory, Richland, Washington. Available at: https://www.pnnl.gov/main/publications/external/technical_reports/PNNL-14702rev1.pdf.
- PNNL-14744, 2004, *Recharge Data Package for the 2005 Integrated Disposal Facility Performance Assessment*, Pacific Northwest National Laboratories, Richland, Washington. Available at: https://www.pnnl.gov/main/publications/external/technical_reports/PNNL-14744.pdf.

PNNL-15443, 2006, *Vadose Zone Transport Field Study Summary Report*, Pacific Northwest National Laboratories, Richland, Washington. Available at: https://www.pnnl.gov/main/publications/external/technical_reports/PNNL-15443.pdf.

PNNL-16688, 2007, *Recharge Data Package for Hanford Single-Shell Tank Waste Management Areas*, Pacific Northwest National Laboratories, Richland, Washington. Available at: https://www.pnnl.gov/main/publications/external/technical_reports/PNNL-16688.pdf.

PNNL-23711, 2015, *Physical, Hydraulic, and Transport Properties of Sediments and Engineered Materials Associated with Hanford Immobilized Low-Activity Waste*, RPT-IGTP-004, Rev. 0, Pacific Northwest National Laboratories, Richland, Washington. Available at: https://www.pnnl.gov/main/publications/external/technical_reports/PNNL-23711.pdf.

RPP-20621, 2004, *Far-Field Hydrology Data Package for the Integrated Disposal Facility Performance Assessment*, Rev. 0, CH2M HILL Hanford Group, Inc., Richland, Washington.

RPP-CALC-61032, 2018, *Vadose Zone and Saturated Zone Flow and Transport Calculations for the Integrated Disposal Facility Performance Assessment*, Rev. 0A, prepared by INTERA Inc. for Washington River Protection Solutions, LLC, Richland, Washington.

RPP-ENV-58782, 2016, *Performance Assessment of Waste Management Area C, Hanford Site, Washington*, INTERA, Inc./CH2M HILL Plateau Remediation Company/Ramboll Environ, Inc./Washington River Protection Solutions, LLC/TecGeo, Inc., Richland, Washington.

RPP-RPT-59958, 2019, *Performance Assessment for the Integrated Disposal Facility, Hanford Site, Washington*, Rev. 1A, Washington River Protection Solutions, LLC, Richland, Washington.

Safe Drinking Water Act of 1974, 42 USC 300, et seq.

SGW-63813, 2019, *Borehole Summary Report for the Installation of Six M-24 Wells in the 200-PO-1, 200-UP-1 and 300-FF-5 Operable Units, FY2019*, CH2M HILL Plateau Remediation Company, Richland, Washington. Available at: <https://pdw.hanford.gov/document/AR-03916>.

WCH-520, 2013, *Performance Assessment for the Environmental Restoration Disposal Facility, Hanford Site, Washington*, Rev. 1, Washington Closure Hanford, Richland, Washington. Available at: <https://pdw.hanford.gov/document/0083701>.

RAI 2-16 (Saturated Zone Hydraulic Conductivity)

Comment

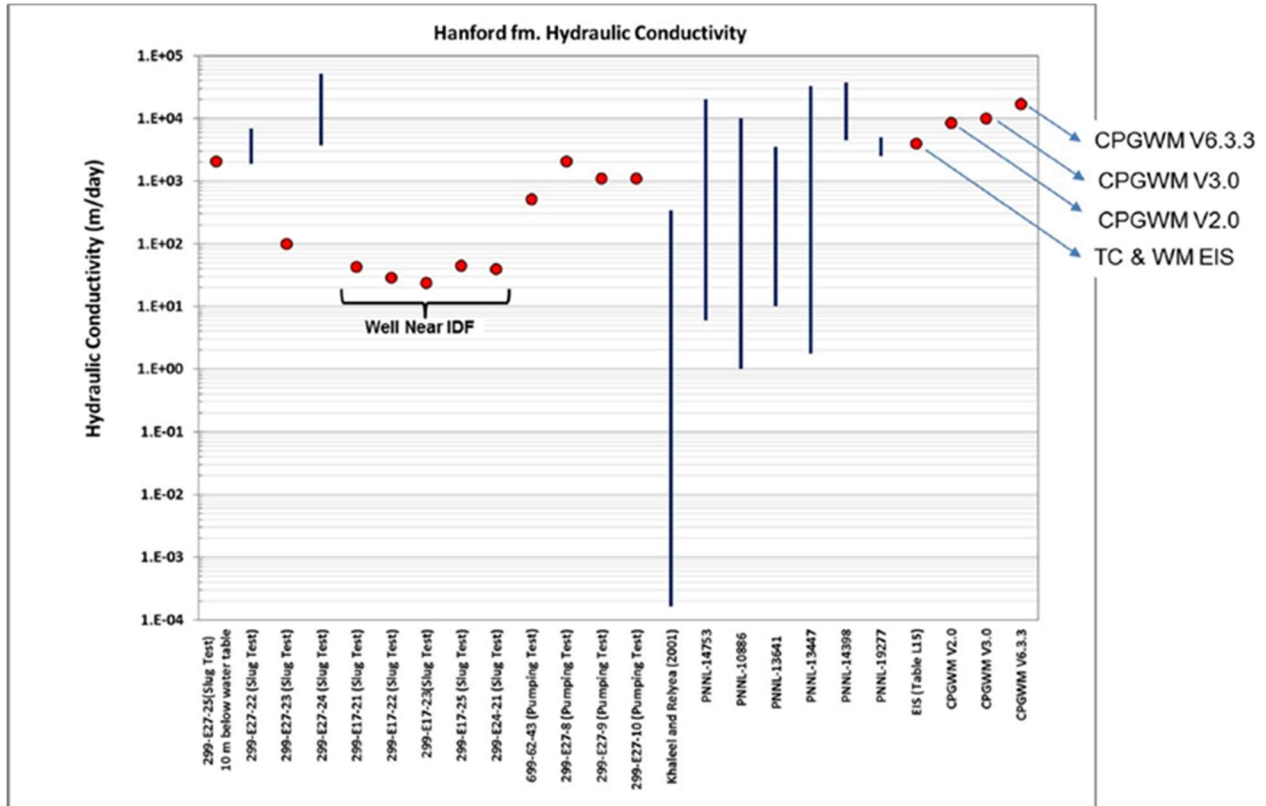
The changes to the estimated hydraulic conductivity values for the saturated zone over time suggest the base case value best estimate may not be reliable.

Basis

The saturated zone hydraulic conductivity, or rather the product of the saturated zone hydraulic conductivity and the gradient, is a key factor with respect to the reduction of risk at the Hanford site. Flux rates of water through the unsaturated zone are relatively low whereas the flow rate of water through the saturated zone are comparably high. This creates a large dilution effect on contaminant fluxes thereby reducing risk to an offsite receptor. DOE has investigated the saturated hydraulic conductivity over numerous decades and produced the very detailed figure (Figure 4-94 in the PA document) shown below. The figure highlights two important features.

First, that the local values can deviate significantly from the global values and secondly, that the estimated values have been highly volatile over time. Since completion of the TC & WM EIS the values have increased almost an order of magnitude. While the specific discharge values may have increased by a lessor amount than estimates of the saturated zone hydraulic conductivity, it isn't apparent why the base case value is thought to be reliable and unlikely to change given the past changes as more data has been collected and additional modeling has been completed.

Figure 2-16-1. Hanford Formation Hydraulic Conductivity Based on Slug Tests, Pumping Tests, and Groundwater Flow Models.



Source: Figure 4-94 of RPP-RPT-59958, *Performance Assessment for the Integrated Disposal Facility, Hanford Site, Washington*.

Path Forward

Please discuss confidence building activities to support the base case saturated zone hydraulic conductivity values assigned. Please discuss plans to verify the base case saturated zone hydraulic conductivity.

DOE Response

DOE acknowledges that there is uncertainty in the hydraulic conductivity of the aquifer sediments underneath the IDF and included an evaluation of this uncertainty in the IDF PA uncertainty analysis. The uncertainty analysis demonstrated that the impact to the environment and dose consequences to a member of the public in the future are very sensitive to the applied value of the aquifer hydraulic conductivity (or Darcy velocity).

The base case hydraulic conductivities of the saturated sediments beneath and downgradient of the IDF are based on the calibrated groundwater models of the Central Plateau. The model basis was the most current available Central Plateau Groundwater Model (CPGWM Version 6.3.3, CP-47631, *Model Package Report: Central Plateau Groundwater Model, Version 6.3.3, Rev. 2*), at the time the IDF-specific groundwater flow model was developed for the IDF PA. The

best-estimate hydraulic conductivity of the gravels of the Hanford formation from CPGWM Version 6.3.3 is 17,000 m/day. This value has evolved with time. This evolution is based on field measurements and model calibrations that are based on additional hydraulic testing information as well as enhancements in the model calibration approach. That evolution is not related to the reliability of the model result, but instead represents the natural evolution of the understanding of the groundwater flow regime in the saturated zone in the 200 East Area of the Central Plateau of the Hanford Site as the area is characterized during ongoing remediation activities related to groundwater operable unit 200-PO-1.

As noted in the RAI basis and the IDF PA, the hydraulic conductivity as well as the related specific discharge in the groundwater regime beneath the IDF are key factors in reducing the groundwater concentration of any radionuclides released from the facility and transported through the vadose zone. As a result, the uncertainty in the groundwater flow regime was identified as a highly significant assumption in Table 8-6 and Section 8.4.3 of the IDF PA (RPP-RPT-59958, *Performance Assessment for the Integrated Disposal Facility, Hanford Site, Washington*) and potential monitoring approaches that could be used to confirm the base case values were recommended in Table 8-8 of RPP-RPT-59958.

This RAI response first summarizes the results of the two CPGWMs that were used to define the base case saturated zone hydraulic conductivity and hydraulic gradient. The response then addresses the confidence-building activities that were planned as part of the IDF PA maintenance plan to verify the base case groundwater flow characteristics. Finally, the response concludes with a summary of the most recent information available based on the maintenance activities conducted since the completion of the IDF PA models and calculations.

Summary of Groundwater Flow Model Results used in the IDF PA (RPP-RPT-59958)

Two groundwater flow models of the 200 East Area of the Central Plateau, which encompass the area upgradient and downgradient of the IDF, were available at the time of the development of the IDF PA saturated zone model and associated calculations (RPP-RPT-59344, *Integrated Disposal Facility Model Package Report: Vadose and Saturated Zone Flow and Transport* and RPP-CALC-61032, *Vadose Zone and Saturated Zone Flow and Transport Calculations for the Integrated Disposal Facility Performance Assessment*, respectively). The available groundwater flow models were the TC&WM EIS groundwater flow model (Appendix L of DOE/EIS-0391, *Final Tank Closure and Waste Management Environmental Impact Statement for the Hanford Site, Richland, Washington*) and the CPGWM Version 6.3.3 (CP-47631, Rev. 2). The results of these two flow models were compared in RPP-CALC-61016, *Saturated Zone Flow – Sensitivity Analyses Using the 3-D EIS Groundwater Flow Model and the Central Plateau Groundwater Flow Model in the Vicinity of the Integrated Disposal Facility* and presented as Figures 4-76, 4-77, 4-92 and 4-93 in RPP-RPT-59958.

The groundwater model comparisons illustrate several relevant aspects of the groundwater flow regime near the IDF, as follows.

- Both groundwater flow models include a high-hydraulic conductivity zone that runs from northwest to southeast through the central part of the 200 East Area and is under the IDF footprint. Both models ascribe this high-hydraulic conductivity zone to the presence of a

paleochannel of an ancestral Columbia River at the time of the deposition of the Hanford and Cold Creek units.

- Both groundwater flow models predict low hydraulic gradients within the high-hydraulic conductivity zone.
- The base case calibrated hydraulic conductivity of the high-hydraulic conductivity zone in the TC&WM EIS was 3,973 m/day and in the CPGWM Version 6.3.3 was 17,000 m/day.
- The specific discharge in the high-hydraulic conductivity zone for both calibrated groundwater flow models is about 0.3 m/day, which was used as the base case specific discharge in the saturated zone in the IDF PA.

As concluded in the IDF PA, the similarity in the predicted specific discharge between the two groundwater flow models provided confidence that the base case value used for the IDF PA was reasonable and representative of the groundwater flow beneath the IDF. Uncertainty in the saturated zone flow velocity along the flow path generating the highest groundwater concentrations at the 100-m boundary was evaluated to account for the differences in the hydraulic conductivity values used in the TC&WM EIS and in CPGWM Version 6.3.3 flow models.

Summary of Planned Maintenance Activities to Verify the Groundwater Flow Model Results
Confidence-building activities to support the assumed base case hydraulic conductivity and specific discharge used in the IDF PA were identified in the IDF PA Maintenance Plan (CHPRC-03348). These activities were identified to confirm the base case values used in the IDF PA (RPP-RPT-59958).

As summarized in CHPRC-03348 Section 4.7, the planned maintenance activities include:

- Evaluate saturated zone flow models and parameter values developed for use in other Central Plateau remediation or related activities
- Evaluate assumptions and analyses used in the Hanford Site Composite Analysis (CA) and other planned and ongoing PAs (including the WMA A-AX PA)
- Evaluate saturated zone flow properties and hydrostratigraphy at the IDF.

The description of each of these activities presented in Section 4.7 of CHPRC-03348 consists of the following.

“The Hanford Site is an area of ongoing characterization and modeling of the groundwater flow domain in the Central Plateau area. These groundwater investigations and models could extend and include the 200 East Area and other areas around the IDF. These studies are expected to be of relevance to IDF, specifically with respect to analyses of the present trends in the water table

surface in the 200 East Area as well as the hydraulic conductivity of the Hanford formation. Although the IDF groundwater flow model uses a projected groundwater flow field after the end of Hanford Site operations (calendar year 2200), understanding the transient behavior of the groundwater flow system near the IDF supports the development of the groundwater flow rates used in the IDF PA.”

“The Hanford Site CA is expected to be completed in 2019 after which it will be reviewed by the LFRG. Until the DOE O 435.1 compliant CA is complete, the TC&WM EIS (DOE/EIS-0391, Section 6.0 and Appendix U) serves as the Hanford site-wide assessment of cumulative impacts. These impacts include impacts from sources immediately upgradient of the IDF, notably the US Ecology site and the BC cribs and trenches. Analyses of COPCs released from these facilities significantly affects the forecast concentration of technetium-99 and iodine-129 beneath the IDF; therefore, these results should be evaluated to determine their impact on the IDF PA monitoring program.”

“The magnitude of dilution for COPCs which reach the saturated zone beneath the IDF is dependent on the hydraulic properties and hydraulic gradient of the hydrostratigraphic units beneath the IDF. While the current site characterization indicates that the present-day and long-term average water table is in the Hanford formation beneath the IDF, this unit is mapped as thinning to the east and south of the IDF and the contact with the Ringold Formation member of Wooded Island – unit E is uncertain. In addition, the single-hole slug tests conducted in the observation wells near the IDF provide only a minimum estimate of the hydraulic properties of the Hanford formation in the small volume stressed around the test wells and are not believed representative of the average hydraulic properties of the Hanford formation at the IDF. Although the properties and extent of the Hanford formation do not affect the PA results during the 1,000-year compliance period, they significantly affect the concentrations in the 1,000-year to 10,000-year sensitivity analysis period. Therefore, opportunities will be explored to conduct larger scale pump tests in the Hanford formation near the IDF.”

Summary of Current Groundwater Flow Models and Results

The following section summarizes the recent groundwater flow modeling and related activities conducted since the PA model was completed that are related to confirming the base case hydraulic conductivity values used in the IDF PA.

Confidence-building activities to verify the representativeness of the hydraulic conductivity of the saturated sediments beneath the IDF used in modeling groundwater flow include pumping tests conducted in 2015, the calibration of hydraulic conductivity parameters in the groundwater models using a tritium plume, and a drawdown test performed on two wells near the IDF.

Pumping Tests at 299-E33-268:

Although no additional site-specific information on the hydraulic conductivity of the saturated sediments near IDF has been collected, constant-rate pumping tests have been performed as part

of the 200-BP-5 treatability test in the Hanford/Cold Creek gravels in borehole 299-E33-268. This well is located about 2 km north of the IDF and is part of the same high conductivity zone that runs under the IDF⁵³. Two constant rate tests were performed by pumping from 299-E33-268 over a 3-day period and a 27-day period and observing the water level response at nearby wells 299-E33-31 (9 m away), 299-E33-267 (4.5 m away), and 299-E33-342 (130 m away). As summarized in Tables 3-3 and 3-4 of DOE/RL-2015-75, *Aquifer Treatability Test Report for the 200-BP-5 Groundwater Operable Unit*, the hydraulic conductivity interpreted from the 3-day constant rate pumping test at 299-E33-268 ranged from 15,800 to 21,300 m/day with an average value of 18,800 m/day, while that from the 27-day constant rate pumping test at 299-E33-268 ranged from 15,100 to 21,100 m/day, with an average value of 18,200 m/day. These values support the base-case value of 17,000 m/day derived from the CPGWM Version 6.3.3. An additional pumping test is being planned to support field investigations for remediation of the groundwater operable units near the IDF.

Central Plateau Groundwater Model Updates:

The CPGWM has been updated multiple times since the IDF PA simulations were completed. The updates include the development of a successor groundwater flow model called the Plateau to River (P2R) model. The recent updates to these models include:

- July 2015 – CPGWM Version 6.3.3 (CP-47631, *Model Package Report: Central Plateau Groundwater Model Version 6.3.3, Rev. 2*) – used as the basis for the IDF PA
- July 2015 – P2R Version 7.1 (CP-57037, *Model Package Report: Plateau to River Groundwater Transport Model Version 7.1, Rev. 0*)
- November 2016 – CPGWM Version 8.3.4 (CP-47631, *Model Package Report Central Plateau Groundwater Model Version 8.3.4, Rev. 3*)
- January 2018 – CPGWM Version 8.4.5 (CP-47631, *Model Package Report: Central Plateau Groundwater Model, Version 8.4.5, Rev. 4*)
- May 2019 – P2R Version 8.2 (CP-57037, *Model Package Report: Plateau to River Groundwater Model Version 8.2, Rev. 1*)
- February 2020 – P2R Version 8.3 (CP-57037, *Model Package Report: Plateau to River Groundwater Model Version 8.3, Rev. 2*).

The modeling updates are summarized below with particular focus on the updates to the calibrated hydraulic conductivity in the suprabasalt sediments beneath the IDF.

Updates to CPGWM Version 6.3.3 (used for the IDF PA) were made in CPGWM Version 8.3.4 and CPGWM Version 8.4.5 completed in November 2016 and January 2018, respectively. The update in CPGWM Version 8.3.4 was relatively minor and the calibrated hydraulic conductivity

⁵³ The suprabasalt sediments in the boreholes near 299-E33-268 are characterized as being part of the Hanford/Cold Creek paleochannel. As noted in the response to RAI 2-14, it is difficult to distinguish between the gravels of the Hanford formation and the gravels of the Cold Creek Unit (CCUg).

of the Hanford channel deposits near the IDF was unchanged from the 17,000 m/day value developed in CPGWM Version 6.3.3. The update in CPGWM Version 8.4.5 was more significant; this update included a modification to the boundary between the Hanford highly conductive channel and the Hanford formation in the western part of the 200 East Area and the lateral extent of the Hanford channel in the southeastern part of the 200 East Area. The new boundary extended the highly conductive channel to be under the IDF, as illustrated in **Figure 2-16-2**. The revision to the location of the Hanford channel in the southeastern part of the 200 East Area effectively replaced the Hanford formation and Rwie gravels near the IDF with Hanford channel deposits⁵⁴. The calibrated hydraulic conductivity for the Hanford channel deposits near the IDF was reduced to 15,000 m/day (CP-47631, Rev. 4 Table 4-4).

A successor groundwater flow model to the CPGWM was developed by expanding the extent of the model to the Columbia River. This model is called the Plateau to River (P2R) groundwater flow model. The initial version of this model (P2R Version 7.1, July 2015) was developed concurrently with CPGWM Version 6.3.3 and is documented in CP-57037, Rev. 0. Because the initial version was based on the calibration of the CPGWM Version 6.3.3, it had the same calibrated hydraulic conductivity of the Hanford channel sediments of 17,000 m/day.

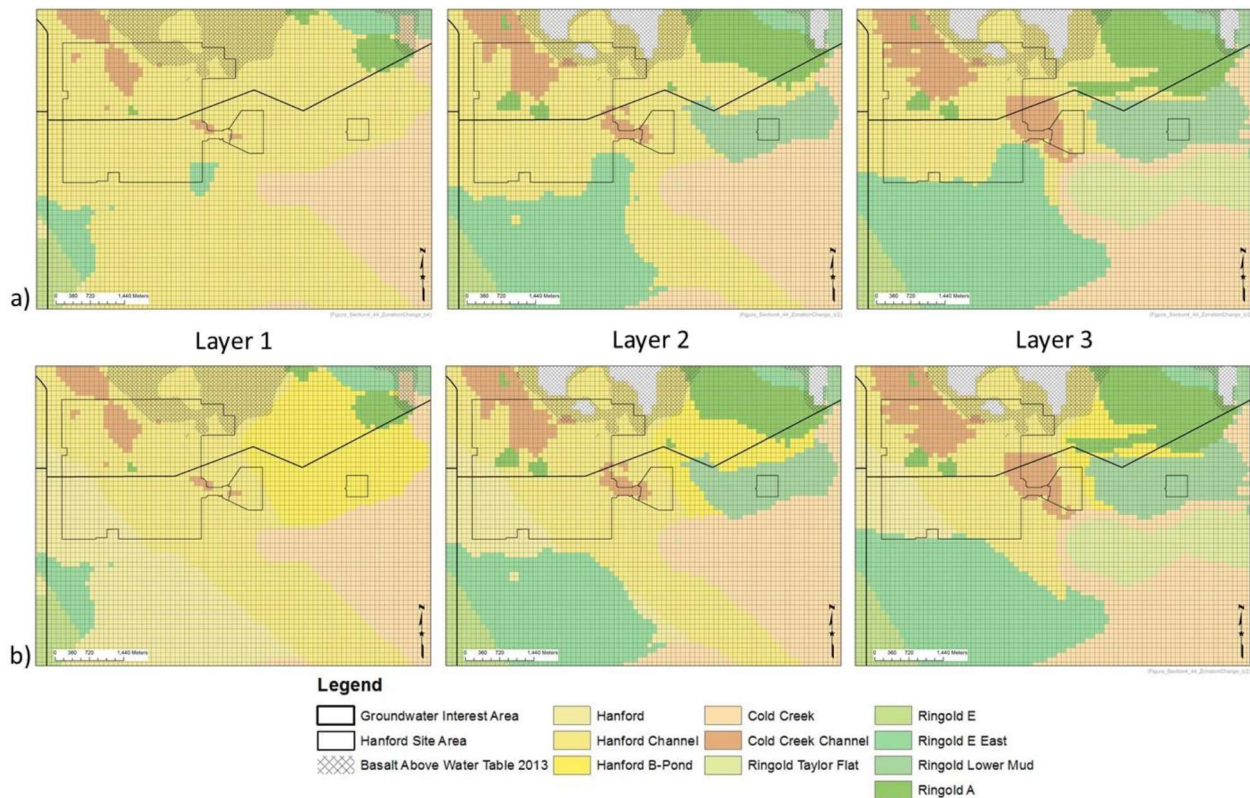
Consistent with the changes made to CPGWM Version 8.4.5, a revised version of the P2R model (Version 8.2, May 2019) was developed that changed the modeled extent of the Hanford channel from the representation in Version 7.1. Adjustments to the extent of Hanford channel sediments were made in the calibration of P2R Version 8.2 as illustrated in **Figure 2-16-3**. These adjustments were made during the calibration to the observed historic tritium plume within and downgradient of the 200 East Area.

The calibrated hydraulic conductivity of the Hanford channel deposits from the P2R Version 8.2 is illustrated in **Figure 2-16-4**. The hydraulic conductivity of the Hanford channel deposits near the IDF is ~15,000 m/day while downgradient of the IDF the calibrated hydraulic conductivity is between 20,000 and 25,000 m/day.

The most current model of groundwater flow in the Central Plateau is the P2R Version 8.3. The approach used to define the extent of the Hanford channel in P2R Version 8.3 differs significantly from the approach adopted in earlier groundwater flow models. In the earlier models, including the TC&WM EIS model, CPGWM Version 8.4.5 and P2R Version 8.2, the Hanford channel was treated as a fixed feature, called the high conductivity zone (HCZ). The extent of the Hanford channel for the various models is shown in **Figure 2-16-3**.

⁵⁴ In addition to presenting the updated calibrated hydraulic conductivity of the suprabasalt aquifer beneath the IDF from revisions to the groundwater flow models, it is appropriate to consider the relevant HSUs beneath and downgradient of the IDF. The identification of the relevant HSUs has evolved with revised interpretations and improved groundwater model calibrations over the past few years. As a result, this RAI is closely related to RAI 2-14 which addresses uncertainty in the presence of the Rwie and the contact between the Rwie and the overlying CCU gravels and the Hanford formation near the IDF. Since the completion of the models and calculations supporting the IDF PA, there have been updates to the GFMs and groundwater flow models that are relevant to address in the responses to RAIs 2-16 and 2-14. Updates to the groundwater flow models are discussed in this RAI response while updates to the GFMs are discussed in the response to RAI 2-14.

Figure 2-16-2. Adjustments to the Hanford Channel Zonation in Layers 1, 2 and 3 of the Central Plateau Groundwater Model Version 8.4.5 in the 200 East Area of the Central Plateau (a) Initial, (b) Modified in Central Plateau Groundwater Model Version 8.4.5.

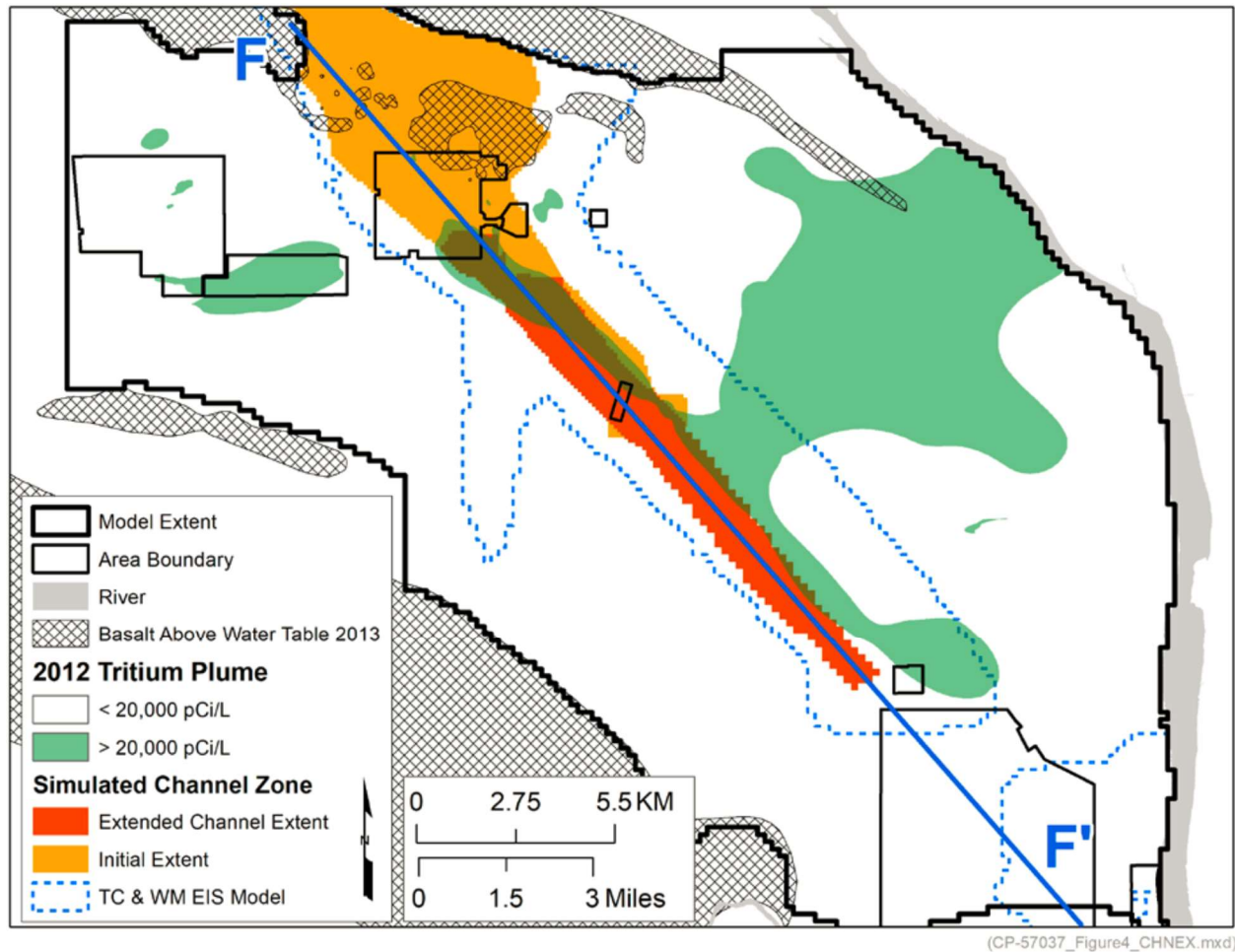


Source: CP-47631, *Model Package Report Central Plateau Groundwater Model Version 8.4.5*, Rev. 4, Figure 4-43.

Note: The initial hydrostratigraphic unit (HSU) zonation is based on a predecessor to the Hanford South geologic framework model (GFM) (ECF-HANFORD-13-0029, *Development of the Hanford South Geologic Framework Model, Hanford Site, Washington*, Rev. 2) and is the same as used in CPGWM Version 6.3.3 (CP-47631, *Model Package Report: Central Plateau Groundwater Model Version 6.3.3*). The modified HSU zonation used in CPGWM Version 8.4.5 (CP-47631, Rev. 4) replaced the Ringold E East in the southeast portion of the 200 East Area, including the area beneath the Integrated Disposal Facility, with the Hanford Channel HSU.

In P2R Version 8.3, the approach taken to calibrate the hydraulic conductivity in the Hanford channel deposits was to first identify an area of the model domain that may contain the Hanford channel, called the HCZ analysis area, and then let the calibration and parameter-estimation process identify the high-hydraulic conductivity within the HCZ analysis area that result in calibrated properties of the Hanford channel deposits to match historical water levels and an existing tritium plume. The location of the HCZ analysis area is illustrated in **Figure 2-16-5**. Within the HCZ analysis area, the four upper HSUs (i.e., the Hanford formation, CCU, Ringold Taylor Flats unit [Rtf], and Rwie) were treated as a single unit and divided into five separate layers in the model grid.

Figure 2-16-3. Location of the Hanford Channel Included Prior to and After Calibration of the Plateau to River (P2R) Groundwater Flow Model Version 8.2.



Source: CP-57037, *Model Package Report: Plateau to River Groundwater Model Version 8.2*, Rev. 1, Figure 4-29.

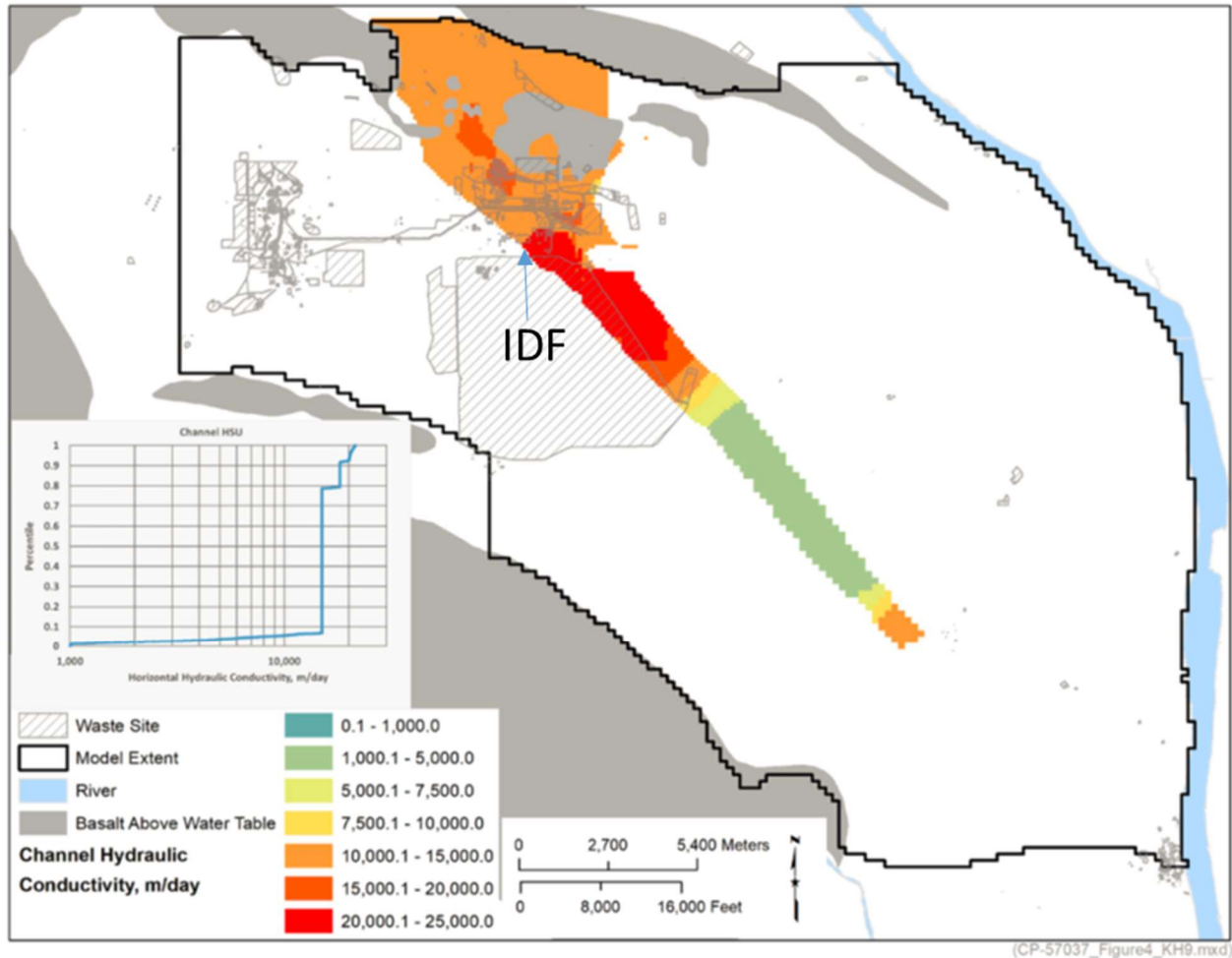
Note: The initial extent of the channel zone is the extent modeled in the CPGWM Version 8.4.5 (CP-47631, *Model Package Report: Central Plateau Groundwater Model, Version 8.4.5*, Rev. 4) and P2R Version 7.1 (CP-57037, *Model Package Report: Plateau to River Groundwater Transport Model Version 7.1*, Rev. 0). The extended channel extent is the result of calibrating the P2R Version 8.2 (CP-57037, Rev. 1) to the observed tritium plume. The extent of the channel zone modeled in the TC & WM EIS (DOE/EIS-0391, *Final Tank Closure and Waste Management Environmental Impact Statement for the Hanford Site, Richland, Washington*) is shown for comparison purposes.

The calibrated hydraulic conductivity of the high conductivity zone (comprised of the paleochannel deposits of the Hanford/Cold Creek unit as well as the Rtf and Rwie⁵⁵) in P2R

⁵⁵ Although there have been no hydraulic tests performed in wells in the southern 200 East Area, evaluation of well development data from monitoring wells drilled in the area indicate that the high-conductivity sediments are not restricted to the Hanford formation and CCU. WMP-27008, *Borehole Summary Report for Wells 299-24-24 (C4647) and 299-E17-26 (C4648), Integrated Disposal Facility*, provides a description of drawdown in wells screened in the Hanford formation and Rwie, respectively. In each case, WMP-27008 noted at least 20 minutes of pumping above 68.1 L/min (18 gal/min) and recorded no measurable drawdown. The hydraulic response of the well screened exclusively in the Rwie supports the results of the DOE/EIS-0391 and P2R Model Version 8.2 that assigned HCZ properties to locations that the Hanford South GFM (ECF-HANFORD-13-0029) assigns to the Rwie.

Version 8.3 are illustrated in **Figures 2-16-6 to 2-16-10** for layers 1 to 5 of the model domain. A transmissivity map illustrated in **Figure 2-16-11** also shows the location of the modeled HCZ.

Figure 2-16-4. Calibrated Hydraulic Conductivity of Hanford Channel – Plateau to River Groundwater Model Version 8.2.



Source: CP-57037, *Model Package Report: Plateau to River Groundwater Model Version 8.2*, Rev. 1, Figure 4-43.

Note: The Hanford channel extends beneath the Integrated Disposal Facility (IDF) footprint and has a calibrated hydraulic conductivity of between 15,000 and 25,000 m/day.

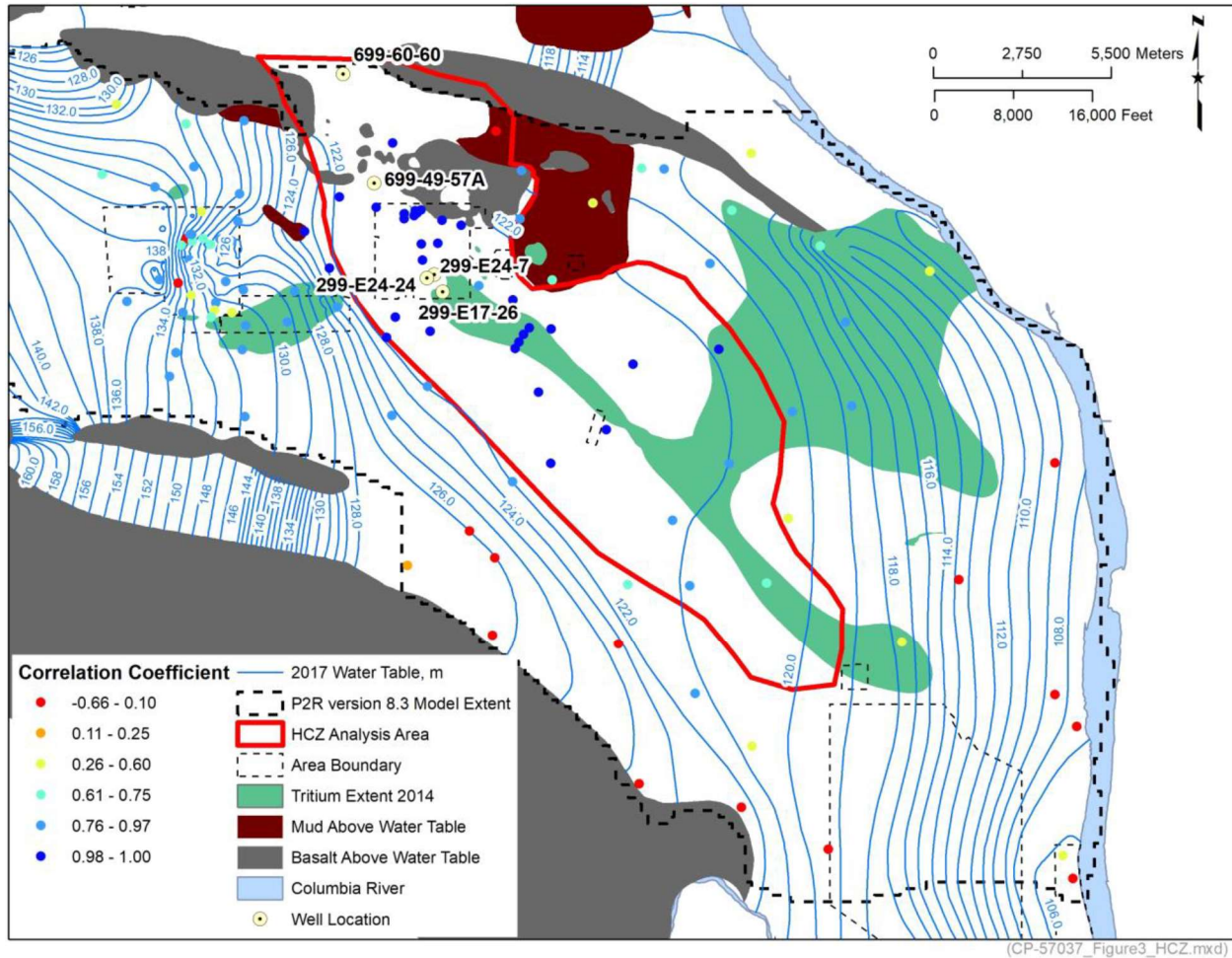
To provide a more detailed representation of the calibrated hydraulic conductivity of the Hanford channel deposits and the HCZ near the IDF, the results of the P2R Version 8.3 in the area near the IDF have been extracted from the model file and this information is presented alongside each regional scale figure.

Summary

As noted in the RAI, the lateral extent and hydraulic conductivity of the Hanford channel sediments beneath the IDF are an important component of the IDF PA, given the role of the saturated zone in diluting radionuclides that may be released from the engineered facility and transported to the water table. This importance was recognized in the IDF PA and resulted in

planned maintenance activity to confirm the base case values used in the IDF PA. The maintenance activities conducted to date have confirmed the hydraulic conductivity value used in the IDF PA base case. Continued maintenance activities will be performed in the future.

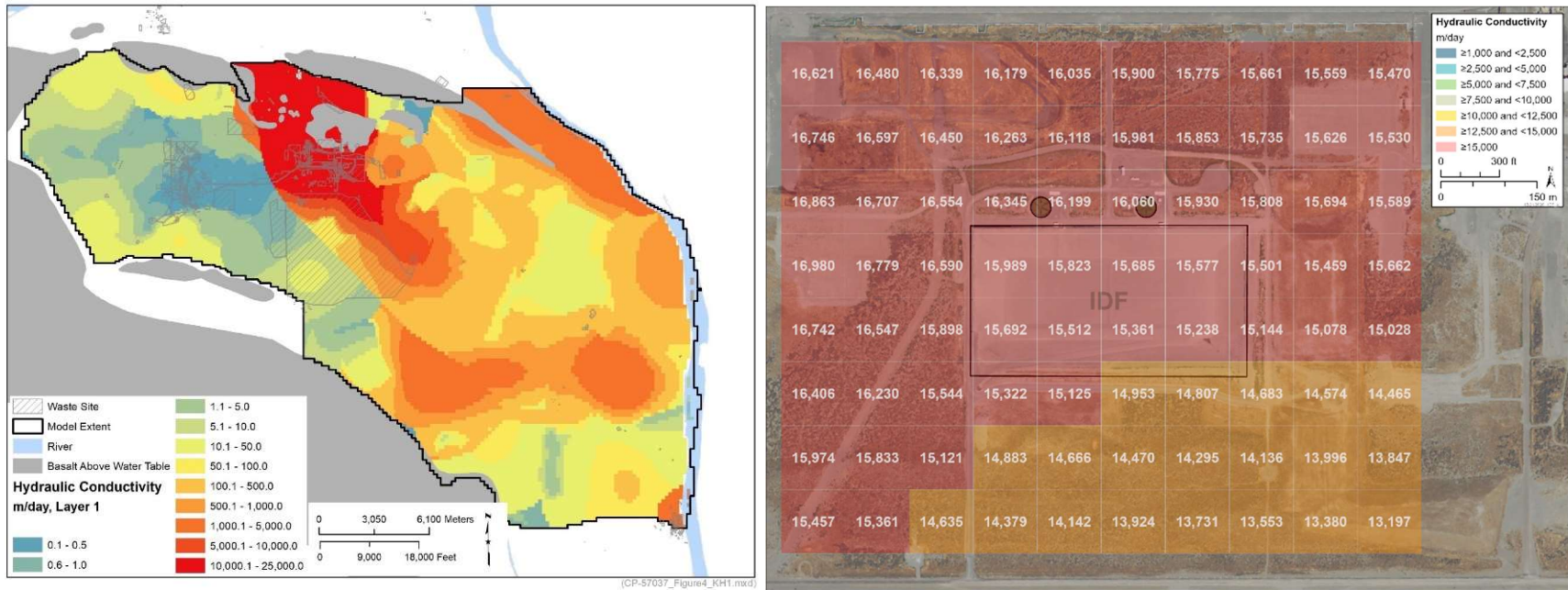
Figure 2-16-5. Location of the High Conductivity Zone Analysis Area used in the Plateau to River Version 8.3.



Source: CP-57037, *Model Package Report: Plateau to River Groundwater Model Version 8.3*, Rev. 2, Figure 3-9.

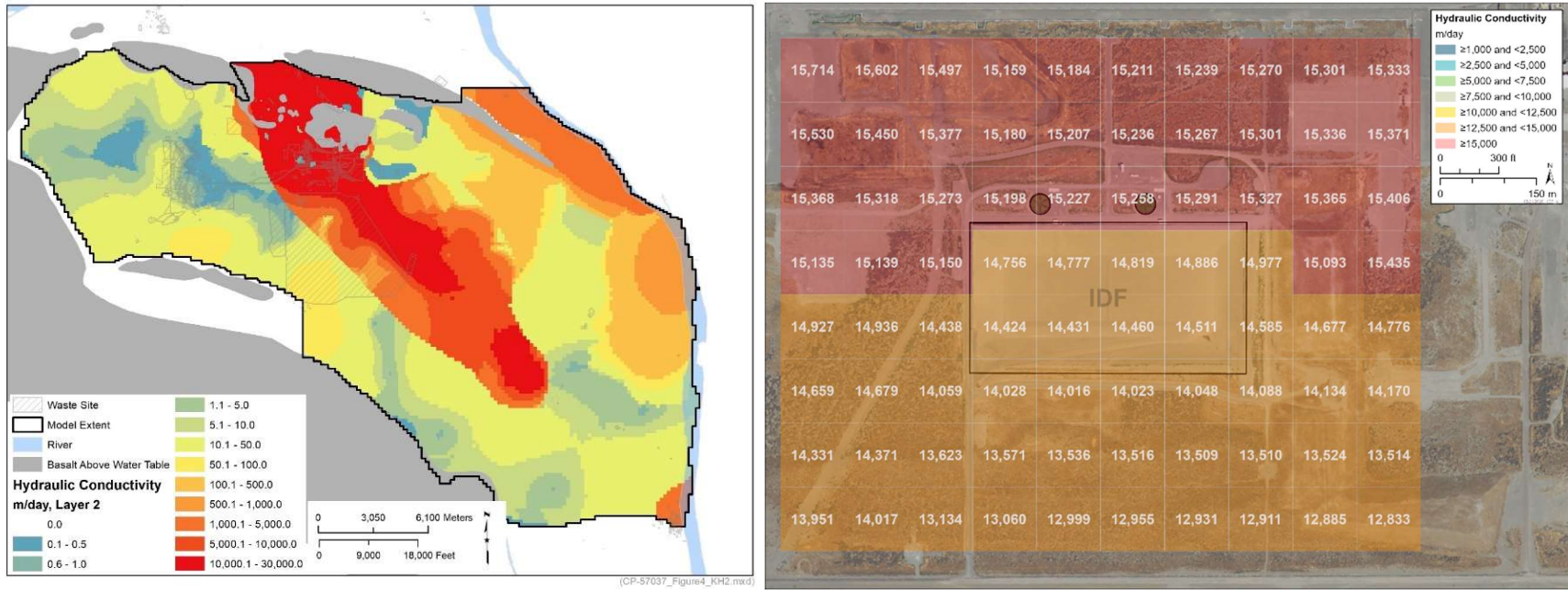
Note: The location of the high conductivity zone (HCZ) analysis area is based on wells that exhibit a similar water level response to anthropogenic water discharges. The HCZ analysis area defines an area that is expected to contain the HCZ; however, the HCZ extent is determined during the model calibration process and is illustrated by the calibrated hydraulic conductivity for Layers 1 to 5 of the Plateau to River (P2R) model in **Figures 2-16-6 to 2-16-10** as well as the calibrated transmissivity illustrated in **Figure 2-16-11**.

Figure 2-16-6. Calibrated Hydraulic Conductivity for Plateau to River Version 8.3 Model Layer 1.



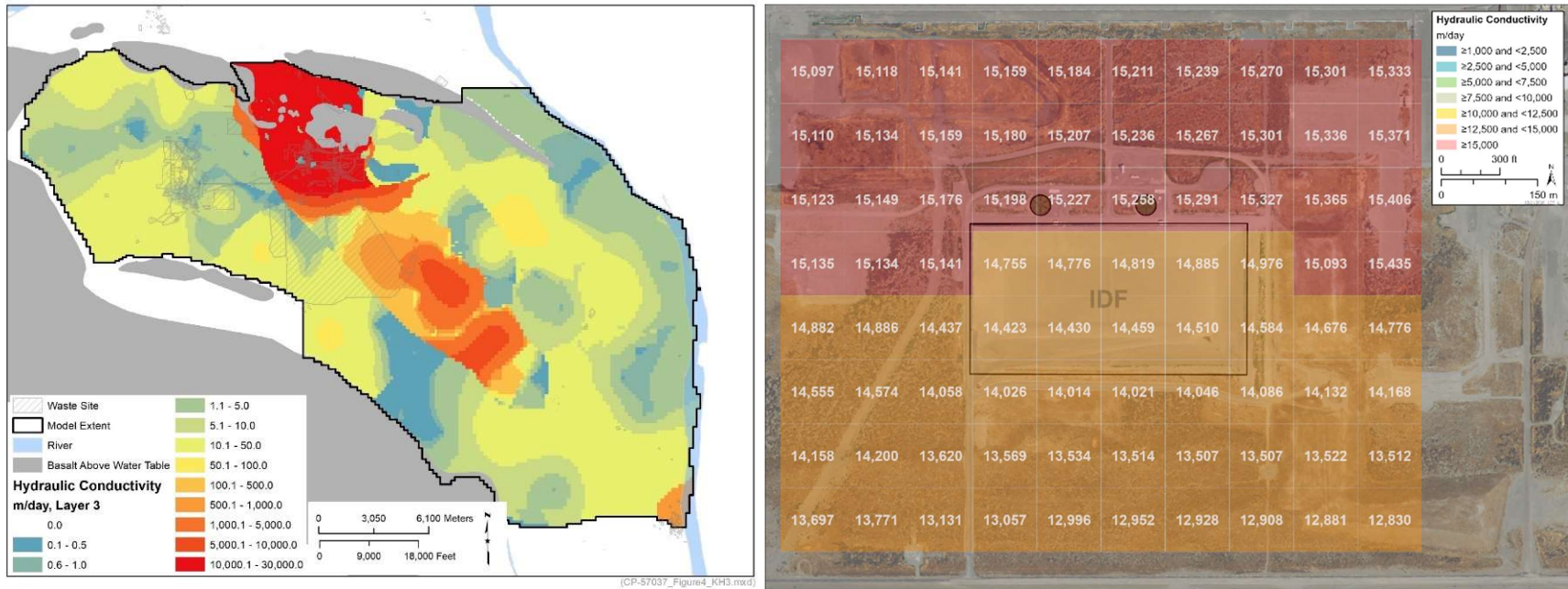
Source: CP-57037, Model Package Report: Plateau to River Groundwater Model Version 8.3, Rev. 2, Figure 4-36.

Figure 2-16-7. Calibrated Hydraulic Conductivity for Plateau to River Version 8.3 Model Layer 2.



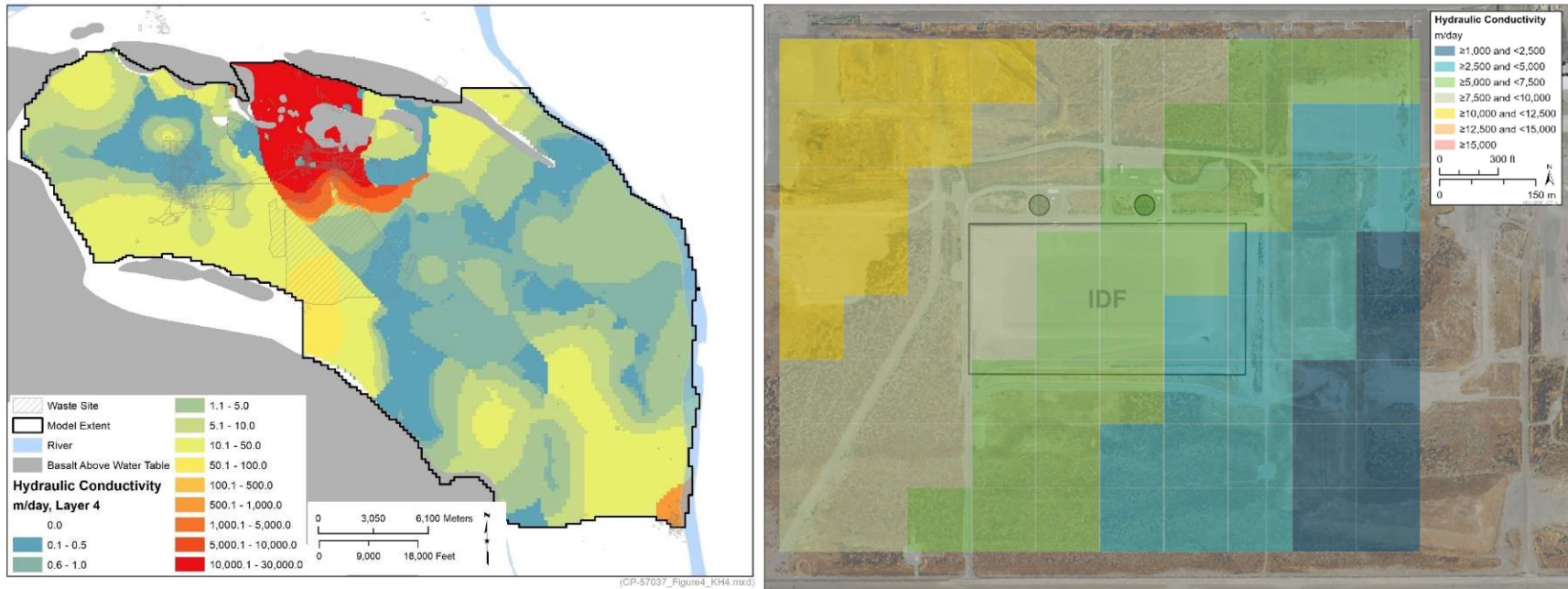
Source: CP-57037, Model Package Report: Plateau to River Groundwater Model Version 8.3, Rev. 2, Figure 4-37.

Figure 2-16-8. Calibrated Hydraulic Conductivity for Plateau to River Version 8.3 Model Layer 3.



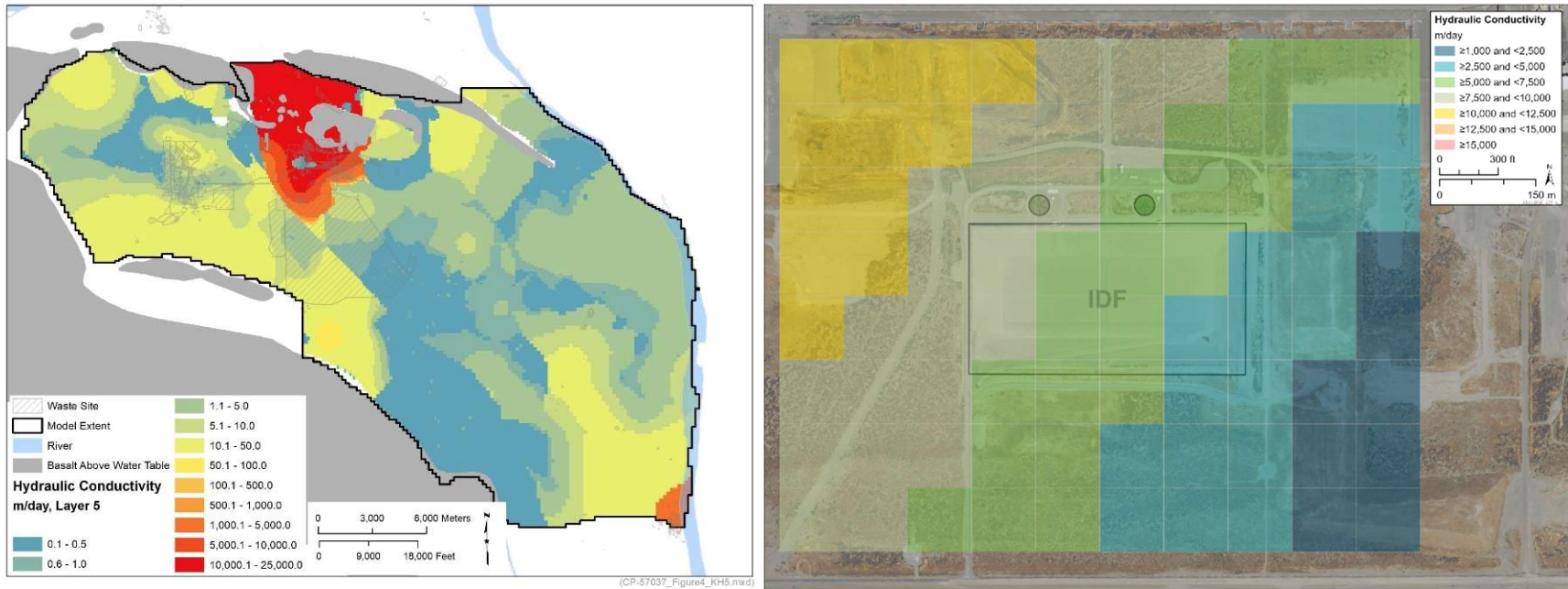
Source: CP-57037, Model Package Report: Plateau to River Groundwater Model Version 8.3, Rev. 2, Figure 4-38.

Figure 2-16-9. Calibrated Hydraulic Conductivity for Plateau to River Version 8.3 Model Layer 4.



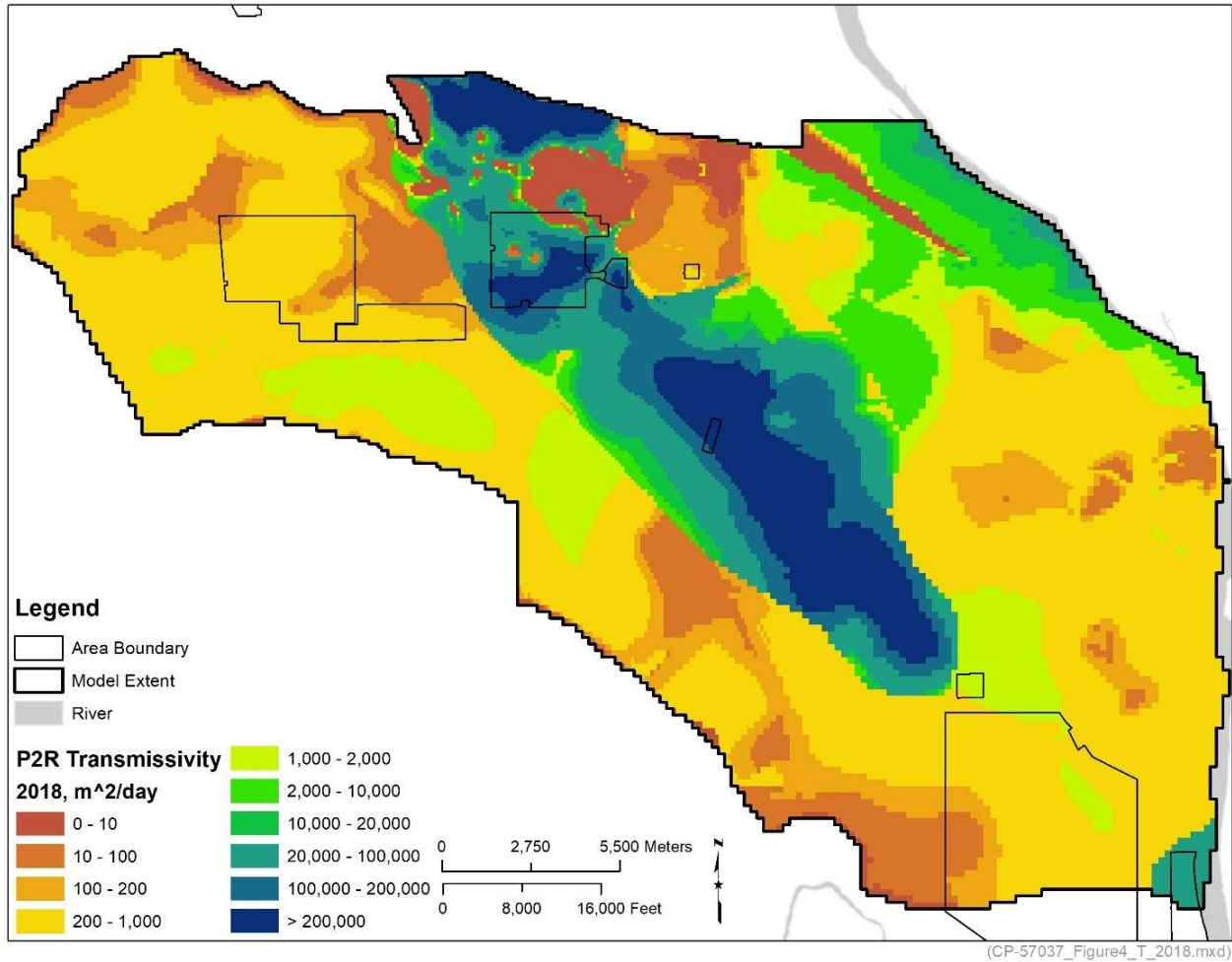
Source: CP-57037, Model Package Report: Plateau to River Groundwater Model Version 8.3, Rev. 2, Figure 4-39.

Figure 2-16-10. Calibrated Hydraulic Conductivity for Plateau to River Version 8.3 Model Layer 5.



Source: CP-57037, *Model Package Report: Plateau to River Groundwater Model Version 8.3*, Rev. 2, Figure 4-40.

Figure 2-16-11. Calibrated Transmissivity for Plateau to River Version 8.3.



Source: CP-57037, *Model Package Report: Plateau to River Groundwater Model Version 8.3*, Rev. 2, Figure 4-44.

Note: The upper surface of the suprabasalt aquifer is assumed to be the modeled 2018 water table surface. The area with transmissivity greater than 20,000 m²/day represents the high conductivity zone (HCZ). Near the Integrated Disposal Facility (in the southcentral part of the 200 East Area) the calibrated transmissivity is about 100,000 m²/day representing the HCZ of the Hanford channel in that area.

References

- CHPRC-03348, 2019, *Performance Assessment Maintenance Plan for the Integrated Disposal Facility*, Rev. 1, CH2M HILL Plateau Remediation Company, Richland, Washington.
- CP-47631, 2015, *Model Package Report: Central Plateau Groundwater Model Version 6.3.3*, Rev. 2, INTERA, Inc., Richland, Washington. Available at: <https://pdw.hanford.gov/document/0077133H>.
- CP-47631, 2017, *Model Package Report: Central Plateau Groundwater Model Version 8.3.4*, Rev. 3, INTERA, Inc./CH2M HILL Plateau Remediation Company, Richland, Washington. Available at: <https://pdw.hanford.gov/document/0069098H>.
- CP-47631, 2018, *Model Package Report: Central Plateau Groundwater Model, Version 8.4.5*, Rev. 4, CH2M HILL Plateau Remediation Company, Richland, Washington. Available at: <https://pdw.hanford.gov/document/0066449H>.
- CP-57037, 2015, *Model Package Report: Plateau to River Groundwater Transport Model Version 7.1*, Rev. 0, CH2M HILL Plateau Remediation Company, Richland, Washington. Available at: <https://pdw.hanford.gov/document/0080149H>.
- CP-57037, 2019, *Model Package Report: Plateau to River Groundwater Model Version 8.2*, Rev. 1, CH2M HILL Plateau Remediation Company, Richland, Washington. Available at: <https://pdw.hanford.gov/document/AR-01336>.
- CP-57037, 2020, *Model Package Report: Plateau to River Groundwater Model Version 8.3*, Rev. 2, CH2M HILL Plateau Remediation Company, Richland, Washington. Available at: <https://pdw.hanford.gov/document/AR-03674>.
- DOE/EIS-0391, 2012, *Final Tank Closure and Waste Management Environmental Impact Statement for the Hanford Site, Richland, Washington*, U.S. Department of Energy, Washington, D.C.
- DOE O 435.1, 2011, *Radioactive Waste Management, Change 2*, U.S. Department of Energy, Washington, D.C.
- DOE/RL-2015-75, 2016, *Aquifer Treatability Test Report for the 200-BP-5 Groundwater Operable Unit*, Rev. 0, U.S. Department of Energy, Richland Operations Office, Richland, Washington. Available at: <https://pdw.hanford.gov/document/0074649H>.
- ECF-HANFORD-13-0029, 2015, *Development of the Hanford South Geologic Framework Model, Hanford Site, Washington*, Rev. 2, prepared by INTERA, Inc. for CH2M HILL Plateau Remediation Company, Richland, Washington. Available at: <https://pdw.hanford.gov/document/0072751H>.

- RPP-CALC-61016, 2017, *Saturated Zone Flow – Sensitivity Analyses Using the 3-D EIS Groundwater Flow Model and the Central Plateau Groundwater Flow Model in the Vicinity of the Integrated Disposal Facility*, Rev. 0, INTERA, Inc. prepared for Washington River Protection Solutions, LLC, Richland, Washington.
- RPP-CALC-61032, 2018, *Vadose Zone and Saturated Zone Flow and Transport Calculations for the Integrated Disposal Facility Performance Assessment*, Rev. 0A, prepared by INTERA Inc. for Washington River Protection Solutions, LLC, Richland, Washington.
- RPP-RPT-59344, 2019, *Integrated Disposal Facility Model Package Report: Vadose and Saturated Zone Flow and Transport*, Rev. 0A, prepared by INTERA Inc. for Washington River Protection Solutions, LLC, Richland, Washington.
- RPP-RPT-59958, 2019, *Performance Assessment for the Integrated Disposal Facility, Hanford Site, Washington*, Rev. 01A, Washington River Protection Solutions, LLC, Richland, Washington.
- WMP-27008, 2005, *Borehole Summary Report for Wells 299-24-24 (C4647) and 299-E17-26 (C4648), Integrated Disposal Facility*, Fluor Hanford Company, Richland, Washington. Available at: <https://pdw.hanford.gov/document/DA01417799>

RAI 2-17 (Intruder)**Comment**

DOE provided the dose result to an inadvertent intruder resulting from the average waste but did not provide the range of potential intruder doses that could be anticipated. NRC provided a number of comments and recommendations associated with intruder analyses for WMA-C that DOE was not able to address in this draft WIR evaluation due to timing differences.

Basis

DOE communicated the dose to an inadvertent intruder resulting from unanticipated future intrusion into a particular waste type. However, DOE did not communicate the range of inadvertent intruder doses that could be anticipated for each waste stream.

The waste will be disposed in the IDF which is a near-surface disposal facility. However, the IDF is a “deep” near-surface disposal facility such that an excavation scenario is highly unlikely. The intruder scenario evaluated was a drilling scenario where the installation of a well to recover resources results in the extraction of geologic materials and some waste in the drill cuttings. The amount of waste potentially disturbed is much lower than what is expected in an excavation scenario. Whereas in the excavation scenario, the concentration of radionuclides in the disturbed waste may more closely approximate the average concentration, for a discrete event like drilling the concentration in the disturbed waste is likely to reflect the variability of radionuclide concentrations in the waste. The risk is a product of probability and consequence, and the probability goes down as drilling at locations of less likely concentrations occur (e.g., the most highly concentrated waste). NRC and most other regulators impose limits that reflect the average concentration of the waste but also impose requirements as to how much averaging can be used (e.g., the NRC’s Branch Technical Position on Concentration Averaging and Encapsulation (ML12254B065)).

NRC issued the technical evaluation report (TER) for review of the draft waste evaluation for WMA-C in May 2020 (ML20128J832). In that report, NRC provided recommendations and comments on the inadvertent intruder analyses. The inadvertent intruder analyses for VLAW used essentially an identical approach, but the VLAW analyses were completed prior to the NRC TER, and therefore, DOE could not address NRC comments. In addition, those comments were not risk-significant in the context of WMA-C but could be risk-significant with respect to the VLAW analyses.

Path Forward

Please provide the range of dose impacts to an inadvertent intruder from each waste stream disposed in the IDF that is within the scope of the draft waste evaluation as discussed previously in this document. The assessment should consider risk-significant comments made on the WMA-C intruder assessment, if applicable to the intruder assessment for VLAW.

DOE Response

The Draft WIR Evaluation addresses the WIR criteria for VLAW produced using the DFLAW approach. Other wastes are outside the scope of the Draft WIR Evaluation, including non-reprocessing secondary waste (see DOE response [Section 2.0]) and vitrified waste assumed

to potentially be produced by supplemental LAW treatment (for which DOE has made no decision to pursue).⁵⁶ To bound the analysis, the IDF PA correctly includes all wastes potentially disposed of in the IDF, including the DFLAW-produced VLAW as well as potential additional VLAW,⁵⁷ and all SSW which may be disposed at IDF. The approach to ensuring that all waste packages are acceptable for disposal at the IDF is described in this RAI response and is the same for all waste streams.

DOE's estimate of long-term consequences from the IDF are based on computer models for: 1) estimating radionuclide inventory in the waste and 2) calculating potential post-closure dose consequences to a member of the public in the future. DOE acknowledges that there will be variability in the DFLAW feed stream to the WTP LAW Vitrification Facility. Because of this variability, the vitrified LAW disposed of in the IDF is expected to have variable compositions.

DOE's hypothetical intruder analysis described in RPP-CALC-61254, *Inadvertent Intruder Dose Calculation Update for the Integrated Disposal Facility Performance Assessment* did not evaluate the variability in the radionuclide concentrations in the VLAW or secondary wastes. Instead, all waste in the IDF was simulated using an average concentration computed using the total inventory in a particular waste stream (e.g., VLAW, SSW, or solidified LSW) and the total as-disposed volume of that waste stream. The total as-disposed volume accounted for debris compaction and any solidification material necessary to encapsulate or stabilize the waste.⁵⁸ To address inventory uncertainty, DOE did evaluate alternative inventory scenarios to demonstrate that the dose to the hypothetical intruder from each radionuclide in the waste was proportional to the radionuclide inventory in the waste. Thus, inventory uncertainty would always be identified as a significant parameter in an importance analysis and potentially could mask the importance of other parameters.

In addition, the intruder dose model was used to compute the concentration of each radionuclide in the impacted waste that would yield a dose to the intruder that is equal to 500 mrem for an acute 40-hour exposure or 100 mrem/yr for a chronic annual exposure, consistent with DOE's

⁵⁶ Information concerning supplemental LAW is provided in this RAI response for additional information and completeness only, and is outside the scope of both the Draft WIR Evaluation and DOE decisions concerning supplemental LAW treatment. DOE has not made decisions concerning the potential path forward for supplemental LAW treatment, as explained in footnote 7 of the Draft WIR Evaluation and 78 FR 75913, "Record of Decision: Final Tank Closure and Waste Management Environmental Impact Statement for the Hanford Site, Richland, Washington." As explained in Section 1.2 of the Draft WIR Evaluation, the Draft WIR Evaluation does not address or include in its scope supplemental LAW. To bound the IDF PA analysis, the IDF PA assumed that supplemental LAW may potentially be vitrified and disposed of in the IDF, although, as explained above, DOE has made no decisions concerning the potential path forward for supplemental LAW treatment.

⁵⁷ See footnote 56.

⁵⁸ RPP-CALC-61254 Rev. 1 evaluated the intruder dose for the eight SSW streams discussed in the PA. The chronic dose after intruding into eight containers of compacted HEPA filters (190 mrem/yr) or eight containers of non-CERCLA, non-tank waste (1,390 mrem/yr) exceeded DOE's performance measure (100 mrem/yr) when the intrusion occurred 100 years after closure. Placing two stacked containers of these low-volume waste streams directly over one another in four separate disposal lifts was not probable. To better represent the mix of waste that will be placed into the IDF over 30 to 50 years of disposal operations, the calculation approach was changed to include an average SSW waste instead of separate waste streams in RPP-CALC-61254 Rev. 2. In addition, WAC were developed to determine concentrations limits for SSW to minimize the placement of waste containers with high intruder consequences above one another.

performance measures for protection of the human intruder in DOE M 435.1-1. Because the IDF waste is disposed of in four lifts, with each lift containing one vitrified waste container or two stacked SSW or solidified LSW containers, the resulting concentration limit is the average concentration in the impacted containers, and is not a limit for each container. The resulting waste concentrations were incorporated into the IDF WAC, IDF-00002, Table G-1. The disposal limits for short-lived radionuclides are sensitive to the time of the inadvertent intrusion. In this analysis, the time of intrusion (2278) was equated to the minimum time that DOE must retain excavation restrictions (through institutional controls) on the Hanford Site to provide reasonable expectation that the dose to an inadvertent intruder would not exceed DOE's performance measures. The recommended institutional control period for the entire Hanford Site is the latest institutional control date specified for a waste site on the Hanford Site in DOE/RL-2001-41, *Sitewide Institutional Controls Plan for Hanford CERCLA Response Actions and RCRA Corrective Actions*. Using this date for intruder analyses is the recommendation from DOE-0431, *Recommendations for Institutional Control Time Period for Conducting DOE Order 435.1 Performance Assessments at the Hanford Site*.

Using a sum of fractions approach (**Equation 2.17-1**), the waste concentration limits in Table G-1 of the WAC are intended to protect the inadvertent intruder from an acute or chronic dose that exceeds DOE performance measures once intruder protections are assumed lost.

$$SOF = \sum_i^n \frac{C_i}{C_{LIMIT,i}} = \sum_i^n \frac{M_i \times SpAct_i \times \frac{1}{V_{WP}}}{C_{LIMIT,i}} \quad (2.17-1)$$

Where:

- SOF = total sum of fractions with respect to WAC limits
- C_i = certified waste profile activity concentration of radionuclide i
- $C_{LIMIT,i}$ = waste acceptance criteria concentration limit of radionuclide i (Table G-1 of IDF-00002)
- M_i = mass of radionuclide i in a container in the waste profile
- $SpAct_i$ = specific activity of radionuclide i
- V_{WP} = as-disposed volume of the container in the waste profile.

Each waste package destined for IDF will have a certified waste profile that is screened against the WAC concentration limits by the IDF waste acceptance team to ensure that each package is not a hot spot for the facility that could result in a dose to the intruder that exceeds DOE's performance measures. Section 2.0 of IDF-00002 describes the waste acceptance process. Waste generators will prepare a certified waste profile for each waste stream prior to shipping waste to the IDF. The IDF waste acceptance team will review the certified waste profile to ensure each profile meets the requirements in the WAC, including calculating the sum of fractions to ensure protection of an inadvertent intruder. In addition, the sum of fractions is calculated for each shipment of waste to the IDF. The concentrations in the shipment cannot exceed concentrations in the certified waste profile. If all waste shipped to the IDF meets the sum of fractions test, then there is not likely to be a hot spot in the facility that would lead to a dose to an intruder that exceeds DOE's performance measures.

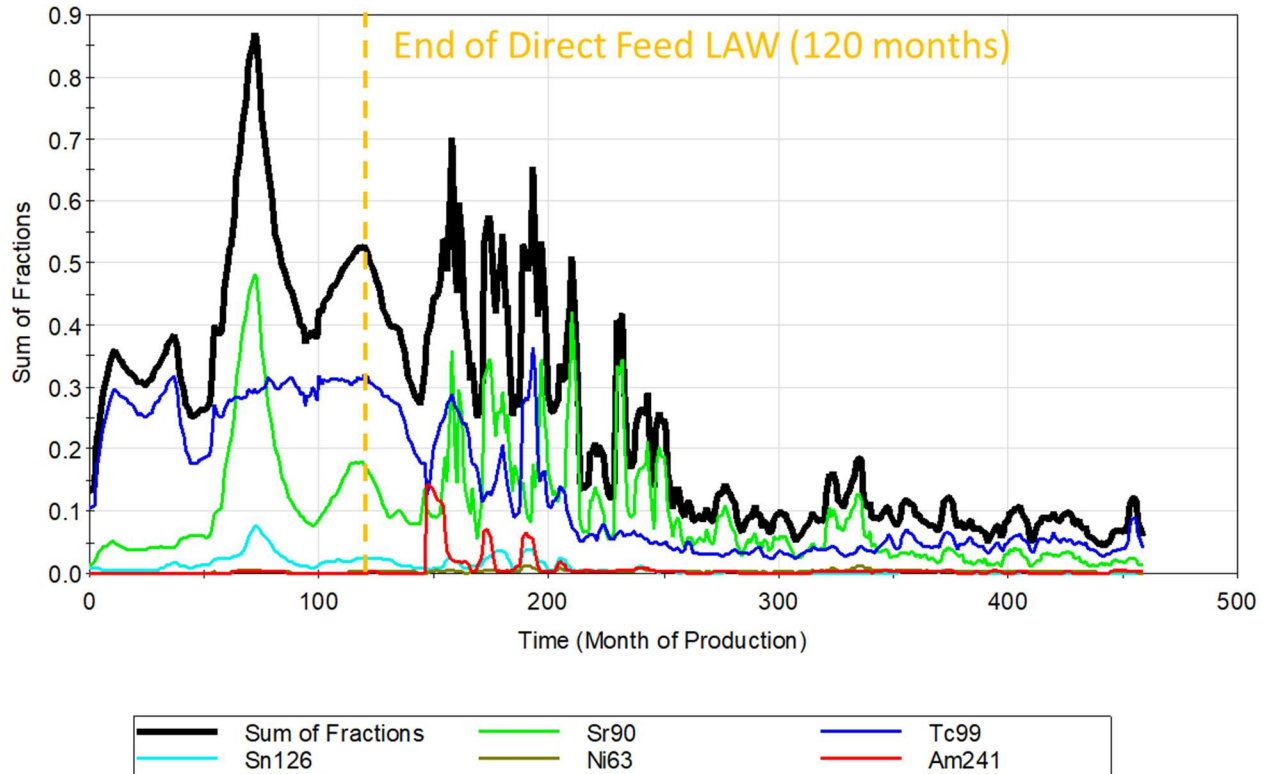
Furthermore, the waste acceptance process could permit disposal of VLAW with a sum of fractions with respect to IDF WAC concentration limits that is greater than 1. However, this requires an evaluation and is done on a case-by-case basis. This allowance occurs because the intruder scenario calculations assume that the intrusion intercepts four VLAW containers, each having one-fourth the inventory that causes the dose. If the drilling event impacts fewer than four VLAW containers or impacts at least one VLAW container with a sum of fractions that is less than one, then it would be possible for one (or more) of the impacted VLAW containers to have a sum of fractions greater than 1 but a dose following an intrusion that is still less than the DOE performance measure. In the event that a forecasted VLAW waste profile has a sum of fractions that is greater than 1, a case-by-case WAC acceptance process will be invoked through the change management process IDF-PRO-EN-54165, *IDF Unreviewed Disposal Question* to ensure that the VLAW container can be safely disposed of in the IDF and to determine if it is necessary to impose any additional constraints on where it can be placed or how much inventory can be placed above it. Although outside the scope of the Draft WIR Evaluation, the same case-by-case evaluation can be performed for SSW and LSW containers that have a sum of fractions greater than 1.

To explore how variability would contribute to the possibility of hot spots in the IDF, the Hanford flowsheet model for LAW vitrification generated a monthly forecast for the amount of each radionuclide that will be incorporated into VLAW and the volume of VLAW produced in that month. This information is reported in RPP-RPT-57991, Rev. 3. The monthly forecasted inventory and volumes were used to compute a monthly average concentration in the VLAW. This monthly average illustrates the variability in the VLAW because of variability in the LAW feed. The resulting concentrations were compared to the concentration limits and a sum of fractions for each month was computed using **Equation 2-17-1**. The results are shown in **Figure 2-17-1** for the WTP LAW Vitrification Facility that includes the DFLAW mission and vitrification in the WTP LAW Vitrification Facility following pre-treatment at the WTP Pre-Treatment Facility after the DFLAW mission is completed. Consistent with the PA that assumes that any LAW exceeding the processing capability of the first vitrification facility will be vitrified in a second vitrification plant, **Figure 2-17-2** shows the sum of fractions result for potential supplemental LAW vitrification for additional information and completeness, although DOE has not made decisions concerning the path forward for Supplemental LAW treatment. In no month did the monthly-average concentration yield a sum of fractions that exceeded 1. Individual radionuclides that exceeded 1% of the disposal limit concentration in any month are also plotted separately to illustrate their contribution to the total sum of fractions. There were only six radionuclides that exceeded 1% of the disposal limit concentration in at least one month: ^{63}Ni , ^{90}Sr ⁵⁹, ^{99}Tc , ^{126}Sn , ^{239}Pu , and ^{241}Am . The variability in the fraction of the disposal limit for a single radionuclide shown in **Figures 2-17-1** and **2-17-2** demonstrate the flowsheet variability in the product concentration. The plotted fraction is the product concentration divided by a fixed value for the disposal concentration limit according to **Equation 2-17-1**. For the six radionuclides that have a peak concentration that is at least 1% of the disposal limit, either the chronic rural pasture scenario or chronic suburban garden scenario have the most restrictive

⁵⁹ The decontamination factor for ^{90}Sr in the Tank-Side Cesium Removal unit is zero in the flowsheet model that produced the input to this calculation. If ^{90}Sr is also captured and retained during the Tank-Side Cesium Removal treatment, ^{90}Sr in the VLAW product will be lower than simulated with a decontamination factor of zero.

concentration limits. The results shown in **Figures 2-17-1 and 2-17-2** can be converted to a dose value by multiplying the fractions by 100 mrem/yr.

Figure 2-17-1. Monthly Radionuclide Sum of Fractions for Vitrified Low-Activity Waste.



Note: Low-activity waste (LAW) vitrification after the end of Direct Feed LAW is outside the scope of the Draft WIR Evaluation.

The highest sum of fractions is 0.87, which means that an intrusion into any vitrified waste container is not expected to result in a chronic dose to the intruder that exceeds 100 mrem/yr or an acute dose that exceeds 500 mrem.

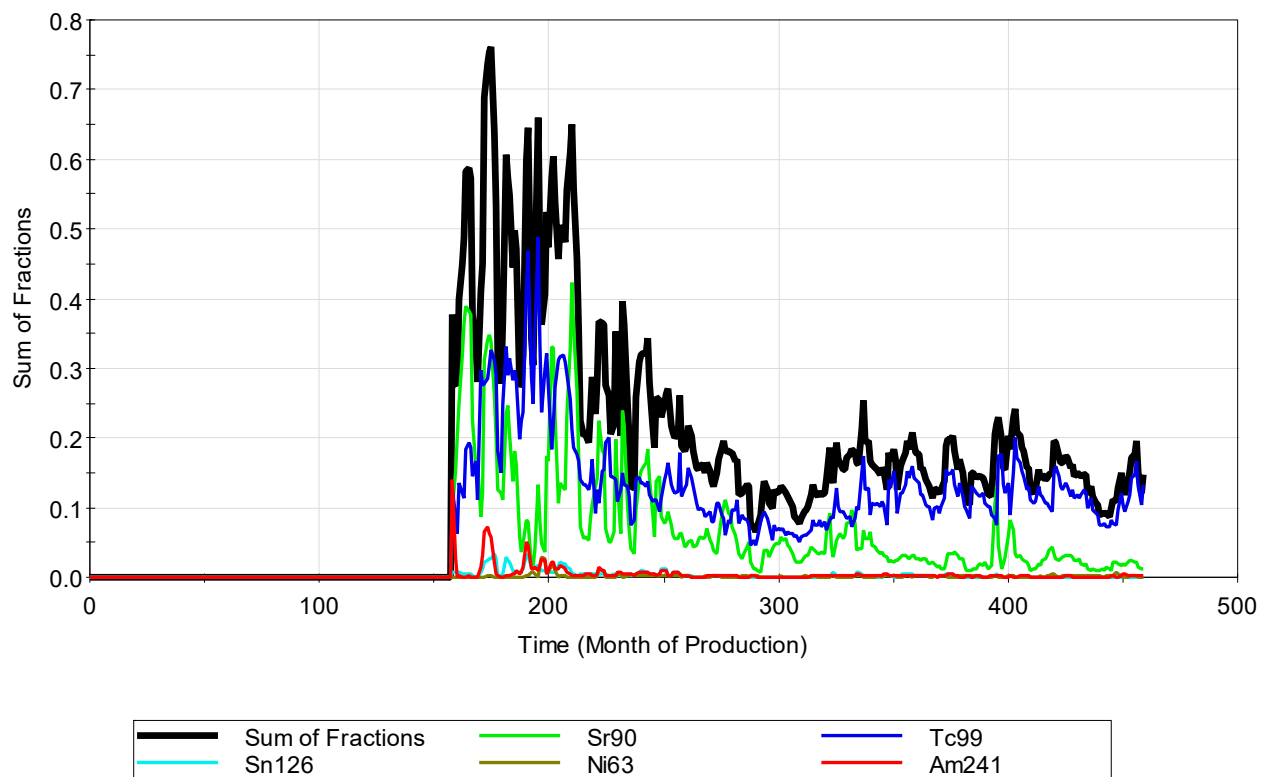
DOE believes that the site-wide institutional control plan, WAC concentration limits, and evaluations comparing the contents of waste packages to the concentration limits will provide reasonable expectation that the performance measures will be met for protection of the hypothetical human intruder at the IDF.

DOE has reviewed NRC's comment on the intruder analysis performed for Hanford WMA C made in their Technical Evaluation Report (TER) (ML20128J832 referred to as WMA C TER). DOE was not able to address NRC's intruder scenario and exposure factor recommendations for the latest revision of the IDF intruder analysis because the recommendations were provided after that IDF intruder analysis was completed. The following list identifies the NRC

comments/recommendations on the WMA C intruder analysis presented in the WMA C TER and a response concerning VLAW in the IDF PA.

- A quantitative basis should be developed that engineered components will deter modern drilling methods for hundreds of years (WMA C TER Recommendation #43). Although the WMA C PA credited the robustness of the tank dome for deterring an inadvertent intrusion into the tank for 500 years, the IDF PA inadvertent intruder calculations do not credit any engineered components for deterring an inadvertent intrusion beyond 100 years of institutional controls after IDF closure.

Figure 2-17-2. Monthly Radionuclide Sum of Fractions for Supplemental Vitrified Low-Activity Waste (after Direct Feed Low Activity Waste Mission).



Note: See footnote 55.

- The drill cuttings are spread over a large area and tilled deep into the soil surface (15 cm) achieving a large amount of dilution. Unless the entire property is tilled, such a deep depth is not consistent with natural phenomenon. Tillage depth should be consistent with future land and exposure scenario assumptions (WMA C TER Recommendation #44). One of the main uses of the inadvertent intruder analyses documented in the IDF PA is the development of disposal concentrations limits that are published in the IDF WAC. According to RPP-CALC-61254 Rev. 3 Table 6-6, there are only six radionuclides in VLAW with mission-averaged concentrations that are greater than 0.5% of the disposal limit calculated for an intrusion that occurs 100 years after closure: ^{241}Am (0.7%), ^{137}Cs (0.6%), ^{239}Pu (0.8%), ^{126}Sn (1.5%), ^{90}Sr (29.8%), and ^{99}Tc (10.5). When the intrusion is

mitigated by DOE's presence on the site and institutional controls until 2278 (as recommended in DOE-0431), the disposal limits increase for short-lived radionuclides so that the projected ^{90}Sr inventory in VLOW drops to 9% of the disposal limit (RPP-CALC-61254 Rev. 3 Table 6-7). When the tillage depth outside the garden area in the Suburban Garden scenario is reduced from 15 cm to 5 cm, the disposal limits reported in RPP-CALC-61254 Rev. 3 Table 6-6 for ^{241}Am , ^{137}Cs , ^{239}Pu , and ^{126}Sn drop by 20 to 44%. Based on the projected inventory of these radionuclides in VLOW relative to the concentration limits reported above, a 20% to 44% reduction in the inventory limit indicates that the intruder dose in these scenarios would not exceed the DOE dose limit set forth in the performance measures for acute or chronic exposures. The disposal limits for ^{90}Sr and ^{99}Tc are unchanged because these limits are determined by the Rural Pasture scenario, which continues to use a 15-cm tillage depth for the pasture. Generally, a reduction in the tilling depth of the pasture will have an inversely proportional change (i.e., increase) on the dose to the intruder and a proportional reduction in the disposal limit concentrations when the rural pasture scenario is the concentration limiting scenario for a radionuclide. The predominant exposure pathway for ^{90}Sr and ^{99}Tc in the Rural Pasture scenario is the milk ingestion pathway. Dairy cow ingestion of fodder is the primary (>99%) bioaccumulation route from the soil for these radionuclides. HNF-SD-WM-TI-707, *Exposure Scenarios and Unit Factors for Hanford Tank Waste Performance Assessment*, Rev. 5, which is the source for the tilling depth value used in the PA, selected 15-cm tillage depths to be consistent with the root depth of garden vegetables (HNF-SD-WM-TI-707 Section 2.1.2). HNF-SD-WM-TI-707 acknowledges that shallower tilling depths would lead to less dilution in the soil after mixing, but would be offset by roots that might extend below the contaminated zone and would ultimately provide the same amount of bioaccumulation. This position was developed for the garden scenarios and was carried over into the pasture scenario without adjustment. The bioaccumulation factors for pasture scenarios were selected for sparsely-vegetated pastures, but the pasture area is computed assuming a heavily-vegetated pasture (crop yield was 1.5 wet kg of fodder per square meter). Due to the differences in the assumed vegetation state for the pasture area and the bioaccumulation factors, the pasture area or bioaccumulation factors may overestimate milk dose by a factor of two or more. Therefore, it is believed that the tilling depth of 15 cm, although it may not be typical of natural mixing, is adequate for this hypothetical analysis and offsets other "conservatisms" included in other parameters used in the dose calculation. The exposure scenario data package providing the scenario-specific inputs is under revision. This recommendation will be added to the list of changes being considered for the data package update.

- The consumption rates between the intruder and on-site receptor are inconsistent. The fruit and vegetable consumption rates used are more applicable to an average member of the public rather than a gardener. (WMA C TER Recommendation #45) The exposure scenario data package providing the scenario-specific inputs is under revision. This recommendation will be added to the list of changes being considered for the data package update.

- Site-specific values for biosphere parameters should be used when available (WMA C TER Recommendation #46). DOE agrees that site-specific data should be used for all parts of the performance assessment when available. In the absence of site-specific information for a representative future person in the hypothetical intruder scenario, the biosphere parameters developed in HNF-SD-WM-TI-707 Rev. 5 that were used in the PA were developed using generalized exposure factors and in some cases were modified to accommodate regional influences (see example below from HNF-SD-WM-TI-707 Rev. 5 page A-17).

“The column labeled “USDA” [*in Table A4 titled Food and Water Consumption Rates*] comes from indirect estimates of average per capita food consumption based on food production in the United States Losses from exports, industrial uses, and end-of-year stocks were taken into account. The other and fruit consumption rates do not include bananas, pineapples, or citrus fruits, because they are not grown in southeastern Washington.”

- Plot sizes are arbitrary. If a gardener is gardening, they would size the garden to provide all the family needs (WMA C TER page 3-139, related to WMA C TER Recommendation #46). The size of the garden and pasture are developed in HNF-SD-WM-TI-707. The garden size is assumed to be ¼ the size necessary to grow all the fruits and vegetables consumed based on exposure factors in EPA/600/P-95/002Fa, *Exposure Factors Handbook Volume 1: General Factors*. The exposure scenario data package providing the scenario-specific inputs is under revision. The size of the contaminated areas will be added to the list of changes being considered for the data package update.
- Site-specific values for exposure parameters should be used when available, such as Hanford mass loading factors from BNWL-2081, *Radioactive Particle Resuspension Research Experiments on the Hanford Reservation*. Mass loading for driller should be re-evaluated (WMA C TER Recommendation #47). DOE anticipates taking a risk-informed approach to potential data collection of mass loading factors. The only application of this data collection effort would be to support calculations in the hypothetical intruder scenarios. For this RAI response, the disposal concentration limits were recalculated using a mass loading factor that is 10 times higher than the base case value, a value consistent with the maximum discussed by the NRC in the WMA C TER, and the tillage depth was changed to 5 cm for the area outside of the garden in the Suburban Garden scenario. The sum of fractions for the projected inventory that includes VLAW, SSW and ETF-LSW reported in RPP-CALC-61254 Rev. 3 Table 6-6 increased from 0.675 to 0.773.
- Recommended including radon in dose calculations to increase transparency with stakeholders as it could be a hidden impact when it is excluded even though a separate standard is used for compliance (WMA C TER Recommendation #48). Consistent with DOE M 435.1-1, the dose to the inadvertent intruder should exclude the dose from radon in air. Therefore, radon contributions to dose are excluded in the inadvertent intruder

dose assessment. Radon release is simulated and compared to the radon flux performance objective, which limits radon releases to 20 pCi/m²/s at the surface of the disposal facility. Therefore, the NRC's TER recommendation is inconsistent with DOE M 435.1-1, and DOE Technical Standard DOE-STD-5002-2017, *Disposal Authorization Statement and Tank Closure Documentation*.

References

- 78 FR 75913, 2013, "Record of Decision: Final Tank Closure and Waste Management Environmental Impact Statement for the Hanford Site, Richland, Washington," *Federal Register*, Vol. 78, pp. 75913–75919 (December 13).
- BNWL-2081, 1977, *Radioactive Particle Resuspension Research Experiments on the Hanford Reservation*, Battelle Pacific Northwest Laboratories, Richland, Washington.
- DOE-0431, 2019, *Recommendations for Institutional Control Time Period for Conducting DOE Order 435.1 Performance Assessments at the Hanford Site*, Rev. 0, U.S. Department of Energy, Office of River Protection, Richland, Washington.
- DOE M 435.1-1, 2011, *Radioactive Waste Management Manual*, Change 2, U.S. Department of Energy, Washington, D.C.
- DOE/RL-2001-41, 2019, *Sitewide Institutional Controls Plan for Hanford CERCLA Response Actions and RCRA Corrective Actions*, Rev. 9, U.S. Department of Energy, Richland Operations Office, Richland, Washington.
- DOE-STD-5002-2017, 2017, *Disposal Authorization Statement and Tank Closure Documentation*, U.S. Department of Energy, Washington, D.C.
- EPA/600/P-95/002Fa, 1997, *Exposure Factors Handbook Volume 1: General Factors*, U.S. Environmental Protection Agency, National Center for Environmental Assessment, Washington, D.C.
- HNF-SD-WM-TI-707, 2007, *Exposure Scenarios and Unit Factors for Hanford Tank Waste Performance Assessment*, Rev. 5, CH2M HILL Hanford Group, Inc., Richland, Washington.
- IDF-00002, 2019, *Waste Acceptance Criteria for the Integrated Disposal Facility*, Rev. 0, CH2M HILL Plateau Remediation Company, Richland, Washington.
- IDF-PRO-EN-54165, 2019, *IDF Unreviewed Disposal Question*, Rev. 1, CH2M HILL Plateau Remediation Company, Richland, Washington.
- ML20128J832, 2020, *Technical Evaluation Report, Draft Waste Incidental to Reprocessing Evaluation for Closure of Waste Management Area C, Hanford Site, Washington*, U.S. Nuclear Regulatory Commission, Rockville, Maryland.

RPP-CALC-61254, 2017, *Inadvertent Intruder Dose Calculation Update for the Integrated Disposal Facility Performance Assessment*, Rev. 1, Washington River Protection Solutions, LLC, Richland, Washington.

RPP-CALC-61254, 2018, *Inadvertent Intruder Dose Calculation Update for the Integrated Disposal Facility Performance Assessment*, Rev. 2, Washington River Protection Solutions, LLC, Richland, Washington.

RPP-CALC-61254, 2019, *Inadvertent Intruder Dose Calculation Update for the Integrated Disposal Facility Performance Assessment*, Rev. 3, Washington River Protection Solutions, LLC, Richland, Washington.

RPP-RPT-57991, 2019, *River Protection Project Integrated Flowsheet*, 24590-WTP-RPT-MGT-14-023, Revision 3, Washington River Protection Solutions, LLC, Richland, Washington.

RAI 2-18 (90Sr Inventory Uncertainty)**Comment**

Additional information is needed regarding the uncertainty in the ⁹⁰Sr inventory estimate and how the inventory uncertainties are propagated into the GoldSim model.

Basis

Strontium-90 is a key radionuclide, especially for the intruder scenario. The projected chronic dose to the hypothetical human intruder 100 years after IDF closure under the rural pasture resident scenario is 43.3 mrem/yr (as compared to DOE's performance metric of 100 mrem/yr). The peak dose is driven by the milk ingestion pathway (40.5 mrem/yr). The total dose is principally due to ⁹⁰Sr and ⁹⁹Tc, which contribute 29.8 mrem/yr and 10.4 mrem/yr, respectively, to the total dose (page 7-38 of the PA document).

There is uncertainty in the inventory of ⁹⁰Sr within the Best Basis Inventory (BBI). The PA document (page 3-232) indicates that ⁹⁰Sr estimates in the BBI could be off by as much as 80 percent. However, it is unclear how uncertainty in ⁹⁰Sr inventory coming from the BBI model is included and propagated into the GoldSim model. In a public teleconference with DOE on September 28, 2020 (ML20311A202), DOE indicated that because of the direct correlation between inventory and dose they intentionally did not include inventory uncertainty in the GoldSim model to be able to see the effects of other aspects of uncertainty more readily. Instead, DOE indicated that they evaluate uncertainty in risk with inventory in RPP-CALC-63176. Specifically, the PA results are scaled to forecast the impact to groundwater in this tool instead of using GoldSim model. DOE also indicated that for the intruder analysis, in RPP-CALC-61254 Rev 3, DOE analyzed different 90Sr levels and how it influences the need for intruder barriers.

Path Forward

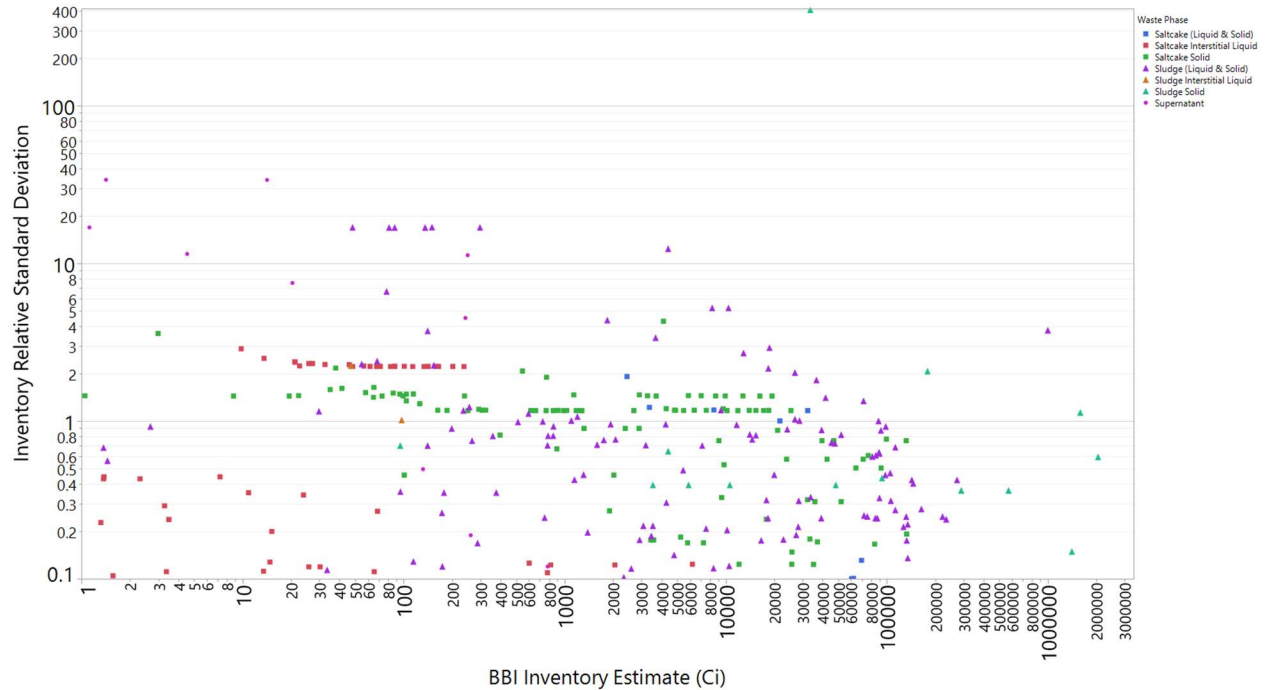
Please provide a description of how ⁹⁰Sr inventory uncertainty impacts the dose to the inadvertent intruder. Please provide the reference RPP-CALC-61254, Rev 3.

DOE Response

The Best-Basis Inventory (BBI) uncertainty estimate discussed on page 3-232 of the IDF PA (RPP-RPT-59958, *Performance Assessment for the Integrated Disposal Facility, Hanford Site, Washington*, Rev. 1A) refers to the uncertainty in the total estimate of the waste in the single- and double-shell tanks at Hanford. The uncertainty estimate is derived from tank waste samples in the BBI database that have an estimate of sample uncertainty. The BBI database includes samples from every waste phase, not just waste phases that will provide feed to the WTP LAW Vitrification Facility. The greatest ⁹⁰Sr activity and highest uncertainty is from samples from the sludge phase (see **Figure 2-18-1**), which is not a phase that will be fed through the LAW vitrification process. To provide an estimate for the uncertainty in the ⁹⁰Sr concentrations that might be present in the LAW feed, the BBI uncertainty analysis discussed in Appendix B of RPP-CALC-62058, *Waste Stream Inventory Calculations for the Integrated Disposal Facility Performance Assessment*, Rev. 1 and discussed in Section 3.3.2.4 of the IDF PA was repeated with just the BBI data for the supernatant phase in 19 double-shell tanks. The uncertainty in the supernatant samples is more representative of the sample uncertainty for staged feed to the WTP LAW Vitrification Facility during DFLAW operations as well as vitrification in the WTP LAW

Vitrification Facility following pre-treatment at the WTP Pre-Treatment Facility after the DFLAW mission is completed⁶⁰ and vitrification for supplemental LAW⁶¹.

Figure 2-18-1. Strontium-90 Inventory in All Waste Phases in the Best-Basis Inventory with Estimates of Sample Uncertainty.



⁶⁰ Vitrification in the WTP LAW Vitrification Facility following pre-treatment at the WTP Pre-Treatment Facility after the DFLAW mission is completed is provided for additional information and completeness, and is outside the scope of the Draft WIR Evaluation.

⁶¹ Information concerning supplemental LAW is provided in this RAI response for additional information and completeness only, and is outside the scope of both the Draft WIR Evaluation and DOE decisions concerning supplemental LAW treatment. DOE has not made decisions concerning the potential path forward for supplemental LAW treatment, as explained in footnote 7 of the Draft WIR Evaluation and 78 FR 75913, “Record of Decision: Final Tank Closure and Waste Management Environmental Impact Statement for the Hanford Site, Richland, Washington.” As explained in section 1.2 of the Draft WIR Evaluation, the Draft WIR Evaluation does not address or include in its scope supplemental LAW. To bound the IDF PA analysis, the IDF PA assumed that supplemental LAW may potentially be vitrified and disposed of in the IDF, although, as explained above, DOE has made no decisions concerning the potential path forward for supplemental LAW treatment.

When the inventory uncertainty analysis⁶² is rerun with just the supernatant samples in the BBI database, the ⁹⁰Sr inventory uncertainty is much lower than the ⁹⁰Sr inventory uncertainty with the other waste phases. When all phases were sampled using the relative sample deviations in the BBI database, the 95th-percentile of the total ⁹⁰Sr inventory in all of the tank waste was 71% higher than the BBI inventory without uncertainty (Table 3-24 in the IDF PA). When only the supernatant samples from double-shell tanks are used in the same evaluation, then the total activity of ⁹⁰Sr included in the BBI uncertainty analysis is 3.45E05⁶³ Ci and the 95th-percentile value is 3.57E05 Ci. The 95th-percentile of the total ⁹⁰Sr inventory is only 3.5% higher than the total ⁹⁰Sr inventory without uncertainty (see **Figure 2-18-2**). When the analysis is re-run using an untruncated normal distribution, the 95th-percentile inventory is lower.

The uncertainty estimate is determined by the relative standard deviation in the BBI database for each waste phase. Supernatant concentrations are determined by laboratory analysis of liquid grab samples collected from different depths in the tank. The number of samples collected from each tank, including duplicates, is determined by the Data Quality Objectives in tank-specific sampling plans. Two of 21 tanks with a supernatant phase contain 91% (3.15E05 Ci of 3.45E05 Ci) of the total ⁹⁰Sr activity in the supernatant phase. The reported uncertainty for these tanks drives the uncertainty in the total uncertainty estimate. The relative standard deviation for the inventory estimate of 1.80E05 Ci of ⁹⁰Sr in tank 241-AN-107 supernate is 0.0223. The relative standard deviation in the inventory estimate of 1.35E05 Ci of ⁹⁰Sr in tank 241-AN-102 supernate is 0.0311. The low relative standard deviations of the grab samples for the ⁹⁰Sr concentrations in the supernate suggests that there will be little uncertainty in the LAW feed once characterization samples are collected and analyzed.

The sum of fraction results for ⁹⁰Sr presented in the response to RAI 2.17 illustrate the variability in the LAW feed and the potential impact to an inadvertent intrusion into four containers of VLAW. The results show that the peak impact to an intruder from just ⁹⁰Sr after drilling into four containers of VLAW is roughly 48% of DOE's dose limits for an intruder, which are 500 mrem for an acute exposure and 100 mrem/yr for a chronic annual exposure⁶⁴. An additional 3.5% inventory uncertainty in the VLAW feed propagated to the VLAW would

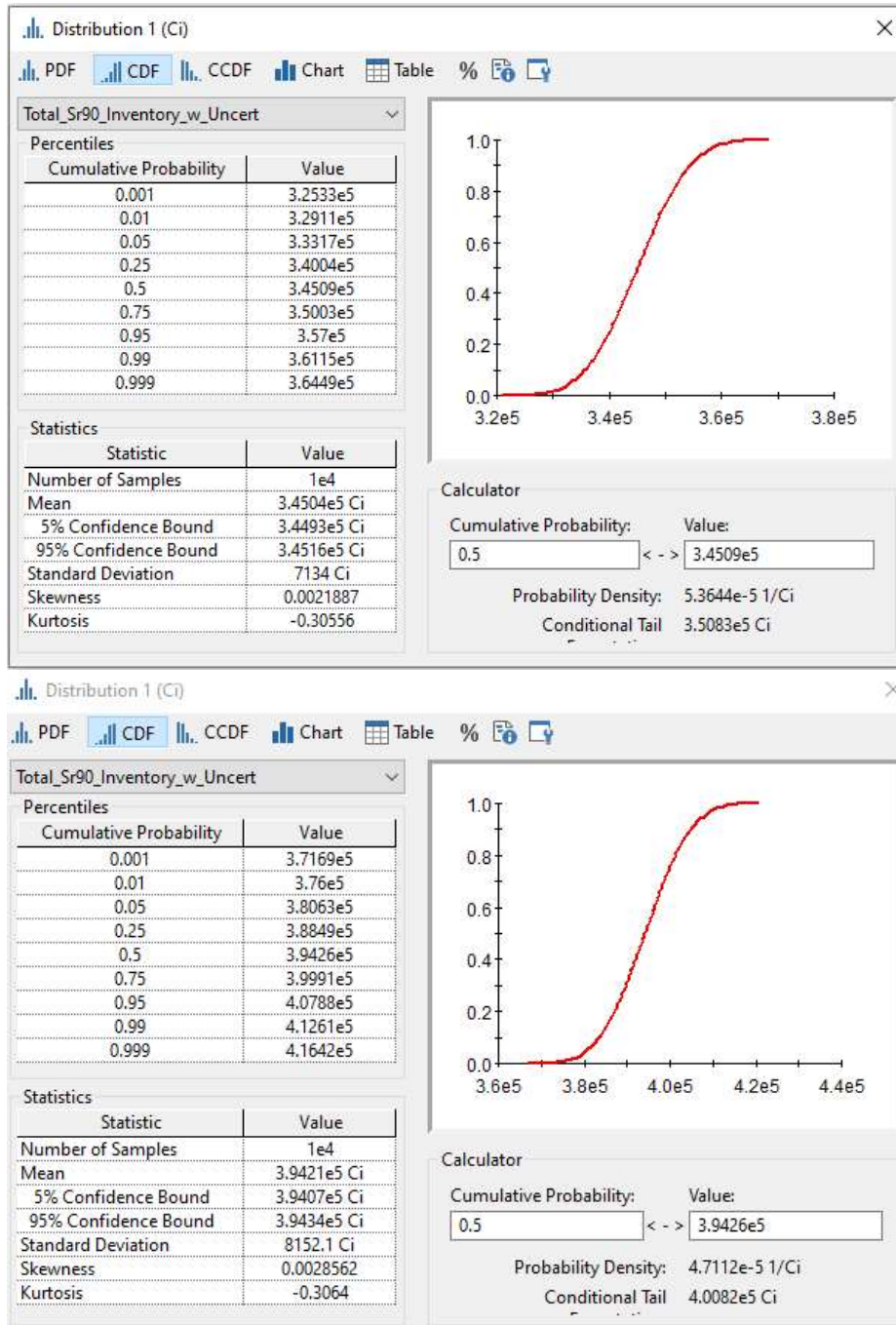
⁶² In the inventory uncertainty analysis, the BBI records were queried to find all double-shell tanks that have ⁹⁰Sr in the supernatant phase. Only the sample records that also had relative standard deviations to characterize the uncertainty in the sample estimate were used. Each estimate and relative standard deviation were used to create a triangular distribution for each sample record. The bounds of the distribution were determined by adding or subtracting three standard deviations from the sample estimate. The mode of the distribution was set equal to the sample estimate without uncertainty. The distributions were sampled and all the values were added together to get the total inventory with uncertainty. The 95th-percentile of 10,000 Monte Carlo realizations was compared to the total inventory without uncertainty to estimate the uncertainty in the total inventory of ⁹⁰Sr in sampled LAW feed.

⁶³ Due to radionuclide decay and processing in the WTP HLW Vitrification Facility, the BBI inventory in supernatant phase of the double-shell tanks is not necessarily the same inventory in the feed stream to the WTP LAW Vitrification Facility. The total ⁹⁰Sr inventory in the BBI supernate can be different from the inventory in the VLAW simulated in the IDF PA.

⁶⁴ The radionuclide concentration limit is the radionuclide concentration in the waste that results in a dose to the intruder that is equal to either DOE's acute dose limit or chronic dose limit. The concentration limits are determined for acute and chronic dose scenarios and the more restrictive concentration is set as the disposal limit. For ⁹⁰Sr, a chronic scenario has a more restrictive concentration limit. Therefore, a waste concentration that is 48% of the ⁹⁰Sr concentration limit yields a chronic dose to the intruder that is 48 mrem/yr from ⁹⁰Sr.

not cause the sum of fractions to exceed 1, so it would also not cause the dose to an inadvertent intruder to exceed DOE performance measures.

Figure 2-18-2. Estimate of Strontium-90 Inventory Uncertainty in Supernate from Best-Basis Inventory Records.



The IDF disposal limit for ⁹⁰Sr is derived from the inadvertent intruder analysis (RPP-CALC-61254, *Inadvertent Intruder Dose Calculation Update for the Integrated Disposal*

Facility Performance Assessment, Rev 3). Subsequent to completion of the IDF PA, the DOE Office of River Protection and DOE Richland Operations Office provided guidance (DOE-0431, *Recommendations for Institutional Control Time Period for Conducting DOE Order 435.1 Performance Assessments at the Hanford Site*) that all Hanford Site intruder analyses should consider that inadvertent intrusion would be mitigated by mandated institutional controls until 2278. A *Comprehensive Environmental Response, Compensation, and Liability Act of 1980* (CERCLA) Record of Decision for a waste site on the Hanford Site requires DOE to maintain institutional controls at Hanford to prevent excavation into that waste site until 2278. Consistent with the recommendation in DOE-0431, IDF disposal limits for all radionuclides were reevaluated in RPP-CALC-61254 Rev. 3 assuming potential intrusion occurs no sooner than 2278. Table 6-5 in RPP-CALC-61254 Rev. 3 shows how the disposal limits for all radionuclides vary with the duration of credited intruder protections, with dates ranging from 100 years after closure (2151) out to calendar year 2278. Disposal limits for short-lived fission products (primarily ^{90}Sr and ^{137}Cs) were very sensitive to the duration of institutional controls used to provide intruder protections; disposal limits for longer-lived radionuclides were not as sensitive to the duration of intruder protections.

The analysis was carried out until 2278 because the analysis included in the previous revision of the IDF PA that assumed institutional controls until 2151 was not sufficient to protect the intruder when VLAW concentrations of ^{90}Sr were as high as the WTP maximum allowable concentration of $20 \text{ Ci } ^{90}\text{Sr} / \text{m}^3$. The results of the analysis revealed that intruder protections until 2242 were necessary to keep doses below DOE performance measures when the VLAW contained $20 \text{ Ci } ^{90}\text{Sr} / \text{m}^3$. However, intruder protections until 2176 were needed to keep doses below DOE performance measures when the VLAW contained an average ^{90}Sr concentration forecasted for the entire DFLAW mission in Table C-7 of RPP-RPT-57991, *River Protection Project Integrated Flowsheet*. When additional radionuclides are disposed of with ^{90}Sr , the duration to protect the intruder must be extended beyond these dates. The sum of fractions calculation in the response to RAI 2-17 calculates disposal limits for ^{90}Sr assuming institutional controls on the Hanford Site until 2278.

Furthermore, the waste acceptance process could permit disposal of VLAW with a sum of fractions with respect to IDF WAC concentration limits that is greater than one. However, this requires an evaluation and is done on a case-by-case basis. This allowance occurs because the intruder scenario calculations assume that the intrusion intercepts four VLAW containers, each having one-fourth the inventory that causes the dose. If the drilling event impacts fewer than four VLAW containers or impacts at least one VLAW container with a sum of fractions that is less than one, then it would be possible for one (or more) of the impacted VLAW containers to have a sum of fractions greater than one but a dose following an intrusion that is still less than the DOE performance measure. In the event that a forecasted VLAW waste profile has a sum of fractions that is greater than 1, a case-by-case WAC acceptance process will be invoked through the change management process in IDF-PRO-EN-54165, *IDF Unreviewed Disposal Question* to ensure that the VLAW container can be safely disposed of in the IDF and determine if it is necessary to impose any additional constraints on where it can be placed or how much inventory can be placed above it. Although outside the scope of the Draft WIR Evaluation, the same case-by-case evaluation can be performed for SSW and LSW containers that have a sum of fractions greater than one.

References

- 78 FR 75913, 2013, “Record of Decision: Final Tank Closure and Waste Management Environmental Impact Statement for the Hanford Site, Richland, Washington,” *Federal Register*, Vol. 78, pp. 75913–75919 (December 13).
- Comprehensive Environmental Response, Compensation, and Liability Act of 1980*, 42 USC 9601 et seq.
- DOE-0431, 2019, *Recommendations for Institutional Control Time Period for Conducting DOE Order 435.1 Performance Assessments at the Hanford Site*, Rev. 0, U.S. Department of Energy, Office of River Protection, Richland, Washington.
- IDF-PRO-EN-54165, 2019, *IDF Unreviewed Disposal Question*, Rev. 1, CH2M HILL Plateau Remediation Company, Richland, Washington.
- ML20311A202, 2020, *Public Teleconference between the Nuclear Regulatory Commission and the Department of Energy on the Hanford Draft WIR Evaluation for Vitrified Low Activity Waste*, September 28, 2020.
- RPP-CALC-61254, 2017, *Inadvertent Intruder Dose Calculation Update for the Integrated Disposal Facility Performance Assessment*, Rev. 1, Washington River Protection Solutions, LLC, Richland, Washington.
- RPP-CALC-61254, 2018, *Inadvertent Intruder Dose Calculation Update for the Integrated Disposal Facility Performance Assessment*, Rev. 2, Washington River Protection Solutions, LLC, Richland, Washington.
- RPP-CALC-61254, 2019, *Inadvertent Intruder Dose Calculation Update for the Integrated Disposal Facility Performance Assessment*, Rev. 3, Washington River Protection Solutions, LLC, Richland, Washington.
- RPP-CALC-62058, 2018, *Waste Stream Inventory Calculations for the Integrated Disposal Facility Performance Assessment*, Rev. 1, Washington River Protection Solutions, LLC, Richland, Washington.
- RPP-CALC-63176, 2020, *Integrated Disposal Facility Risk Budget Tool Analysis*, Rev. 0A, Washington River Protection Solutions, LLC, Richland, Washington.
- RPP-RPT-57991, 2019, *River Protection Project Integrated Flowsheet*, 24590-WTP-RPT-MGT-14-023, Rev. 3, Washington River Protection Solutions, LLC, Richland, Washington.
- RPP-RPT-59958, 2019, *Performance Assessment for the Integrated Disposal Facility, Hanford Site, Washington*, Rev. 1A, Washington River Protection Solutions, LLC, Richland, Washington.

RAI 2-19 (Releases from the ETF-LSW Waste)**Comment**

Additional information is needed on the modeled release of ^{129}I and ^{99}Tc from the ETF-LSW waste.

Basis

Several aspects of the modeling used for the release from the ETF-LSW waste could result in the underestimation of the potential release. The ETF-LSW waste originates from the treatment of liquid waste from WTP operations, including the liquid effluent from the melter primary off-gas treatment system and the LAW vitrification secondary off-gas/vessel vent treatment system. As described above in RAI 1-3, there is uncertainty in how much of key radionuclides, such as ^{129}I and ^{99}Tc , will end up in the ETF-LSW waste stream due to uncertainty in how well these radionuclides will be incorporated into the glass. For example, in Case 7, the inventories of ^{129}I and ^{99}Tc in the ETF-LSW waste are assumed to be a small percentage of the total, while in Cases 10A and 10B, the inventories of ^{129}I and ^{99}Tc are assumed to be much higher. In the GoldSim model, the calculated fractional release rates of ^{129}I and ^{99}Tc from the ETF waste on a unit inventory basis (i.e., “fractional_release_rate_all”) are approximately an order of magnitude less than the release rates from other waste streams, such as the ion exchange waste stream and the waste streams that are encapsulated in cementitious mortar or paste.

The basis for the best-estimate parameter values assumed for the release from the solidified ETF-LSW waste is provided in PNNL-25194 (2016) and is summarized in the PA document. One key modeling assumption for the release from the ETF-LSW stream, that appears to be non-conservative, is the assumed probability distribution of the effective diffusivity coefficient. A log-uniform distribution with a range of 1.8×10^{-13} cm²/s to 5.5×10^{-8} cm²/s was assumed for the ETF-LSW waste, while the probability distribution assumed for the diffusivity for the other cementitious materials was higher. The data cited in PNNL-25194 includes effective coefficient data for iodine and technetium, which are expected to sorb slightly, as well as data from sodium, nitrate, and nitrite. The measured diffusivity coefficients at the low end of the observed range were for iodine and technetium and likely include sorption. This item was also identified by the Low-Level Waste Disposal Facility Federal Review Group (LFRG) as Issue Number IDF-S19-PA12-05. The corrective action stated for this item was to add a clarifying discussion to Section 6.3.2.3 of the PA document. This discussion acknowledges that the effective diffusivities include sorption and states that the minimum value of the distribution was based on the assumption that the K_d of the species in question (iodine and technetium) is equal to 0. The assumption that the K_d values for these elements is equal to 0 is inconsistent with the assumed K_d values in the model. Additionally, the response to the LFRG comment stated that “the ETF-LSW waste form is a negligible contributor to dose as shown in Figure 6-63”. This figure reference appears to be incorrect. However, Figure 6-58 does show the dose contribution from the ETF-LSW waste being less when the Case 7 inventory is assumed. This figure does not provide any information as to the relative dose contribution of the ETF-LSW waste if a higher inventory of ^{129}I and ^{99}Tc end up in this waste stream.

Additionally, the diffusive length assumed in the GoldSim model for the ETF-LSW waste (0.2 m) is approximately an order of magnitude longer than the diffusive lengths for the other waste

forms, but it is not clear what the basis is for this waste length being longer. It also is not clear what effect this assumption has on the modeled diffusive fluxes of the radionuclides out of the wasteform and the potential dose from this release.

Path Forward

Please provide additional information on the expected fractional release rate for ^{129}I and ^{99}Tc for the ETF-LSW wasteform and describe whether the modeled performance is consistent with this wasteform's expected performance as compared to the other cementitious wasteforms included in the PA. Consider providing an evaluation of the potential fractional release and the dose from the ETF waste using an effective diffusion coefficient value that does not include sorption. Also consider providing an evaluation of the potential dose if the inventory in this waste stream is higher than assumed in Case 7 (i.e., a Case 10A/10B inventory) using a revised effective diffusion coefficient value. Please provide additional information on the basis for the diffusive length assumed for the ETF-LSW waste. If this diffusive length was an error, provide an updated evaluation of the fractional release rate from the ETF-LSW waste that incorporates a corrected value for the diffusive length. Consider providing an updated value for the diffusive length, if appropriate, in the evaluation requested above.

DOE Response

The Draft WIR Evaluation addresses the WIR criteria for VLAW produced during the DFLAW operations only. As such, vitrified waste assumed to be produced after DFLAW operations and all SSW and LSW, assumed during DFLAW operations or assumed after DFLAW operations, is outside the scope of this WIR evaluation. See DOE response (Section 2.0). However, DOE recognizes the importance of the IDF PA, which is a reference for the Draft WIR Evaluation, and is providing the information below in response to the RAI, including a discussion of the full potential treatment mission, SSW, and LSW for additional information. The approach to ensuring that all waste packages are acceptable for disposal at the IDF is described in this RAI response and is the same for all waste streams.

The grout used to solidify LSW from the Hanford ETF is different from the grout used to encapsulate debris and solidify other non-debris waste streams from the WTP such as carbon adsorption media, ion exchange resin, and silver mordenite. The grout used in the PA calculations to solidify ETF-LSW was specifically designed for the expected composition of the secondary waste from the treatment of liquid waste streams at the ETF. The grout formulation was designed to achieve specific performance requirements. Specifically, the hydrated lime was added to sequester sulfate in ettringite [$\text{Ca}_6\text{Al}_2(\text{SO}_4)_3(\text{OH})_{12}\cdot 26(\text{H}_2\text{O})$] early in the curing phase, avoiding late ettringite formation that can lead to undesired swelling and cracking of the waste form and to increase the pH to activate the blast furnace slag to maintain reducing conditions to help immobilize ^{99}Tc (PNNL-25194, *Secondary Waste Cementitious Waste Form Data Package for the Integrated Disposal Facility Performance Assessment* and PNNL-26443, *Updated Liquid Secondary Waste Grout Formulation and Preliminary Waste Form Qualification*). Consequently, compared to an encapsulating or void fill grout, DOE believes that it is appropriate to assign different properties to the grouted ETF-LSW waste form. DOE continues to evaluate alternative grout formulations for ETF-LSW waste streams. An alternative formulation to that used in the PA has been specified by the ETF Modular Grout Project. This grout formulation results in a low-pH, sulphur-activated blast furnace slag waste form with

upfront struvite precipitation to prevent release of ammonia gas. Laboratory studies evaluating the necessary properties to use in PA calculations are expected to be published in a research report in FY 2021. Once completed, DOE will use its change control process to evaluate the new grout formulation for possible implications on the conclusions of the PA.

In the process models used to determine compliance with DOE performance objectives, radionuclide releases from containers of solidified LSW were simulated using an effective diffusion coefficient for non-sorbing species and accounted for sorption using a radionuclide-specific distribution coefficient (K_d) (RPP-CALC-61030, *Cementitious Waste Form Release Calculations for the Integrated Disposal Facility Performance Assessment*, Section 4.2.2). The effective diffusion coefficient used in the compliance case simulations of ETF-LSW with hydrated lime was $1.6E-09 \text{ cm}^2/\text{s}$ (RPP-CALC-61030 Table 6-10), which is the geometric average value for sodium reported in PNNL-25194 Table 3.1. The geometric average for the apparent diffusion coefficient for ^{99}Tc , which accounts for sorption and redox conditions, was $1.8E-13 \text{ cm}^2/\text{s}$ (PNNL-25194 Table 3.1). No apparent diffusion coefficient value was reported in PNNL-25194 for ^{129}I in a hydrated lime-based waste form; the laboratory work developing the values for technetium, sodium, and nitrate did not include iodine (PNNL-25194 Section 3.1.2).

In a subsequent report that was not available in time to support the PA calculations, additional tests with hydrated lime grout for the ETF-LSW were reported in PNNL-26443. This report included a diffusion coefficient for iodine in the different tests that were performed. The results are compared to diffusion coefficients for sodium in **Figure 2-19-1**. The results indicate that iodine has some affinity for the grout solids since the diffusion coefficients are lower than for non-sorbing sodium. When the K_d is backed out of the reported diffusion coefficient using Equations 4-5 and 4-6 in RPP-CALC-61030, the K_d values for iodine without getters range from 0.2 to 4 mL/g with an arithmetic average equal to 1 mL/g⁶⁵. However, it is noted that the effective diffusion coefficients for sodium reported in PNNL-26443 increased by a factor of up to 18 over the values reported in PNNL-25194. The reported diffusion coefficients in PNNL-26443 for iodine including sorption were comparable to the effective diffusion coefficient for non-sorbing species in PNNL-25194 (equal to $1.6E-09 \text{ cm}^2/\text{s}$).

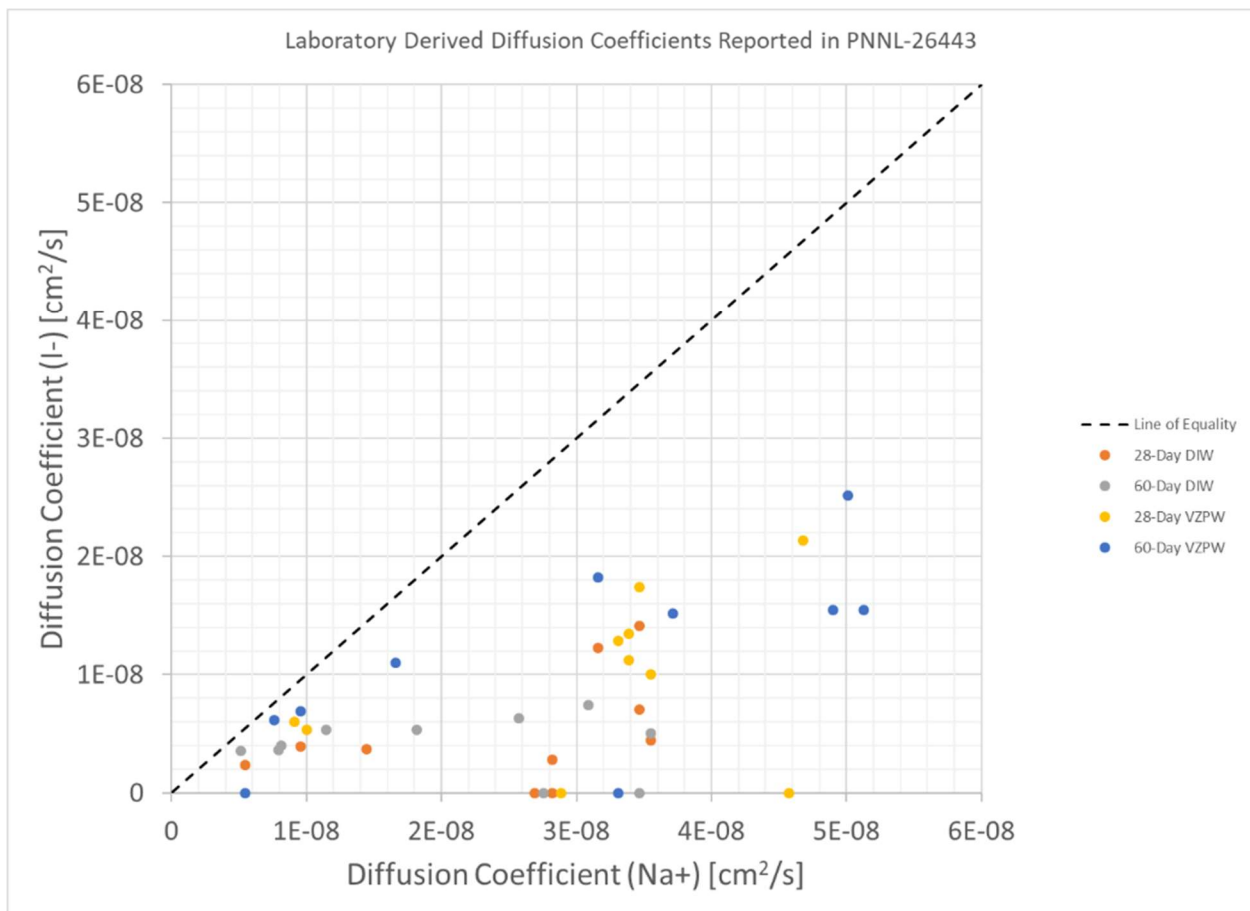
Simulations treating iodine as non-sorbing in the grouted waste form were performed in the sensitivity analyses described in RPP-CALC-61030. In addition, the initial and updated values for the apparent iodine diffusion coefficient in ETF-LSW are within the range of values included in the uncertainty analysis that are computed from sampled values using Equations 4-5 and 4-6 in RPP-CALC-61030 (**Figure 2-19-2**).

Simulations in RPP-CALC-61030 for the compliance case used a grout K_d of 0.8 mL/g for ^{99}Tc and 4.0 mL/g for ^{129}I (RPP-CALC-61030 Tables 6-10 and 6-11). RPP-CALC-61030 Figure 7-56 shows the ETF-LSW release rates that are used to compute the dose in the groundwater pathway analysis and provide the basis for comparison of alternative cases. In addition to the compliance case, sensitivity cases evaluated the release of iodine and technetium to the vadose zone from ETF-LSW using alternative values for K_d , effective diffusion coefficients, saturated hydraulic

⁶⁵ Distribution coefficient estimates assume a porosity of 0.5 and saturation of 1 from Table 3.4 in PNNL-25194 because these properties were not reported in PNNL-24463.

conductivity, cement type, waste package type, net infiltration rate, and inventory (RPP-CALC-61030 Tables 6-12 through 6-15). The compliance case and sensitivity cases for ETF-LSW in RPP-CALC-61030 include 77 process model simulations. Multiple simulations reported in RPP-CALC-61030 included simulations with the diffusion coefficient derived for sodium and no iodine or technetium sorption to the grout. The results reported in RPP-CALC-61030 are limited to release rates and cumulative amounts released at 1,000 and 10,000 years of simulation time; additional results from select simulations are presented and discussed in this RAI response. The simulated results presented in RPP-CALC-61030 Table 7-22 reveal that the fractional release rates and cumulative fraction released in 1,000 and 10,000 years for Case 7 and Case 10A inventories are the same. Thus, the fractional release rates are independent of initial inventory and simulated results can be scaled to consider uncertainties in inventories. The results presented below are expressed as fractional values.

Figure 2-19-1. Comparison of Laboratory Measured Effective Diffusion Coefficients for Iodine and Sodium.

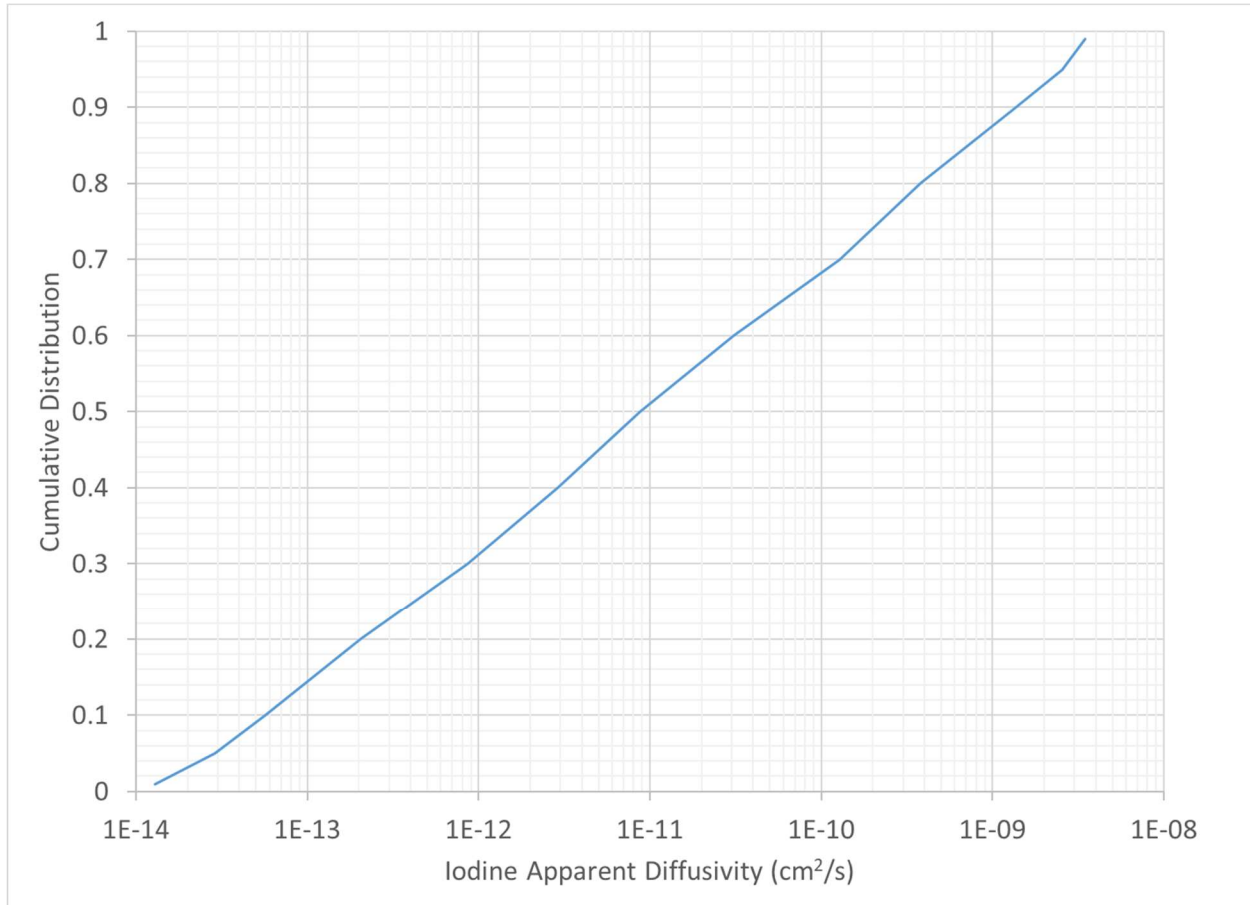


DIW = de-ionized water

VZPW = vadose zone pore water

Values from PNNL-26433, *Updated Liquid Secondary Waste Grout Formulation and Preliminary Waste Form Qualification*, Tables 6.6 and 6.7.

Figure 2-19-2. Distribution of Iodine Apparent Diffusion Coefficients in Integrated Disposal Facility Performance Assessment Uncertainty Analysis.



Reference: RPP-RPT-59958, *Performance Assessment for the Integrated Disposal Facility, Hanford Site, Washington*.

Iodine:

The IDF PA compliance case simulated ¹²⁹I releases from the ETF-LSW stream using a grout distribution coefficient of 4 mL/g and an effective diffusion coefficient of 1.6E-09 cm²/s. Measured values for the apparent diffusion coefficient of iodine in PNNL-26443 suggest that the applied K_d may underestimate iodine release rates. RPP-CALC-61030 simulated iodine release from ETF-LSW without sorption onto the grout and reported cumulative fractions released at 1,000 and 10,000 years. Time histories of the releases rates with and without sorption to the grout are compared in **Figures 2-19-3** and **2-19-4**. The peak release rate, which is roughly proportional to the peak impact to groundwater and peak ¹²⁹I dose result from this waste stream, increases by a factor of 8 for the case with no sorption and a factor of 17 for the case with no sorption and an effective diffusion coefficient that is a factor of three higher than the base case.

Knowing that the peak impact to groundwater and the peak dose are proportional to the peak release rate from the waste form because of the linear transport processes imposed in the vadose and saturated zones, an estimate of the peak dose can be inferred by scaling the base case results by 8 or 17 to estimate doses for these release conditions. In the base case the peak groundwater

concentration from ^{129}I in ETF-LSW, which included 0.064 Ci ^{129}I in 18,900 m³ of grouted waste, is approximately 0.016 pCi/L (RPP-RPT-59958, Rev 1A, Figure 1-7). Using a unit dose conversion factor of 0.69 mrem/yr per pCi/L, this yields a dose at the 100-m buffer zone of 0.011 mrem/yr. Scaling this dose result by a factor of up to 17 to evaluate higher apparent diffusivity values yields a dose rate of 0.2 mrem/yr from ^{129}I in ETF-LSW. If 0.282 Ci of ^{129}I (1% of all the tank waste) ended up in ETF-LSW with an apparent diffusion coefficient equal to 5E-9 cm²/s and a K_d of 0 mL/g, then the peak dose rate from ^{129}I in ETF-LSW would be approximately 3.5 mrem/yr.

Figure 2-19-3. Comparison of Fractional Release Rates to Vadose Zone from Solidified Liquid Secondary Waste for Background Infiltration Rates of 1.7 mm/yr: Iodine-129.

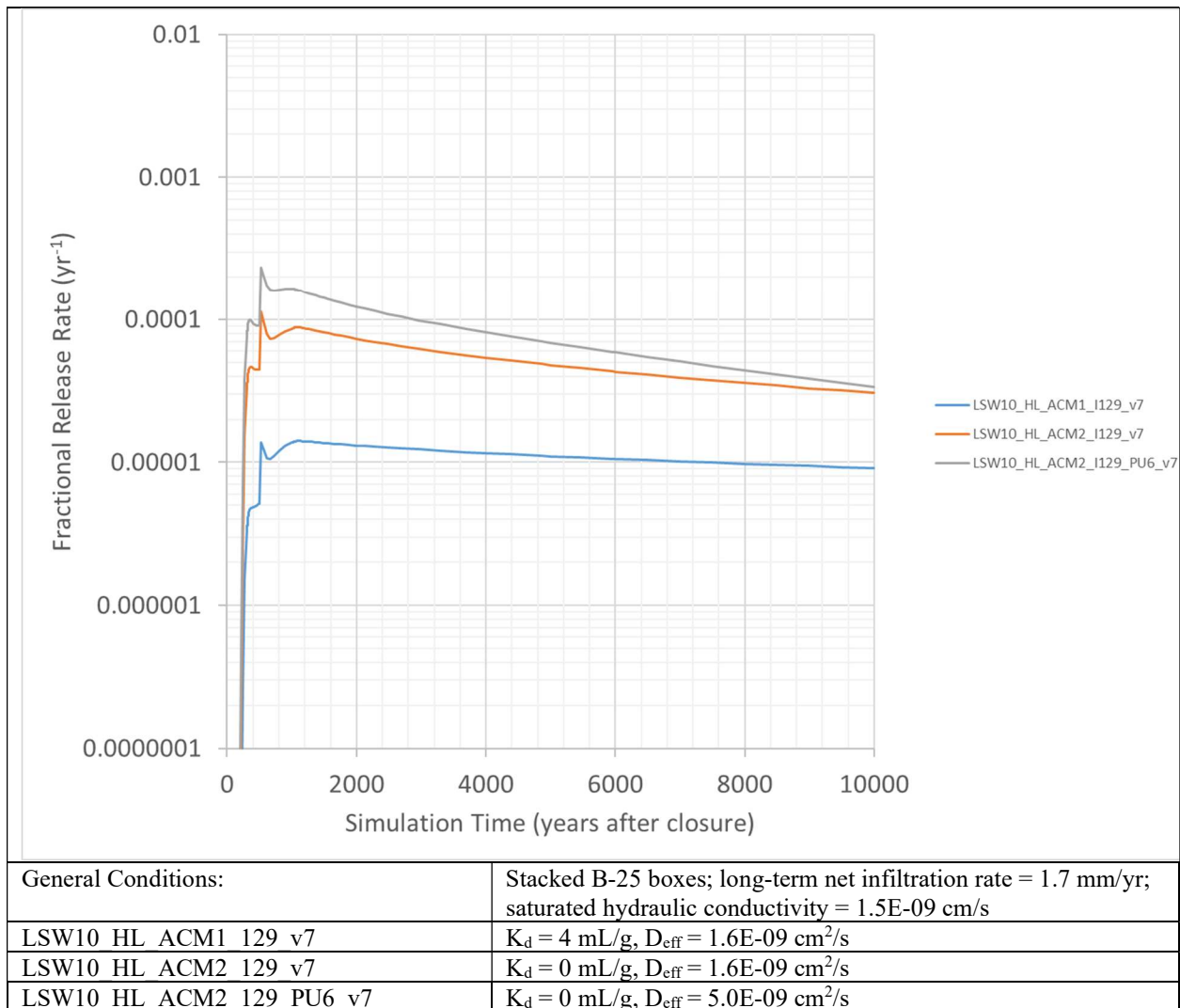
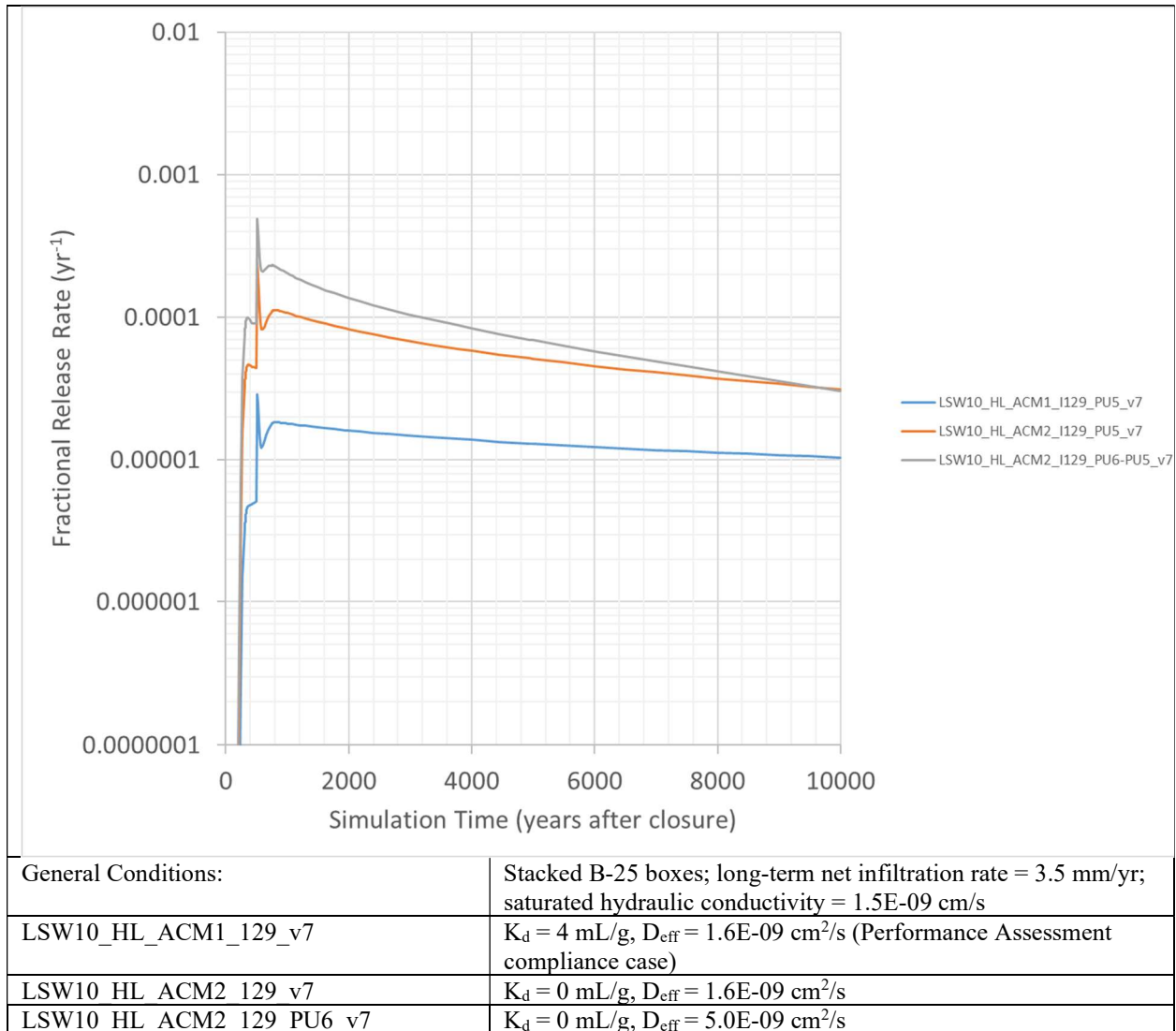


Figure 2-19-4. Comparison of Fractional Release Rates to Vadose Zone from Solidified Liquid Secondary Waste for Background Infiltration Rates of 3.5 mm/yr: Iodine-129.



Technetium:

The applied K_d for ^{99}Tc (0.8 mL/g) in the PA compliance case assumes oxidizing conditions for the grout; the simulation does not account for the strong reducing capability of the engineered grout that could have been simulated using a K_d value greater than 1,000 mL/g as long as the reducing capacity of the grout remains. As a result, DOE believes that the simulations for ^{99}Tc overestimate release and are appropriate for simulating this designed waste form in the PA dose assessment.

In addition, the only simulated difference between iodine and technetium when the waste form K_d is set to zero for both radionuclides is the decay rate and molecular weight. The primary transport parameters would be the same so that fractional release rates for both would be similar. This is verified by comparing the cumulative fractions released for process model simulations

LSW10_HL_ACM2_I129_PU6-PU5_v7 and LSW10_HL_ACM1_Tc99_PU6-PU5_v7. In both of these cases the simulated conditions are the same: two stacked B25 boxes; $D_{\text{eff}}=5\text{E-}9\text{ cm}^2/\text{s}$; $K_d=0\text{ mL/g}$; long-term net infiltration rate= 3.5 mm/yr ; and $K_{\text{sat}}=1.5\text{E-}9\text{ cm/s}$. In these runs 80.1% of the ^{129}I is released to the vadose zone in 10,000 years compared to 79.2% of the ^{99}Tc (RPP-CALC-61030 Tables 7-23 and 7-24). For the cases with $D_{\text{eff}}=1.6\text{E-}9\text{ cm}^2/\text{s}$ and $K_d=0\text{ mL/g}$ the percentage of each radionuclide released to the vadose zone are 53.9% for ^{129}I and 53.1% for ^{99}Tc (RPP-CALC-61030 Tables 7-23 and 7-24).

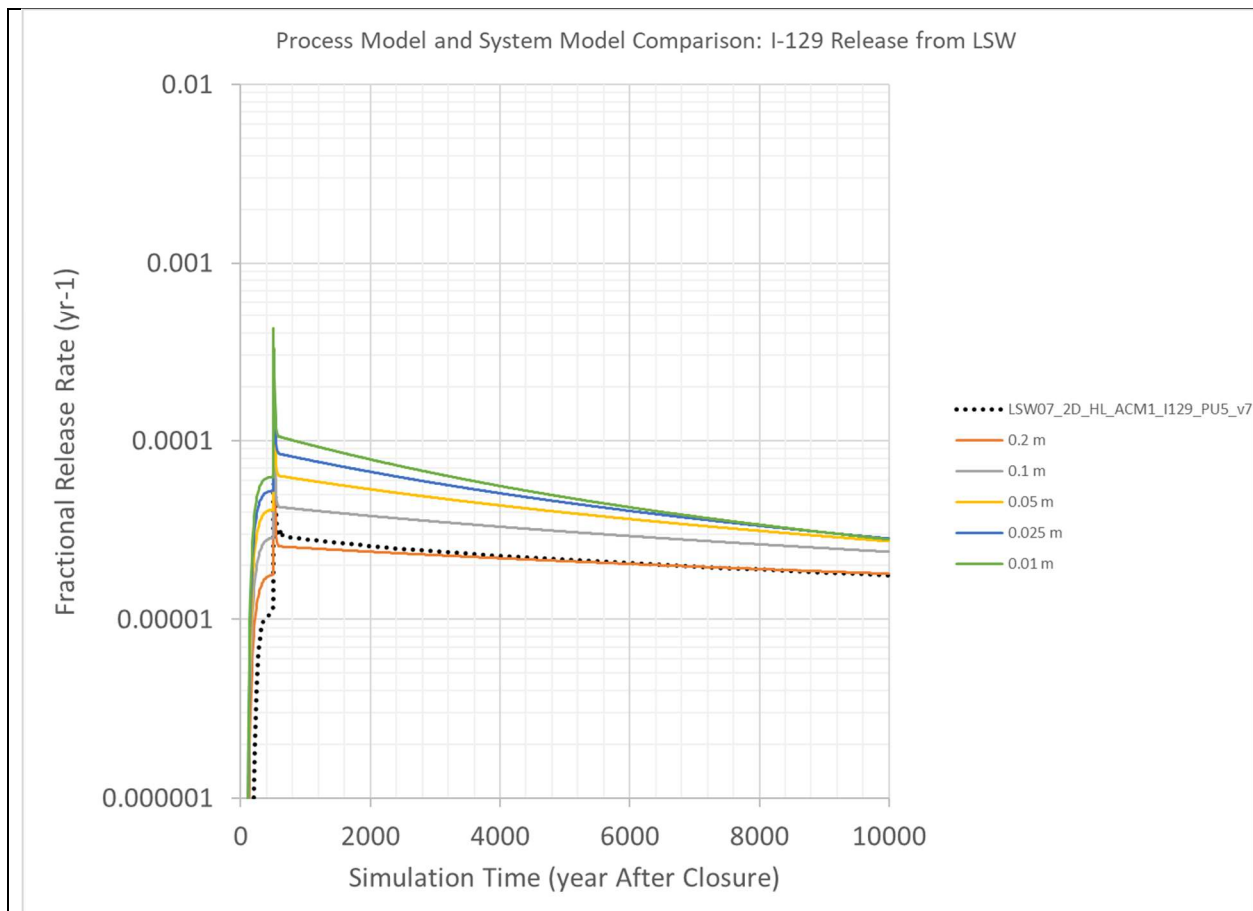
System Model Representation:

The implementation of the cementitious waste release model in the compliance case calculations and the abstracted model included in the system model are described in RPP-CALC-61030 and RPP-RPT-59726, *Integrated Disposal Facility Model Package Report: System Model*, respectively. Of particular distinction between the two models is the treatment of diffusion in the backfill surrounding the waste containers and how it influences diffusion out of a breached container. In the process model simulation (referred to in RPP-CALC-61030 as the Advective Diffusive Transport [ADT] model), the backfill diffusivity was artificially increased above the value that would be determined from the Millington-Quirk model for partially saturated media (see RPP-RPT-59958 Section 4.4.1.3.3 for discussion of the Millington-Quirk model for these waste forms). The diffusivity was increased by setting the tortuosity of the backfill to 1. Consequently, the effective diffusivities differ only by the different porosity and saturation in the waste form and the backfill⁶⁶. These changes were implemented to minimize the influence of harmonic averaging of the diffusive conductance between adjacent nodes representing the waste form and backfill. Owing to the low saturations in the backfill surrounding the waste containers, the Millington-Quirk model would have predicted very low tortuosity in the backfill, which due to harmonic averaging of the diffusive conductance between adjacent nodes in the computational grid, would have limited diffusion into the backfill from the waste form. This was verified using an alternate representation of waste form release referred to in DOE/EIS-0391 as the Shrinking Core Diffusion Model for cementitious waste forms. Because the backfill also has an advective component to transport and this component was previously shown to be the dominant transport mechanism in the backfill in DOE/EIS-0391, it was decided to equate the effective diffusion coefficient for the backfill to the diffusion coefficient of the waste and set the tortuosity in the backfill to unity to minimize the influence of harmonic averaging that would constrain releases from the ETF-LSW waste package. When this change was made, the releases to the vadose zone had much better agreement with results reported in DOE/EIS-0391. An alternate method to increase the node discretization by using smaller grid block sizes near the waste form / backfill interface was considered. However, the amount of discretization necessary to minimize harmonic average affects would have made computational times excessively long to represent a minor transport pathway in the backfill.

⁶⁶ By setting the tortuosity of the backfill to 1, the backfill has the same effective diffusivity as the LSW, because the diffusion coefficient specified in STOMP is per species (i.e., Tc-99 or I-129), not material. Thus, the only difference arises from the porosity and saturation assigned to the backfill and LSW (in Stomp the measured diffusivity is multiplied by porosity and saturation). For SSW, the tortuosity of the backfill was also set such that the diffusivity of the grout and backfill was the same.

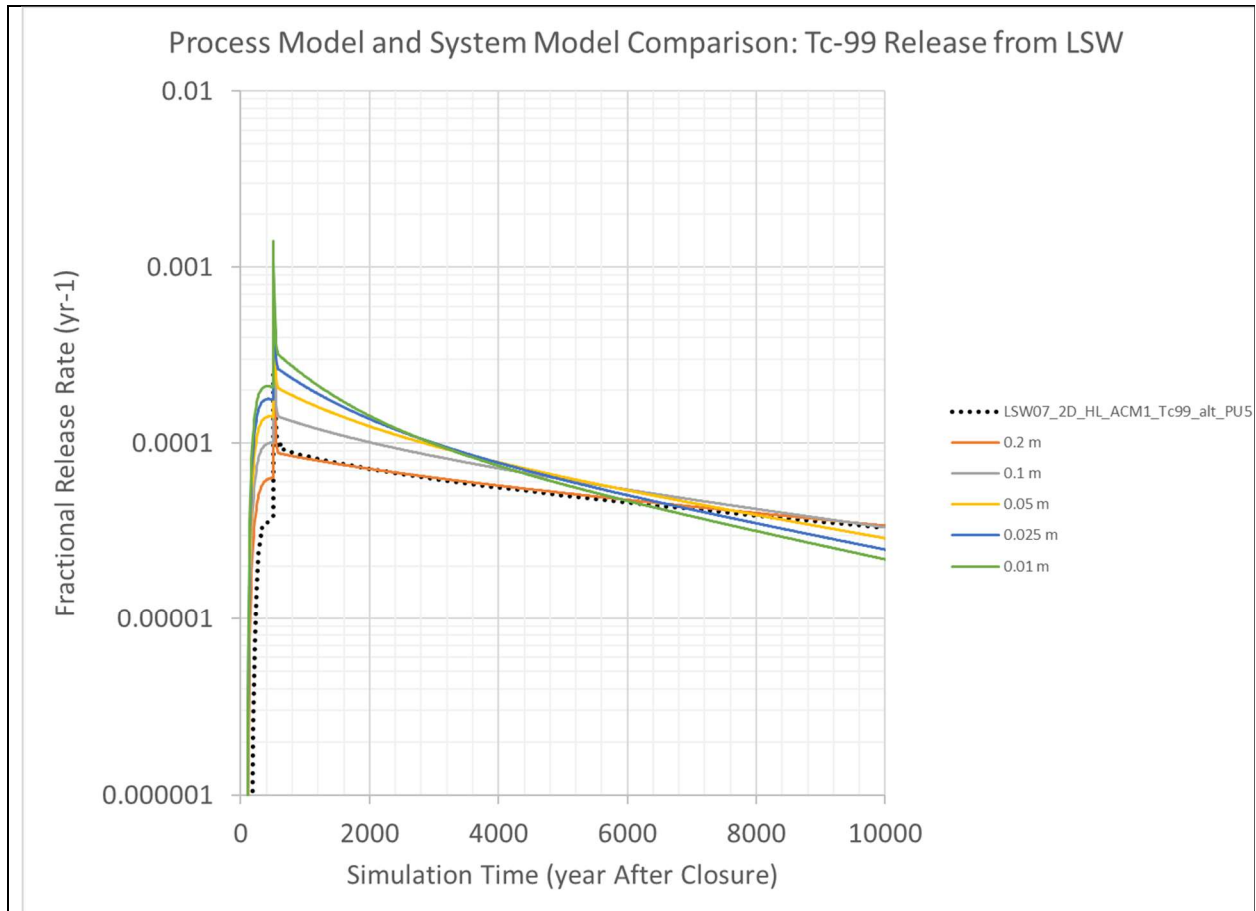
In the process model, separate simulations are performed for each waste form and contaminant; therefore, it is possible to specify different backfill properties for SSW and LSW to account for the condition specified above. However, in the system model the effective diffusion coefficient for the backfill (and the tortuosity) is shared by the LSW and SSW release models. Therefore, it was not possible to impose the same manipulation of backfill properties for LSW releases that was used in the process model without defining two different media elements to represent the same backfill material. To ensure that waste form releases from the LSW were still controlled by diffusion across the waste form / backfill interface, the diffusive length was adjusted until the simulated releases using the system model abstraction had good agreement with the process model result. Examples of system model calculations evaluating different diffusive lengths for a comparison to the process model results are shown in **Figures 2-19-5** and **2-19-6**. Note that these are new calculations developed for this RAI response; however, a similar analysis was performed during system model development but those results have not been reported previously. A good agreement was determined by comparing peak release rates to the vadose zone and total cumulative releases in 10,000 years. Faster releases in the system model were acceptable when both metrics could not be obtained within 5%.

Figure 2-19-5. System Model Development of the Diffusive Length in the Backfill near Packages of Liquid Secondary Waste: Iodine-129.



LSW = liquid secondary waste

Figure 2-19-6. System Model Development of the Diffusive Length in the Backfill near Packages of Liquid Secondary Waste: Technetium-99.



LSW = liquid secondary waste

When the diffusive length was set to the maximum anticipated spacing between waste containers (0.2 m), the peak release rates, which drive groundwater impacts and dose in the groundwater pathway scenario, were 63% and 77% higher in the system model than in the process model for ^{129}I and ^{99}Tc , respectively. The cumulative releases of ^{129}I and ^{99}Tc from LSW in the two models had better agreement. The total ^{129}I released in the process model was 21.1% of the initial inventory (RPP-CALC-61030 Table 7-29) compared to 20.9% of the initial inventory in the system model. The cumulative release of ^{99}Tc from LSW was 51.0% of the initial inventory (RPP-CALC-61030 Table 7-29) in the process model and 53.6% of the initial inventory in the system model. These system model results were considered acceptable for the intended use of the system model to evaluate parameter uncertainty and perform other sensitivities knowing that the peak impacts to groundwater and a member of the public in the future occur in the sensitivity analysis period that follows DOE's time of compliance.

References

DOE/EIS-0391, 2012, *Final Tank Closure and Waste Management Environmental Impact Statement for the Hanford Site*, Richland, Washington, U.S. Department of Energy, Washington, D.C.

PNNL-25194, 2016, *Secondary Waste Cementitious Waste Form Data Package for the Integrated Disposal Facility Performance Assessment*, RPT-SWCS-006, Rev. 0, Pacific Northwest National Laboratory, Richland, Washington.

PNNL-26443, 2017, *Updated Liquid Secondary Waste Grout Formulation and Preliminary Waste Form Qualification*, RPT-SWCS-009, Rev. 0, Pacific Northwest National Laboratory, Richland, Washington.

RPP-CALC-61030, 2017, *Cementitious Waste Form Release Calculations for the Integrated Disposal Facility Performance Assessment*, Rev. 0, INTERA, Inc. for Washington River Protection Solutions, LLC, Richland, Washington.

RPP-RPT-59726, 2017, *Integrated Disposal Facility Model Package Report: System Model*, Rev. 0, INTERA, Inc. for Washington River Protection Solutions, LLC, Richland, Washington.

RPP-RPT-59958, 2019, *Performance Assessment for the Integrated Disposal Facility, Hanford Site, Washington*, Rev. 1A, Washington River Protection Solutions, LLC, Richland, Washington.

RAI 2-20 (I Sorption on the SSW-GAC and SSW-AGM Wasteforms)**Comment**

Additional information is needed for the assumed sorption of ^{129}I on the SSW-GAC (Granular Activated Carbon) and SSW-AgM (Silver Mordenite) wasteforms.

Basis

The modeled release of ^{129}I from the SSW-GAC and SSW-AgM wasteforms is significantly reduced by the assumed sorption of the ^{129}I onto these wasteforms. The assumed distributions of the distribution coefficient (Kd) values for ^{129}I on the SSW-GAC and SSW-AgM wasteforms are much larger than the distributions assumed for the other cementitious wasteforms in this model and are much larger than typically observed Kd values for ^{129}I on cementitious materials.

The Kd values assumed for ^{129}I for the SSW-GAC and the SSW-AgM wasteforms are based on an average of a Kd value for sorption of ^{129}I onto a typical cementitious material and the sorption of ^{129}I onto GAC or AgM. Although the sorption of the ^{129}I onto the GAC and AgM contained in these wasteforms could improve the overall sorption of ^{129}I on these wasteforms compared to typical cementitious wasteforms, the sorption on the combined material might not be equal to the average sorption of its components due to changes in the chemical environment in the wasteform. It is not clear what support exists for the Kd values assumed in the GoldSim Model, and it is not clear if analytical measurements of the ^{129}I sorption on simulated wasteforms comparable to the SSW-GAC and SSW-AgM wasteforms have been performed.

The sorptive capacity of ^{129}I on the waste forms for the SSW-GAC and the SSW-AgM waste streams was identified during the LFRG review as issue number ISF-S09-PA03-02. As a corrective action/resolution for this issue, a sensitivity case was performed for the air pathway that used Kd values that were lower than were previously assumed but were still much higher than for typical cementitious materials. However, a sensitivity analysis was not performed to evaluate the potential effect of less sorption of ^{129}I on these wasteforms on the dose. The corrective action/resolution states that the “full range of uncertainty in the Kd values was considered in the probabilistic analysis” for the groundwater pathway. However, the entire range of Kd values included in the GoldSim model is high and this range does not appear to capture the potential for the sorption of ^{129}I to be much lower than assumed. The corrective action/resolution to this issue also stated that R&D activities were expected to be performed in the future to characterize the Kd on the carbon media and silver mordenite waste forms.

Path Forward

Please provide additional information to support the assumed Kd values for ^{129}I on the SSWGAC and the SSW-AgM wasteforms, and if any R&D activities have taken place on this topic to date, provide the results of those activities. Alternatively, provide a sensitivity analysis showing the effect on the release rates and potential dose from ^{129}I from these two wasteforms if the sorption on these wasteforms is lower than assumed in the model.

DOE Response

The Draft WIR Evaluation addresses the WIR criteria for VLAW produced using the DFLAW approach. Other wastes are outside the scope of the Draft WIR Evaluation, including secondary

waste and vitrified waste produced after the DFLAW mission is completed. Vitrified waste produced after the DFLAW mission is completed includes vitrification at the WTP LAW Vitrification Facility following pre-treatment at the WTP Pre-Treatment Facility⁶⁷ and vitrification at a potential WTP Supplemental LAW Facility (for which DOE has made no decision to pursue).⁶⁸ To bound the analysis, the IDF PA correctly includes all wastes potentially disposed of in the IDF, including the DFLAW-produced VLAW as well as additional VLAW,⁶⁹ and all SSW which may be disposed at IDF. DOE recognizes the importance of the IDF PA to the WIR evaluation and provides the following response for additional information only on this RAI that addresses the SSW included in the PA.

DOE acknowledges that there is uncertainty in the capability of the cement waste forms for carbon adsorption media (SSW-GAC) and silver mordenite (SSW-AgM⁷⁰) to retain iodine. In the PA models, enhanced retention of iodine was simulated in these two waste forms relative to other cementitious waste forms to be consistent with the known enhanced sorptive characteristics of the types of pure media included in these waste forms. The enhanced sorptive characteristics of these two media are the reason that they are used in the operation of the off-gas treatment systems. Iodine sorption onto SSW-GAC was simulated in the base case with a sorption coefficient of 302 mL/g and a range of values from 70 mL/g to 989 mL/g in the uncertainty analysis. Iodine sorption onto SSW-AgM was simulated in the base case with a sorption coefficient of 502 mL/g and a range of values from 96 mL/g to 4,750 mL/g in the uncertainty analysis. As discussed in the RAI, these distribution coefficients are the arithmetic average of values for grout and the media. These values do not account for any chemical change to the waste form environment or loss of performance over time. These assumed values in the IDF PA were noted as a critical assumption requiring confirmation in Section 1.5.5 of the IDF PA (RPP-RPT-59958). As a critical assumption that needs to be verified, laboratory research to

⁶⁷ After DFLAW operations are completed, vitrification of additional LAW in the WTP LAW Vitrification Facility will follow pre-treatment at the WTP Pre-Treatment Facility. The Draft WIR Evaluation only includes vitrified LAW produced using the DFLAW approach; therefore, vitrification at the WTP LAW Vitrification Facility after DFLAW is outside the scope of the Draft WIR Evaluation. The discussion of the PA results for WTP-vitrified LAW generated during this post-DFLAW time period is provided for additional information and completeness, and is outside the scope of the Draft WIR Evaluation.

⁶⁸ Information concerning the secondary waste associated with the supplemental LAW is provided in this RAI response for additional information and completeness only, and is outside the scope of both the Draft WIR Evaluation and DOE decisions concerning supplemental LAW treatment. DOE has not made decisions concerning the potential path forward for supplemental LAW treatment, as explained in footnote 7 of the Draft WIR Evaluation and the 78 FR 75913, "Record of Decision: Final Tank Closure and Waste Management Environmental Impact Statement for the Hanford Site, Richland, Washington." As explained in Section 1.2 of the Draft WIR Evaluation, the Draft WIR Evaluation does not address or include in its scope supplemental LAW. To bound the IDF PA analysis, the IDF PA assumed that supplemental LAW may potentially be vitrified and disposed of in the IDF, although, as explained above, DOE has made no decisions concerning the potential path forward for supplemental LAW treatment.

⁶⁹ See footnotes 67 and 68.

⁷⁰ Silver mordenite columns are part of the off-gas treatment system in the WTP HLW Vitrification Facility, which will not be operational during the DFLAW time period covered by the Draft WIR Evaluation.

collect data to verify the assumed values was included in the Research and Development section of the PA Maintenance Plan (CHPRC-03348).

“Evaluate bulk (i.e., average) transport properties (notably distribution coefficient [K_d]) of solidified nondebris waste streams, with special focus on the retention of iodine-129 on the granular activated carbon (GAC) and silver mordenite substrate materials”.

Beginning in FY 2019, DOE began collecting data to support this critical assumption. The most recent work to develop data to support this critical assumption was completed in September 2020 in PNNL-28545, *Development and Characterization of Cementitious Waste Forms for Immobilization of Granular Activated Carbon, Silver Mordenite, and HEPA Filter Media Solid Secondary Waste*.

The report concluded that grout formulations that were used in the IDF PA to solidify non-debris waste streams such as spent carbon adsorption media and AgM are capable of stabilizing the media. The research report included results from sorption experiments and EPA 1315 leaching experiments with stabilized GAC and AgM. For the carbon adsorption media stabilized with a typical Hanford grout formulation (like Hanford Grout Mix 5 used as the representative grout in the IDF PA), the iodide diffusivities were lower than the best-estimate and optimistic values reported for a mobile species from a mortar in the SSW data package that developed input values for the PA (SRNL-STI-2016-00175, *Solid Secondary Waste Data Package Supporting Hanford Integrated Disposal Facility Performance Assessment*). Releases from the waste form decrease with decreases in diffusivities. The stabilized AgM grout samples using a typical Hanford grout formulation did not produce measurable iodide in the leachates, and only “maximum” diffusivity values could be reported⁷¹. These values were more than four orders of magnitude lower than the mobile species value in the data package. The diffusivity values reported in PNNL-28545 for a typical Hanford grout formulation were used to estimate a K_d value for these waste forms that is consistent with the disposal conditions. The K_d is estimated from the measured properties using RPP-RPT-59958 Rev 1A, Equations 4.4.1.3-10 and 4.4.1.3-11, which are combined in Equation 2.20-1. The apparent or observed diffusion coefficient is a lumped parameter that accounts for diffusion and sorption. In contrast, the effective diffusion coefficient in the following equations does not account for sorption and is estimated in the laboratory using a non-sorbing species.⁷²

$$D_{app} = \frac{D_{eff}}{\left[1 + \frac{(1-n)\rho_s K_d}{Sn}\right]} \quad (2.20-1a)$$

⁷¹ The values are referred to as “maximum” values but are very low. The values are determined using leachate concentrations that are higher than observed in the leachate, which means they overestimate the diffusivity.

⁷² These definitions of effective and apparent diffusion coefficients are consistent with the usage in the SSW data package (SRNL-STI-2016-00175) and the IDF PA. PNNL-28545 uses laboratory experiments to measure the diffusion coefficient, but these measurements determine the lumped parameter that accounts for diffusion and sorption. PNNL-28545 refers to the lumped parameter as the observed or effective diffusivity; however, the lumped value that accounts for sorption is consistent with the term apparent diffusivity used in the PA and SSW data package and in this RAI response.

Or,

$$K_d = \left[\frac{D_{eff}}{D_{app}} - 1 \right] \left[\frac{Sn}{(1-n)\rho_s} \right] = \left[\frac{D_{eff}}{D_{app}} - 1 \right] \left[\frac{Sn}{\rho_b} \right] \quad (2.20-1b)$$

Where:

D_{app}	=	“apparent” or “observed” diffusion coefficient
D_{eff}	=	“effective” diffusion coefficient
n	=	porosity
ρ_s	=	solid density
ρ_b	=	dry bulk density (= $(1 - n)\rho_s$)
K_d	=	distribution coefficient
S	=	saturation

Distribution Coefficient Estimation

For carbon adsorption media stabilized using a typical Hanford grout (SSW-GAC) contacted by a simulant representing Hanford pore water, the apparent diffusivity from the EPA 1315 leachate test (performed in duplicate) was $4.80E-10 \text{ cm}^2/\text{s}$ (PNNL-28545 Table 7-2). The measured value leached with de-ionized water (DIW) was $1.1E-09 \text{ cm}^2/\text{s}$ (PNNL-28545 Table 7-2). The measured porosity of a 30% GAC/grout mixture was 0.388 (PNNL-28545 Table 5-4). The average bulk density of a 30% GAC/grout mixture was 1.509 g/cm^3 (PNNL-28545 Table E.6). Saturation and the diffusivity for a non-sorbing species were not reported in PNNL-28545. A saturation for the leaching test of 99% was assumed. The diffusivity for a non-sorbing contaminant used in the PA was assumed for the calculation to estimate the K_d observed in the leaching tests.

$$K_d = \left[\frac{5.4E - 08 \frac{\text{cm}^2}{\text{s}}}{4.8E - 10 \frac{\text{cm}^2}{\text{s}}} - 1 \right] \left[\frac{0.99 \times 0.388}{1.509 \frac{\text{g}}{\text{cm}^3} \times 1 \frac{\text{cm}^3}{\text{ml}}} \right] = 28.4 \text{ ml/g}$$

Following the same methodology for the experiment conducted in DIW, the estimated K_d value for SSW-GAC with an average reported density of 1.482 g/cm^3 leached by DIW is 12.5 mL/g . These estimated values are lower than the PA base case and lower than the range of values considered in the uncertainty analysis. The values are similar to the adsorption K_d for iodine and GAC in a pore water equilibrated with grout (16 mL/g reported in PNNL-28545 Table 6-3). A process model simulation reported in RPP-CALC-61030 evaluated a distribution coefficient as low as 50 mL/g . Although this result was not carried forward to dose, the cumulative releases to the vadose zone were reported and can be quantitatively compared. In this sensitivity case, the cumulative fractions released to the vadose zone in 1,000 and 10,000 years increased by factors of 5.9 and 5.5, respectively, compared to the equivalent case that used a 302 mL/g for the distribution coefficient⁷³. This comparison uses the cumulative fractions released in case

⁷³ Although the increase is nearly proportional to the change in distribution coefficients, the relationship between cumulative fraction released and distribution coefficient is non-linear. Disproportionally higher releases would be expected using distribution coefficient values that are lower than 50 mL/g .

GAC_ACM1_I129_v7 that are reported in RPP-CALC-61030 Table 7-4 and the fractions released in case GAC_ACM2_I129_PU7_v7 reported in RPP-CALC-61030 Table 7-15.

Because the effective diffusion coefficient for a non-sorbing species in SSW-GAC was not reported in PNNL-28545, there is uncertainty in this value, which means there is uncertainty in the K_d determined using this value. If the effective diffusion coefficient for a non-sorbing species is an order of magnitude lower than the value used from the PA for a mortar, then the K_d value decreases to 2.6 g/mL, a value that is consistent for cementitious material without accounting for any sorption onto the spent media that was used to capture it by sorption in the off-gas treatment system.

$$K_d = \left[\frac{5.4E - 09 \frac{cm^2}{s}}{4.8E - 10 \frac{cm^2}{s}} - 1 \right] \left[\frac{0.99 \times 0.388}{1.505 \frac{g}{cm^3} \times 1 \frac{cm^3}{ml}} \right] = 2.6 \text{ ml/g}$$

Following the same methodology for the experiment conducted in DIW, the estimated K_d value for SSW-GAC with a reported density of 1.482 g/cm³ leached by DIW is 1.0 mL/g.

The second part of this RAI response evaluates the dose using these revised parameter values for SSW-GAC.

For AgM stabilized using a typical Hanford grout (SSW-AgM) contacted by a simulant representing Hanford pore water, the apparent diffusivity from the EPA 1315 leachate test (performed in duplicate) was 4.90E-13 cm²/s (PNNL-28545 Table 7-2 and page 7.5). This value is determined by detection limits because iodine was not measured in the leachate. The average bulk density of the stabilized AgM was 1.169 g/cm³ (PNNL-28545 Table E.8). Porosity, saturation and the effective diffusivity for a mobile species were not measured in PNNL-28545. Therefore, the values used in the PA are substituted into Equation 2.20-1b to estimate the K_d observed in the leaching tests.

$$K_d = \left[\frac{5.4E - 08 \frac{cm^2}{s}}{4.9E - 13 \frac{cm^2}{s}} - 1 \right] \left[\frac{0.99 \times 0.24}{1.169 \frac{g}{cm^3} \times 1 \frac{cm^3}{ml}} \right] = 22,400 \text{ ml/g}$$

The estimated value is much greater than the PA base case and greater than the range of values considered in the uncertainty analysis. Even when the diffusivity for a non-sorbing species is reduced by a factor of 10 and the porosity is changed to values between 0.1 and 0.6, the calculated K_d values are still above what was simulated in the PA. Based on this analysis, SSW-AgM does not warrant a re-evaluation following DOE's change control process.

Re-Evaluation of SSW-GAC

The IDF PA system model was re-run with iodine distribution coefficients in SSW-GAC set to 28.4 mL/g, 12.5 mL/g, and 2.6 mL/g. The initial inventory of iodine sorbed to the GAC prior to disposal was unchanged despite the observation in this report that iodine retention on GAC is

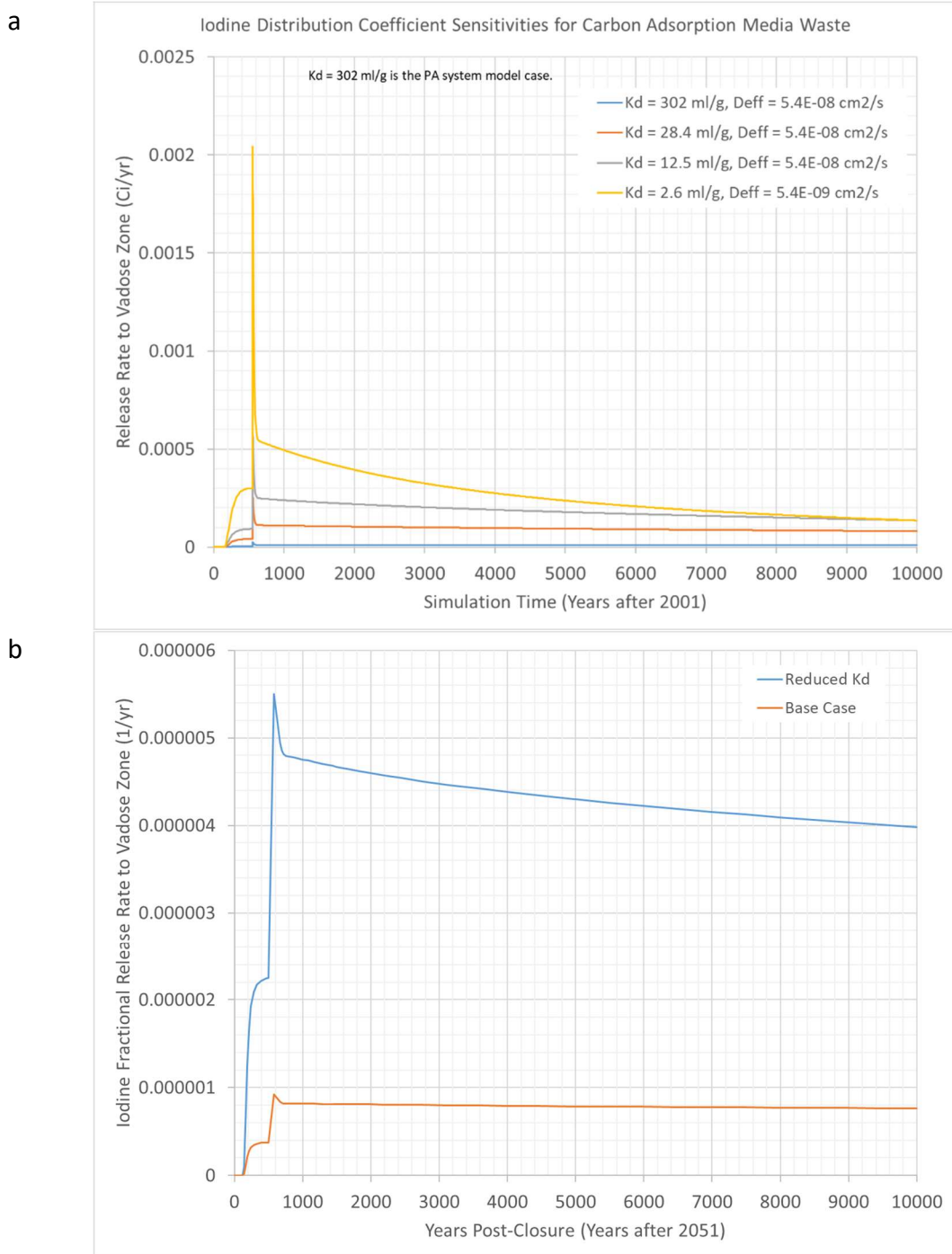
lower than previously thought. The effective diffusivity for a non-sorbing species was also reduced to $5.4\text{E-}09\text{ cm}^2/\text{s}$ in the latter sensitivity case. **Figure 2-20-1** and **Figure 2-20-2** show the comparable release rates and cumulative releases from the IDF to the vadose zone and **Figure 2-20-3** shows the simulated groundwater concentrations and corresponding dose results. Consistent with the dose results presented in the PA, the system model dose for SSW sources includes all SSW sources. Therefore, the dose results shown in **Figure 2-20-3** include other SSW sources, but the dose from the other SSW sources are computed using the base case conditions for those waste streams.

The iodine release rates to the vadose zone from SSW-GAC shown in **Figure 2-20-1** illustrate that release rates using the new acquired K_{ds} for the SSW-GAC waste stream are higher than the PA reference case. These release rates have a similar shape, with a release rate that slowly increases as iodine released from the waste containers reaches the bottom of the IDF. There is a sudden increase in the release rate 500 years after closure when the surface barrier performance degrades and a greater amount of water flows into the IDF. At this time all of the mass that was in the process of being transported to the bottom of the IDF before the increase in flow occurred is rapidly transported to the bottom of the IDF with the increased flow. After this sharp increase the rates drop and releases are governed by the diffusive release from the waste package. The release rates are generally higher for lower K_d values, which is expected for the diffusive release model with some sorption.

Figure 2-20-2 shows the cumulative release to the vadose zone when the rates applied in **Figure 2-20-1** are integrated. The cumulative release in 10,000 years is about 9 times higher for the 28.4 mL/g case than it is in the system model base case. This can be compared with the STOMP simulations that showed a 5.5 to 6 factor increase for a 50 mL/g case (the integrated rates shown in **Figure 2-20-1b**). In the case with the highest releases, the cumulative amount released in 10,000 years amounts to about 20% of the initial inventory allocated to the SSW-GAC.

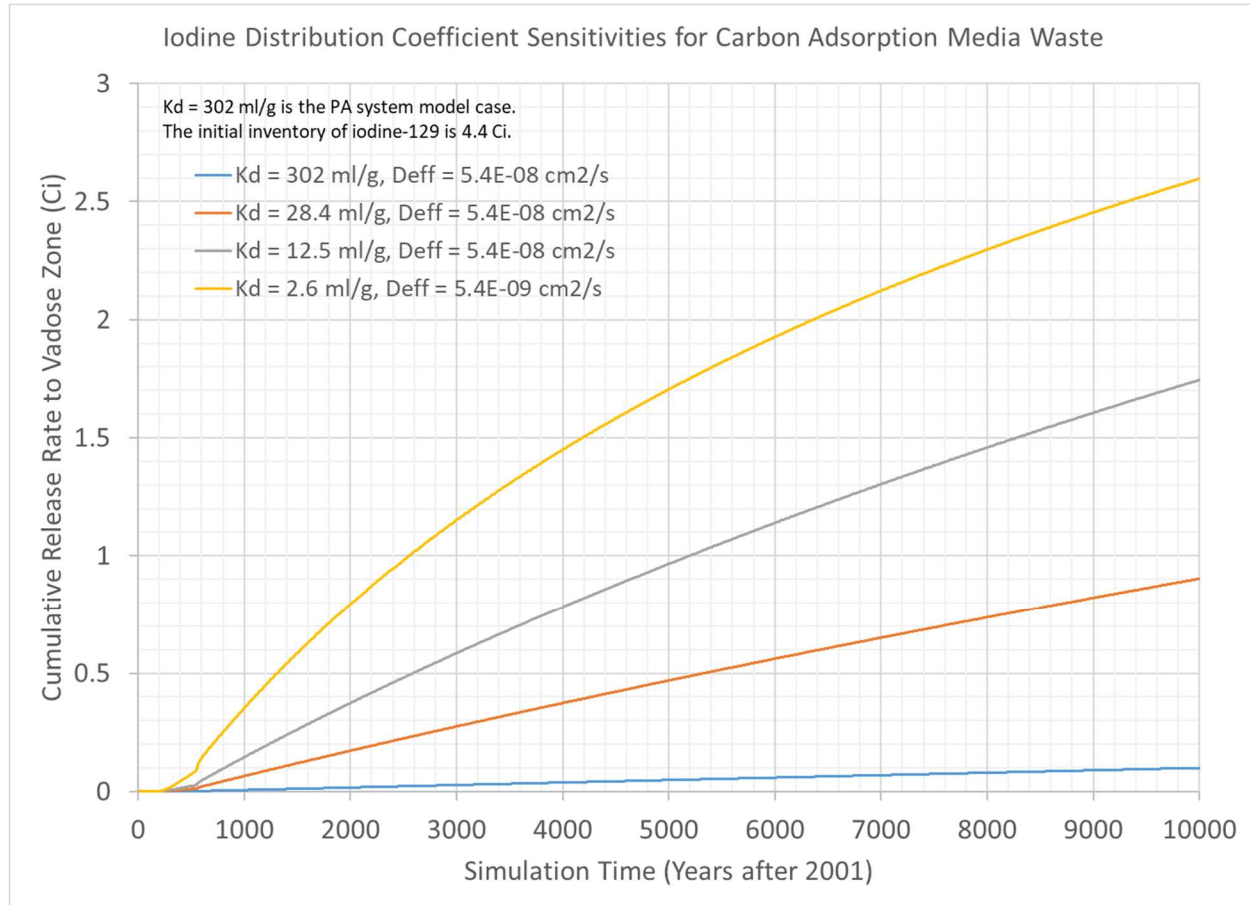
Figure 2-20-3 shows the simulated groundwater concentrations from all SSW waste streams for the different sensitivity cases. All of the difference is attributed to the change in iodine retention in SSW-GAC. Due to sorption in the vadose zone, iodine reaches the groundwater after the DOE time of compliance has passed. After this time, the iodine concentrations in the groundwater increase to levels that exceed the safe drinking water level, which is 1 pCi/L. However, the simulated concentrations are all lower than the concentration that results in a 4 mrem/yr drinking water dose using conversion factors from DOE-STD-1196-2011, *Derived Concentration Technical Standard*. The peak iodine dose from all SSW sources increased by a factor of 3.2 from 1.1 mrem/yr to 3.5 mrem/yr when the SSW-GAC distribution coefficient for iodine decreased from 302 mL/g to 28.4 mL/g. The peak dose was 6.3 mrem/yr when the SSW-GAC k_d is reduced to 12.5 mL/g. In both cases the peak dose occurred more than 7,000 years after closure. The peak dose occurs after the DOE time of compliance and is lower than DOE's All-Pathways dose limit (25 mrem/yr).

Figure 2-20-1. Iodine-129 Release Rate to Vadose Zone from Carbon Adsorption Media: Solid Secondary Waste-Granular Activated Carbon Sensitivity Studies
a) System Model, b) Process Model (fractional release rate).



Note: In the Performance Assessment system model, some inventory is provided with a decay date in 2001. This inventory is decayed within the model until the time of assumed Integrated Disposal Facility closure in 2051. Therefore, time zero in the simulations shown in Figure 2-20-1a is 2001. For Figure 2-20-1b, closure was assumed to be 30 years after the start of low-activity waste vitrification in 2021.

Figure 2-20-2. Iodine-129 Cumulative Release to Vadose Zone from Solidified Carbon Adsorption Media: Solid Secondary Waste-Granular Activated Carbon Sensitivity Studies.



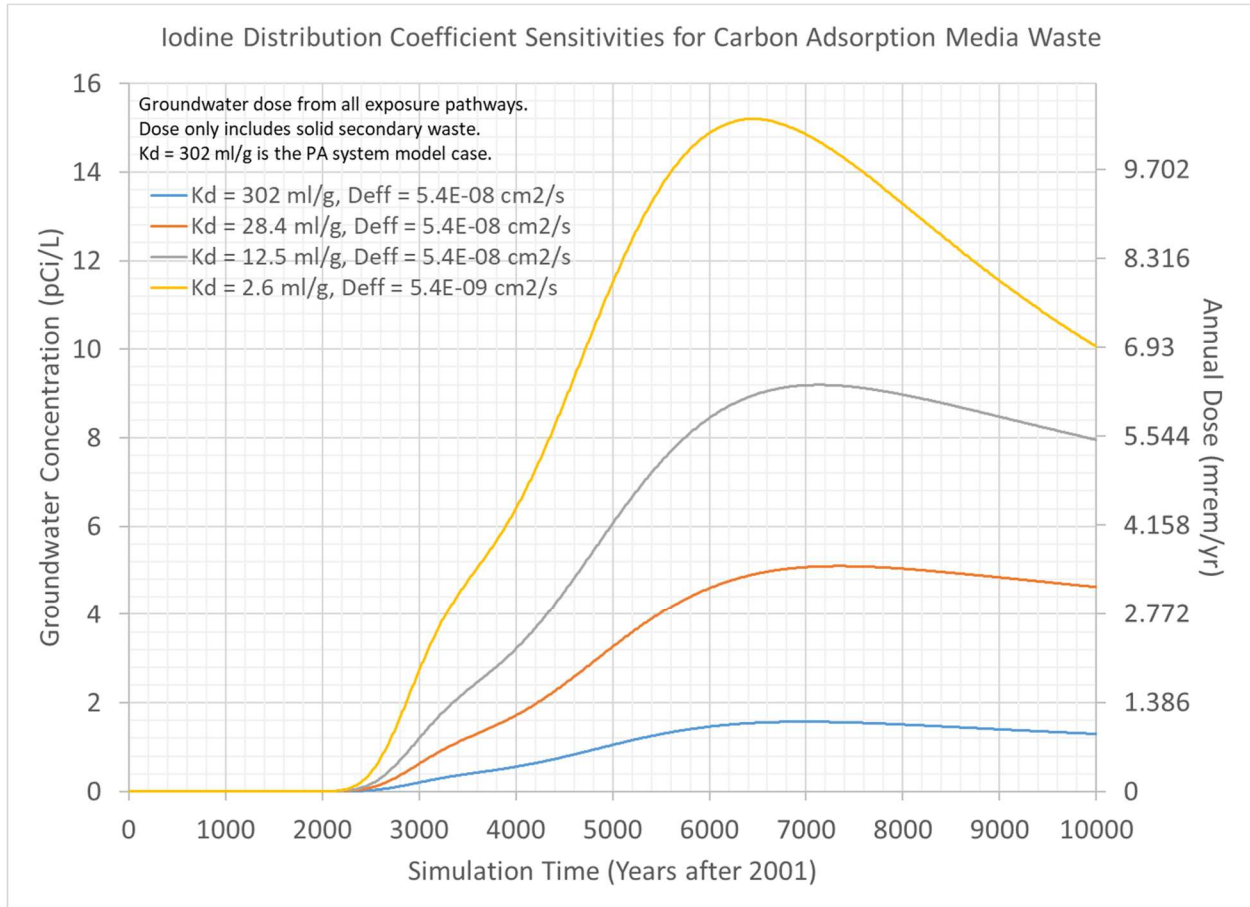
Note: In the Performance Assessment (PA) system model, some inventory is provided with a decay date in 2001. This inventory is decayed within the model until the time of assumed Integrated Disposal Facility closure in 2051. Therefore, time zero in the simulations is 2001.

When the SSW-GAC distribution coefficient for iodine decreased from 302 mL/g to 2.6 mL/g and the effective diffusion coefficient for a non-sorbing species is reduced from 5.4E-08 cm²/s to 5.4E-09 cm²/s, the peak dose increased to 10.5 mrem/yr, but occurred more than 6,300 years after closure.

Additional Information

The new data collection effort completed in September 2020 includes new parameter values for SSW other than the distribution coefficients that are the subject of this RAI response, which has been provided as additional information because SSW is outside the scope of the Draft WIR Evaluation. These other measured SSW properties include: porosity, density, and saturated hydraulic conductivity. The new information will be evaluated using the established PA change control process later this year.

Figure 2-20-3. Iodine-129 Groundwater Concentration and Annual Dose Solidified Carbon Adsorption Media: Solid Secondary Waste-Granular Activated Carbon Sensitivity Studies.



Note: The groundwater concentration can be converted to an annual dose using the conversion factor 0.69 (mrem/yr) / (pCi/L).

Note: The inventory of ¹²⁹I simulated in the carbon adsorption bed waste is 4.4 Ci, which is 15% of the ¹²⁹I estimated to be in the tank farm tanks. More recent flowsheets indicate 96% of the ¹²⁹I estimated to be in the tank farm tanks is vitrified. This means that the amount of ¹²⁹I expected to be in this waste stream will be much lower than 4.4 Ci.

The initial results presented in this RAI response will be formally evaluated in a Special Analysis that becomes part of the IDF PA technical basis. However, because the peak dose impact is less than the DOE performance objective and occurs more than 1,000 years after closure, the conclusions of the PA will not change. An evaluation of other parameters reported in PNNL-28545 will also be included in the forthcoming Unreviewed Waste Disposal Question analysis.

References

- 78 FR 75913, 2013, “Record of Decision: Final Tank Closure and Waste Management Environmental Impact Statement for the Hanford Site, Richland, Washington,” *Federal Register*, Vol. 78, pp. 75913–75919 (December 13).
- CHPRC-03348, 2019, *Performance Assessment Maintenance Plan for the Integrated Disposal Facility*, Rev. 1, INTERA, Inc./CH2M HILL Plateau Remediation Company, Richland, Washington.
- DOE-STD-1196-2011, 2011, *Derived Concentration Technical Standard*, U.S. Department of Energy, Washington, D.C.
- PNNL-28545, 2020, *Development and Characterization of Cementitious Waste Forms for Immobilization of Granular Activated Carbon, Silver Mordenite, and HEPA Filter Media Solid Secondary Waste*, Rev. 1, RPT-SWCS-014, Rev. 1.0, Pacific Northwest National Laboratory, Richland, Washington.
- RPP-CALC-61030, 2017, *Cementitious Waste Form Release Calculations for the Integrated Disposal Facility Performance Assessment*, Rev. 0, INTERA, Inc. for Washington River Protection Solutions, LLC, Richland, Washington.
- RPP-RPT-59958, 2019, *Performance Assessment for the Integrated Disposal Facility, Hanford Site, Washington*, Rev. 1A, Washington River Protection Solutions, LLC, Richland, Washington.
- SRNL-STI-2016-00175, 2016, *Solid Secondary Waste Data Package Supporting Hanford Integrated Disposal Facility Performance Assessment*, Rev. 0, Savannah River National Laboratory, Savannah River Nuclear Solutions, Aiken, South Carolina.

RAI 2-21 (Releases from Cementitious Wasteforms)**Comment**

More information is needed on the process for determining and evaluating the final cementitious grout specifications for waste streams stabilized with cementitious grout.

Basis

In the PA document, DOE indicated that secondary waste streams generated as the result of WTP operations will be solidified or encapsulated using cementitious materials. The PA document states that the “final specification of the solidification and encapsulation matrices, however, are currently uncertain and will eventually be selected on the bases of several performance factors: adequate mechanical strength for handling, transportation and emplacement; compatibility with other engineered barriers and waste forms in the IDF; [and] limited rates of release of COPCs into the IDF.” The PA document further states “[b]ecause the details of the SSW cementitious grout mix specification(s) and final disposal configuration for SSW have not been defined, the SSW data package relied on available information from existing studies of cementitious materials considered representative of mixes that may be used for SSW encapsulation and/or solidification”. It is not clear if any further information on the proposed specifications for the cementitious matrices has been developed since the PA document was written.

Additionally, in the LFRG review, one of the key issues identified was that the Waste Acceptance Criteria (WAC) for the current PA has not been developed to protect key assumptions and limits. The corrective action/resolution for this item is that a WAC document will be developed based on the analysis documented in this revision of the PA. It is not clear if this document has been developed yet and/or if any other documents have been prepared that describe the methodology that will be used to ensure that the performance of the selected grout mixtures is consistent with the performance assumed in the PA for key parameters (e.g., parameters related to the chemical and hydraulic performance of the wasteform).

Path Forward

Please provide additional information, if any, that has been developed on the planned specifications for the cementitious grout mixes to be used to stabilize waste generated as part of WTP operations. Provide the WAC for the current PA, if available. Provide a description of the process that will be used to design and the cementitious grout mixes to ensure that the performance of the grout mixtures will be consistent with the performance assumed in the PA for all of the expected compositions of the waste streams.

DOE Response

The Draft WIR Evaluation addresses the WIR criteria for VLAW produced using the DFLAW approach. Other wastes are outside the scope of the Draft WIR Evaluation, including non-reprocessing secondary waste (see DOE response [Section 2.0]) and vitrified waste assumed to potentially be produced by supplemental LAW treatment (for which DOE has made no decision to pursue).⁷⁴ To bound the analysis, the IDF PA correctly includes all wastes

⁷⁴ Information concerning SSW generated from supplemental LAW is provided in this RAI response for additional information and completeness only, and is outside the scope of both the Draft WIR Evaluation and DOE

potentially disposed of in the IDF, including the DFLAW-produced VLAW as well as, potentially, additional VLAW,⁷⁵ and all SSW which may be disposed at IDF. However, DOE recognizes the importance of the PA, which is a reference for the Draft WIR Evaluation, and is providing the information below in response to the RAI, including a discussion of the full potential treatment mission, SSW, and LSW for additional information. The approach to ensuring that all waste packages are acceptable for disposal at the IDF is described in this RAI response and is the same for all waste streams.

A copy of the WAC was uploaded to the NRC share site on December 8, 2020.

The grout used in the PA to solidify or encapsulate SSW, referred to as Hanford Grout Mix 5, is a commercially-available product from a local concrete supplier. For other waste, this mix was developed in the early 1990s⁷⁶ (see **Figure 2-21-1**). The grout mix and variations of the mix used onsite were studied in the laboratory to develop the necessary parameters for simulating releases in a computer model. The developed parameters are reported in SRNL-STI-2016-00175.

At the time the PA data collection effort was performed to establish the inputs that were used in modeling SSW, waste generation from WTP operations was still five or more years away. At that time, no decisions were being made about the expected grout formulation for SSW. For this reason, the PA assumed that the disposal practice that was being used at the time was appropriate for waste form release modeling and identified this as a key assumption. Since the PA had been completed, no decision has been made to develop and use an alternative to Hanford Grout Mix 5. Therefore, the use of Hanford Grout Mix 5 is still the expected path forward for disposal in the IDF. Any variations to the proposed grout mix, including the addition of sand, would be subject to change management controls to ensure that key assumptions in the PA are protected. For different grout formulations, laboratory measurements for the grout density, porosity, saturation, saturated hydraulic conductivity, and effective diffusion coefficients would be required to perform the evaluations. The response to RAI 2-20 identifies data collection efforts in PNNL-28545 to evaluate these properties for the three SSW streams included in the IDF PA.

decisions concerning supplemental LAW treatment. DOE has not made decisions concerning the potential path forward for supplemental LAW treatment, as explained in footnote 7 of the Draft WIR Evaluation and 78 FR 75913, "Record of Decision: Final Tank Closure and Waste Management Environmental Impact Statement for the Hanford Site, Richland, Washington." As explained in Section 1.2 of the Draft WIR Evaluation, the Draft WIR Evaluation does not address or include in its scope supplemental LAW. To bound the IDF PA analysis, the IDF PA assumed that supplemental LAW may potentially be vitrified and disposed of in the IDF, although, as explained above, DOE has made no decisions concerning the potential path forward for supplemental LAW treatment.

⁷⁵ See footnote 74.

⁷⁶ This mix is the basis for what is currently used by an offsite treatment vendor to prepare containerized waste for disposal on the Hanford Site. Variations of this mix add sand as an aggregate. Certain other waste destined for disposal onsite is sent offsite for treatment prior to disposal; the waste generator has the opportunity to specify a grout mix or rely upon the treatment contractor to select the treatment method and use a grout formulation that ensures the treated product meets both the disposal facilities WAC and also land disposal requirements in the State of Washington.

Figure 2-21-1. Mix Design Worksheet for Hanford Grout Mix 5.

MIX DESIGN WORKSHEET

MIX NO: 5 CALCULATED BY: Jerry L. England DATE: 3-11-93
 GEL: 11 DATE ISSUED: _____ LAB NOTEBOOK NO: N/A PAGE: N/A
 CEMENT TYPE: ASH GROVE I-II W/C: 0.30

AGGREGATE	SIZE	SPECIFIC GRAVITY
_____	_____	_____
_____	_____	_____
SAND	FLY ASH	_____
CENTRALIA	_____	_____

	DESCRIPTION	ABSOLUTE VOLUME (FT ³)	SSD WEIGHTS (LB)
CEMENT	I-II	3.00	588
WATER	TAP	11.33	706
AIR	N/A		
AGGREGATE	N/A		
SAND	FLY ASH	12.53	1706
WRA			
OTHER			
OTHER			
OTHER	0.5%	0.14	

REMARKS Add 8 oz. WRA per 100 lbs of cement material. Add 1.5 lbs fiber per cubic yard (PRO MESH).

MIXING _____

INSTRUCTIONS Water cure 73°F ± 3°F for 28 Days.

CHECKED BY: HL Beatty DATE: 8/12/93

Section 4.6 in CHPRC-03348 (referred to as the IDF PA Maintenance Plan) identifies activities to continually evaluate national and international research on grout properties and release models to see if useful insights can be learned and used to compare with conceptual and numerical model assumptions and parameter values used in the IDF PA. PNNL-28545 illustrates this data collection effort to protect key assumptions in the IDF PA. Another research opportunity identified ultra-high performance cementitious composites as a possible candidate to encapsulate SSW at Hanford. DOE and WRPS Chief Technology Office awarded two contracts to investigate this material for treatment of SSW prior to disposal at IDF. Initial studies showed promise for this material having very low leaching characteristics (Hasan et al. 2019). Subsequently, in FY 2020 Savannah River National Laboratory began investigating the application of Ultra-High Performance Cementitious Composites to encapsulate waste streams. The final report for this work is expected to be completed mid-FY 2021.

References

- 78 FR 75913, 2013, “Record of Decision: Final Tank Closure and Waste Management Environmental Impact Statement for the Hanford Site, Richland, Washington,” *Federal Register*, Vol. 78, pp. 75913–75919 (December 13).
- CHPRC-03348, 2019, *Performance Assessment Maintenance Plan for the Integrated Disposal Facility*, Rev. 1, INTERA, Inc./CH2M HILL Plateau Remediation Company, Richland, Washington.
- Hasan, T. W., S. Allena, L. Gilbert, and M. R. Choma, 2019, *Investigating Ultra-High-Performance Cementitious Composite (UHPCC) as a Possible Encapsulation Grout for Hanford Solid Secondary Waste – FY2018 Report*, Washington State University Tri-Cities, Richland, Washington.
- PNNL-28545, 2020, *Development and Characterization of Cementitious Waste Forms for Immobilization of Granular Activated Carbon, Silver Mordenite, and HEPA Filter Media Solid Secondary Waste*, Rev. 1, RPT-SWCS-014, Rev. 1.0, Pacific Northwest National Laboratory, Richland, Washington.
- SRNL-STI-2016-00175, 2016, *Solid Secondary Waste Data Package Supporting Hanford Integrated Disposal Facility Performance Assessment*, Rev. 0, Savannah River National Laboratory, Savannah River Nuclear Solutions, Aiken, South Carolina.

5.0 ASSESSMENT OF WASTE CONCENTRATION AND CLASSIFICATION

No RAI Responses fall into this categorization.

6.0 REFERENCES

- 10 CFR 61, “Licensing Requirements for Land Disposal of Radioactive Waste,” Subpart C—Performance Objectives, *Code of Federal Regulations*, as amended.
- 10 CFR 61.55, “Waste Classification,” *Code of Federal Regulations*, as amended.
- Atomic Energy Act of 1954*, 42 USC 2011, et seq., as amended.
- DOE G 435.1-1, 1999, *Implementation Guide for Use with DOE M 435.1-1, Radioactive Waste Management Manual*, U.S. Department of Energy, Washington, D.C.
- DOE M 435.1-1, 2011, *Radioactive Waste Management Manual*, Change 2, U.S. Department of Energy, Washington, D.C.
- DOE O 435.1, 2011, *Radioactive Waste Management*, Change 2, U.S. Department of Energy, Washington, D.C.
- DOE/ORP-2020-01, 2020, *Draft Waste Incidental to Reprocessing Evaluation for Vitrified Low-Activity Waste Disposed Onsite at the Hanford Site*, Washington, U.S. Department of Energy, Office of River Protection, Richland, Washington.
- DOE-ORP-PPD-EM-50168, 2020, *Waste Incidental to Reprocessing Determinations*, Rev. 2, U.S. Department of Energy, Office of River Protection, Richland, Washington.
- IDF-00002, 2019, *Waste Acceptance Criteria for the Integrated Disposal Facility*, Rev. 0, CH2M HILL Plateau Remediation Company, Richland, Washington.
- Interagency Agreement 89304019SEM000003/P0000, 2020, *Consulting Services concerning DOE WIR evaluations on Vitrified Low Activity Waste*, U.S. Department of Energy, Office of River Protection, Richland, Washington/U.S. Nuclear Regulatory Commission, Rockville, Maryland.
- MR-50461-00, 2019, *2019 Flowsheet Integration Joint Scenarios*, Rev. 3, Washington River Protection Solutions, LLC, Richland, Washington.
- NRC, 2020, “Request for Additional Information on the Draft Waste Incidental to Reprocessing Evaluation for Vitrified Low-Activity Waste Disposed Onsite at the Hanford Site, (Docket Number PROJ0736)” (letter from C. McKenney to M. Gilbertson, U.S. Department of Energy, Office of Environmental Management, November 06), U.S. Nuclear Regulatory Commission, Washington, D.C.
- Nuclear Waste Policy Act of 1982*, 42 USC 10101, et seq.

NUREG-1854, 2007, *NRC Staff Guidance for Activities Related to U.S. Department of Energy Waste Determinations – Draft Final Report for Interim Use*, U.S. Nuclear Regulatory Commission, Office of Federal and State Materials and Environmental Management Programs, Washington, D.C.

RPP-RPT-57991, 2019, *River Protection Project Integrated Flowsheet*, 24590-WTP-RPT-MGT-14-023, Rev. 3, Washington River Protection Solutions, LLC, Richland, Washington.

RPP-RPT-59958, 2019, *Performance Assessment for the Integrated Disposal Facility, Hanford Site, Washington*, Rev. 1A, Washington River Protection Solutions, LLC, Richland, Washington.

Waste Isolation Pilot Plant Land Withdrawal Act, Public Law 102-579, as amended.

This page intentionally left blank.

ATTACHMENT A

Reserved